Southern Ocean phytoplankton under multiple stressors: The modulation of Ocean Acidification effects by iron and light

Clara Jule Marie Hoppe

Fachbereich 2

Universität Bremen

Dissertation zur Erlangung des akademischen Grades eines Doktors der Naturwissenschaften

Dr. rer. nat

Dezember 2013

"What we observe is not nature itself,
but nature exposed to our method of questioning."

Werner Heisenberg (1962)

Acknowledgements

First and foremost, I would like to express my gratitude to my supervisor Björn Rost for his unlimited enthusiasm, encouragement and support throughout the past years. I feel really lucky to be part of his truly inspiring group.

In addition, I am grateful to Dieter Wolf-Gladrow for his support and willingness to review this thesis. Especially, I thank him for his input to and help with the 'CC riddle'.

I would also like to thank Kai Bischof for agreeing to be on my thesis committee despite his extremely busy schedule.

Furthermore, I would like to thank Scarlett Trimborn for the opportunity to join her on two expeditions to the Southern Ocean and for her support during the early stage of this thesis.

Special thanks also go to the further members of my PhD committee Philippe Tortell, Christoph Völker and Philipp Assmy for their useful advice and questions that helped me to plan and structure the work for this thesis.

In addition, I would like to thank my co-authors, office buddies, lunch group members, many AWI co-workers and friends, and fellow cruise-participants for interesting and instructive discussions.

This work would not have been possible without the support from the cruise leaders, captains and crew of the RV Polarstern cruises ANT-XXVII/2 and ANT-XXVIII/3.

Abbreviations

ACC	Antarctic circumpolar current
ANOVA	Analysis of variance
APF	Antarctic polar front
ASW	Artificial seawater
ATP	Adenosine triphosphate
AWW	Antarctic winter water
BSi	Biogenic silica
C_i	Inorganic carbon
$CaCO_3$	Calcium cabonate
CCM	Carbon concentrating mechnisms
Cd	Cadmium
Chl *a*	Chlorophyll *a*
Co	Copper
CO_2	Carbon dioxide
CO_3^{2-}	Carbonate ion
CRM	Certified reference material
CTD	Conductivity temperature depth
D1	Photosystem II reaction center protein
DFB	Desferrioxamine B siderophore
DIC	Dissolved inorganic carbon
DOM	Dissolved organic matter
DPM	Disintegrations per minute
E_z-ratio	Exported organic matter : NPP ratio
ETR	Electron transfer rates through PSII
ETR_{max}	Light-saturated, maximal electron transfer rates through PSII
F_0	Minimum fluorescence
Fe	Iron
F_m	Maximum fluorescence
F_q'/F_m'	Quantum yield (efficiency) of electron transport through PSII in the light
FRRF	Fast repetition rate fluorometry
F_v	Variable fluorescence
F_v/F_m	Quantum yield (efficiency) of electron transport through PSII in the dark
H_2O	Water
HCl	Hydrochloric acid
HCO_3^-	Bicarbonate ion
HNLC	High-nutrient low-chlorophyll
HPLC	High performance liquid chromatography

HSO_4	Sulfuric acid
I_K	PSII light saturation index
LET	Linear electron transport
MOX	Midstream terminal oxidase
NADPH	Nicotineamide-adenine-dinucleotide-phosphate
$NaHCO_3$	Sodium-bicarbonate
NO_2^-	Nitrite
NO_3^-	Nitrate
NPP	Net primary production
NPQ	Non-photochemical quenching
NSW	North Sea water
O_2	Oxygen
OA	Ocean Acidification
PAR	Photosynthetically active radiation
P^b	Chlorophyll-specific carbon fixation
pCO_2	Carbon dioxide partial pressure
PI curve	Photosynthesis-irradiance curve
PIC	Particulate inorganic carbon
PO_4^{3-}	Phosphate
POC	Particulate organic carbon
PON	Particulate organic nitrogen
PQ	Plastoquinone pool
PS	Photosystem
ROS	Reactive oxygen species
pH	Negative logarithm of the hydronium ion activity of a solution
RubisCO	Ribulose-1,5-bisphosphate carboxylase/oxigenase
SG	South Georgia
$Si(OH)_4$	Ortho-Silicate
SO	Southern Ocean
STF	Single turnover flash
TA	Total alkalinity
Zn	Zinc
α	Light-use efficiency of PSII
$\Phi_{e,C}$	Energy conversion efficiency from photochemistry to biomass production
ρ	Connectivity between PSII reaction centres in the dark
ρ'	Connectivity between PSII reaction centres in the light
σ_{PSII}	Functional absorption cross-section for PSII in the dark
σ_{PSII}'	Functional absorption cross-section for PSII in the light
τ	PSII turnover (i.e. reoxidation of PQ) time in the dark
τ '	PSII turnover (i.e. reoxidation of PQ) time in the light

Contents

Chapter 1

Summary

The uptake of anthropogenic carbon dioxide (CO_2) by the world's oceans has led to pronounced perturbations of the marine carbonate system, which are collectively termed Ocean Acidification (OA). The Southern Ocean (SO) contributes significantly to the sequestration of anthropogenic CO_2 via the physical and biological carbon pumps and is furthermore especially prone to OA. On this account, the sensitivity of SO phytoplankton towards OA has gained increasing attention in the recent years. Most studies investigated OA effects in isolation, even though co-occurring changes in sea surface temperature and stratification can strongly alter light and nutrient availabilities. The aim of this thesis was therefore to investigate how key environmental factors for SO primary productivity influence the manifestation of OA effects on phytoplankton physiology and ecology.

Effects of OA are typically investigated in pCO_2 perturbation experiments, in which carbonate chemistry is altered and monitored. Over-determination of the carbonate system (i.e. the measurement of more than two parameters) revealed systematically occurring inconsistencies between pCO_2 values calculated from different pairs of input parameters. As described in *Publication I*, these inconsistencies were found to be as high as 30%, having the largest impact under OA scenarios. Since there is no general agreement on which pair of input parameters is used, these discrepancies hamper the comparability and quantitative validity of past and future OA studies. Until the reasons are found and abolished, it is suggested to agree on one specific set of parameters (i.e. pH and total alkalinity) to increase comparability between studies. These findings also emphasizes the need for high pCO_2 standards.

Iron is one of the most important limiting factors for phytoplankton growth and primary production in the SO. It could therefore be hypothesised that iron availability exerts an influence on the manifestation of OA effects in this region. As presented in *Publication II*, iron limitation drastically altered the responses of a natural phytoplankton assemblage to OA. After iron enrichment, primary production increased with increasing pCO_2 levels, whereas OA had no influence on carbon fixation under iron limitation. Changes in productivity were accompanied by pronounced functional shift in species composition. The results indicate that under increased iron availability, OA could potentially lead to a stimulation of SO primary production and strengthen the biological carbon pump. Over much of the SO, however, iron limitation likely prevents 'CO_2 fertilization' effects.

Next to iron availability, also irradiance levels and dynamics are controlling the development of SO phytoplankton blooms. Therefore, also a strong interaction between light fields and increasing pCO_2 levels can be expected. In *Publication III*, dynamic light was found to strongly alter the effects of OA on the diatom *Chaetoceros debilis*. High pCO_2 had little effect on primary production under constant but a negative effect under dynamic light. Results indicate a lowered capacity to sink excess energy, pssibly causedby a down-regulation

of the carbon concentrating mechanisms under OA. Thus, consequences of high-light stress were most pronounced in the light peaks of the dynamic light treatment under OA. The results question the applicability of findings from OA studies conducted under constant irradiances to varying light conditions in the oceans and furthermore emphasise the need for more complex experimental setups.

In the natural environment not only light conditions are variable, phytoplankton encounter simultaneous changes in several drivers and stressors. The aim of *publication IV* was to understand how concurrent variability in iron, light and other factors controls SO phytoplankton blooms. Therefore, two large-scale phytoplankton blooms in the Antarctic Polar Frontal zone were compared with respect to phytoplankton standing stocks, primary production, photosynthetic efficiencies and nutrient deficits. The blooms were mainly controlled by interactions between iron and light limitation, as well as zooplankton grazing. The results of this field study confirm the environmental importance of the two co-variables investigated in *Publication II* and *III*.

In conclusion, there is no universal phytoplankton response to OA. More specifically, the effects of OA will always be modulated by the respective set of environmental conditions prevailing in the ecosystem of interest, which themselves may be subject to global change. Similarly, the setup of CO_2 perturbation experiments (e.g. with respect to light, nutrients, temperature) will to some extent determine its results. The modulation of OA effects by these variables can explain seemingly contradictory results from previous studies and helps to increase our understanding of the underlying physiological mechanisms. Based on the findings of this thesis, differential responses for the coastal and open ocean regimes of the SO can be proposed. While climate change may enhance primary and export production in coastal and shelf areas, iron limitation and highly dynamic light regimes could jointly reverse the beneficial effects of elevated pCO_2 levels in open ocean regions of the SO.

Zusammenfassung

Die Aufnahme von anthropogenem Kohlenstoffdioxid (CO_2) durch die Ozeane führt zu ausgeprägten Veränderungen in der Karbonatchemie des Meerwassers, dem Phänomen der sogenannten Ozeanversauerung. Über die physikalische sowie biologische Kohlenstoffpumpe nimmt das Südpolarmeer einen signifikanten Anteil des anthropogenen CO_2 auf und ist zudem besonders anfällig für Veränderungen in der Karbonatchemie. Da die CO_2-Aufnahmekapazität des Südpolarmeeres wesentlich vom Phytoplankton beeinflusst wird, ist dessen Reaktion auf Ozeanversauerung von besonderem Interesse. Obwohl der CO_2-Anstieg zu einer zunehmenden Erwärmung und Stratifizierung der Meeresoberfläche führt, welche Veränderungen in der Licht- und Nährstoffverfügbarkeit zur Folge haben, wurden die Auswirkungen von Ozeanversauerung meist nur isoliert untersucht. Das Hauptziel der vorliegenden Dissertation war es daher, den Einfluss der wichtigsten Umweltfaktoren im Südpolarmeer in Hinblick auf die Folgen von Ozeanversauerung für die Physiologie und Ökologie des Phytoplanktons im Südpolarmeer zu untersuchen.

Die Folgen von Ozeanversauerung für marine Organismen werden üblicherweise in pCO_2-Manipulationsexperimenten untersucht, in denen die Karbonatchemie verändert und überwacht werden muss. Eine Überbestimmung des Karbonatsystems (d.h. das Messen von mehr als 2 Parametern) deckte Abweichungen zwischen den von unterschiedlichen Parameter-Paaren berechneten pCO_2-Werten auf. *Publikation I* beschreibt systematische Abweichungen von bis zu 30%, welche sich am stärksten in den Zukunftszenarien von Ozeanversauerungsstudien auswirken. Da bisher verschiedene Parameter-Kombinationen verwendet werden, stellen die beschriebenen Diskrepanzen die Vergleichbarkeit von Ozeanversauerungsstudien und deren quantitativen Ergebnisse in Frage. Diese Studie unterstreicht die Notwendigkeit eines Karbonatchemie-Standards für hohe pCO_2-Bereiche, welche zur Zeit nicht existieren.

Eisen ist einer der wichtigsten, häufig limitierenden Faktoren der Primärproduktion im Südpolarmeer. Es wurde daher vermutet, dass unterschiedliche Eisenkonzentrationen die Auswirkungen von Ozeanversauerung modulieren. Wie in *Publikation II* dargestellt, führen unterschiedliche Eisenverfügbarkeiten zu stark veränderten Ozeanversauerungseffekten in natürlichen Phytoplanktongemeinschaften. Während Ozeanversauerung unter erhöhter Eisenverfügbarkeit zu gesteigerten Primärproduktionsraten führte, blieben diese unter Eisenlimitation bei ansteigendem pCO_2-Gehalt konstant. Die hierdurch zu erwartenden Auswirkungen auf die Exportproduktion wurden des Weiteren durch eine Verschiebung in der Artzusammensetzung und einem veränderten Silifizierungsgrad der dominierenden Diatomeen verstärkt. Die Ergebnisse deuten an, dass sich erhöhte pCO_2-Gehalte unter ausreichenden Eisenkonzentrationen positiv auf das Phytoplankton des Südpolarmeeres auswirken könnten. Im eisenlimitierten offenen Ozean ist das Potential für eine CO_2-bedingte Steigerung in der Primärproduktion hingegen stark eingeschränkt.

Weiterhin wird das Wachstum vom Phytoplankton des Südpolarmeeres auch von im Mittel niedrigen, jedoch hoch dynamischen Lichtintensitäten begrenzt. In *Publikation III* wurde gezeigt, dass auch zwischen den Auswirkungen von Ozeanversauerung und dynamischen Lichtverhältnissen eine Interaktion besteht. Während die Diatomee *Chaetoceros debilis* unter konstanten Lichtbedingungen kaum auf erhöhte pCO_2-Werte reagierte, führte Ozeanversauerung unter dynamischem Licht zu einer drastischen Reduktion im Biomasseaufbau. Photophysiologische Untersuchungen deuten eine verringerte Energietransfer-Effizienz von den Licht- zu den Dunkelreaktionen der Photosynthese unter dynamischem Licht und Ozeanversauerung an. Diese könnte auf eine CO_2-bedingte Regulation im Kohlenstofferwerb und einer damit einhergehenden Kapazitätserniedrigung für die Ableitung überschüssiger Energie in den Hochlichtphasen des dynamischen Lichtfeldes hindeuten. Diese Studie stellt die Übertragbarkeit von Ozeanversauerungsexperimenten, die unter konstanten Lichtbedingungen durchgeführt wurden, in Frage und unterstreichen die Notwendigkeit, zukünftige Experimente unter komplexeren Bedingungen durchzuführen.

In ihrer natürlichen Umgebung erfahren Phytoplanktonzellen nicht nur hoch-dynamische Lichtbedingungen, vielmehr sind sie einer Vielzahl an unterschiedlichen und oft variablen Einflussgrössen und Stressfaktoren ausgesetzt. Um zu verstehen, wie sich gleichzeitige Veränderungen in diversen Umweltparametern auf das Phytoplankton des Südpolarmeeres auswirken, sind daher Felduntersuchungen unumgänglich. *Publikation IV* zeigt in diesem Zusammenhang, dass sich Unterschiede in Biomasse, Primärproduktion, Photosynthese-Effizienz und Nährstoffaufnahme von zwei Phytoplankton-Blüten im Südpolarmeer durch die jeweils vorherrschenden Licht- und Eisenverfügbarkeiten sowie das Vorkommen von Fressfeinden erklärt werden können. Des Weiteren bestätigen diese Ergebnisse, dass mit Eisen- und Lichtverfügbarkeit die wichtigsten Umweltvariablen des Südpolarmeeres in *Publikation II* und *III* untersucht wurden.

Von den Ergebnissen dieser Dissertation kann geschlussfolgert werden, dass es kein allgemeingültiges Reaktionsmuster des Phytoplanktons auf Ozeanversauerung gibt. Vielmehr werden die Folgen des Klimawandels von den jeweils vorherrschenden, sich ebenfalls im Wandel befindlichen Umweltbedingungen abhängen. Ebenso werden die Rahmenbedingen von Ozeanversauerungsexperimenten (z.B. Licht, Nährstoffe, Temperatur) einen grossen Einfluss auf deren Ergebnisse haben. Das Wissen um die Modulation von Ozeanversauerungseffekten auf das Phytoplankton kann dabei helfen, widersprüchliche Messergebnisse zu erklären und zugrundeliegende physiologischen Mechanismen zu entschlüsseln. In Hinblick auf das Südpolarmeer kann davon ausgegangen werden, dass sich der Klimawandel unterschiedlich auf verschiedene Phytoplanktongemeinschaften auswirkt. Während Ozeanversauerung in Küstennähe zu erhöhter Primär- und Exportproduktion führen könnte, werden kombinierte

Effekte von Eisenlimitation und stark dynamischen Lichtbedingungen im offenen Ozean einen vermutlich entgegengesetzten Trend zur Folge haben.

Chapter 2

Introduction

Preface

Humankind is dependent on diverse marine ecosystem services such as food supply or coastal protection (Peterson & Lubcheno 1997). For example, more than 150 million people live within one metre of the high tide level (Rowley et al. 2007) and at least one billion people directly depend on fish for food, while hundreds of millions depend on fishing for their livelihood (Schorr 2004). The Millennium Ecosystem Assessment (2005) concluded that the degradation and loss of marine ecosystem services affects especially poor and already vulnerable people, hence being a significant barrier to the reduction of poverty. Essential ecosystem services are seriously threatened by climate change (Rowley et al. 2007, Hoegh-Guldberg & Bruno 2010). At the same time are oceans absorbing and storing heat and anthropogenic carbon dioxide (CO_2), thereby attenuating the effects of climate change but also exerting strong feedbacks on global climate (Bindoff et al. 2007). The understanding of climate change, its consequences for marine ecosystems and potential feedbacks on climate is therefore one of the most urgent tasks of human society.

2.1 The global carbon cycle

2.1.1 Earth's climate and it's perturbation by anthropogenic CO_2 emissions

CO_2 is the ultimate source of carbon for phototrophic production of organic matter, which is required by all higher trophic levels. Furthermore, without greenhouse gases such as CO_2 in the atmosphere, temperatures on Earth would be too low to support life as we know it (Mitchell 1989).

Over geological timescales, the release of CO_2 to the atmosphere, mainly by tectonic activities, has been balanced by its uptake mainly due to weathering of silicate rocks (Kasting et al. 1988). According to ice core data, atmospheric CO_2 concentrations have been fairly constrained over the past 800,000 years, during which CO_2 partial pressure (pCO_2) has been oscillating between 170 μatm in glacial and 300 μatm in interglacial phases (Petit et al. 1999, Lüthi et al. 2008; Figure 2.1 A). Since the industrial revolution, however, humankind has significantly changed the Earth's atmospheric composition, mainly by the release of CO_2 from fossil fuels (Keeling 1973, Sundquist 1985; Figure 2.1 B). Until today, atmospheric pCO_2 levels increased to about 395 μatm (Keeling et al. 2013; http://keelingcurve.ucsd.edu) and are expected to rise to 750 μatm (IPCC scenario IS92a, IPCC, 2007) or even beyond

1000 μatm by the end of this century (Raupach et al. 2007). The increase in atmospheric CO_2 concentrations leads to various phenomena such as global warming, sea level rise, ocean acidification, as well as changes in wind and precipitation patterns, collectively termed *climate change*.

The oceans play a key role in the manifestation of climate change effects. Firstly, they take up over 80% of the heat added to the climate system by the anthropogenic greenhouse effect (Levitus et al. 2005, Bindorff et al. 2007). As a result also the oceans are warming, which can lead to increased stratification of the water column, with concurrent declines in mixed layer depth (MLD) and upwelling of nutrients into the well-lit surface mixed layer (Steinacher et al. 2010). Even though atmospheric CO_2 levels are now 40% higher than before the industrial revolution, their rise is much slower than expected from the emissions of anthropogenic CO_2. This is the case, because a large fraction of it has been removed from the atmosphere by the other components of the global carbon cycle (Canadell et al. 2007). As the largest sink, the oceans have taken up more than 40% of the anthropogenic CO_2 from the atmosphere so far (Khatiwala et al. 2009). This addition of at least 140 Pg carbon (Khatiwala et al. 2009) has led to significant perturbations of the marine carbonate system (Figure 2.2), which are collectively called *Ocean Acidification* (OA; Broeker & Clark 2002, Caldeira & Wickett 2003). Since the onset of the industrial revolution the mean surface pH has already dropped by about 0.1 pH units. Until the end of this century, surface pH is expected to decrease by additional 0.3 units, which would represent an increase in acidity by 150% (Feely et al. 2009).

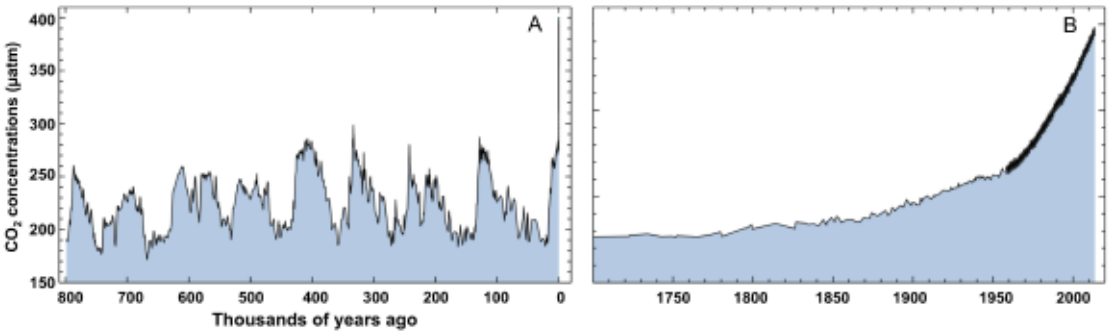

Figure 2.1: - Atmospheric pCO_2 levels over the past 800.000 years (A) and since the onset of the industrial revolution (B) as reconstructed from ice cores (Lüthi et al. 2008) and from atmospheric measurements (Keeling et al. 2013). Modified after Keeling et al. (2013; http://keelingcurve.ucsd.edu/).

2.1.2 Marine carbonate chemistry

The ocean's capacity to take up and store enormous amounts of CO_2 is caused by the dissociation of CO_2 into several forms of inorganic carbon (C_i) as well as by the high CO_2-buffering capacity of seawater (Zeebe & Wolf-Gladrow 2001). CO_2 enters the surface ocean via equilibration with the atmosphere. According to Henry's law, the concentrations of CO_2 in seawater relative to those of the atmosphere depend on the solubility coefficient of CO_2 (K_0) at a certain temperature and salinity (Weiss 1974):

$$[CO_2](aq) = K_0(T, S) \times pCO_2 \tag{2.1}$$

In seawater, CO_2 is not only present in its dissolved form ($CO_2(aq)$), but also reacts with water (H_2O) to form carbonic acid (H_2CO_3), which almost immediately dissociates to bicarbonate (HCO_3^-) under the release of protons (H^+). HCO_3^- and H^+ are also formed from the reaction of CO_2 with carbonate ions (CO_3^{2-}) present in seawater. All carbonate species are related to each other by the following equilibria:

$$CO_2(aq) + H_2O \rightleftharpoons H_2CO_3 \overset{K_1}{\rightleftharpoons} HCO_3^- + H^+ \overset{K_2}{\rightleftharpoons} CO_3^{2-} + 2H^+ \tag{2.2}$$

where K_1 and K_2 are the first and second dissociation constants of carbonic acid, respectively. As the dissolution of CO_2 leads to the formation of H^+ ions, it also causes a decrease in seawater pH. These reactions between CO_2 and water also control the equilibrium between the different components of the carbonate system, as the concomitant changes in speciation are linked to the pH through the pK values of the dissociation constants (Figure 2.3).

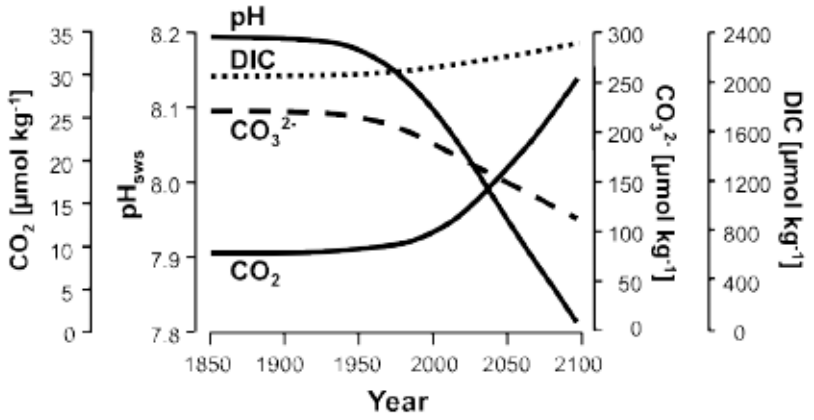

Figure 2.2: - Projected changes in marine seawater chemistry in response to increased uptake of anthropogenic CO_2 by the worlds oceans. Calculations are based on a 'business as usual' scenario for CO_2 emissions (IPCC 1995). Modified after Wolf-Gladrow et al. (1999).).

The exact knowledge of temperature, salinity, pressure and two parameters of the carbonate system allows calculating the concentrations of all other components with the help of the dissociation constants of carbonic acid. The two most commonly measured carbonate chemistry parameters are the sum of all inorganic carbon species (CO_2(aq), H_2CO_3, HCO_3^- and CO_3^{2-}), collectively termed *dissolved inorganic carbon* (DIC), and the *total alkalinity* (TA). According to Dickson (1981), TA is defined as the excess of proton acceptors (bases formed from weak acids with a pK $\leq$4.5) over proton donors (acids with a pK >4.5):

$$\begin{aligned} TA = [HCO_3^-] + 2[CO_3^{2-}] + [B(OH)_4^-] + [OH^-] + [HPO_4^{2-}] + 2[PO_4^{3-}] \\ + [H_3SiO_4^-] + [NH_3] + [H^+]_F - [HSO_4^-] - [HF] - [H_3PO_4] \end{aligned} \quad (2.3)$$

As a conservative parameter, TA is not affected by changes in temperature or pressure, nor does it change due to in- or outgassing of CO_2. Biological activity, however, can greatly alter TA. For example, the precipitation of calcium carbonate ($CaCO_3$) reduces TA by two units per unit DIC (Eq. 2.3, Figure 2.4). But also the removal of nitrate, which does not show up in the traditional alkalinity expression (Eq. 3), has an effect on TA. In order to understand such changes in TA, an expression in which all components are conservative, was developed by Wolf-Gladrow et al. (2007):

$$\begin{aligned} TA_{ec} = [Na^+] + 2[Mg^{2+}] + 2[Ca^{2+}] + [K^+] + 2[Sr^{2+}] + ... - [Cl^-] - [Br^-] \\ - [NO_3^-] - ... + TPO_4 + TNH_3 - 2TSO_4 - THF - THNO_2 \end{aligned} \quad (2.4)$$

where $TPO_4 = [H_3PO_4] + [H_2PO_4^-] + [HPO_4^{2-}] + [PO_4^{3-}]$, $TNH_3 = [NH_3] + [NH_4^+]$, $TSO_4 = [SO_4^{2-}] + [HSO_4^-]$, $THF = [F^-] + [HF]$, and $THNO_2 = [NO_2^-] + [HNO_2]$ are

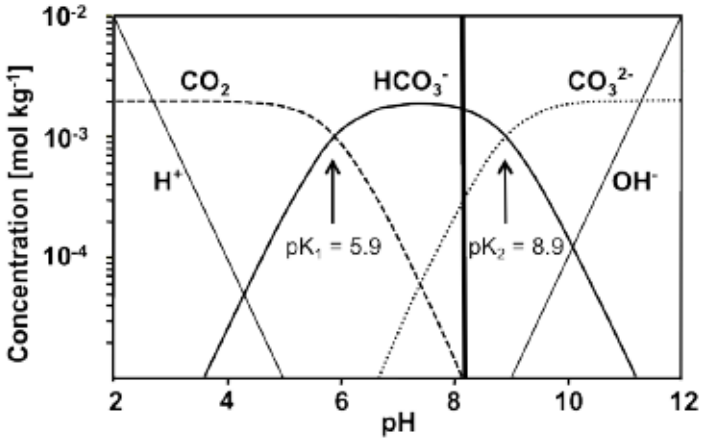

Figure 2.3: - Bjerrum plot showing the relative contributions of the different species of the marine carbonate system as a function of pH at a given DIC concentrations (2100 μmol kg^{1-}), temperature (25 °C) and salinity (35). pK_1 and pK_2 are the pK values of the first and second dissociation constants of carbonic acid. Modified after Zeebe & Wolf-Gladrow (2001).

total phosphate, ammonia, sulphate, fluoride, and nitrite, respectively. With the help of the explicit conservative expression of TA (Eq. 2.4), the influence of biological processes such as biomass production or remineralisation on the marine carbonate system can be explained easily (Wolf-Gladrow et al. 2007). For example, it can be seen that the assimilation of one unit nitrate will increase TA by one unit, while the assimilation of one unit ammonia will decrease TA by the same amount. The uptake of DIC by marine photoautotrophs has no net effect on TA (Figure 2.4).

2.1.3 The ocean's carbon pumps

Organisms living in the ocean's surface can not only lead to changes in the carbonate system of their immediate surroundings, they can also collectively influence atmospheric pCO_2 levels by rising or decreasing the pCO_2 levels of the surface waters. The *biological carbon pump* is operated by the sinking of particulate carbon from the euphotic zone to greater depth. After remineralisation and dissolution, this carbon is stored in the deep ocean, so that a concentration gradient with depth is established (Volk & Hoffert 1985, Heinze & Maier-Reimer 1991; Figure 2.5). The biological carbon pump consists of two components: The *soft-tissue pump* transports carbon, which has been incorporated into organic material, to depth. As carbon is removed from the surface, seawater re-equilibrates with the atmosphere by the uptake of CO_2. The *carbonate (counter) pump* can lead to a net efflux of CO_2 from the ocean to the atmosphere, as the biologically-mediated precipitation of $CaCO_3$ lowers the

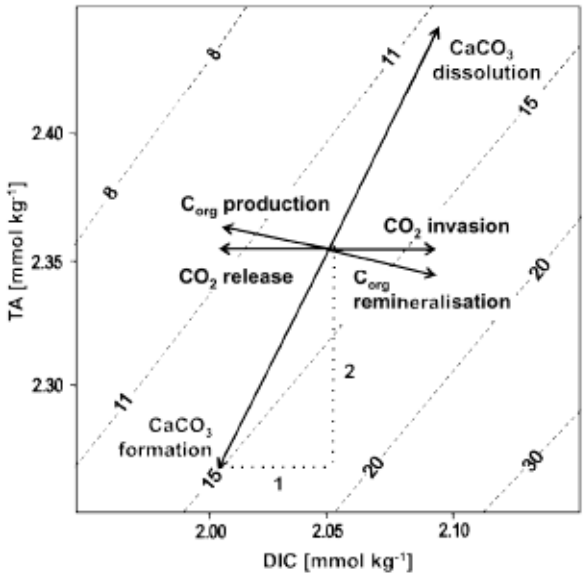

Figure 2.4: - Effects of various biotic and abiotic processes on DIC and TA of seawater. Modified after Wolf-Gladrow et al. (1999).

alkalinity by the removal of calcium ions. The subsequent downward transport of $CaCO_3$ contributes to the depth-gradient of inorganic carbon and alkalinity.

In addition to the biological pumps, also a physical carbon pump exists. The so-called *solubility pump* is driven by the different CO_2 solubility in warm and cold water in combination with deep water formation when cold CO_2-rich water from the surface sinks to greater depth (Volk & Hoffert 1985). The strength of this pump depends on the intensity of the overturning circulation (Broeker & Peng 1992, Sarmiento & Bender 1994, Marshall & Speer 2012).

As the *soft-tissue pump* is driven by the production of biomass by organisms, it is not only transporting carbon, but also other elements such as nitrogen and phosphorus. Hence, the *biological pump* (Longhurst & Harrison 1989, De La Rocha & Passow 2007) establishes concentration gradients of carbon as well as other nutrients. As the downward transport of organic matter can lead to a surface depletion in nitrate or phosphate (that unlike carbon, cannot be resupplied by equilibration with the atmosphere), production of organic matter and its export via the biological pump need to be balanced by the supply of new nutrients, typically from water masses below (Eppley & Peterson 1979). Primary production based on these new nutrients (i.e. *new production*) sets an upper limit to export

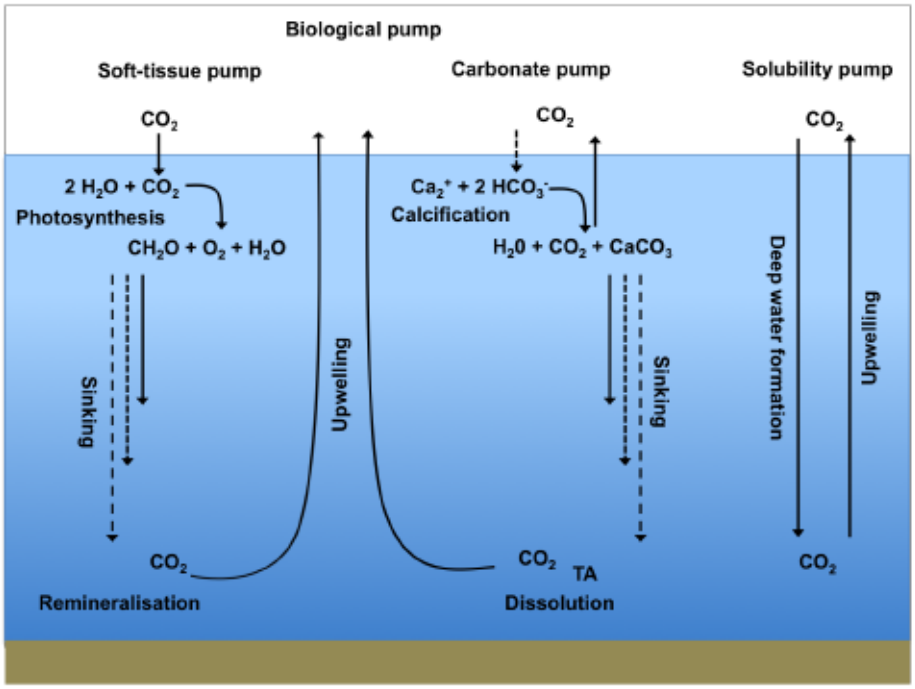

Figure 2.5: - Simplified illustration of the oceans carbon pumps comprising the biologically mediated soft-tissue and carbonate (counter) pumps as well the physically driven solubility pump and their effects on atmospheric CO_2 concentrations. Modified after Heinze & Maier-Reimer (1991).

production, even though total production also includes biomass build-up based on nutrients that are recycled within the surface ocean (i.e. *recycled production*; Dugdale & Goering 1967). The strength of the biological pump and its potential to sequester anthropogenic carbon is therefore determined by the surface concentrations of nutrients, the degree to which these nutrients are consumed, as well as the ratio of carbon to these nutrients in the organic matter that sinks to greater depths (Sigman et al. 2010). The latter is strongly affected by grazing and aggregation (De La Rocha & Passow 2007). Under current conditions, the biological carbon pumps account for about one third of the sequestration of carbon into the deep oceans (Falkowski et al. 1998).

2.2 Marine primary producers

2.2.1 Diatoms and other phytoplankton – small but mighty

The organisms that are responsible for the largest fraction of marine primary production, i.e. the main drivers behind the biological pumps, are microscopic photoautotrophs. The term *phytoplankton* (greek: 'phyton' = 'plant' and 'plankton' = 'wanderer') describes all unicellular aquatic organisms that utilize sunlight to turn inorganic nutrients into organic matter, and that are too small or immobile to actively resist the movement of ocean currents. Generally, phytoplankton provide three important 'services' to their environment: Firstly, due to the conversion of inorganic to organic matter they represent the base of aquatic food webs, which also include the world's fisheries (Lindeman 1942, Field et al. 1998). In fact, global oceanic net primary production is as high as 45-50 Pg carbon per year, and most of it is mediated by phytoplankton. Secondly, the production of oxygen during aquatic photosynthesis does not only provide half of the oxygen we breathe today (Field et al. 1998), it also led to the initial oxygenation of Earth's atmosphere 2.3 billion years ago (Bekker et al. 2004). Finally, phytoplankton biomass, mostly in converted forms such as aggregates or zooplankton fecal pellets, is transported to the deep ocean by the soft-tissue pump described above (Volk & Hoffert 1985).

Even though all phytoplankton possess these basal characteristics, the term actually describes a highly diverse group that comprises at least 25,000 different species (Falkowski & Raven 1997, Falkowski et al. 2004). One of the most common as well as diverse phytoplankton taxa is that of the diatoms (*Bacillariophyceae*; Figure 2.6), which are characterised by their silica frustules (Falkowski et al. 2004). Diatoms first evolved about 190-250 million years ago (Sims et al. 2004; Sorhannus 2007) and became a dominant phytoplankton group about 35 million years ago (Katz et al. 2004). Today, diatoms account for about 40% of the ocean's primary production and are the main players in the biogeochemical cycles of carbon,

nitrogen, phosphorus, silicon and iron (Nelson et al. 1995, Buessler 1998, Sartou et al. 2005). The competitive success of diatoms over other phytoplankton groups has been attributed to their high intrinsic growth rates under nutrient-replete conditions (Sartou et al. 2005), photoacclimation and -protection capacities (Lavaud 2007) as well as quantum-to-biomass conversion efficiencies (Wagner et al. 2006).

2.2.2 Phytoplankton photosynthesis and its limitation

Primary production, i.e. the build-up of organic matter, is dependent on the successful realization of various physiological processes (Figure 2.7). Unfavourable environmental conditions (e.g. low irradiances or nutrient concentrations) can impair phytoplankton productivity by interrupting any of these processes. To assess the responses to stressors, phytoplankton researchers often focus on measurements that integrate over all physiological levels (e.g. growth rate, production of particulate organic carbon (POC)) as well as specific levels of photosynthesis (e.g. electron transport, O_2 evolution, carbon uptake).

During the light reactions of photosynthesis, solar energy is transformed into chemical energy. During the linear electron transport (LET) through the photosystems, carriers of energy and reductive power (ATP and NADPH) are produced in a 1:1 ratio. A large

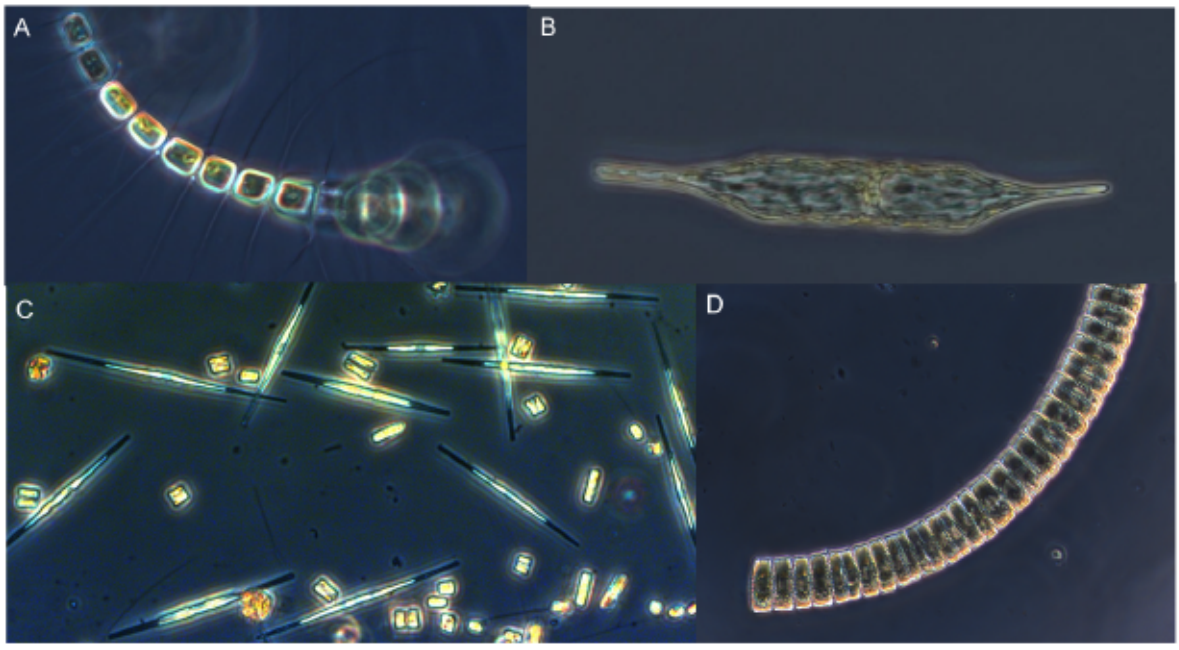

Figure 2.6: - Light microscopic pictures of different diatom species from the SO: *Chaetoceros debilis* (A; C. Hoppe), *Rhizosolenia* sp. (B; C. Hoppe), mixed community dominated by *Pseudo-nitzschia turgiduloides* and *Fragilariospsis cylindrus* (C; S. Trimborn), and *Fragilariopsis kergulensis*(D; C. Hoppe).

proportion of these carriers is used for the transformation of inorganic to organic carbon in the dark reactions of the Calvin cycle (Raven et al. 2005):

$$3CO_2 + 6NADPH + 9ATP + 5H_2O \rightarrow C_3H_7O_6P + 6NADP^+ + 9ADP + 8P_i + 3H^+ \quad (2.5)$$

As the Calvin cycle consumes NADPH and ATP in a 2:3 ratio, ATP also needs to be generated from other sources than the LET. One important additional source of ATP is cyclic electron transport within the photosynthetic apparatus (Asada 2000, Raven et al. 2005). Such alternative electron pathways are also used to overcome varying demands of NADPH and ATP as they may be imposed by different environmental stressors (Prasil et al. 1996, Asada 1999, Wagner et al. 2006, Behrenfeld & Milligan 2013). During the dark reactions of photosynthesis, the carboxylation is catalysed by the enzyme Ribulose-1,5-bisphosphate carboxylase/oxygenase (RubisCO). RubisCO has a poor affinity to its substrate CO_2, with a higher K_M (20-70 μmol L^{-1}) than the current concentrations of dissolved CO_2 in seawater (8-20 μmol L^{-1}; Badger et al. 1998). To overcome substrate-limitation of RubisCO, phytoplankton employ so-called carbon concentrating mechanisms (CCMs) that increase the concentration of CO_2 at the enzyme's catalytic site, and also act against CO_2 leakage out of the cells (Raven et al. 2008, Reinfelder 2011).

Even though the largest share of ATP and NADPH is needed for the fixation of carbon, a substantial part is consumed in other processes such as the uptake and assimilation of nutrients as well as the performance of the CCM. Changes in light harvesting need to be

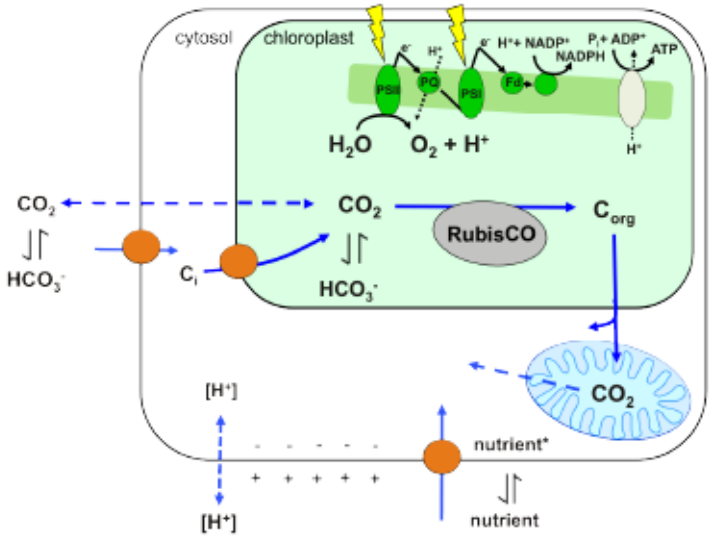

Figure 2.7: - Simplified illustration of the physiological key processes determining biomass build-up by phytoplankton cells. Processes include light and dark reactions of photosynthesis, carbon concentration mechanisms, mitochondrial respiration, nutrient uptake and assimilation, pH homeostasis and maintenance of proton gradients.

balanced by the sum of all downstream metabolic processes. The short-term evolution of O_2 and production of photosynthates (seconds to hours), however, does not directly translate into biomass build-up or growth on longer time scales (hours to days). In between these very different levels of observations, a number of energy consuming processes (e.g. protein biosynthesis, cell division, production of storage compounds) as well as complex cascades of sensing, signalling and regulation take place (Wilson et al. 2006, Behrenfeld et al. 2008). The investigation of processes on the subcellular level helps to thoroughly understand why certain responses are observed on the cellular level, and how they could be altered by differential environmental forcing.

2.2.3 Ocean Acidification effects on phytoplankton

In view of the increased uptake of anthropogenic carbon by the oceans, also the limitation of photosynthesis by its substrate CO_2 has gained increasing attention in the past two decades (Riebesell et al. 1993, Badger et al. 1998, Rost et al. 2003). Already in some early work, a potential for 'CO_2 fertilisation' of marine primary production was proposed (Riebesell et al. 1993). It was shown that an increase in seawater concentrations of dissolved CO_2, i.e. *Ocean Carbonation*, could directly increase the carboxylation reaction of RubisCO or reduce the costs of carbon acquisition (e.g. Burkhardt et al. 2001, Rost et al. 2003, Trimborn et al. 2009). For instance, cyanobacteria were shown to reduce their investment into CCMs under OA and thereby save significant amounts of energy, which then could be allocated to other processes (Kranz et al. 2009, Kranz et al. 2010). In fact, photosynthesis and growth rates of many investigated diatom and cyanobacteria species were found to be enhanced under pCO_2 levels expected for the end of this century (e.g. Riebesell et al. 1993, Rost et al. 2006, Burkhardt et al. 1999, Levitan et al. 2007, Wu et al. 2010, Kranz et al. 2010). Furthermore, species-specific differences in carbon acquisition are likely to affect the competitive success of species. OA therefore has the potential to affect overall productivity as well as composition of natural phytoplankton assemblages (Tortell 2000, Beardall & Giordano 2002), as seen in the Equatorial Pacific and the Southern Ocean (Tortell et al. 2002, Tortell et al. 2008a). For the intensively studied group of coccolithophores, however, contradictory results on growth and photosynthesis under OA have been published (e.g. Riebesell et al. 2000, Rost et al. 2002, Sciandra et al. 2003, Iglesias-Rodriguez et al. 2008, Langer et al. 2009, Hoppe et al. 2011). Similar to other calcifying organisms, also calcification in coccolithophores has been shown to be particularly sensitive to increased pCO_2 levels, i.e. the majority of the studies showed declining calcification rates and PIC:POC ratios (e.g. Riebesell et al. 2000, Langer et al. 2006, Langer et al. 2009, Hoppe et al. 2011). The decline in calcification is most likely

caused by another aspect of carbonate chemistry perturbation, namely the decline in pH (i.e. *Ocean Acidification* in its literal sense; Rost & Riebesell 2004).

2.2.4 Beyond Ocean Acidification research – Multiple stressors

Most OA experiments have examined CO_2 effects alone, even though this phenomenon does not occur in isolation. Other environmental parameters such as temperature, nutrient input and light availability are concomitantly changing (Rost et al. 2008, Steinacher et al. 2010; Figure 2.8). Multiple drivers and stressors will influence the effects of OA on phytoplankton, both directly and indirectly (Rost et al. 2008, Boyd et al. 2010). The effects of these single environmental drivers often do not simply add up but interact in more complex ways, i.e. they antagonistically diminish or synergistically amplify the effects of each other (Folt et al. 1999, Saito et al. 2008). For example, increasing temperature and pCO_2 have been shown to synergistically enhance photosynthesis of a coccolithophore (Feng et al. 2008) and to differentially alter species composition of natural phytoplankton communities (Hare et al. 2007). Furthermore, OA effects are often more pronounced under low compared to high light (Kranz et al. 2010), hinting towards the importance of energization for the manifestation of OA effects. An assessment of multiple drivers and stressors controlling primary production is most essential for those regions that are pivotal for global biogeochemical cycles.

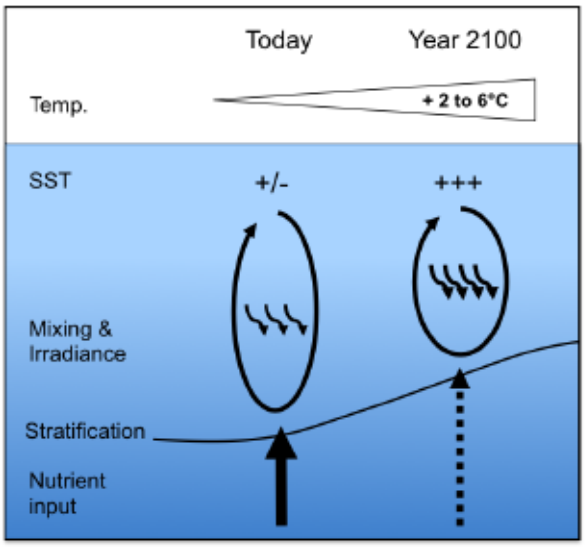

Figure 2.8: - Simplified illustration of the projected impact of increased surface temperatures on seawater stratification, MLD, light intensities and nutrient input until the end of the century. Modified after Rost & Riebesell (2004).

2.3 The Southern Ocean

2.3.1 Overturning circulation and ocean carbon storage

The Southern Ocean (SO) is one of the regions that most strongly contribute to the sequestration of anthropogenic carbon (Gruber et al. 2009). It extends from the Southern Subtropical front (approx. 40°S) to the Antarctic continent. It contains the largest current of the world's oceans, the Antarctic Circumpolar Current (ACC), which transports water around the Antarctic continent at a rate of about 150 Sverdrup (150×10^6 m^3 s^{-1}; Rintoul & Sokolov 2001). The SO is a central connection between the Atlantic, Pacific and Indian Ocean basins, as well as between the surface and deep waters in the global overturning circulation (Figure 2.9; Macdonald & Wunsch 1996, Schmitz et al. 1996). The latter connection is mediated through wind-induced upwelling of southwards-flowing deep water masses towards the SO's surface (Marshall & Speer 2012). Subsequent cooling leads to the formation of bottom water along the Antarctic continent and intermediate water north of the ACC, removing carbon from the oceans surface by the solubility pump and storing it on timescales of decades to hundreds of years (Broeker & Peng 1992; Figure 2.5). At the same time, the overturning circulation also leads to the upwelling of 'old' DIC- and nutrient-rich water masses.

Over geological timescales, changes in the biological and physical carbon pumps as

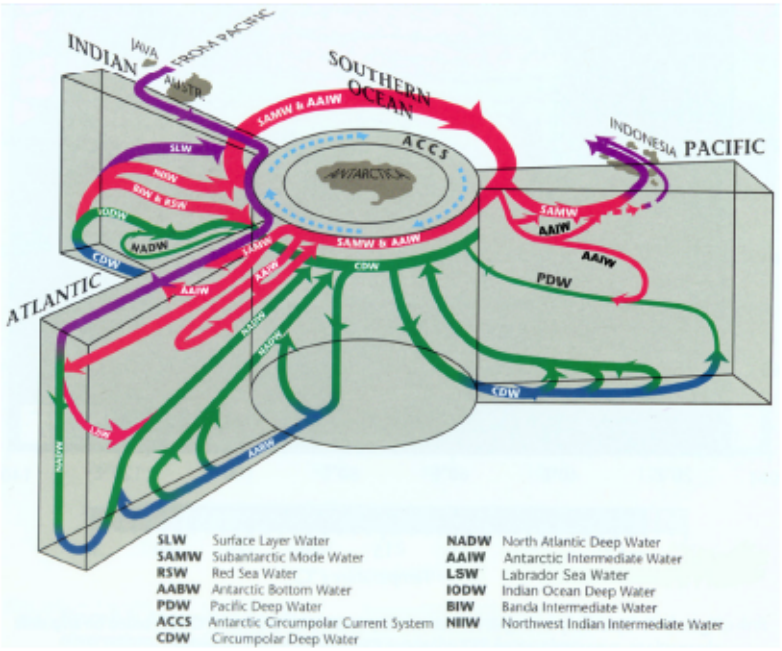

Figure 2.9: - Simplified illustration of the role of the Southern Ocean for the global ocean circulation system and the pathways of the different water masses. Adopted from Schmitz et al. (1996).

well as the changes in ice coverage and its effect on stemming CO_2 efflux to the atmosphere have drastically influenced global climate and are held at least partly responsible for the glacial-interglacial dynamics (Sigman et al. 2010).

Today, the SO contributes 20-40% to the oceanic uptake of anthropogenic CO_2, a large fraction of which is mediated by phytoplankton primary and export production (Takahashi et al. 2002, Sabine et al. 2004, Khatiwala et al. 2009, Gruber et al. 2009). The future strength of carbon sequestration in the SO is under debate: With respect to the solubility pump, some model estimates predict reduced CO_2 sequestration due to changes in wind patterns (LeQuéré et al. 2007), while other models forecast a unaltered or even strengthened CO_2 sink caused by the increased pCO_2 gradient between atmosphere and surface ocean (Böning et al. 2008, LeQuéré et al. 2008, Zickfeld et al. 2008). Furthermore, also the future fate of the biological carbon pumps themselves is uncertain (Rost et al. 2008). It is clear, however, that due to the large proportion of unused nitrate and phosphate in the surface waters, primary as well as export production in the SO are currently far below their potential (Falkowski et al. 1998).

2.3.2 The world's largest high-nutrient low-chlorophyll region

The fact that the SO acts as a net source of CO_2 for the atmosphere, is partly due to the inability of the phytoplankton to transform the carbon and nutrients into biomass (Sigman et al. 2010). This incomplete exploitation of the SO's potential for new and export production, has been called the *Antarctic paradox* (Gran 1931). This term describes the fact that SO standing stocks and productivity of phytoplankton are quite low despite high insolation rates in summer and non-limiting concentrations of nitrate, phosphate and silicate in most parts of the open SO (Gran 1931, Nelson et al. 1989). These characteristics are nicely summarized by the term *high-nutrient low-chlorophyll* (HNLC; de Baar et al. 1994). The apparent mismatch between potential and actual productivity was first theoretically, then experimentally attributed to the limiting concentrations of trace metals in SO surface waters, especially with respect to iron (Hart 1934, Martin 1990, Martin et al. 1990).

Iron (Fe) is the fourth most abundant element in the Earth's crust (Wedepohl 1995). In today's oceans, however, it is often limiting phytoplankton growth because its solubility depends on the redox status: While reduced iron (ferrous Fe_{II}) is highly soluble in seawater, the oxidised (ferric Fe_{III}) form is nearly insoluble (Cooper 1937). When photosynthetic organisms evolved, the anoxic oceans contained high concentrations of dissolved iron (approx. 25 mM; Holland 1984). Due to the oxygenation of oceans by photosynthesis, iron got progressively oxidised. Today, its concentrations rarely exceed the nanomolar range (Johnson et al. 1997). Besides the difficulties of measuring iron in these low concentrations, a thorough

understanding of iron biogeochemistry is hindered by the extremely complex and highly dynamic interplay between iron chemistry and biology (Ye et al. 2009, Hassler et al. 2011; Figure 2.10). The distribution of dissolved iron reflects a large range of processes such as input from various sources, chemical and physical speciation, organic complexation, biological uptake, particle scavenging, as well as recycling, export and remineralization (Johnson et al. 1997, Boyd & Ellwood 2010). In the SO, iron sources include resuspension of coastal and shallow sediments, dust deposition, melting sea-ice and icebergs, hydrothermal activity, island wakes, vertical diffusive flux, and the interaction between the bathymetry and currents (Boyd & Ellwood 2010). Surface concentrations of dissolved iron in that region range from 0.03 to 0.65 nM (on average 0.16 nM; Boye et al. 2001, Boye et al. 2010).

Owing to its central role in cellular redox reactions and the consequences for biosynthesis, iron limitation leads to diminished biomass build-up by phytoplankton (Geider & LaRoche 1994, Hutchins & Bruland 1998, Raven et al. 1999). Regarding photophysiology, for example, iron limitation causes strong changes in the photosynthetic capacities due to altered architecture of the photosynthetic apparatus, interrupted electron transport chains, and lowered photosynthetic energy transfer efficiencies as well as maximum chlorophyll *a*-specific rates of photosynthesis (Greene et al. 1991, McKay et al. 1999). As iron is the electron carrier in nitrate and nitrite reductases, also nitrate assimilation is impaired under iron limitation. Under these conditions, the usage of recycled nitrogen sources such as ammonium or urea is preferred (Brzezinski et al. 2003). For iron-limited phytoplankton

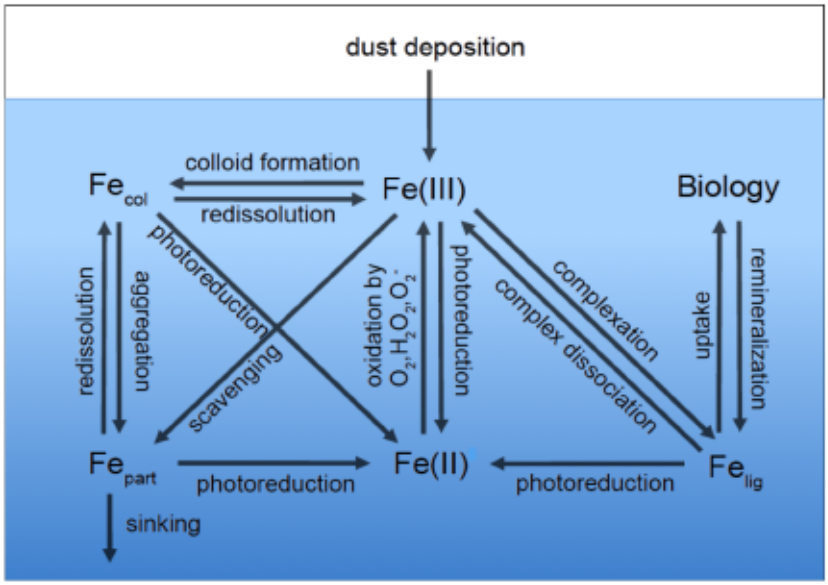

Figure 2.10: - Simplified illustration of the seawater iron chemistry including dissolved ferric (Fe_{III}) and ferrous (Fe_{II}) redox forms as well as iron bound to colloids (Fe_{col}), particles (Fe_{part}) and ligands (Fe_{lig}). Modified after Ye et al. (2009).

in the SO, the uptake of ammonium can therefore represent a large fraction of the nitrogen uptake, even though ammonium concentrations are usually particularly low (Goeyens et al. 1995, Brezezinski et al. 2003).

Next to iron, also light limitation has been identified as a key factor controlling the growth of SO phytoplankton (Mitchell et al. 1991, Boyd 2002). Strong seasonality leads to high annual variability in day length, solar angle, winds, ice cover and water-column structure and thus a high variability in the integrated light that cells encounter in the water column (Arrigo et al. 1998). While photosynthesis is light limited most parts of the year (Sakshaug & Slagstad 1991, Arrigo et al. 1998), high irradiance levels can lead to photoinhibtion in summer (Alderkamp et al. 2010). In addition, the deep MLD of the open SO, which regularly exceeds 100 m even in summer, and the movement of phytoplankton cells within the water column on time scales of 0.01-0.03 m s^{-1} lead to rapid changes in the encountered light regime. As phytoplankton cells can experience shifts between complete darkness and irradiances exceeding 2000 μmol photons m^{-2} s^{-1} within a few hours, they need efficient photoacclimation strategies to cope with a wide range of irradiance levels (Denman & Gargett 1983, MacIntyre et al. 2000, Dong et al. 2008). Organisms living in such dynamic light environments have to compromise between investing in light-harvesting efficiency and photoprotection (van de Poll et al. 2007). Besides efficient photosynthetic machinery, phytoplankton therefore also developed diverse photoprotective strategies that allow them to cope with changes in light intensities on different timescales (Niyogi 1999).

In the SO, light stress and iron limitation often occur simultaneously and also interact on the physiological level (Sunda & Huntsman 1997, Timmermann et al. 2001). As iron limitation impairs electron transport and photoprotective mechanisms, it will strongly limit cells abilities to acclimate to both low (Galbraith et al. 2010) and high light (Strzepek & Harrison 2004). In addition to light and iron availability, also silicon (Si) limitation and grazing pressure are regularly identified as controlling factors for diatoms-dominated blooms in the SO, even though these do not seem to determine the initiation but rather the termination of blooms (Priddle et al. 1992, Banse 1996, Dubischar & Bathmann 1997, Atkinson et al. 2001, Nelson et al. 2001).

Despite these strong bottom-up as well as top-town controls on phytoplankton, large-scale phytoplankton blooms with up to 35 mg Chlorophyll *a* m^{-3} occur along the Antarctic continent, the marginal ice zone, as well as near islands and along the frontal zones (Park et al. 2010; Figure 2.11). SO phytoplankton blooms are mostly dominated by diatoms (Tréguer et al. 1995, Smetacek 1999) and, to a lesser degree, by the prymnesiophyte *Phaeocystis antarctica* (Arrigo et al. 1999). The dominance of diatoms translates in significant export of organic matter to depth (Wefer & Fischer 1991, Schlitzer 2002) and biogenic Si-rich sediments

(Bareille et al. 1991). The timing and intensity of bloom development, as well as the amount and composition of organic matter transported to depth depend on the species composition of the phytoplankton (Smetacek 1999, Abelmann et al. 2006, Sachs et al. 2009). The success of the different species in the phytoplankton assemblages, in turn, is determined by their ability to cope with the conditions in their environment.

2.3.3 Southern Ocean primary production under climate change

Due to the high CO_2 solubility of seawater at cold temperatures as well as the global ocean circulation patterns, the SO naturally has lower pH compared to mid and low latitude waters. Additionally, the projected changes in carbonate chemistry will be most severe in polar oceans (Fabry et al. 2009). Already by the mid 21th century, for example, surface waters of the SO may be under-saturated with respect to aragonite, which is one important form of carbonate found in shells of organisms (Orr et al. 2005). This does not only mean that OA may have a larger impact on marine organisms in the SO compared to other parts of the global ocean, but also that this region could serve as the perfect 'miner's canary' for OA research. Therefore, the potential effect of OA as an additional driver for primary production and ecosystem

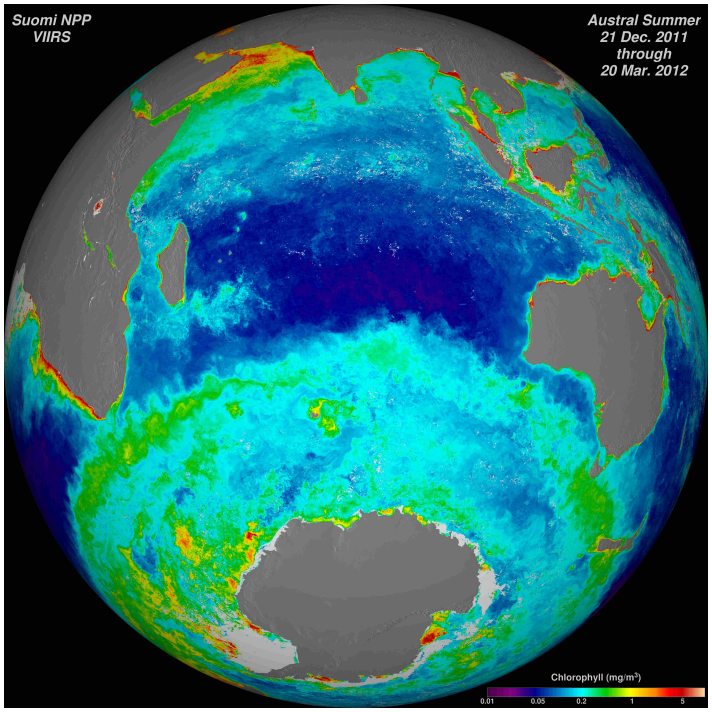

Figure 2.11: - SO summer chlorophyll *a* concentrations from remote sensing. Season-long composite of ocean chlorophyll *a* concentrations derived from visible radiometric measurements made by the VIIRS instrument on Suomi NPP satellite (Norman Kuring, Suomi NPP, NASA, 2012, www.nasa.gov).

functioning in the SO has gained increasing attention in recent years. Growth and primary production of single species as well as natural diatom assemblages from the SO have been shown to increase with increasing pCO_2 levels (Riebesell et al. 1993, Tortell et al. 2008b). In addition, also the competitive success of the dominant species was shown to be strongly altered under OA (Tortell et al. 2008a, Feng et al. 2010). SO phytoplankton has been shown to posses efficient CCMs that prevent CO_2 limitation under current conditions (Cassar et al. 2004, Tortell et al. 2008a), but species could benefit indirectly from increased pCO_2 through lowered metabolic costs of carbon acquisition.

As everywhere else, not only carbonate chemistry but also other environmental factors are subject to change. For instance, heat uptake may change wind patterns and surface ocean stratification, which has been shown to be a key determinant for SO spring bloom development (Banse 1996, Bathmann et al. 1997, Abbott et al. 2000, Steinacher et al. 2010). Changes in stratification may also influence upwelling of iron (Landry et al. 2002), the other main limiting factor of phytoplankton growth in the SO. The combined effects of OA and other important environmental variables on SO phytoplankton, however, are still largely unknown.

2.4 Aims of this thesis

While some understanding about OA impacts on SO phytoplankton was gained in recent years (Tortell et al. 2008a, 2008b), almost nothing is known about the combined effects of OA and other stressors in this region. The aim of this thesis is therefore to shed light on the interactions between rising pCO_2 levels and key environmental drivers occurring in the SO. For this purpose, different future scenarios were applied to single species or natural phytoplankton communities, measuring responses on the level of primary productivity, growth or species composition as well as underlying physiology such as photochemistry. In addition, this thesis attempts to put the applied stressors in the context of naturally occurring variability and interactive effects between environmental drivers, especially with respect to iron and light.

2.4.1 The carbonate chemistry riddle

Scientists interested in the effects of climate change on marine organisms face the problem that they have to understand and deal with complex marine chemistry in order to perform and interpret CO_2 perturbation experiments. Unfortunately, the uncertainties associated with the pCO_2 treatments of these experiments are often not quantified. When assessing the uncertainties of pCO_2 calculations from perturbation studies, discrepancies between pCO_2 values calculated from different measured parameter pairs (TA & DIC, TA & pH, and DIC & pH) were as high as 30%. *Publication I* presents the calculated discrepancies and their systematic occurrence. As these discrepancies can hamper the comparability and quantitative validity of studies, their implications for the interpretation of OA experiments are discussed.

2.4.2 The modulation of OA effects by iron availability

Because iron is considered one of the most important limiting factors for phytoplankton growth and primary production in the SO, the effects of iron enrichment have gained a lot of attention (e.g. de Baar et al. 2005, Pollard et al. 2009). The aim of *Publication II* was to unravel the potential interactive effects of iron limitation and OA on SO phytoplankton productivity, which remain largely unknown so far. It presents the results of an incubation experiment investigating OA effects on phytoplankton assemblages from the Weddell Sea under both iron-limited and -enriched conditions. In the final phytoplankton assemblages resulting from the different treatments, interactive effects between OA and iron availability were observed with respect to species composition, carbon and iron uptake, POC:Chl *a* and photophysiology.

2.4.3 The modulation of OA effects by dynamic light

Light intensities were shown to modulate OA effects on phytoplankton (Rost et al. 2006, Kranz et al. 2010, Wu et al. 2010) and may further be influenced by dynamic light fields as they prevail in the ocean's mixed layer. The aim of *Publication III* was therefore to investigate combined effects OA and dynamic light, mimicking irradiances occurring under natural mixing regimes of the SO. To do so, the Antarctic diatom *Chaetoceros debilis* was grown under two different pCO_2 (390 & 1000 μatm) and light conditions (constant & dynamic), the latter yielding the same integrated irradiance. The responses were characterised in terms of growth, cellular quotas of POC, PON, BSi and Chl *a* as well as carbon fixation and photophysiology. Opposing trends in OA-responses under constant and dynamic light can be explained by interactions between light harvesting and carbon acquisition.

2.4.4 Controls of primary production in SO phytoplankton blooms

Irrespective of the differences between using phytoplankton strains or natural assemblages, there are shortcomings associated to bottle incubations as they simplify natural conditions. The aim of *Publication IV* was therefore to understand how SO phytoplankton blooms are controlled by environmental key drivers and natural variations therein. To this end, two large-scale phytoplankton blooms in the Antarctic Polar Frontal zone were investigated with respect to phytoplankton standing stocks, primary production, photosynthetic efficiencies and nutrient deficits. Differences between the two blooms were explained by the specific set of conditions with respect to iron, light and grazing.

2.4.5 What have we learned?

In the synthesis chapter, the main findings of this thesis are summarized and discussed on a more general level. Special emphasis is put on the impacts of experimental setup and multiple stressors as well as sampling on different spatial and temporal scales. Finally, overall findings are exploited to make predictions for ecosystem structure and functioning of the future SO.

2.4.6 List of publications and declaration of own contribution

Hoppe C. J. M., Langer G., Rokitta S. D., Wolf-Gladrow D. A., Rost B. (2012): Implications of observed inconsistencies in carbonate chemistry measurements for Ocean Acidification studies. Biogeosciences 9: 2401-2405
The experiments were planned together with the co-authors. I have conducted the experiments, measurements, and data analysis. I wrote the manuscript in cooperation with the co-authors.

Hoppe C. J. M., Hassler C. S., Payne C. D., Tortell P. D., Rost B., Trimborn S. (2013): Iron limitation modulates Ocean Acidification effects on Southern Ocean phytoplankton communities. PlosOne 8: e79890
The experiments and subsequent measurements were conducted together with the co-authors. I have performed most data analysis. The manuscript was written in cooperation with the co-authors.

Hoppe C. J. M., Holtz L.-M., Trimborn S., Rost B.: Contrasting responses of *Chaetoceros debilis* to Ocean Acidification under constant and dynamic light. Under review for *New Phytologist*
The experiments were planned together with the co-authors. I have conducted the experiments, measurements and data analysis. I drafted the manuscript and finalised it in cooperation with the co-authors.

Hoppe, C. J. M., Ossebaar, S., Soppa, M. A., Cheah, W., Klaas, C., Rost, B., Wolf-Gladrow, D., Hoppema, M., Bracher, A., Strass, V., de Baar, H. J. W., and Trimborn, S.: Controls of primary production in two different phytoplankton blooms in the Antarctic Circumpolar Current. To be submitted to *Deep-Sea Research II*
I have conducted the ^{14}C-based primary production measurements and performed all data analysis except those from satellite products. I drafted the manuscript and finalised it in cooperation with the co-authors.

Chapter 3

Publication I

Implications of observed inconsistencies in carbonate chemistry measurements for ocean acidification studies

Biogeosciences, 9, 2401–2405, 2012
www.biogeosciences.net/9/2401/2012/
doi:10.5194/bg-9-2401-2012

Biogeosciences

Implications of observed inconsistencies in carbonate chemistry measurements for ocean acidification studies

C. J. M. Hoppe, G. Langer, S. D. Rokitta, D. A. Wolf-Gladrow, and B. Rost

Alfred Wegener Institute for Polar and Marine Research, 27570 Bremerhaven, Germany

Correspondence to: C. J. M. Hoppe (clara.hoppe@awi.de)

Received: 23 January 2012 – Published in Biogeosciences Discuss.: 14 February 2012
Revised: 9 May 2012 – Accepted: 3 June 2012 – Published: 3 July 2012

Abstract. The growing field of ocean acidification research is concerned with the investigation of organism responses to increasing pCO_2 values. One important approach in this context is culture work using seawater with adjusted CO_2 levels. As aqueous pCO_2 is difficult to measure directly in small-scale experiments, it is generally calculated from two other measured parameters of the carbonate system (often A_T, C_T or pH). Unfortunately, the overall uncertainties of measured and subsequently calculated values are often unknown. Especially under high pCO_2, this can become a severe problem with respect to the interpretation of physiological and ecological data. In the few datasets from ocean acidification research where all three of these parameters were measured, pCO_2 values calculated from A_T and C_T are typically about 30 % lower (i.e. ∼300 μatm at a target pCO_2 of 1000 μatm) than those calculated from A_T and pH or C_T and pH. This study presents and discusses these discrepancies as well as likely consequences for the ocean acidification community. Until this problem is solved, one has to consider that calculated parameters of the carbonate system (e.g. pCO_2, calcite saturation state) may not be comparable between studies, and that this may have important implications for the interpretation of CO_2 perturbation experiments.

1 Introduction

Since the beginning of the Industrial Revolution, CO_2 emissions from the burning of fossil fuels and changes in land use have increased atmospheric CO_2 levels from preindustrial values of 280 ppm to currently 390 ppm (www.esrl.noaa.gov/gmd/ccgg/trends; data by Tans and Keeling, NOAA/ESRL). Values are expected to rise to 750 ppm (IPCC scenario IS92a, IPCC, 2007) or even beyond 1000 ppm by the end of this century (Raupach et al., 2007). In addition to its contribution to the broadly discussed greenhouse effect, about 25 % of anthropogenic CO_2 has been taken up by the ocean (Canadell et al., 2007), causing a shift of the carbonate chemistry towards higher CO_2 concentrations and lower pH (Broecker et al., 1971). This process, commonly referred to as ocean acidification (OA), is already occurring and is expected to intensify in the future (Kleypas et al., 1999; Wolf-Gladrow et al., 1999; Caldeira and Wickett, 2003). Ocean acidification will affect marine biota in many different ways (for reviews see Fabry et al., 2008; Rost et al., 2008).

To shed light on potential responses of organisms and ecosystems, numerous national and international research projects have been initiated (see Doney et al., 2009). An essential part of OA research is based on CO_2 perturbation experiments, which represent the primary tool for studying responses of key species and marine communities to acidification of seawater. Marine biologists working in this field have to deal with several problems associated with this type of experiment: being especially interested in high pCO_2 scenarios, seawater carbonate chemistry needs to be adjusted and kept quasi-constant over the duration of an experiment (in many cases, the carbonate chemistry is not at all controlled after initial adjustment). Also, the correct determination of at least two parameters is necessary to obtain a valid description of the whole carbonate system and hence correctly interpret organism responses.

Aqueous pCO_2 is difficult to measure in small-scale experiments, and also pH has been under debate due to intricacies concerning pH scales and measurement protocols (Dickson, 2010; Liu et al. 2011). Total alkalinity (A_T) and dissolved inorganic carbon (C_T) are usually favoured as

Published by Copernicus Publications on behalf of the European Geosciences Union.

input parameters for carbonate chemistry calculations, because sample preservation and measurements are relatively straightforward. This combination of parameters had also been thought to lead to the most accurate calculations of CO_2 concentrations and carbonate saturation states (Riebesell et al., 2010). Still, there is no agreement of which two parameters are to be measured, and, as a consequence, carbonate system calculations in different studies are often based on different input parameters. As will be shown here, this may severely impair comparability of different datasets.

Even though detailed literature on measurement protocols has been published (Dickson et al., 2007; Gattuso et al., 2010), potential pitfalls and problems with uncertainty estimations remain and, as certified reference materials (CRMs) are only available for current surface ocean conditions, the quality of carbonate chemistry measurements at high pCO_2 levels is often unknown. Uncertainties of estimated pCO_2 values are generally considered to be smaller than 10 % (c.f. Gattuso et al., 2010; Hydes et al., 2010). An examination of the few over-determined datasets assessed in OA laboratories (including data from our own laboratory; reported in the Supplement) reveals up to 30 % discrepancies between estimated pCO_2 levels derived from different input pairs (A_T & C_T; A_T & pH; C_T & pH). This potentially widespread phenomenon has major implications for the comparability and quantitative validity of studies in the OA community. In view of the growing body of OA literature and its impact on public opinion and policy makers (Raven et al., 2005), the identification, quantification and prevention of common errors has to be an issue of high priority.

This publication is based on an earlier manuscript entitled "On CO_2 perturbation experiments: Over-determination of carbonate chemistry reveals inconsistencies" (Hoppe et al. 2010).

2 Results

We present here a comparison of over-determined carbonate chemistry datasets found in the literature together with our own datasets. Only one dataset with more than two parameters of the carbonate system measured in OA-laboratories was found in the list of "EPOCA relevant publications" archived in the PANGEA® database (Nisumaa et al., 2010; http://www.epoca-project.eu/index.php/data.html): Schneider and Erez, (2006); another study was excluded from this analysis because of con icting values between database and manuscript. In addition, the data from Iglesias-Rodriguez et al. (2008), Thomsen et al. (2010) and our own laboratory (Hoppe et al. 2010) are shown. For all datasets, values reported for relevant parameters (e.g. salinity, temperature, pH scale, etc.) and the dissociation constants of carbonic acid of Mehrbach et al. (1973; as refit by Dickson and Millero, 1987) were used to calculate pCO_2 values at 15 °C using the program CO_2sys (Pierrot et al., 2006). As information on nutrient concentrations was lacking in the datasets used, values were based on appropriate literature data (see Supplement for details).

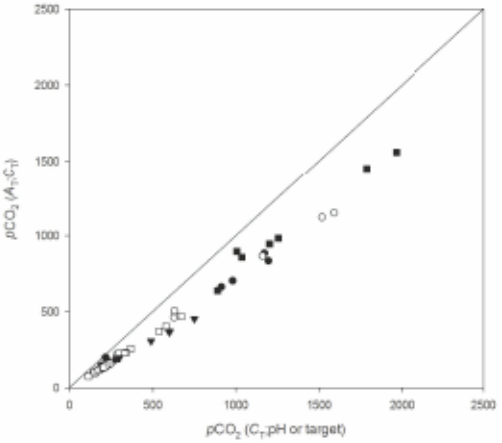

Fig. 1. Calculated pCO_2 (A_T; C_T) versus calculated pCO_2 (C_T; pH) in μatm from this study (closed circles, natural seawater; open circles, artificial seawater), Schneider and Erez, 2006 (open squares), Thomsen et al., 2010 (closed squares) and Iglesias-Rodr´guez et al., 2008 (closed triangles; here pCO_2(target) instead of pCO_2(C_T; pH) is given). pCO_2 values were calculated for the respective salinity, nutrients and carbonate chemistry parameters at 15 °C for all datasets.

These calculations revealed discrepancies in the pCO_2 calculated from different input pairs, which increased systematically with increasing pCO_2 (Fig. 1). The pCO_2 calculated from C_T and A_T was ~ 30 % lower than the pCO_2 calculated from either C_T and pH or from A_T and pH, the latter pairs yielding comparable results (±5 %). The carbonate system of Iglesias-Rodriguez et al. (2008; as shown in the PANGEA® database) was not strictly over-determined. However, if one assumes equilibration of the aerated seawater with the gas mixtures used (280–750 ppm), the deviation of the pCO_2 values (calculated from A_T and C_T) from the target pCO_2 reveals a similar relationship to that observed in the other datasets (Fig. 1). Even though outgassing in C_T samples cannot be completely excluded as a potential source of the discrepancies in this particular study, the consistent pattern among studies argues strongly against this explanation.

With respect to our own dataset, further information is available. Discrepancies of ~30 % were observed irrespective of whether C_T or A_T was manipulated, and in both natural and artificial seawaters (NSW and ASW, respectively; Supplement, Table 2).

3 Discussion

Underestimation of pCO_2 calculated from measured values of A_T and C_T has been described in a number of studies from the marine chemistry community, in which direct measurements over a range of pCO_2 levels (approx. 200–1800 μatm) were compared to calculations from A_T and C_T (Lee et al., 1996, 2000; Wanninkhof et al., 1999; Luecker et al., 2000; Millero et al., 2002). The magnitude of these deviations is, however, much smaller than found in our study (5–10 %; cf. Fig. 4 in Luecker et al., 2000). The latter datasets and those from the OA community differ in the magnitude of the discrepancies (~5–10 % and ~30 %, respectively). Thus, the phenomenon observed in our study seems to be different from the one documented by marine chemists.

Currently, we do not have an explanation for the discrepancies described here, although a few simple explanations, such as the uncertainties of dissociation constants or uncertainties attributed to A_T, C_T or pH measurements, can be ruled out: Systematic errors in measured A_T (5 μmol kg^{-1}; based on repeated CRM measurements, our own data), C_T (7 μmol kg^{-1}; based on repeated CRM measurements, our own data), pH (0.02; Liu et al., 2011) and in equilibrium constants (0.01 in pK_1^*, 0.02 in pK_2^*; Dickson, 2010) would be much too small to explain the large discrepancies in calculated pCO_2.

The contribution of dissolved organic matter (DOM) to alkalinity has recently gained a lot of attention (Kim and Lee, 2009; Koeve et al., 2010). However, changes in A_T due to DOM cannot cause the discrepancies described here, since the phenomenon was also observed in an experiment in which artificial seawater without any organic compounds or organisms was used (Supplement, Table 2). Furthermore, experiments with nutrient-enriched North Sea seawater (our data), probably DOM-rich water from Kiel Bight (Thomsen et al., 2010) and from the oligotrophic Red Sea (Schneider and Erez, 2006) show essentially identical discrepancies (Fig. 1). Nonetheless, DOM contributions can become a significant source of error in high biomass cultures (Kim and Lee, 2009).

It remains puzzling that these discrepancies are observed in experiments involving both A_T and C_T adjustments, different seawater compositions, as well as in several datasets produced with different equipment and procedures (e.g. coulometric, colourimetric and manometric C_T measurements). The fact that several independent studies carried out within the framework of ocean acidification research show similar discrepancies between calculated pCO_2 values (Fig. 1) suggests a systematic, as opposed to a random, deviation that will hinder a realistic judgement of the quality of datasets.

Regardless of the reasons for its occurrence, this phenomenon will have consequences for ocean acidification research. Firstly, published pCO_2 values may not be comparable if different input parameters were measured and used to calculate pCO_2. Secondly, if calculated pCO_2 values are underestimated by up to 30 %, an organism s respective sensitivity to acidification might be severely overestimated. This is especially important at pCO_2 levels $\geq$750 μatm, which are typically applied for the year 2100 scenario and therefore crucial for all CO_2 perturbation experiments. As an example, one might refer to the responses of four *Emiliania huxleyi* strains to different pCO_2 levels reported by Langer et al. (2009). For strain RCC1256, the authors report strongly decreasing calcification rates above pCO_2 values of 600 μatm (pCO_2 values were derived from A_T and C_T measurements). As the study of Langer et al. (2009) was conducted in the same laboratory as this one, the presence of the described discrepancies can be assumed. If the pCO_2 values from Langer et al. (2009) are indeed ~30 % lower than the ones calculated from A_T and pH (or C_T and pH), our study could suggest that calcification increases until a pCO_2 of 750 μatm and only declines at values above 800 μatm. Predictions for this strain for the often proposed 2100 scenario of 750 μatm would thus differ substantially. The discrepancies in calculated pCO_2 values described here might also explain the differing results reported by Langer et al. (2009) and Hoppe et al. (2011) with respect to the sensitivity of this strain. Thirdly, depending on the input pair chosen, the calculated carbonate ion concentration and hence the calcite and aragonite saturation states might differ significantly. In this study, discrepancies in saturation states were found to be in the range of 15–30 %.

Care must therefore be taken when comparing studies that use different pairs of input parameters or when reporting threshold levels of pCO_2 harmful to an organism. To improve comparability between future studies, it may be useful to agree on a certain pair of input parameters as long as the described discrepancies remain. We suggest, for the time being, that the OA community should use A_T and pH as input parameters when calculating the carbonate chemistry and, whenever possible, measure and report additional parameters. This suggestion does, however, not mean that the resulting pCO_2 values are "correct". Although choosing a particular pair of parameters provides a pragmatic approach to dealing with such discrepancies, it is unsatisfying and – if the choice results in inaccurate calculations of pCO_2 and $[CO_3^{2-}]$ – may lead to inappropriate interpretations of organism responses. Currently, we have neither sufficient understanding of the uncertainties of carbonate chemistry measurements, nor a clear demonstration that it is possible to get thermodynamically consistent data of A_T, C_T, pH and pCO_2 for seawater samples with $pCO_2 > 600$ μatm (A. Dickson personal communication, 2011). Further investigations on source and occurrence of this phenomenon are necessary. Certified reference material with high pCO_2, as well as calculation programs including the propagation of errors, could improve estimations of uncertainties in carbonate chemistry measurements and therewith calculations of pCO_2 values. It should become common practise to provide and defend

estimates of uncertainty. A large-scale inter-comparison of the quality of carbonate chemistry measurements between different laboratories (from the OA but also from the marine chemistry community) would help revealing whether the phenomenon described here is indeed widespread.

Supplementary material related to this article is available online at: http://www.biogeosciences.net/9/2401/2012/bg-9-2401-2012-supplement.zip.

Acknowledgements. This work was supported by the European Research Council under the European Community s Seventh Framework Programme (FP7/2007-2013)/ ERC grant agreement No. 205150 and 2010-NEWLOG ADG-267931 HE). It also contributes to EPOCA under the grant agreement No. 211284, to MedSeA under grant agreement No. 265103 and to the BIOACID program (FKZ 03F0608). We thank A. Dickson who helped to improve this manuscript substantially. Also, we would like to thank T. Tyrrell for his helpful review as well as comments on an earlier version of this manuscript.

Edited by: J.-P. Gattuso

References

Broecker, W. S., Li, Y. H., and Peng, T. H.: Carbon Dioxide – Man s Unseen Artifact, in: Impingement of Man on the Ocean, edited by: Hood, D. W., Wiley, New York, USA, 287–324, 1971.

Caldeira, K. and Wickett, M. E.: Oceanography: Anthropogenic carbon and ocean pH, Nature, 425, p. 365, 2003.

Canadell, J. G., C. Le Quere, C., Raupach, M. R., Field, C. B., Buitenhuis, E. T., Ciais, P., Conway, T. J., Gillett, N. P., Houghton, R. A. and Marland, G.: Contributions to accelerating atmospheric CO(2) growth from economic activity, carbon intensity, and efficiency of natural sinks, P. Natl. Acad. Sci. USA, 104, 18866–18870, 2007.

Dickson, A. G.: The carbon dioxide system in sea water: equilibrium chemistry and measurements, in: Guide for Best Practices in Ocean Acidification Research and Data Reporting, edited by: Riebesell U., Fabry V. J., Hansson L. and Gattuso J.-P., Office for Official Publications of the European Union, Luxembourg, 2010.

Dickson, A. G. and Millero F. J.: A comparison of the equilibrium constants for the dissociation of carbonic acid in seawater media, Deep-Sea Res., 34, 1733–1743, 1987.

Dickson, A. G., Sabine, C. L., and Christian, J. R. (Eds.): Guide to best practices for ocean CO_2 measurements, PICES Special Publication, 3, Sidney, Canada, 2007.

Doney, S. C., Balch, W. M. Fabry, V. J., and Feely, R. A.: Ocean Acidification: A Critical Emerging Problem for the Ocean Sciences, Oceanography, 22, 16–25, 2009.

Fabry, V. J., Seibel, B. A., Feely, R. A., and Orr, J. C.: Impacts of ocean acidification on marine fauna and ecosystem processes, ICES J. Mar. Sci., 65, 414–432, 2008.

Gattuso, J.-P., Lee, K., Rost, B., and Schulz, K.: Approaches and tools to manipulate the carbonate chemistry, in: Guide for Best Practices in Ocean Acidification Research and Data Reporting, edited by: Riebesell, U., Fabry, V. J., Hansson, L., and Gattuso, J.-P., Office for Official Publications of the European Union, Luxembourg, 2010.

Hoppe, C. J. M., Langer, G., Rokitta, S. D., Wolf-Gladrow, D. A., and Rost, B.: On CO_2 pertubation experiments: over-determination of carbonate chemistry reveals inconsistencies, Biogeosciences Discuss., 7, 1707–1726, doi:10.5194/bgd-7-1707-2010, 2010.

Hoppe, C. J. M., Langer, G., and Rost, B.: *Emiliania huxleyi* shows identical responses to elevated pCO_2 in TA and DIC manipulations, J. Exp. Mar. Biol. Ecol., 406, 54–62, 2011.

Hydes, D. J., Loucaides, S., and Tyrrell, T.: Report on a desk study to identify likely sources of error in the measurements of carbonate system parameters and related calculations, Supplement to DEFRA contract ME4133 "DEFRApH monitoring project. National Oceanography Centre, Southampton Research and Consultancy Report, No.x, 54 pp., 2010.

Iglesias-Rodriguez, M. D., Buitenhuis, E. T., Raven, J. A., Schofield, O. M., Poulton, A. J., Gibbs, S., Halloran, P. R., and Baar, H. J. W. d.: Phytoplankton Calcification in a High-CO_2 world, Science, 322, 336–340, 2008.

IPPC: Climate Change 2007: Synthesis Report, Contribution of Working Groups I, II and III to the Fourth Assessment Report of the Intergovernmental Panel on Climate Change (Core Writing Team Pachauri, R. K. and Reisinger, A. (Eds.)) IPCC, Geneva, Switzerland, 2007.

Kim, H.-C. and Lee, K.: Significant contribution of dissolved organic matter to seawater alkalinity, Geophys. Res. Lett., 36, L20603, 5 pp., 2009.

Kleypas, J. A., Buddemeier, R. W., Archer, D. E., Gattuso, J.-P., Langdon, C., and Opdyke, B. N.: Geochemical consequences of increased atmospheric carbon dioxide on coral reefs, Science, 284, 118–120, 1999.

Koeve, W., Kim, H.-C., Lee, K., and Oschlies, A.: Potential impact of DOC accumulation on fCO_2 and carbonate ion computations in ocean acidification experiments, Biogeosciences Discuss., 8, 3797–3827, doi:10.5194/bgd-8-3797-2011, 2011.

Langer, G., Nehrke, G., Probert, I., Ly, J., and Ziveri, P.: Strain-specific responses of *Emiliania huxleyi* to changing seawater carbonate chemistry, Biogeosciences, 6, 2637–2646, 2009, http://www.biogeosciences.net/6/2637/2009/.

Lee, K., Millero, F. J., and Campbell, D. M.: The reliability of the thermodynamic constants for the dissociation of carbonic acid in seawater, Mar. Chem., 55, 233–245, 1996.

Lee, K., Millero, F. J., Byrne, R. H., Feely, R. A., and Wanninkhof, R.: The recommended dissociation constants for carbonic acid in sea water, Geophys. Res. Lett., 27, 229–232, 2000.

Liu, X., Patsavas, M. C., and Byrne, R. H.: Purification and Characterization of meta-Cresol Purple for Spectrophotometric Seawater pH Measurements, Environ. Sci. Technol., 45, 4862–4868, 2011.

Lueker, T. J., Dickson, A. G., and Keeling, C. D.: Ocean pCO_2 calculated from dissolved inorganic carbon, alkalinity, and equations for K_1 and K_2: validation based on laboratory measurements of CO_2 in gas and seawater at equilibrium, Mar. Chem., 70, 105–119, 2000.

Mackey, K. R., Rivlin, T., Grossman, A. R., Post, A. F., and Paytan, A.: Picophytoplankton responses to changing nutrient and light regimes during a bloom, Mar. Biol., 158, 1531–1546, 2009.

Mehrbach, C., Culberson, C. H., Hawley, J. E., and Pytkowicz, R. M.: Measurement of the apparent dissociation constants of carbonic acid in seawater at atmospheric pressure, Limnol. Oceanogr., 18, 897–907, 1973.

Millero, F. J., Pierrot, D., Lee, K., Wanninkhof, R., Feely, R., Sabine, C. L., Key, R. M., and Takahashi, T.: Dissociation constants for carbonic acid determined from field measurements, Deep-Sea Res., 49, 1705–1723, 2002.

Pierrot, D. E., Lewis, E., and Wallace, D. W. R.: MS Exel Program Developed for CO_2 System Calculations, ORNL/CDIAC-105aCarbon Dioxide Information Analysis Centre, Oak Ridge National Laboratory, US Department of Energy, 2006.

Raupach, M. R., Marland, G., Ciais, P., Le Quéré, C., Canadell, J. G., Klepper, G., and Field, C. B.: Global and regional drivers of accelerating CO_2 emissions, Proc. Natl. Acad. Sci. USA, 104, 10288–10293, 2007.

Raven, J. A., Caldeira, K., Elderfield, H., Hoegh-Guldberg, O., Liss, P., Riebesell, U., Shepherd, J., Turley, C., and Watson, A.: Ocean acidification due to increasing atmospheric carbon dioxide, The Royal Society, Cardiff, UK, 2005.

Riebesell U., Fabry V. J., Hansson L., and Gattuso J.-P. (Eds.): Guide for Best Practices in Ocean Acidification Research and Data Reporting, Office for Official Publications of the European Union, Luxembourg, 2010.

Rost, B., Zondervan, I., and Wolf-Gladrow, D. A.: Sensitivity of phytoplankton to future changes in ocean carbonate chemistry: current knowledge, contradictions and research directions, Mar. Ecol. Prog. Ser., 373, 227–237, 2008.

Schneider, K. and Erez, J.: The effect of carbonate chemistry on calcification and photosynthesis in the hermatypic coral *Acropora eurystoma*, Limnol. Oceanogr., 51, 1284–1293, 2006.

Thomsen, J., Gutowska, M. A., Saphörster, J., Heinemann, A., Trübenbach, K., Fietzke, J., Hiebenthal, C., Eisenhauer, A., Körtzinger, A., Wahl, M., and Melzner, F.: Calcifying invertebrates succeed in a naturally CO_2 enriched coastal habitat but are threatened by high levels of future acidification, Biogeosciences Discuss., 7, 5119–5156, doi:10.5194/bgd-7-5119-2010, 2010.

Wanninkhof, R., Lewis, E., Feely, R. A., and Millero, F. J.: The optimal carbonate dissociation constants for determining surface water pCO_2 from alkalinity and total inorganic carbon, Mar. Chem., 65, 291–301, 1999.

Wolf-Gladrow, D. A., Riebesell, U., Burkhardt, S., and Bijma, J.: Direct effects of CO_2 on growth and isotopic composition of marine plankton, Tellus, 51, 461–476, 1999.

Chapter 4

Publication II

Iron limitation modulates Ocean Acidification effects on Southern Ocean phytoplankton communities

OPEN ACCESS Freely available online

PLOS ONE

Iron Limitation Modulates Ocean Acidification Effects on Southern Ocean Phytoplankton Communities

Clara J. M. Hoppe[1]*, Christel S. Hassler[2¤], Christopher D. Payne[3], Philippe D. Tortell[3], Björn Rost[1], Scarlett Trimborn[1]

1 Alfred Wegener Institute Helmholtz Centre for Polar and Marine Research, Bremerhaven, Germany, **2** University of Technology Sydney, Plant Functional Biology and Climate Chance Cluster, New South Wales, Australia, **3** University of British Columbia, Vancouver, British Columbia, Canada

Abstract

The potential interactive effects of iron (Fe) limitation and Ocean Acidification in the Southern Ocean (SO) are largely unknown. Here we present results of a long-term incubation experiment investigating the combined effects of CO_2 and Fe availability on natural phytoplankton assemblages from the Weddell Sea, Antarctica. Active Chl *a* fluorescence measurements revealed that we successfully cultured phytoplankton under both Fe-depleted and Fe-enriched conditions. Fe treatments had significant effects on photosynthetic efficiency (F_v/F_m; 0.3 for Fe-depleted and 0.5 for Fe-enriched conditions), non-photochemical quenching (NPQ), and relative electron transport rates (rETR). pCO_2 treatments significantly affected NPQ and rETR, but had no effect on F_v/F_m. Under Fe limitation, increased pCO_2 had no influence on C fixation whereas under Fe enrichment, primary production increased with increasing pCO_2 levels. These CO_2-dependent changes in productivity under Fe-enriched conditions were accompanied by a pronounced taxonomic shift from weakly to heavily silicified diatoms (i.e. from *Pseudo-nitzschia* sp. to *Fragilariopsis* sp.). Under Fe-depleted conditions, this functional shift was absent and thinly silicified species dominated all pCO_2 treatments (*Pseudo-nitzschia* sp. and *Synedropsis* sp. for low and high pCO_2, respectively). Our results suggest that Ocean Acidification could increase primary productivity and the abundance of heavily silicified, fast sinking diatoms in Fe-enriched areas, both potentially leading to a stimulation of the biological pump. Over much of the SO, however, Fe limitation could restrict this possible CO_2 fertilization effect.

Citation: Hoppe CJM, Hassler CS, Payne CD, Tortell PD, Rost B, et al. (2013) Iron Limitation Modulates Ocean Acidification Effects on Southern Ocean Phytoplankton Communities. PLoS ONE 8(11): e79890. doi:10.1371/journal.pone.0079890

Editor: Erik V. Thuesen, The Evergreen State College, United States of America

Received June 27, 2013; **Accepted** October 7, 2013; **Published** November 20, 2013

Funding: S.T. was funded by the German Science Foundation (DFG; www.dfg.de), project TR 899/2. B.R. and C.J.M.H. were funded by the European Research Council (ERC; erc.europa.eu) under the European Community's Seventh Framework Programme (FP7/2007-2013), ERC grant agreement no. 205150. C.H. was funded by the Australian Research Council (www.arc.gov.au; DP1092892) and a UTS Chancellor Fellowship (www.uts.edu.au). P.D.T. was funded by an Alexander von Humboldt research fellowship (http://www.humboldt-foundation.de)and grants from the Natural Sciences and Engineering Research Council of Canada (www.nserc-crsng.gc.ca). The funders had no role in study design, data collection and analysis, decision to publish, or preparation of the manuscript.

Competing Interests: The authors have declared that no competing interests exist.

* E-mail: Clara.Hoppe@awi.de

¤ Current address: University of Geneva, Institute F. A. Forel, Versoix, Switzerland

Introduction

The Southern Ocean (SO) exerts a disproportionate control on the global carbon cycle over glacial-interglacial timescales [1,2] and contributes significantly to the oceanic sequestration of anthropogenic CO_2 [3]. Besides abiotic drivers such as ocean circulation and sea-ice cover, biological carbon uptake and drawdown also control the air-sea-flux of CO_2 in the SO [1,2]. These biological processes are mediated by phytoplankton communities, dominated mainly by silicifying diatoms [4].

The surface waters of the SO are rich in major nutrients such as nitrate and phosphate, but in vast areas of this region primary production is limited by low iron (Fe) availability [5]. Both laboratory and *in-situ* fertilisation experiments have demonstrated that the growth of SO phytoplankton is strongly enhanced by the addition of Fe [6,7,8]. As Fe is a key nutrient for biochemical pathways including photosynthesis and nitrate assimilation [9], limiting Fe concentrations lead to decreased photochemical efficiencies and photosynthetic rates [10,11]. One important source of iron in open-ocean waters is the melting of sea-ice, which causes seasonal and localized phytoplankton blooms and strong vertical particle fluxes [12,13]. These factors make the marginal sea-ice zone a biogeochemically important region of the SO [12].

The effects of seawater carbonate chemistry on SO phytoplankton have received increasing attention over recent years. Laboratory studies suggest that Antarctic phytoplankton can be growth-limited by CO_2 supply under present-day CO_2 concentrations [14,15]. Field data from continental shelf waters of the Ross Sea have demonstrated CO_2-dependent changes in primary productivity and phytoplankton assemblages [16,17]. In these prior studies, phytoplankton assemblages were not demonstrably Fe-limited (e.g. high F_v/F_m reported in [17]), making the extrapolation of results to the open SO waters difficult. Recently, pH-dependent shifts in Fe speciation have been reported [18], suggesting a strong potential for ocean acidification (OA) to reduce Fe bioavailability as seen in experiments with Arctic phytoplankton assemblages [19].

Given the Fe-limited status of much of the SO, there is a great need to investigate combined effects of OA and Fe limitation in this region. Here we present results from a CO_2-Fe-incubation experiment (190, 390 and 800 µatm pCO_2 under Fe-enriched and

Fe-depleted conditions) using an open ocean phytoplankton assemblage from the Weddell Sea, an important region for SO primary productivity. The aim of this study was to investigate the interactive effects of OA and Fe availability on species composition, primary production, as well as iron uptake and photophysiology of Fe-limited phytoplankton assemblages.

Materials and Methods

Experimental Setup

A ship-board incubation experiment was designed using a CO_2-Fe-matrix-approach to examine potential interactive effects between CO_2 and Fe availability on SO phytoplankton communities. A natural phytoplankton assemblage from the Weddell Sea (66°50′S, 0°W) was sampled during mid Dec. 2010 on the *RV Polarstern* ANT-XXVII/2 cruise. The permission for field work according to the Antarctic Treaty was issued by the Umweltbundesamt (Germany). Seawater was collected from 30 m depth using a "torpedo fish" towed outside the ship's wake [20]. To eliminate large grazers, we filtered seawater through an acid-cleaned 200 µm mesh. Water containing the natural phytoplankton community was transferred into acid-cleaned 4L polycarbonate bottles and incubated in growth chambers at 3±1°C with a constant daylight irradiance of 40±5 µmol photons m^{-2} s^{-1} (Master TL-D 18W daylight lamps, Philips, adjusted by neutral density screens). The applied irradiance was based on several light measurements in the SO at the sampling depth (data by Mitchell; e.g. DOI: 10.1594/PANGAEA.132802). To provide sufficient time for changes in the phytoplankton assemblages to occur and achieve ecologically relevant information, experiments lasted between 18 and 30 days depending on experimental treatment (18–20 days in case of Fe-enriched and 27–30 days in case of Fe-depleted treatments). In order to prevent significant changes in chemical conditions due to phytoplankton growth, incubations were diluted with 0.2 µm filtered seawater when nitrate concentrations were about 10 µmol kg^{-1}. Dilution water was obtained from the initial sampling location and filtered through acid-cleaned 0.2 µm filter cartridges (AcroPak 1500, PALL). Experiments were run with triplicate treatments of two Fe levels (Fe-enriched and Fe-depleted; see below) and 3 pCO_2 levels (190, 390 and 800 µatm).

Tubing, bubbling systems, reservoir carboys, incubation bottles and other equipment were acid-cleaned prior to the cruise using trace metal-clean techniques: After a 2-day Citranox detergent bath and subsequent rinsing steps with Milli-Q (MQ, Millipore), equipment was kept in acid (5N HCl for polyethylene and 1N HCl for polycarbonate materials) for 7 days, followed by 7 rinses with MQ. Equipment was kept triple-bagged during storage and experiments. Incubation bottles were stored under acidified conditions (addition of 500 µL 10N suprapure quarz destilled HCl, Carl Roth, in 500 mL MQ) and rinsed twice with seawater prior to the start of the experiment.

In order to mimic different pCO_2 conditions, the incubation bottles were continuously sparged with air of different CO_2 partial pressures (190, 390 and 800 µatm) delivered through sterile 0.2 um air-filters (Midisart 2000, Sartorius stedim). Gas mixtures were generated using a gas flow controller (CGM 2000 MCZ Umwelttechnik), in which CO_2-free air (<1 ppmv CO_2; Dominick Hunter) was mixed with pure CO_2 (Air Liquide Deutschland). The CO_2 concentration in the mixed gas was regularly monitored with a non-dispersive infrared analyzer system (LI6252, LI-COR Biosciences) calibrated with CO_2-free air and purchased gas mixtures of 150±10 and 1000±20 ppmv CO_2 (Air Liquide Deutschland).

To promote phytoplankton growth, 1 nM Fe ($FeCl_3$, ICP-MS standard, TraceCERT, Fluka) was added to the Fe-enriched treatments. In the Fe-depleted treatments, 10 nM of the hydroxamate siderophore desferrioxamine B (DFB, Sigma) was added to bind and thereby reduce the bioavailable Fe [21,22]. No additional macronutrients were added to the incubation bottles. Abiotic control bottles, used to assess changes in Fe chemistry, contained filtered seawater (0.2 µm) exposed to each treatment condition over the duration of the experiment.

Chemical parameters

Nutrients were determined colorimetrically on-board with a Technicon TRAACS 800 Auto-analyzer on a daily basis over the course of the experiments, following procedures improved after [23]. Samples for total alkalinity (TA) were 0.6 µm-filtered (glass fibre filters, GF/F, Whatman), fixed with 0.03% $HgCl_2$ and stored in 150 mL borosilicate bottles at 4°C. TA was estimated at the Alfred Wegener Institute (Germany) from duplicate potentiometric titration [24] using a TitroLine alpha plus (Schott Instruments). The calculated TA values were corrected for systematic errors based on measurements of certified reference materials (CRMs provided by Prof. A. Dickson, Scripps, USA; batch #111; reproducibility ±5 µmol kg^{-1}). Dissolved inorganic carbon (DIC) samples were filtered through 0.2 µm cellulose-acetate filters (Sartorius stedim), fixed with 0.03% $HgCl_2$ and stored in 5 mL gas-tight borosilicate bottles at 4°C. Also in the home laboratory, DIC was measured colourimetrically in triplicate with a QuAAtro autoanalyzer (Seal) [25]. The analyser was calibrated with $NaHCO_3$ solutions (with a salinity of 35, achieved by addition of NaCl) with concentrations ranging from 1800 to 2300 µmol DIC kg^{-1}. CRMs were used for corrections of errors in instrument performance (e.g. baseline drift). Seawater pH was measured potentiometrically on the NBS scale (pH_{NBS}; overall uncertainty 0.02 units) with a two-point calibrated glass reference electrode (IOline, Schott Instruments). Values for pH were reported on the pH_{total} scale for better comparability with other datasets. Following suggestions by Hoppe et al. [26], seawater carbonate chemistry (including pCO_2) was calculated based on TA and pH using CO_2SYS [27]. The dissociation constants of carbonic acid of Mehrbach et al. (refit by Dickson and Millero) were used for calculations [28,29]. Dissociation constants for HSO_4 were taken from Dickson [30]. Iron chemistry was analyzed using the competitive ligand exchange adsorptive cathodic stripping voltammetry using the ligand 2-(2-thiazolylazo)-p-cresol (TAC, 10 µmol kg^{-1} [31]). Total dissolved (<0.2 um) Fe concentrations were analyzed following a 45 min UV-photo-oxidation step (acid washed quartz tubes closed with Teflon lids) and concentrations were determined in triplicate using standard additions of a freshly made $FeCl_3$ standard (ICP-MS standard, TraceCERT, Fluka, 1–4 nM).

Biological Parameters

To determine the taxonomic compositions at the end of the experiment, duplicate aliquots of 200 mL unfiltered seawater were preserved with both hexamine-buffered formalin solution (2% final concentration) and Lugols (1% final concentration). Preserved samples were stored at 4°C in the dark until further analysis by inverted light microscopy (Axiovert 200, Zeiss). Additionally, species dominating the final communities were identified using scanning electron microscopy (Philips XL30) according to taxonomic literature [32]. Average biovolume of the dominant species was calculated based on representative cell size measurements [33]. Values were in good agreement with the MAREDAT database [34]. For analysis of particulate organic carbon (POC),

cells were collected onto precombusted GF/F-filters (15 h, 500°C), which were subsequently stored at −20°C and dried for >12 h at 60°C prior to sample analysis. Analysis was performed using an Automated Nitrogen Carbon Analyser mass spectrometer system (ANCA-SL 20-20, SerCon Ltd.). Samples for determination of chlorophyll *a* (Chl *a*) concentration were filtered onto 0.45 µm cellulose acetate filters (Sartorius stedim) and stored at −20°C until analysis onboard. Chl *a* was subsequently extracted in 10 mL 90% acetone (overnight in darkness, at 4°C) and concentrations determined on a fluorometer (10-000 R, Turner Designs), using an acidification step to determine phaeopigments [35].

Physiological assays

Primary production of the final phytoplankton assemblages was determined in 100 mL incubations after addition of a 10 µCi (0.37 MBq) spike of $NaH^{14}CO_3$ (PerkinElmer, 53.1 mCi mmol^{-1}). From the incubations, 0.5 mL aliquots were immediately removed and mixed with 10 mL of scintillation cocktail (Ultima Gold AB, PerkinElmer) to determine the total amount of added $NaH^{14}CO_3$. For blank determination, samples were filtered and acidified immediately after ^{14}C spikes. After 24 h of incubation under acclimation light intensity, samples were filtered onto GF/F-filters, acidified with 6N HCl and left to degas overnight. Filters were then transferred into scintillation vials, to which 10 mL of scintillation cocktail was added. After ≥2 h, the samples were measured on a ship-board liquid scintillation counter (Tri-Carb 2900TR, PerkinElmer), using automatic quench correction and a maximum counting time of 5 minutes.

Maximum Fe uptake capacity of the final phytoplankton assemblages was estimated after 2–4 h dark-acclimation in 500 mL acid-cleaned PC-bottles. In case of the Fe- treatments, cells were gently concentrated by filtration over an HCl-cleaned 2 µm membrane filter (Isopore, Millipore), rinsed and resuspended in 500 mL filtered seawater from the initial sampling location in order to dispose all DFB. From this, 50 mL were taken for Chl *a* measurements. Subsequently, 1 nM of ^{55}Fe (Perkin Elmer, 33.84 mCi mg^{-1} as $FeCl_3$ in 0.5 N HCl) was added to each sample (both Fe- and -enriched). Generally, 2 mL were taken from all samples to determine the initial amount of ^{55}Fe. Subsequently, cells were exposed for at least 24 h to the acclimation light intensity. At the end of the incubation time, the sample was filtered onto GF/F-filters and rinsed 5 times with oxalate solution (gravity filtered, 2 min between rinses) and 3 times with natural seawater [36]. Each filter was then collected in a scintillation vial, amended with 10 mL scintillation cocktail (Ultima Gold A, PerkinElmer) and mixed thoroughly (Vortex). ^{55}Fe counts per minute were estimated for each sample on the ship-board liquid scintillation counter (Tri-Carb 2900TR, PerkinElmer), and converted into disintegrations per minute considering the radioactive decay and custom quench curves. ^{55}Fe uptake was then calculated taking into account the initial ^{55}Fe concentration and the total dissolved Fe concentration (background and added). Fe uptake rates were normalized to POC using Chl *a*:POC ratios from the respective treatments.

Photophysiological parameters were measured using a Fluorescence Induction Relaxation System (FIRe; Satlantic, Canada; 37). Samples were 1 h dark-acclimated prior to measurements to ensure that all photosystem II (PSII) reaction centers were fully oxidized and non-photochemical quenching (NPQ) was relaxed. The duration of the dark acclimation was chosen after testing different time intervals (data not shown). Samples were then exposed to a strong short pulse (Single Turnover Flash, STF), which was applied in order to cumulatively saturate PSII. Afterwards, a long saturating pulse (Multiple Turnover Flash, MTF) was applied in order to fully reduce the PSII and the plastoquinone (PQ) pool. The minimum (F_0) of the STF phase and maximum (F_m) fluorescence of the MTF was used to calculate the apparent maximum quantum yield of photochemistry in PSII (F_v/F_m) according to the equation $(F_m-F_0)/F_m$. This parameter was calculated for all bottles on a regular basis (every 6–7 days). Values of these parameters as well as of the functional absorption cross section of PSII (σ_{PSII} [Å^2 quanta^{-1}]) were derived using the FIRePro software provided by Satlantic [37]. Additional fluorescence measurements were performed under increasing irradiances (21, 41, 66, 88, 110 and 220 µmol photons m^{-2} s^{-1}) provided by an external actinic light source (warm white 350 mA LEDs, ILL3A003, CML Innovative Technologies). After 5 minutes acclimation to the respective light level, the light-acclimated minimum (F_q') and maximum (F_m') fluorescence were estimated. The effective quantum yield of photochemistry in open reaction centers of PSII was derived according to the equation $(F_m'-F_q')/F_m'$ [38]. Relative electron transport rates (rETR) were then calculated as the product of effective quantum yield and applied growth irradiance of 40 µmol photons m^{-2} s^{-1}. Using the Stern-Volmer equation [39], NPQ of Chl *a* fluorescence under growth irradiance was calculated as $F_m/F_q'-1$. NPQ was relaxed (values <0.1) at lowest light levels for all treatments (data not shown). All measurements were conducted at the growth temperature.

Statistics

All data is given as the mean of the replicates ($n=3$) with 1 standard deviation. To test for significant differences between the treatments, Two Way Analyses of Variance (ANOVA) with additional normality tests (Shapiro-Wilk; passed for all data shown) were performed. The significance level was set to 0.05. Statistical analyses were performed with the program SigmaPlot (SysStat Software Inc).

Results

Seawater chemistry

The initial carbonate system (pH: 7.93±0.01; DIC 2210±17 µmol kg^{-1}; TA: 2303±14 µmol kg^{-1}) shifted to experimental treatment levels (average pH of 8.39±0.02, 8.13±0.02, and 7.80±0.03 for the three CO_2 treatments) within the first 2 days of the experiment (Figure 1 A). The semi-continuous dilute-batch approach led to stable seawater carbonate chemistry over the course of the experiment (Figure 1 A). Compared to abiotic controls, drift was <8% and <5% for TA and DIC, respectively (Table 1). Initial seawater nutrient concentrations were 29 µmol kg^{-1} nitrate, 76 µmol kg^{-1} silicate and 2 µmol kg^{-1} phosphate. Over the course of the experiment, concentrations of nitrate never fell below 7 µmol kg^{-1}, while silicate and phosphate concentrations were always above 40 and 0.8 µmol kg^{-1}, respectively. Initial Fe concentration in the water sampled for incubations was 1.12±0.15 nmol kg^{-1}. In 0.2 µm filtered seawater (i.e. abiotic control treatments) enriched with 10 nM DFB, dissolved Fe concentrations remained 1.16±0.08 nmol kg^{-1} until the end of the experiment (Table 1), indicating that the experimental bottles remained free of Fe contamination. Dissolved Fe concentrations decreased in Fe-enriched seawater (1 nM Fe added, Table 1).

Photophysiology

Over the course of the experiment, we observed significant Fe-dependent differences in the apparent maximum quantum yield of PSII reaction centres (F_v/F_m; Figure 1 B; $p<0.001$). Average values of F_v/F_m at the end of the experiment were 0.51±0.04 and

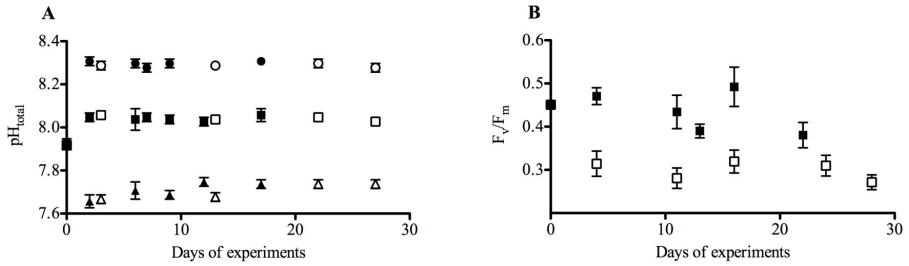

Figure 1. pH and F_v/F_m over the course of the experiment. Experimental conditions over the course of the experiment. A: Development of pH_{total} (n = 3; mean ±1 s.d.) in Fe-enriched (solid circles, 190 µatm CO_2; solid squares, 390 µatm CO_2; solid triangles, 800 µatm CO_2) and Fe-depleted treatments (open circles, 190 µatm CO_2; open squares, 390 µatm CO_2; open triangles, 800 µatm CO_2). B: Development of dark-adapted F_v/F_m (n = 3; mean ±1 s.d.) in Fe-enriched (solid squares) and Fe-depleted treatments (open squares).
doi:10.1371/journal.pone.0079890.g001

0.32±0.03 for Fe-enriched and -depleted treatments, respectively (Table 2). In contrast, the pCO_2 treatments had no effects on F_v/F_m under either of the Fe treatments. Relative electron transfer rates from PSII (rETR) were significantly higher in Fe-enriched treatments, and also showed pCO_2-dependent increases under both Fe-enriched (5.7±0.8 at low and 7.5±0.9 at high pCO_2; $p<0.001$) and Fe-depleted conditions (4.2±0.4 at low and 5.3±0.1 at high pCO_2; $p<0.001$). Significant interactive effects between Fe- and pCO_2-treatments were also observed in photoprotective non-photochemical quenching (NPQ; Table 2; $p<0.001$). Under Fe-limitation, NPQ decreased from 0.22±0.03 at low pCO_2 to 0.11±0.00 at high pCO_2, while under Fe-enriched conditions, NPQ was independent of pCO_2 (0.06±0.01 at all pCO_2 levels; $p<0.001$).

The ratios of Chl *a* to POC of the final phytoplankton assemblages (Table 1) were significantly higher ($p<0.001$) in Fe-enriched (0.023±0.003 at low and 0.017±0.004 at high pCO_2) compared to Fe-depleted treatments (0.012±0.001 at low and 0.010±0.001 at high pCO_2). Chl *a*:POC ratios furthermore decreased significantly with increasing pCO_2 levels ($p = 0.012$), irrespective of the Fe-status.

Fe and C uptake

For all pCO_2 levels, carbon-normalized Fe uptake capacities at the end of the experiment were 10-fold higher in Fe-depleted compared to Fe-enriched treatments (Figure 2; $p<0.001$), but with no significant CO_2 effect. Combining data across pCO_2 treatments, mean Fe uptake capacities were 7.50±3.35 pmol Fe (µmol POC)$^{-1}$ h^{-1} and 0.72±0.38 pmol Fe (µmol POC)$^{-1}$ h^{-1} at low and high Fe, respectively. Under Fe-enriched conditions, we observed a significant CO_2-dependent increase in C-specific primary productivity (Figure 3; $p<0.001$). Primary productivity increased from 4.21±0.44 nmol C (µmol POC)$^{-1}$ h^{-1} at low pCO_2 to 8.15±0.75 nmol C (µmol POC)$^{-1}$ h^{-1} at high pCO_2. In contrast, no CO_2-dependent productivity responses were observed in Fe-depleted treatments, with values of 3.62±0.38 nmol C (µmol POC)$^{-1}$ h^{-1} at low pCO_2 and 3.93±0.16 nmol C (µmol POC)$^{-1}$ h^{-1} at high pCO_2. Thus, there was a significant interactive effect of the CO_2- and Fe-treatments on NPP ($p = 0.023$).

Species composition

We observed pronounced shifts in the diatom-dominated phytoplankton assemblages in association with the CO_2-dependent changes in primary productivity (Figure 4; Table 3). Shifts in species composition did not lead to changes in average cell size in the different assemblages (data not shown). After Fe-enrichment, *Pseudo-nitzschia* cf. *turgiduloides* was the most abundant species under low and intermediate pCO_2 (39±5% and 40±9%, respectively), whereas *Fragilariopsis cylindrus* dominated communities under high pCO_2 levels (72±5%). Furthermore, *Chaetoceros* cf. *simplex* abun-

Table 1. Seawater chemistry.

Treatment		Fe_{diss}		DIC		TA		pH		pCO_2	
		[µmol kg^{-1}]		[µmol kg^{-1}]		[µmol kg^{-1}]		[total]		[µatm]	
Initial seawater	1.12	±0.15	2071		2271		7.93		518		
+Fe	190 µatm CO_2	0.45	±0.07	2002	±11	2208	±36	8.31	±0.01	188	±6
	390 µatm CO_2	0.32	±0.04	2082	±4	2230	±8	8.06	±0.03	369	±30
	800 µatm CO_2	0.21	±0.03	2175	±14	2215	±8	7.74	±0.02	801	±51
−Fe	190 µatm CO_2	1.13	±0.16	2018	±18	2209	±5	8.28	±0.01	204	±5
	390 µatm CO_2	1.25	±0.21	2096	±41	2219	±21	8.03	±0.02	398	±22
	800 µatm CO_2	1.11	±0.09	2155	±41	2241	±52	7.74	±0.01	813	±11

Parameters of the seawater carbonate chemistry were sampled at the beginning ($n = 1$) and the end of the experiment ($n = 3$; mean ±1 s.d.). Total dissolved Fe measurements in abiotic control treatments after 0.2 µm filtration as measured by voltammetry ($n = 2$; mean ± 1 s.d.). The decreased dissolved Fe concentration in the +Fe treatment can be attributed to precipitation/absorption of colloidal iron. pCO_2 was calculated from TA and pH_{total} at 3°C and a salinity of 34 using CO_2SYS [27], using average final nutrient concentrations of 1 and 60 µmol kg^{-1} for phosphate and silicate, respectively.
doi:10.1371/journal.pone.0079890.t001

Table 2. Physiological differences between treatments.

Treatment		Chl a: POC			F_v/F_m			σ_{PSII}			NPQ			rETR		
+Fe	190 µatm CO_2	**0.023**	**±0.003**	**$F_{[Fe]}$ = 59.57**	**0.55**	**±0.02**	**$F_{[Fe]}$ = 162.69**	**270**	**±37.1**	**$F_{[Fe]}$ = 36.89**	**0.06**	**±0.00**	**$F_{[Fe]}$ = 166.34**	**5.72**	**±0.78**	**$F_{[Fe]}$ = 59.03**
	390 µatm CO_2	0.025	±0.005	**$p_{[Fe]}$<0.001**	0.50	±0.03	**$p_{[Fe]}$<0.001**	230	±34.9	**$p_{[Fe]}$<0.001**	0.05	±0.02	**$p_{[Fe]}$<0.001**	5.47	±1.32	**$p_{[Fe]}$<0.001**
	800 µatm CO_2	0.017	±0.004	F_{CO2} = 6.84	0.52	±0.01	F_{CO2} = 0.02	229	±19.5	F_{CO2} = 5.29	0.06	±0.01	F_{CO2} = 0.34	7.5	±0.87	F_{CO2} = 22.75
−Fe	190 µatm CO_2	0.012	±0.001	**p_{CO2} = 0.012**	0.31	±0.02	p_{CO2} = 0.894	345	±21.1	p_{CO2} = 0.136	0.22	±0.03	p_{CO2} = 0.568	4.16	±0.40	**p_{CO2}<0.001**
	390 µatm CO_2	0.013	±0.001		0.33	±0.03		330	±26.1		0.19	±0.02	$F_{[Fe],CO2}$ = 36.07	4.48	±0.34	
	800 µatm CO_2	0.01	±0.001		0.32	±0.02		301	±35.9		0.11	±0.00	**$p_{[Fe],CO2}$<0.001**	5.29	±0.08	

Final Chl a: POC ratios (µg:µg) and photophysiological parameters (apparent maximum quantum yield of PSII F_v/F_m, proportion of non-photochemical quenching, NPQ, functional absorption cross section of PSII (σ_{PSII} [Å^2 quanta^{-1}]), and relative electron transport rates from PSII, rETR) of the final communities grown under different CO_2 and Fe levels (n = 3; mean ±1 s.d.). Fe-depleted (−Fe) and Fe-enriched (+Fe) conditions were achieved by the addition of 10 nmol kg^{-1} DFB and 1 nmol kg^{-1} $FeCl_3$, respectively. Bold *p* values indicate statistically significant differences between treatments ($p<0.05$; 2-way ANOVA).

doi:10.1371/journal.pone.0079890.t002

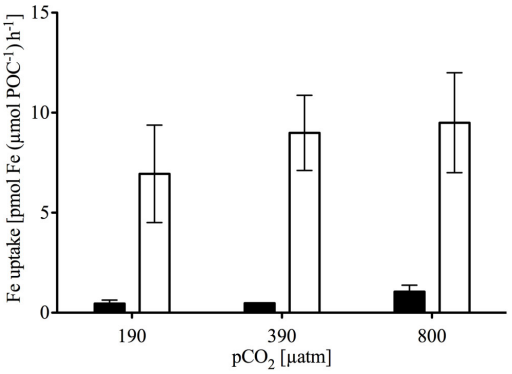

Figure 2. Iron uptake capacities of final phytoplankton communities. Fe uptake capacities [pmol Fe (µmol POC)$^{-1}$ h^{-1}] of Fe-enriched (solid bars) and -depleted (open bars) final phytoplankton communities (n = 3; mean ±1 s.d.) estimated from 24 h incubation with 1 nM ^{55}Fe as a function of pCO_2 [µatm]. Statistical analysis (2-way ANOVA) revealed significant differences between Fe-treatments ($F = 62.217$, $p = <0.001$) but not between CO_2-treatments ($F = 1.205$, $p = 0.349$).

doi:10.1371/journal.pone.0079890.g002

dances increased with rising CO_2 (from 11±0% at low pCO_2 to 17±1% at high pCO_2). Phytoplankton composition changes were also observed under Fe limitation, but the nature of these species shifts differed significantly from those seen under high Fe levels (Figure 4; Table 3). Under Fe-depleted conditions, *Pseudo-nitzschia* cf. *turgiduloides* dominated the low pCO_2 treatment (55±16%), while *Synedropsis* sp. was the most prevalent species under high pCO_2 (78±2%).

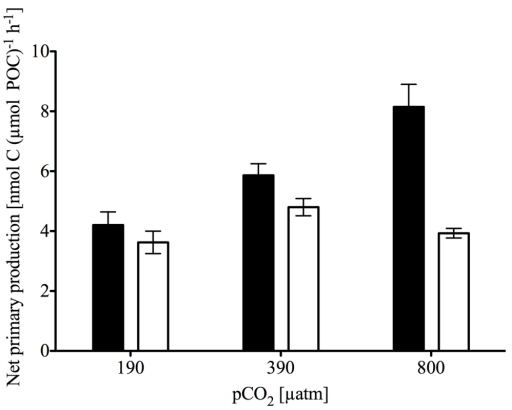

Figure 3. Net primary production of final phytoplankton communities. NPP [nmol C (µmol POC)$^{-1}$ h^{-1}] was estimated from ^{14}C incubations over 24 h as a function of pCO_2 [µatm]. Black and grey bars indicate Fe-enriched (solid bars) and -depleted treatments (open bars), respectively (n = 3; mean ± s.d.). ANOVA analysis revealed significant effects of pCO_2 levels as well as a significant interaction term of [Fe] and pCO_2 levels ($F_{[Fe]} = 0.01$, $p_{[Fe]} = 0.92$; $F_{pCO2} = 15.56$, $p_{pCO2} < 0.001$; $F_{[Fe],pCO2} = 5.85$, $p_{[Fe],pCO2} = 0.023$).

doi:10.1371/journal.pone.0079890.g003

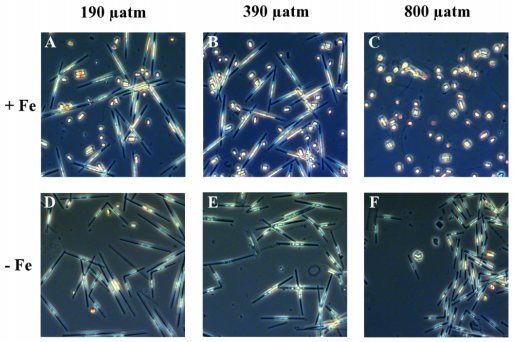

Figure 4. Representative microscopy pictures of species composition of the final communities. A, Fe-enriched 190 µatm (39±5% *Pseudo-nitzschia*, 43±4% *Fragilariopsis*); B, Fe-enriched 390 µatm (40±9% *Pseudo-nitzschia*, 42±12% *Fragilariopsis*); C, Fe-enriched 800 µatm (72±5% *Fragilariopsis*); D, Fe-depleted 190 µatm (55±16% *Pseudo-nitzschia*, 26±20% *Synedropsis*); E, Fe-depleted 390 µatm (51±15% *Pseudo-nitzschia*, 29±16% *Synedropsis*); F, Fe-depleted 800 µatm (78±2% *Synedropsis*).
doi:10.1371/journal.pone.0079890.g004

Discussion

Confirmation of Fe limitation

Dissolved Fe concentrations in Fe-depleted abiotic controls remained at initial concentrations, showing that experimental manipulations and CO_2 bubbling resulted in no significant Fe contamination (Table 1). In Fe-enriched abiotic controls, dissolved Fe concentrations decreased over the course of the experiment. This can be attributed to precipitation and absorption of colloidal iron in the absence of significant concentrations of Fe-binding ligands [40]. Fe limitation of phytoplankton in the DFB treatments was confirmed by significant differences in F_v/F_m between Fe-enriched and -depleted treatments (Table 2; Figure 1 B). F_v/F_m values of Fe-depleted treatments are comparable to those observed in naturally Fe-limited phytoplankton communities [41]. In line with previous findings on SO phytoplankton, also other photophysiological parameters like NPQ and rETR differed significantly between Fe treatments (Table 2, [42,43]). Moreover, the significantly higher Fe uptake capacity in Fe-depleted treatments likely reflects the induction of high-affinity uptake systems and/or the selection of phytoplankton communities with greater Fe affinities [21,22]. All of these observations confirm Fe limitation in the Fe-depleted treatments.

OA response under Fe-enriched conditions

The observed CO_2-dependent increase in primary productivity under Fe-enriched conditions (Figure 3) confirms that CO_2 fixation in SO phytoplankton can be limited by carbon supply under current CO_2 concentrations [14,16]. This hypothesis is further supported by the decrease in Chl *a*:POC ratios and the increase in rETRs with increasing pCO_2 (Table 2). Similarly, Ihnken et al. [44] observed ETR_{max} in Fe-sufficient *Chaetoceros muelleri* to increase with increasing CO_2. These findings suggest that the Calvin cycle, the major sink of photosynthetic energy [9], is the rate-limiting step of photosynthesis under low pCO_2 levels. NPQ was not affected under high pCO_2, Fe-enriched conditions. Under the applied irradiance of 40 µmol photons m^{-2} s^{-1}, however, NPQ values were generally very low (Table 2) suggesting that there is little requirement for dissipation of light. For one of

Table 3. Microscopic cell counts.

Taxonomic group	Initial	+Fe						−Fe					
		190 µatm		390 µatm		800 µatm		190 µatm		390 µatm		800 µatm	
Pseudo-nitzschia cf. *turgiduloides*	5	39	±5	40	±9	3	±3	55	±16	51	±15	<0.5	
Synedropsis sp.	1	1	±1	1	±0	3	±2	26	±20	29	±16	78	±2
Fragilariopsis cylindrus	32	43	±4	42	±12	72	±5	3	±2	2	±1	5	±3
Chaetoceros cf. *simplex*	6	11	±0	10	±2	17	±1	1	±1	3	±2	1	±1
Phaeocystis antarctica	18	1	±0	2	±2	2	±1	7	±2	6	±3	5	±1
unidentified flagellates	9	3	±1	2	±2	3	±3	<0.5		<0.5		3	±1
Choanoflagellates	6	<0.5		1	±1	<0.5		4	±2	6	±3	6	±0
Ceratoneis closterium	1	<0.5		<0.5		<0.5		1	±0	1	±1	1	±0
Dinoflagellates	6	<0.5		<0.5		<0.5		1	±1	<0.5		<0.5	
Pseudo-nitzschia cf. *turgidula*	2	<0.5		<0.5		<0.5		<0.5		<0.5		<0.5	
Fragilariopsis kerguelensis	7	<0.5		<0.5		<0.5		<0.5		<0.5		<0.5	
Thalassiosira sp.	3	<0.5		<0.5		<0.5		<0.5		<0.5		<0.5	
Large *Chaetoceros* sp.	2	<0.5		<0.5		<0.5		<0.5		<0.5		<0.5	
Rhizosolenia sp.	11	-		<0.5		<0.5		<0.5		<0.5		<0.5	
Thalassiothrix sp.	1	-		-		-		<0.5		-		-	
Guinardia sp.	<0.5	-		<0.5		<0.5		-		<0.5		<0.5	
Eucampia sp.	<0.5	<0.5		-		<0.5		-		<0.5		-	
Ciliates	<0.5	-		-		-		<0.5		<0.5		<0.5	
Silicoflagellates	<0.5	-		-		-		-		<0.5		-	

Species composition of the initial community (n = 1) and at the end of the experiment (% of total cell count; n = 3; average ±1s.d.).
doi:10.1371/journal.pone.0079890.t003

the dominant species in the Fe-enriched treatments, *Fragilariopsis cylindrus*, a significant induction of NPQ was only found at irradiances larger than 200 µmol photons m^{-2} s^{-1} [43]. We can therefore conclude that even when photosynthesis was carbon limited under low pCO_2, the applied irradiance was too low to induce NPQ under Fe-enriched conditions and other pathways were operated as electron sinks (e.g. midstream-oxidases [9]).

The changes in physiological responses in Fe-enriched phytoplankton assemblages were accompanied by a pronounced shift in the species composition (Figure 4; Table 3) from *Pseudo-nitzschia* cf. *turgiduloides* under low and intermediate pCO_2 to *Fragilariopsis cylindrus* under high pCO_2 levels. Likely mechanisms for this floristic shift include species-specific differences in carbon acquisition [15,45], as well as pH-mediated differences in cellular physiology, e.g. changes in electrochemical membrane potentials and ion transport processes [46]. *Pseudo-nitzschia* has also been observed to dominate in bloom situations after Fe fertilization [7], where pH increases due to biomass build-up and drawdown of CO_2. This is in line with results from CO_2 manipulations on SO phytoplankton assemblages, which were dominated by *Pseudo-nitzschia* at high pH [16]. In a laboratory study under Fe-enriched conditions, growth and rETRs of *Pseudo-nitzschia subcurvata* were unaffected by pCO_2, suggesting that this species shows little to no responses to CO_2 fertilization [15]. Our field experiment suggests that *Fragilariopsis cylindrus*, in contrast, benefited from increased pCO_2. Even though information of OA responses for this species is lacking, the related *Fragilariopsis kerguelensis* showed enhanced rETRs with increasing pCO_2 (S. Trimborn, unpublished data). We thus speculate that *F. cylindrus* increased its photosynthetic activity under elevated pCO_2, thereby outcompeting the otherwise faster growing *Pseudo-nitzschia*. Under OA, also the relative abundance of *Chaetoceros* sp. increased by 50% (Table 3), which is consistent with previous findings on SO phytoplankton assemblages [16] as well as growth responses of *Chaetoceros debilis* to increased pCO_2 [15].

OA response under Fe-limitation

The observation that under Fe-limitation, productivity was not stimulated by increasing pCO_2 (Figure 3) may indicate that Fe acts as the main limiting factor suppressing the effects of other nutrients such as inorganic carbon. Alternatively, the apparent insensitivity of primary production to OA may arise from antagonistic physiological responses to pCO_2 and pH.

Under Fe limitation, elevated pCO_2 significantly increased rETRs and decreased NPQ, while the functional absorption cross section was not affected (Table 2). These results suggest a greater electron sink associated with the Calvin cycle and thus a decreased need for energy dissipation under OA [44]. It is also known that linear electron transport (LET) towards the Calvin cycle is not the sole sink for photosynthetic energy and that, depending on the ATP demand of the cells, alternative electron pathways can play an important role (*e.g.* Mehler reaction, MOX pathway, pseudocyclic electron flow around PSI) [9]. Increased pCO_2, however, is known to decrease photorespiration and/or the need for carbon concentrating mechanism (CCMs), which would lead to a decrease in cellular ATP demand [47]. The observed increase in rETRs in Fe-limited cells at high pCO_2 levels (Table 2) may therefore rather be linked to higher LET rates than to alternative electron pathways. The higher LET, enabled by the enhanced CO_2 fixation in the Calvin cycle, could counteract the generally greater need for photoprotection under Fe limitation [42,43]. This could explain the opposing CO_2 effects on NPQ under Fe-depleted and Fe-enriched conditions. The CO_2 effect, apparent in photophysiology, is potentially masked in primary production by co-occurring pH effects on Fe bioavailability. According to the observed decline in Fe bioavailability with decreasing pH [18,19], Fe-depleted phytoplankton would experience the greatest Fe stress under high pCO_2.

In this study, Fe-limitation was achieved by the addition of the chelator DFB. Even though DFB has been shown to form strong complexes with Fe and thereby decrease Fe availability by >90% [36], phytoplankton can still access DFB-bound Fe to some extent [48,49]. Since the phytoplankton assemblages in our DFB-treatments were strongly Fe-limited (as demonstrated by photophysiology, Fe and C uptake), bioavailability of Fe must have been largely reduced. Fe bioavailability also seems to be slightly reduced with increasing pCO_2 (Figure 2), as has been observed in natural phytoplankton communities (i.e. without any added chelators) and in studies using different chelators such as EDTA and DFB [18,19,50]. Also, Maldonado et al. [49] suggest that the in-situ organic Fe-complexes observed in the SO have similar bioavailability compared to DFB. Although the chemical nature of in-situ organic Fe-binding ligands is not fully resolved, hydroxamate siderophores have been reported [51]. It is thus possible that at least some of the organically bound Fe exhibits a similar pH-dependent bioavailability as induced by DFB, and thus may allow for the extrapolation of our results to field situations. In order to study the bioavailability of Fe associated with in-situ Fe-binding organic ligands under OA scenarios, future experiments without added chelators should be conducted. As the nature of Fe-binding ligands remains largely unknown and can vary spatially [52,53], one should address the Fe bioavailability of various compounds (e.g., humic acids, saccharids, exopolymeric substances) that were reported to affect iron biogeochemistry [36,54,55]. Furthermore, organic ligands control the bioavailability and the physicochemistry of trace metals in general [52,56]. As some of those (Co, Cd, Zn) are also essential for phytoplankton physiology (e.g. for the activity of the carbonic anhydrase) [57], joint measurements of other trace metals as well as their ligands would be desirable.

Although primary productivity was not sensitive to OA under Fe limitation, we did observe CO_2-dependent species shifts, with *Pseudo-nitzschia* sp. dominating under low and *Synedropsis* sp. under high pCO_2 (Figure 4). The low abundances of *F. cylindrus* in Fe-depleted treatments probably reflect the rather high sensitivity of this species towards Fe limitation [43], which could be due to low Fe uptake capacities observed for this species [21]. In contrast, *Pseudo-nitzschia* has been shown to be an efficient user of Fe under limiting concentrations [58] and sporadic Fe input events [59]. Interestingly, the final proportion of *Pseudo-nitzschia* declined strongly with increasing pCO_2, irrespectively of the Fe status (Table 3), suggesting that its growth rates must have been significantly lower than those of the dominant species (*F. cylindrus* and *Synedropsis* sp. under Fe-enriched and -depleted conditions, respectively). This observation is in line with a recent study on *P. pseudodelicatissima*, whose growth rates were not affected by OA under either Fe-deplete nor -replete conditions [50]. As *Pseudo-nitzschia* generally does not seem to benefit from increased pCO_2 levels ([15,16,50], this study), one could expect OA to have a negative effect on the abundances of this genus under on-going climate change. At present, nothing is known about the Fe and CO_2 requirements of *Synedropsis* [60]. However, a possible appearance of *Synedropsis* in phytoplankton assemblages or incubation experiments might have been overlooked in past studies, as their delicately silicified frustules are very prone to dissolution [61] and not distinguishable from *Pseudo-nitzschia* by light microscopy (Figure 4).

Our results clearly demonstrate a strong difference in CO_2-dependent community structure between Fe-enriched and Fe-depleted conditions (Figure 4). To explain these shifts, more information on species-specific differences in Fe requirements, uptake, as well as allocation strategies [21,62,63], and inorganic carbon acquisition [15,16] is needed for all dominant species.

Biogeochemical implications

The findings of our study suggest that the effects of OA on primary production and community structure are strongly modulated by the prevailing Fe concentrations. Our results, and those of others [16,64], indicate a potential stimulation of the biological pump as a result of increased pCO_2 in Fe-replete regions. Under Fe enrichment and increasing pCO_2 levels, we observed a shift from weakly silicified *Pseudo-nitzschia* towards more heavily silicified *Fragilariopsis*. *Pseudo-nitzschia* remineralizes quickly in subsurface waters [65], while *Fragilariopsis* is a more efficient vector of carbon export [12]. Thus, enhanced primary production, in concert with potentially higher export efficiencies, could lead to a stronger downward flux of organic matter in Fe-replete areas under OA.

The described feedback by 'CO_2-fertilisation', however, may not operate over the broad expanse of the Fe-limited SO. These regional differences in CO_2-sensitivity might be even more pronounced in terms of carbon export efficiencies, as under Fe-depleted conditions no functional shifts in species composition were observed. Here, all assemblages were dominated by weakly silicified species such as *Pseudo-nitzschia* cf. *turgiduloides* [54] or *Synedropsis* sp. [60]. Frustules of both species are delicate and only preserved in shallow waters or under special circumstances such as large aggregation events in combination with anoxia [61,65]. Irrespective of their potential for carbon export, all species dominating our incubations are ecologically important [61,66,67]. Furthermore, both *F. cylindrus* and *P. turgiduloides* are not only characteristic sea-ice algae but also dominate phytoplankton assemblages in open waters [66,67]. In fact, most genera being characteristic for SO phytoplankton assemblages were present in initial and final phytoplankton assemblages (Table 3). Overall, species in the incubations resemble a mixture of typical open-ocean and sea-ice associated species [68–71]. Hence, our interpretations may not be restricted to sea-ice influenced habitats only.

Our results suggest that the potential 'CO_2 fertilization' effect critically depends on the availability of Fe, determining how strongly the biological pump will serve as a carbon sink in the future SO. Realistic projections of primary production and CO_2 sequestration thus remain difficult as long as scenarios for Fe input as well as its bioavailability to phytoplankton remain poorly constrained [18,72]. The results of this study furthermore highlight the need to assess combined effects of important environmental factors in order to understand and predict responses to single stressors such as OA. In this respect, irradiance levels should also be considered as a potentially interacting factor. Indeed, the level of energization has been shown to strongly influence the strength of phytoplankton responses to OA [73], suggesting that also the interaction between Fe and CO_2 availability could be modulated by light conditions. To thoroughly assess consequences of OA, multi-factorial perturbation experiments (including factors such as different Fe sources or grazing) should target physiological as well as ecological responses of SO phytoplankton assemblages.

Acknowledgments

We thank A. McMinn as well as two anonymous referees for helpful comments on this manuscript. We also thank K. Bakker for nutrient analysis, L. Norman, U. Richter, K.-U. Richter, C. Couture, and B. Müller for laboratory or field assistance. L. Wischnewski measured DIC, T. Brenneis measured TA and POC. We also thank P. Assmy, M. Montresor, and D. Sarno for help with taxonomic identifications, F. Hinz and U. Bock for SEM pictures, and the cruise leader, captain and crew of RV Polarstern during ANTXXVII/2. We gratefully thank H.W. de Baar for providing a towed fish for trace-metal clean sampling of seawater.

Author Contributions

Conceived and designed the experiments: CJMH ST BR CH PDT. Performed the experiments: CJMH ST CDP. Analyzed the data: CJMH ST CH CDP. Contributed reagents/materials/analysis tools: CJMH ST BR CH PDT CDP. Wrote the paper: CJMH ST BR CH PDT. Wrote the revised manuscript: CJMH ST BR CH PDT. Wrote the response to the reviewers: CJMH ST BR CH PDT.

References

1. Moore JK, Abbott MR, Richman JG, Nelson DM (2000) The southern ocean at the Last Glacial Maximum: A strong sink for atmospheric carbon dioxide. Global Biogeochem Cycles 14: 455–475.
2. Sigman DM, Hain MP, Haug GH (2010) The polar ocean and glacial cycles in atmospheric CO_2 concentration. Nature 466: 47–55.
3. Le Quéré C, Takahashi T, Buitenhuis ET, Rödenbeck C, Sutherland SC (2010) Impact of climate change and variability on the global oceanic sink of CO_2. Global Biogeochem Cycles 24.
4. Sakshaug E, Slagstad D, Holm-Hansen O (1991) Factors controlling the development of phytoplankton blooms in the Antarctic Ocean - a mathematical model. Mar Chem 35: 259–271.
5. Martin J, Fitzwater S, Gordon R (1990) Iron Deficiency Limits Phytoplankton Growth in Antarctic Waters. Global Biogeochem Cycles 4: 5–12.
6. Timmermans KR, Gerringa LJA, de Baar HJW, van der Wagt B, Veldhuis MJW, et al. (2001) Growth rates of large and small Southern Ocean diatoms in relation to availability of iron in natural seawater. Limnol Oceanogr 46: 260–266.
7. de Baar HJW, Boyd PW, Coale KH, Landry MR, Tsuda A, et al. (2005) Synthesis of iron fertilization experiments: From the Iron Age in the Age of Enlightenment. J Geophys Res 110: C09S16.
8. Smetacek V, Klaas C, Strass VH, Assmy P, Montresor M, et al. (2012) Deep carbon export from a Southern Ocean iron-fertilized diatom bloom. Nature 487: 313–319.
9. Behrenfeld MJ, Milligan AJ (2013) Photophysiological Expressions of Iron Stress in Phytoplankton. Ann Rev Mar Sci 5: 217–247.
10. Greene RM, Geider RJ, Falkowski PG (1991) Effect of Iron Limitation on Photosynthesis in a Marine Diatom. Limnol Oceanogr 36: 1772–1782.
11. Strzepek RF, Hunter KA, Frew RD, Harrison PJ, Boyd PW (2012) Iron-light interactions differ in Southern Ocean phytoplankton. Limnol Oceanogr 57: 1182–1200.
12. Fischer G, Futterer D, Gersonde R, Honjo S, Ostermann D, Wefer G (1988) Seasonal variability of particle flux in the Weddell Sea and its relation to ice cover. Nature 335: 426–428.
13. Lizotte MP (2001) The Contributions of Sea Ice Algae to Antarctic Marine Primary Production. Am Zool 41: 57–73.
14. Riebesell U, Wolf-Gladrow DA, Smetacek V (1993) Carbon dioxide limitation of marine phytoplankton growth rates. Nature 361: 249–251.
15. Trimborn S, Brenneis T, Sweet E, Rost B (2013) Sensitivity of Antarctic phytoplankton species to ocean acidification: Growth carbon aquisition, and species interaction. Limnol Oceanogr 58: 997–1007.
16. Tortell PD, Payne CD, Li Y, Trimborn S, Rost B, et al. (2008) CO_2 sensitivity of Southern Ocean phytoplankton. Geophys Res Lett 35: L04605.
17. Feng Y, Hare CE, Rose JM, Handy SM, DiTullio GR, et al. (2010) Interactive effects of iron, irradiance and CO_2 on Ross Sea phytoplankton. Deep-Sea Res Part 1 Oceanogr Res Pap 57: 368–383.
18. Shi D, Xu Y, Hopkinson BM, Morel FMM (2010) Effect of Ocean Acidification on Iron Availability to Marine Phytoplankton. Science 327: 676–679.
19. Sugie K, Endo H, Suzuki K, Nishioka J, Kiyosawa H, Yoshimura T (2013) Synergistic effects of pCO_2 and iron availability on nutrient consumption ratio of the Bering Sea phytoplankton community. Biogeosciences 10: 6309–6321.
20. de Jong JTM, den Das J, Bathmann U, Stoll MHC, Kattner G, et al. (1998) Dissolved iron at subnanomolar levels in the Southern Ocean as determined by ship-board analysis. Anal Chim Acta 377: 113–124.
21. Hassler CS, Schoemann V (2009) Bioavailability of organically bound Fe to model phytoplankton of the Southern Ocean. Biogeosciences 6: 2281–2296.
22. Maldonado MT, Price NM (2001) Reduction and transport of organically bound iron by *Thalassiosira oceanica* (Bacillariophyceae). J Phycol 37: 298–310.

23. Grasshoff K, Kremling K, Ehrhardt M (1999) Methods of Seawater Analysis pp 600. Weinheim: Wiley-VCH.
24. Brewer PG, Bradshaw AL, Williams RT (1986) Measurement of total carbon dioxide and alkalinity in the North Atlantic ocean in 1981. In The Changing Carbon Cycle – A Global Analysis ed. JR . Trabalka, DE . Reichle, Heidelberg Berlin: Springer Verlag. 358–381 pp.
25. Stoll MHC, Bakker K, Nobbe GH, Haese RR (2001) Continous-Flow Analysis of Dissolved Inorganic Carbon Content in Seawater. Anal Chem 73: 4111–4116.
26. Hoppe CJM, Langer G, Rokitta SD, Wolf-Gladrow DA, Rost B (2012) Implications of observed inconsistencies in carbonate chemistry measurements for ocean acidification studies. Biogeosciences 9: 2401–2405.
27. Pierrot DE, Lewis E, Wallace DWR (2006) MS Excel Program Developed for CO_2 System Calculations. ed. ORNL ORNL/CDIAC-105a Carbon Dioxide Information Analysis Centre. US Department of Energy.
28. Mehrbach C, Culberson CH, Hawley JE, Pytkowicz RM (1973) Measurement of the apparent dissociation constants of carbonic acid in seawater at atmospheric pressure. Limnol Oceanogr 18: 897–907.
29. Dickson AG, Millero FJ (1987) A comparison of the equilibrium constants for the dissociation of carbonic acid in seawater media. Deep-Sea Res 34: 1733–1743.
30. Dickson AG (1990) Standard potential of the reaction: $AgCl(s)+\frac{1}{2}H_2(g)=Ag(s)+HCl(aq)$, and the standard acidity constant of the ion HSO_4^- in synthetic seawater from 273.15 to 318.15 K. J Chem Thermodyn 22: 113–127.
31. Croot PL, Johansson M (2000) Determination of Iron Speciation by Cathodic Stripping Voltammetry in Seawater Using the Competing Ligand 2-(2-Thiazolylazo)-p-cresol (TAC). Electroanalysis 12: 565–576.
32. Tomas CR, Hasle GR (1997) Identifying Marine Phytoplankton. Academic Press. 858 pp.
33. Hillebrand H, Dürselen CD, Kirschtel D, Pollingher U, Zohary T (1999) Biovolume calculation for pelagic and benthic microalgae. J Phycol 35: 403–424.
34. Leblanc K, Arístegui J, Armand L, Assmy P, Beker B, et al. (2012) A global diatom database – abundance, biovolume and biomass in the world ocean. Earth Sys Sci Data 4: 149–165.
35. Knap A, Michaels A, Close AH, Dickson A. (1996) Protocols for the Joint Global Ocean Flux Study (JGOFS) Core Measurements. In JGOFS Report Nr. 19, UNESCO, pp. 170
36. Hassler CS, Schoemann V, Nichols CM, Butler ECV, Boyd PW (2011) Saccharides enhance iron bioavailability to Southern Ocean phytoplankton. Proc Natl Acad Sci USA 108: 1076–8101.
37. Gorbunov M, Falkowski P (2004) Fluorescence Induction and Relaxation (FIRe) Technique and Instrumentation for Monitoring Photosynthetic Processes and Primary Production in Aquatic Ecosystems, Lawrence.
38. Genty B, Briantais J-M, Baker NR (1989) The relationship between the quantum yield of photosynthetic electron transport and quenching of chlorophyll fluorescence. BBA 990: 87–92.
39. Bilger W, Björkman O (1991) Temperature dependence of violaxanthin de-epoxidation and non-photochemical fluorescence quenching in intact leaves of *Gossypium hirsutum* L. and *Malva parviflora* L. Planta 184: 226–234.
40. Johnson KS, Gordon RM, Coale KH (1997) What controls dissolved iron concentrations in the world ocean? Mar Chem 57: 137–161.
41. Kolber ZS, Barber RT, Coale KH, Fitzwateri SE, Greene RM, et al. (1994) Iron limitation of phytoplankton photosynthesis in the equatorial Pacific Ocean. Nature 371: 145–149.
42. van Oijen T, van Leeuwe MA, Gieskes WWC, de Baar HJW (2004) Effects of iron limitation on photosynthesis and carbohydrate metabolism in the Antarctic diatom *Chaetoceros brevis* (Bacillariophyceae). Eur J Phycol 39: 161–171.
43. Alderkamp A-C, Kulk G, Buma AGJ, Visser RJW, Van Dijken GL, et al. (2012) The effect of iron limitation on the photophysiology of *Phaeocystis antarctica* (Prymnesiophyceae) and *Fragilariopsis cylindrus* (Bacillariophyceae) under dynamic irradiance. J Phycol 48: 45–59.
44. Ihnken S, Roberts S, Beardall J (2011) Differential responses of growth and photosynthesis in the marine diatom *Chaetoceros muelleri* to CO_2 and light availability. Phycologia 50: 182–198.
45. Tortell PD, Payne CD, Gueguen C, Strzepek RF, Boyd PW, Rost B (2008) Inorganic carbon uptake by Southern Ocean phytoplankton. Limnol Oceanogr 53: 1266–1278.
46. Taylor AR, Chrachri A, Wheeler G, Goddard H, Brownlee C (2011) A Voltage-Gated H+ Channel Underlying pH Homeostasis in Calcifying Coccolithophores. PLoS Biol 9.
47. Beardall J, Raven JA (2004) The potential effects of global climate change on microalgal photosynthesis, growth and ecology. Phycologia 43: 26–40.
48. Maldonado MT, Price NM (1999) Utilization of iron bound to strong organic ligands by plankton communities in the subarctic Pacific Ocean. Deep-Sea Res Part 2 Top Stud Oceanogr 46: 2447–2473.
49. Maldonado MT, Strzepek RF, Sander S, Boyd PW (2005) Acquisition of iron bound to strong organic complexes, with different Fe binding groups and photochemical reactivities, by plankton communities in Fe-limited subantarctic waters. Global Biogeochem Cycles 19: GB4S23.
50. Sugie K, Yoshimura T (2013) Effects of pCO_2 and iron on the elemental composition and cell geometry of the marine diatom *Pseudo-nitzschia pseudodelicatissima* (Bacillariophyceae). J Phycol 49: 475–488.
51. Velasquez I, Nunn BL, Ibisanmi E, Goodlett DR, Hunter KA, et al. (2011) Detection of hydroxamate siderophores in coastal and Sub-Antarctic waters off the South Eastern Coast of New Zealand. Mar Chem 126: 97–107.
52. Hassler CS, Schoemann V, Boye M, Tagliabue A, Rozmarynowycz M, et al. (2012) Iron Bioavailability in the Southern Ocean. In Oceanography and Marine Biology: An Annual Review, ed. A. R. Gibson RN, Gordon JDM, Hughes RN, 1–64. London: CRC Press.
53. Shaked Y, Lis H (2012) Disassembling iron availability to phytoplankton. Front Microbiol 3: 123.
54. Laglera LM, van den Berg CMG (2009) Evidence for the geochemical control of iron by humic substances in seawater. Limnol Oceanogr 54: 610–619.
55. Hassler CS, Alasonati E, Mancuso Nichols CA, Slaveykova VI (2011) Exopolysaccharides produced by bacteria isolated from the pelagic Southern Ocean - Role in Fe binding, chemical reactivity, and bioavailability. Mar Chem 123: 88–98.
56. Gledhill M, Buck KN (2012) The organic complexation of iron in the marine environment: A review. Front Microbiol 3:69.
57. Morel FMM, Price NM (2003) The Biogeochemical Cycles of Trace Metals in the Oceans. Science 300: 944–947.
58. Marchetti A, Maldonado MT, Lane ES, Harrison PJ (2006) Iron Requirements of the Pennate Diatom *Pseudo-nitzschia*: Comparison of Oceanic (High-Nitrate, Low-Chlorophyll Waters) and Coastal Species. Limnol Oceanogr 51: 2092–2101.
59. Coale KH, Johnson KS, Chavez FP, Buesseler KO, Barber RT, et al. (2004) Southern Ocean Iron Enrichment Experiment: Carbon Cycling in High- and Low-Si Waters. Science 304: 408–414.
60. Hasle GR, Medlin LK, Syvertsen EE (1994) *Synedropsis* gen. nov., a genus of araphid diatoms associated with sea ice. Phycologia 33: 248–270.
61. Stickley CE, St John K, Koc N, Jordan RW, Passchier S, et al. (2009) Evidence for middle Eocene Arctic sea ice from diatoms and ice-rafted debris. Nature 460: 376–9.
62. Sarthou G, Timmermans KR, Blain S, Tréguer P (2005) Growth physiology and fate of diatoms in the ocean: a review. J Sea Res 53: 25–42.
63. Marchetti A, Schruth DM, Durkin CA, Parker MS, Kodner RB, et al. (2012) Comparative metatranscriptomics identifies molecular bases for the physiological responses of phytoplankton to varying iron availability. Proc Natl Acad Sci USA 109: 317–325.
64. Riebesell U, Schulz KG, Bellerby RGJ, Botros M, Fritsche P, et al. (2007) Enhanced biological carbon consumption in a high CO_2 ocean. Nature 450: 545–550.
65. Parsons ML, Dortch Q, Turner RE (2002) Sedimentological evidence of an increase in *Pseudo-nitzschia* (Bacillariophyceae) abundance in response to coastal eutrophication. Limnol Oceanogr 47: 551–558.
66. Almandoz GO, Ferreyra GA, Schloss IR, Dogliotti A, Rupolo V, et al. (2008) Distribution and ecology of *Pseudo-nitzschia* species (Bacillariophyceae) in surface waters of the Weddell Sea (Antarctica). Polar Biol 31: 429–442.
67. Kang S-H, Fryxell GA (1993) Phytoplankton in the Weddell Sea, Antarctica: composition, abundance and distribution in water-column assemblages of the marginal ice-edge zone during austral autumn. Mar Biol 116: 335–348.
68. Garibotti IA, Vernet MA, Smith RC, Ferrario ME (2005) Interannual variability in the distribution of the phytoplankton standing stock across the seasonal sea-ice zone west of the Antarctic Peninsula. J Plankton Res 27: 825–843.
69. Armand LK, Crosta X, Romero O, Pichon J-J (2005) The biogeography of major diatom taxa in Southern Ocean sediments: 1. Sea ice related species. Palaeogeogr Palaeoclimatol Palaeoecol 223: 93–126.
70. Crosta X, Romero O, Armand LK, Pichon J-J (2005) The biogeography of major diatom taxa in Southern Ocean sediments: 2. Open ocean related species. Palaeogeogr Palaeoclimatol Palaeoecol 223: 66–92.
71. Assmy P, Henjes J, Klaas C, Smetacek V (2007) Mechanisms determining species dominance in a phytoplankton bloom induced by the iron fertilization experiment EisenEx in the Southern Ocean. Deep-Sea Res Part I Oceanogr Res Pap 54: 340–362.
72. Boyd PW, Ellwood MJ (2010) The biogeochemical cycle of iron in the ocean. Nat Geosci 3: 675–682.
73. Rokitta SD, Rost B (2012) Effects of CO_2 and their modulation by light in the life-cycle stages of the coccolithophore *Emiliania huxleyi*. Limnol Oceanogr 57: 607–618.

Chapter 5

Publication III

Contrasting responses of *Chaetoceros debilis* to Ocean Acidification under constant and dynamic light

Contrasting responses of *Chaetoceros debilis* to Ocean Acidification under constant and dynamic light

Clara J. M. Hoppe[1], Lena-Maria Holtz[1], Scarlett Trimborn[1,2], and Björn Rost[1]

[1]Alfred Wegener Institute - Helmholtz Centre for Polar and Marine Research, Am Handelshafen 12, 27570 Bremerhaven, Germany
[2]University Bremen, Leobener Strasse NW2-A, 28359 Bremen, Germany

Under review for New Phytologist

5.1 Summary

- There is increasing evidence that different light intensities strongly modulate the effects of Ocean Acidification (OA) on marine phytoplankton. The aim of the present study was to investigate interactive effects of OA and dynamic light, mimicking natural mixing regimes.

- The Antarctic diatom *Chaetoceros debilis* was grown under two pCO_2 (390 & 1000 μatm) and two light conditions (constant & dynamic), the latter yielding the same integrated irradiance over the day. To characterise possible interactive effects between treatments, growth, elemental composition, primary production and photophysiology were investigated.

- Dynamic light reduced growth and strongly altered the effects of OA on primary production, being unaffected by elevated pCO_2 under constant yet significantly reduced under dynamic light. Interactive effects between OA and light were also observed for Chl *a* production and POC quotas.

- Response patterns can be explained by changes in the cellular energetic balance: While the energy conversion efficiency from photochemistry to biomass production ($\Phi_{e,C}$) was not affected by OA under constant light, it was drastically reduced under dynamic light. Contrasting responses under different light conditions need to be considered when making predictions for a more stratified and acidified future ocean.

Keywords: CO_2; diatoms; multiple stressors; photophysiology; phytoplankton; primary production; Southern Ocean

5.2 Introduction

The Southern Ocean (SO) plays a pivotal role in the global carbon cycle (Marinov et al. 2006), strongly influencing atmospheric CO_2 concentrations on glacial-interglacial timescales (Moore et al. 2000, Sigman et al. 2010). Today, the SO takes up 15-40% of the anthropogenic CO_2 (Khatiwala et al. 2009, Takahashi et al. 2009), a large proportion of which is mediated by phytoplankton (Takahashi et al. 2002, Gurney et al. 2004). Yet, the potential for carbon sequestration via the biological pump (Volk & Hoffert 1985) is even higher in this region, as primary producers are restricted by the availability of trace metals (Martin 1990, de Baar et al. 2005) as well as prevailing light conditions (Mitchell et al. 1991, Sakshaug et al. 1991). Deep vertical mixing, induced by strong winds, leads to rapid changes in the light regime as well as low integrated irradiances that phytoplankton cells encounter in the upper mixed layer (MacIntyre et al. 2000).

Primary and export production in the SO are dominated by diatoms (Nelson et al. 1995, Brzezinski et al. 1998). Therefore, a lot of the research has focussed on this functional group. Diatoms tend to dominate well-mixed nutrient rich environments, in which light is the main factor controlling growth rates (Sarthou et al. 2005). Even though diatom species were found to differ in light responses, this group can generally be characterised by high photochemical efficiencies, low susceptibilities towards photoinhibition, and high plasticity in photoacclimation (Wagner et al. 2006, Lavaud et al. 2007, Kropuenske et al. 2009, Su et al. 2012, Li & Campbell 2013). Overall, diatoms seem to be less compromised by fluctuating irradiances than other phytoplankton groups (van Leeuwe et al. 2005, Wagner et al. 2006, Lavaud 2007). These physiological features can, to a large degree, explain the dominance of diatoms in natural phytoplankton assemblages exposed to deep-mixing regimes like the SO (Sarthou et al. 2005), even though the prymnesiophyte *Phaeocystis* has been shown to outcompete diatoms in the deep-mixing regimes of the Ross Sea (Arrigo et al. 2010, Alderkamp et al. 2012, Smith et al. 2013).

Studies investigating the effects of dynamic light on diatoms often showed that while C : N ratios stayed constant, photosynthetic efficiencies increased and growth rates decreased compared to constant light regimes (e.g. van Leeuwe et al. 2005, Wagner et al. 2006, Kropuenske et al. 2009, Mills et al. 2010, Shatwell et al. 2012). This indicates increased costs imposed by continuous photoacclimation and/or time spent under non-optimal configuration of the core physiological apparatus. Despite these general trends, large differences in the magnitude of responses were observed between studies. Furthermore, some species were shown to acclimate their photosynthetic apparatus to average light levels (van Leeuwe et al. 2005, Shatwell et al. 2012), but other species to the highest irradiances of a dynamic

light field (Kropuenske et al. 2009, van de Poll et al. 2007). These differences can be attributed to a high level of interspecific variability, but also to the fact that these studies varied greatly in amplitude, frequency and average levels of applied irradiances. Furthermore, the effects of other environmental conditions (e.g. temperatures, nutrient concentrations, seawater carbonate chemistry) on the integrated physiological configuration of phytoplankton cells (Behrenfeld et al. 2008) may also influence their ability to cope with fluctuating light fields.

Primary production is dependent on the successful realization of various physiological processes that phytoplankton cells have to keep in balance (Falkowski & Raven 1997). For instance, changes in light harvesting need to be balanced by the sum of all downstream processes. The short-term evolution of O_2 and production of energy carriers and reductive equivalents (ATP and NADPH), however, does not directly translate into biomass build-up or growth on longer time scales (Behrenfeld et al. 2008). In between stages, at which the rates of photosynthesis and primary production can be measured, a number of energy consuming processes (e.g. protein biosynthesis, cell division, carbon concentrating mechanisms; CCMs) as well as complex cascades of sensing, signalling and regulation take place (Wilson et al. 2006). Changes in environmental conditions (e.g. light regime) will inevitably impact the balance of cellular processes, affecting the coupling of photosynthetic light harvesting to carbon fixation. Therefore, short- and long-term processes as well as the balance between both need to be studied under different environmental settings, especially with respect to climate change (e.g. Ocean Acidification).

Owing to the high solubility of CO_2 under low water temperatures (Sarmiento et al. 2004), the effects of increased CO_2 concentrations and decreased pH on SO phytoplankton have gained increasing attention (Tortell et al. 2008, Feng et al. 2010, Boelen et al. 2011, Hoogstraten et al. 2012a, Hoogstraten et al. 2012b, Hoppe et al. 2013, Trimborn et al. 2013). The observed sensitivity of phytoplankton to these changes, commonly referred to as Ocean Acidification (OA), can be attributed to different aspects of carbonate chemistry. On the one hand, OA might influence electrochemical membrane potentials and enzyme activities through changes in pH (Kramer et al. 2003) and possibly increases the energetic costs for pH homeostasis (Taylor et al. 2011). On the other hand, phytoplankton may benefit from OA through the increased supply of CO_2, which is the substrate of the enzyme ribulose-1,5-bisphosphate carboxylase/oxigenase (RubisCO). This carbon-fixing enzyme has a poor affinity for CO_2, with half-saturation constants (K_M) being higher than the current levels of aquatic CO_2 (K_M = 20-70 μmol L^{-1}; Badger et al. 1998). To overcome substrate-limitation arising from this, phytoplankton employ so-called carbon concentrating mechanisms (CCMs), which increase the CO_2 concentration at RubisCO (Reinfelder 2011). An increase of external

CO_2 availability may lead to lowered metabolic costs to run the CCM (Burkhardt et al. 2001, Rost et al. 2003, Trimborn et al. 2008). Results on the CO_2-sensitivity of diatom-dominated SO phytoplankton assemblages vary greatly between studies, indicating little to high potential for CO_2 fertilisation (Tortell et al. 2008, Feng et al. 2010, Hoppe et al. 2013). Also, observed changes in growth and physiology of isolated diatom species differ in this respect (Riebesell et al. 1993, Boelen et al. 2011, Hoogstraten et al. 2012a, Trimborn et al. 2013, Trimborn et al. 2014).

There is more and more evidence that besides intra- and interspecific variability (Langer et al. 2009, Trimborn et al. 2013), also experimental conditions significantly impact OA responses. Besides the impact of temperature (Feng et al. 2008, Tatters et al. 2013) and nutrient availability (Fu et al. 2010, Lefebvre et al. 2012, Sugie & Yoshimura 2013, Hoppe et al. 2013), the effect of light intensities on OA responses has been proven especially important (Kranz et al. 2010, Ihnken et al. 2011, Gao et al. 2012a). In the haptophyte *Emiliania huxleyi*, for example, the CO_2-sensitivity of carbon fixation and calcification was greatly enhanced under low compared to high light (Rokitta & Rost 2012). Several studies on diatoms have furthermore shown an increased susceptibility towards photoinhibition under elevated pCO_2 levels (Wu et al. 2010, McCarthy et al. 2012, Li & Campell 2013). Even though all of these studies increased our knowledge on interactive effects between OA and light intensities, the transferability on processes in the ocean, where light intensities are highly dynamic, is questionable.

In addition, also photoacclimation can be influenced by CO_2 concentrations, as changes in CCM and RubisCO activity alter not only the amount of electrons being used in the Calvin cycle, but also its short-term plasticity (Tortell et al. 2000, Reinfelder 2011). It therefore seems likely that OA and dynamic light regimes interactively affect phytoplankton cells. Up to date, only very limited and somehow contradictory data on this interaction is available. Boelen et al. (2011) did not observe significant effects of OA under neither constant nor dynamic light for the Antarctic diatom *Chaetorecos brevis*. In the coccolithophore *Gephyrocapsa oceanica*, the combination of high pCO_2 and short-term (2 h) exposure to dynamic light led to lowered carbon fixation compared to ambient pCO_2 and constant light (Jin et al. 2013). To further investigate possible interactive effects of dynamic light and OA, we acclimated a strain of the bloom-forming SO diatom species *Chaetoceros debilis* to two pCO_2 levels (390 and 1000 μatm) as well as two light regimes (constant and dynamic light), the latter yielding the same integrated irradiance over the day (90 μmol photons m^{-2} s^{-1}). This matrix approach was applied in order to test the hypothesis that dynamic light may diminish the beneficial effect of elevated pCO_2 often observed under constant light, and to understand the physiological mechanisms underlying the general acclimation responses.

5.3 Material and methods

5.3.1 Culture conditions

Monoclonal cultures of the diatom *Chaetoceros debilis* Cleve 1894 (isolated in 2004 by P. Assmy during R/V Polarstern cruise ANT-XXI/3, European Iron Fertilization Experiment [EIFEX], In-Patch, 49°36'S, 02°05'E; re-isolated by C. Hoppe in 2011) were grown in 1L semi-continuous dilute-batch cultures (2000 - 65000 cells mL^{-1}; diluted every 4-5 days) at 3 ±0.4°C in a 16:8 light:dark cycle. Media consisted of 0.2 μm sterile-filtered Antarctic seawater with a salinity of 33 enriched with 100 μmol L^{-1} nitrate, 6.25 μmol L^{-1} phosphate and 100 μmol L^{-1} silicate. Trace metals and vitamins were added according to F/2 medium (Guillard & Ryther 1962).

For the constant light treatments (Figure 5.1), an irradiance of 90 ±10 μmol photons m^{-2} s^{-1} was applied. Also for the dynamic light treatments (Figure 5.1), an integrated irradiance of 90 ±10 μmol photons m^{-2} s^{-1} was applied. The dynamic light field was calculated assuming a spring situation with a mixed layer depth of 80 m, a mixing speed of 0.014 m s^{-1} (Denman & Gargett 1983), 5 mixing cycles per day and an attenuation coefficient of 0.04 m^{-1}, leading to a maximum irradiance of 490 μmol photons m^{-2} s^{-1}. The dynamic light modulation was controlled via the Control2000 programme of a Rumed incubator (1301, Rubarth Apparate). In both light treatments, irradiance was provided by identical daylight lamps (Philips Master TL-D 18W; emission peaks at wavelength of 440, 560 and 635 nm), i.e. exposing the phytoplankton to the same spectral composition in all

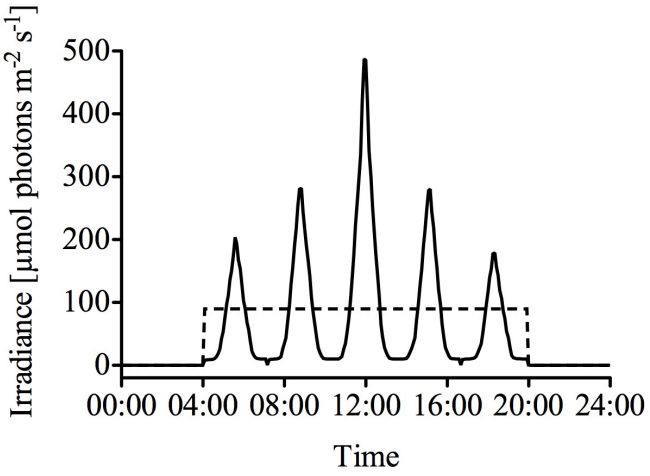

Figure 5.1: - Irradiances [μmol photons m^{-2} s^{-1}] over the day in the constant (dashed line) and dynamic (solid line) light regimes.

treatments. Light intensities were adjusted by neutral density screens and monitored using a LI-1400 data logger (Li-Cor) equipped with a 4π-sensor (Walz).

Different pCO_2 conditions were achieved by continuously and gentle aeration of the incubation bottles with air of different CO_2 partial pressures (390 and 1000 μatm; gas flow rates approx. 90 $\pm$10 mL min^{-1}) delivered through sterile 0.2 μm air-filters (Midisart 2000, Sartorius stedim). Gas mixtures were generated using a gas flow controller (CGM 2000 MCZ Umwelttechnik), in which CO_2-free air (<1 ppmv CO_2; Dominick Hunter) was mixed with pure CO_2 (Air Liquide Deutschland). The pCO_2 in the mixed gas was regularly monitored with a non-dispersive infrared analyzer system (LI6252, LI-COR Biosciences) calibrated with CO_2-free air and purchased gas mixtures of 150 $\pm$10 and 1000 $\pm$20 ppmv CO_2 (Air Liquide Deutschland). Cultures were acclimated to treatments conditions for at least 10 generations prior to sampling, never exceeding 65,000 cells L^{-1} during this time period.

5.3.2 Carbonate chemistry

Samples for total alkalinity (TA; n=14) were 0.6 μm filtered (glass fibre filters, GF/F, Whatman) and stored in borosilicate bottles at 3°C. TA was estimated from duplicate potentiometric titration (Brewer et al. 1986) using a TitroLine alpha plus (Schott Instruments) and corrected for systematic errors based on measurements of certified reference materials (CRMs provided by Prof. A. Dickson, Scripps, USA; batch #111; reproducibility $\pm$5 μmol kg^{-1}). Dissolved inorganic carbon (DIC; n=14) samples were filtered through 0.2 μm cellulose-acetate filters (Sartorius stedim) and stored in gas-tight borosilicate bottles at 3°C. DIC was measured colorimetrically in triplicates with a QuAAtro autoanalyzer (Seal; Stoll et al. 2001). The analyser was calibrated with $NaHCO_3$ solutions (with a salinity of 35, achieved by addition of NaCl) to achieve concentrations ranging from 1800 to 2300 μmol DIC kg^{-1}. CRMs were used for corrections of errors in instrument performance such as baseline drifts (reproducibility $\pm$8 μmol kg^{-1}). Seawater pH_{total} (n=14) was measured potentiometrically with a two-point calibrated glass reference electrode (IOline, Schott Instruments). An internal TRIS-based reference standard (Dickson et al. 2007) was used to correct for variability on electrode performance (reproducibility $\pm$0.015 pH units). Following suggestions by Hoppe et al. (2012), seawater carbonate chemistry (including pCO_2) was calculated from TA and pH using CO_2SYS (Pierrot et al. 2006). The dissociation constants of carbonic acid of Mehrbach et al. (1973; refit by Dickson & Millero, 1989) were used for calculations. Dissociation constants for $KHSO_4$ were taken from Dickson (1990).

5.3.3 Growth, elemental composition and production rates

Samples for cell counts were fixed with Lugols solution (1% final concentration) and counted on a light microscope (Axio Observer.D1, Zeiss) after 24 h sedimentation time in 10 mL Utermöhl chambers (Hydro-Bios; >1700 cells counted per sample). Samples for determination of chlorophyll *a* (Chl *a*) were filtered onto 0.6 μm glass-fibre filters (GF/F, Whatman), immediately placed into liquid nitrogen and stored at -80°C until analysis. Chl *a* was subsequently extracted in 8 mL 90% acetone (2-3 h at 4°C). After removal of the filter, concentrations were determined on a fluorometer (TD-700, Turner Designs), using an acidification step (1M HCl) to determine phaeopigments (Knap et al. 1996). Growth rate determinations started 1-2 days after re-dilution from daily Chl *a* sampling (n=3) over 4 days within the first 15 min of the dark-phase and calculated as

$$\mu = (\ln([\mathrm{Chl}a]_{\mathrm{t1}}) - \ln([\mathrm{Chl}a]_{\mathrm{t2}}))/\Delta_{\mathrm{t}} \tag{5.1}$$

where [Chl v]$_{t1}$ and [Chl a]$_{t2}$ denote the Chl *a* concentrations at the respective sampling days t_1 and t_2 and Δ_t is the corresponding incubation time in days. Particulate organic carbon (POC) and nitrogen (PON) were measured after filtration onto precombusted (15h, 500°C) glass-fibre filters (GF/F 0.6 μm nominal pore size; Whatman). Filters were stored at -20°C and dried for at least 12 h at 60°C prior to sample preparation. Analysis was performed using a CHNS-O elemental analyser (Euro EA 3000, HEKAtech). Contents of POC and PON were corrected for blank measurements and normalised to filtered volume and cell densities to yield cellular quotas. Biogenic silica (BSi) filtered onto 0.5 μm cellulose-acetate filters and determined spectrophotometrically after treatment with a molybdate solution as described in Koroleff (1983). Production rates of Chl *a*, POC, PON and BSi were calculated by multiplying the cellular quota with the growth rate of the respective culture. In order to diminish possible short-term effects arising from changes in irradiance fields in the dynamic treatments, all samples were taken within the first 30 min of the dark-phase.

5.3.4 Chl *a*-specific Primary production

Chl *a*-specific net primary production (NPP) rates were determined in triplicates by incubation of 20 mL of culture with 20 μCi $NaH^{14}CO_3$ spike (53.1 mCi mmol^{-1}; Perkin Elmer) in 20 mL glass scintillation vials for 24 h under experimental conditions. From these incubations, 0.1 mL aliquots were immediately removed, mixed with 15 mL of scintillation cocktail (Ultima Gold AB, PerkinElmer) and counted after 2 h with a liquid scintillation counter (Tri-Carb 2900TR, PerkinElmer) to determine the total amount of added $NaH^{14}CO_3$ ($DPM_{100\%}$). For blank determination ($DPM_{0\%}$), one replicate was immediately acidified with

0.5 mL 6M HCl. After 24 h of incubation, ^{14}C incorporation was stopped by adding 0.5 mL 6M HCl to each vial. The entire sample was then left to degas and dry in a custom-build chamber. When samples were completely dry (1-2 d), 5 mL milli-Q water were added to resuspend the sample. Subsequently, 15 mL of scintillation cocktail (Ultima Gold AB, PerkinElmer) were added and samples were measured after 2 h with a liquid scintillation counter (Tri-Carb 2900TR, PerkinElmer). NPP rates [mol C (mol Chl a)$^{-1}$ d^{-1}] were calculated as

$$\mathrm{NPP} = ([\mathrm{DIC}] \times (\mathrm{DPM_{sample}} - \mathrm{DPM_{0\%}}) \times 1.05)/(\mathrm{DPM_{100\%}} \times \mathrm{t} \times [\mathrm{Chl}\ a]) \tag{5.2}$$

where [DIC] and [Chl a] denote the concentrations of dissolved inorganic carbon and Chl a in the sample, respectively. DPM_{sample} denotes the disintegrations per minute (DPM) in the samples, $\mathrm{DPM_{0\%}}$ reflects the blank value, and $\mathrm{DPM_{100\%}}$ denotes the DPM of the total amount of $NaH^{14}CO_3$ added to the samples, and t is the duration of the incubation.

5.3.5 Variable Chl *a* fluorescence

Photophysiological characteristics (Table 5.1), based on photosystem II (PSII) variable Chl a fluorescence, were measured using a fast repetition rate fluorometer (FRRF; FastOcean PTX, Chelsea Technologies) in combination with a FastAct Laboratory system (Chelsea Technologies). The excitation wavelength of the fluorometers light-emitting diodes (LEDs) was 450 nm, and the applied light intensity was 1.3 × 1022 photons m^{-2} s^{-1}.The FRRf was used in single turnover mode, with a saturation phase comprising 100 flashlets on a 2 μs pitch and a relaxation phase comprising 40 flashlets on a 50 μs pitch. All measurements (n=3) were conducted in a temperature-controlled chamber at 3 ±0.3°C.

In the middle of the dark phase (4h after offset of light), minimum (F_0, F_0') and maximum Chl a fluorescence (F_m, F_m'$_{90}$), absorption cross section of PS II photochemistry (σ_{PSII}, σ_{PSII}'$_{90}$), reoxidation time of the plastoquinone pool (τ, τ'$_{90}$), connectivity between PSIIs (ρ, ρ'$_{90}$; assuming the homogeneous model), all both after dark acclimation for 3 minutes and acclimation to an average light level of 90 mol photons m^{-2} s^{-1} for 90 seconds, as well as relative electron transfer rates through PSII (rETR) from each light- and dark-acclimated measurements were estimated from iterative algorithms for induction (Kolber et al. 1998) and relaxation phase (Oxborough 2012). Maximum quantum yield efficiencies of PSII (apparent PSII photochemical quantum efficiency; F_v/F_m) was estimated as

$$\mathrm{F_v/F_m} = (\mathrm{F_m} - \mathrm{F_0})/\mathrm{F_m} \tag{5.3}$$

Fluorescence based photosynthesis-irradiance curves (PI) were conducted four times a day (1h and 8h after the onset of light as well as directly after and 4h after the onset of darkness) at 15 irradiance levels between 6 and 650 μmol photons m^{-2} s^{-1}, with an acclimation time

of 90 s per light step. Longer acclimation time (6 min) yielded generally higher $rETR_{max}$, but under these conditions no differences between treatments were observed (data not shown; Ihnken et al. 2010).

Non-photochemical quenching of Chl fluorescence (NPQ) at irradiances of 490 and 650 μmol photons m^{-2} s^{-1} (i.e. the maximum irradiance applied in the dynamic light cycle as well as the maximum irradiance step of the PI curve) were calculated using the normalized Stern-Volmer coefficient as described in Oxborough (2012) and McKew et al. (2013):

$$NPQ = (F'_q/F'_v) - 1 = F'_0/F'_v \tag{5.4}$$

where F_0' was measured after each light step (with a duration of 90 s).

Following the suggestion by Silsbe & Kromkamp (2012), the light-use efficiency (α [mol e^- m^2 (mol Chl a)$^{-1}$ (mol photons)$^{-1}$]), and the light saturation index (I_K [mol photons m^{-2} s^{-1}]) were estimated by fitting the data to the model by Webb et al. (1974). The maximum electron transport rates (ETR_{max} [mol e^- (mol Chl a)$^{-1}$ s^{-1}]) were estimated after applying a beta phase fit as described by Oxborough (2012). The relative ETR (rETR) were converted to absolute rates by applying a correction factor derived from the relationship between rETR and JV_{PSII} ([mol e^- m^{-3} d^{-1}]; provided by FastPro software as described in Oxborough et al. 2012) from each individual dataset and dividing it by the Chl a concentration of the sample. Daily integrated electron transport rates (ETR_{24h} [mol e^- (mol Chl a)$^{-1}$ d^{-1}]) were estimated by calculating electrons transported in 5 minute steps of I values of both light regimes using α, I_K and ETR_{max} from the PI curve measured closest to the time point of interest. Chl a concentrations for normalizations were corrected using the growth rate and the time difference between FRRF and Chl a measurements. To estimate the energy transfer efficiency from photochemistry to biomass build-up, the electron requirement for carbon fixation ($\Phi_{e,C}$ [mol e^- (mol C)$^{-1}$]) was calculated for each treatment by dividing the ETR_{24h} by NPP (expressed as molar quantities).

5.3.6 Statistics

All data is given as the mean of the replicates with ± one standard deviation. To test for significant differences between the treatments, two-way analyses of variance (ANOVA) with additional normality (Shapiro-Wilk) and Post Hoc (Holm-Sidak method) tests were performed. The significance level was set to 0.05. Statistical analyses were performed with the program SigmaPlot (SysStat Software Inc).

Table 5.1: Summary of abbreviations and units of physiological measurements

Parameter	Unit	Description
α	mol e^- m^2 (mol Chl a)$^{-1}$ (mol photons)$^{-1}$	Light use efficiency of PSII
ETR_{24h}	mol e^- (mol Chl a)$^{-1}$ d^{-1}	Absolute daily electron transfer rates through PSII
ETR_{max}	mol e^- (mol Chl a)$^{-1}$ s^{-1}	Light-saturated, maximal absolute electron transfer rates through PSII
I_K	μmol photons m^{-2} s^{-1}	PSII light saturation index
F_q'/F_m'$_{90}$	(dimensionless)	Quantum yield (efficiency) of electron transport through PSII in the light
F_v/F_m	(dimensionless)	Quantum yield (efficiency) of electron transport through PSII in the dark
μ	d^{-1}	Chl a-specific growth rate (constant)
NPP	μg C (μg Chl a)$^{-1}$ d^{-1}	Chl a-specific net primary production from 24h ^{14}C-incubations
NPQ_{490}	dimensionless	Non-photochemical quenching of Chl fluorescence
$\Phi_{e,C}$	mol e^- (mol C)$^{-1}$	Energy conversion efficiency from photochemistry to biomass production
ρ	(dimensionless)	Connectivity between PSII reaction centres in the dark
ρ'$_{90}$	(dimensionless)	Connectivity between PSII reaction centres in the light
σ_{PSII}	$\AA^2$ quantum^{-1}	Functional absorption crosssection for PSII in the dark
σ_{PSII}'$_{90}$	$\AA^2$ quantum^{-1}	Functional absorption crosssection for PSII in the light
τ	μs	PSII turnover (i.e. reoxidation) time in the dark
τ'$_{90}$	μs	PSII turnover (i.e. reoxidation) time in the light

5.4 Results

5.4.1 Carbonate chemistry

Continuous aeration with air of desired CO_2 partial pressure (390 and 1000 μatm) as well as regular dilution of cultures with pre-aerated seawater medium led to stable carbonate chemistry over the course of the experiment (Table 5.2) and to significant differences between pCO_2 (ANOVA, p<0.001 for DIC, pH and pCO_2), but not light treatments (ANOVA, p>0.05). In the ambient treatments, pCO_2 were 385 ±31 μatm for constant and 396 ±30 μatm for dynamic light. In the OA treatments, pCO_2 levels were 972 ±35 μatm for constant and 1007 ±30 μatm for dynamic light. Over the duration of the experiment (>5 weeks), the drift in DIC and TA compared to abiotic controls were <2 and <4%, respectively.

5.4.2 Growth rates and elemental composition

Chl *a*-specific growth rates (Table 5.3, Figure 5.2A) under constant light conditions were similarly high, being 0.53 ±0.03 d^{-1} and 0.56 ±0.03 d^{-1} in ambient and high pCO_2 treatments, respectively. Under dynamic light, growth rates were significantly lower than under constant light (ANOVA, F=51; p<0.001). Under these conditions, growth rates were unaffected by the applied pCO_2 treatments, being 0.44 ±0.01 d^{-1} at ambient and 0.42 ±0.03 d^{-1} at high pCO_2.

With respect to the amount of Chl *a* per cell (Table 5.3), we observed significant effects of both pCO_2 (ANOVA, F=28; p<0.001) and light treatments (ANOVA, F=6; p=0.047). Under dynamic light, Chl *a* quotas significantly decreased with increasing pCO_2 (post-hoc, p<0.001), while they remained unaffected by OA under constant light, leading to a significant interactive effect of pCO_2 and light level on cellular Chl *a* quotas (ANOVA, F=21; p=0.002). Similarly, also the production of Chl *a* per cell (Table 5.3, Figure 5.2 B) was significantly affected by both pCO_2 (ANOVA, F=28; p<0.001) and light (ANOVA,

Table 5.2: Seawater carbonate chemistry - DIC [μmol kg^{-1}], TA [μmol kg^{-1}], pH_{total} and pCO_2 [μatm] were sampled regularly over the course of the experiments (n=14; mean ±1 s.d.). pCO_2 was calculated from TA and pH_{total} at 3°C and a salinity of 34 using CO_2SYS (Pierrot et al. 2007), and concentrations of 12 and 108 μmol kg^{-1} for phosphate and silicate, respectively.

Treatment	**DIC**	**TA**	**pH_{total}**	**pCO_2**
Constant light 390 μatm CO_2	2092 ±15	2250 ±27	8.05 ±0.02	385 ±18
Constant light 1000 μatm CO_2	2202 ±29	2258 ±18	7.66 ±0.03	973 ±28
Dynamic light 390 μatm CO_2	2101 ±27	2263 ±33	8.03 ±0.02	400 ±17
Dynamic light 1000 μatm CO_2	2203 ±25	2252 ±27	7.65 ±0.02	1026 ±31

Table 5.3: Acclimation Parameter - Chl *a*-specific growth rates, cellular quotas and production rates of Chl *a*, POC, PON and BSi as well as NPP, integrated ETR and energy converison efficiency (n=3; mean ±1 s.d.) of *C. debilis* under two pCO_2 levels at constant and dynamic light regimes.

Parameter		**Constant light**		**Dynamic light**	
		390 μatm CO_2	**1000 μatm CO_2**	**390 μatm CO_2**	**1000 μatm CO_2**
Growth rate	μ [d^{-1}]	0.53 ±0.03	0.56 ±0.03	0.44 ±0.01	0.42 ±0.03
Cellular quotas	Chl *a* [pg $cell^{-1}$]	0.66 ±0.04	0.62 ±0.06	0.72 ±0.04	0.45 ±0.04
	POC [pg $cell^{-1}$]	40.49 ±4.29	43.66 ±4.13	43.28 ±4.91	30.91 ±4.72
	PON [pg $cell^{-1}$]	7.69 ±0.39	6.76 ±0.89	7.94 ±0.77	5.65 ±0.87
	BSi [μg $cell^{-1}$]	55.20 ±1.15	41.87 ±2.89	47.43 ±4.88	39.75 ±1.13
Production rates	Chl *a* [pg $cell^{-1}$ d^{-1}]	0.35 ±0.02	0.36 ±0.03	0.31 ±0.02	0.19 ±0.02
	POC [pg $cell^{-1}$ d^{-1}]	21.34 ±2.26	24.32 ±2.30	18.88 ±2.14	12.87 ±1.96
	PON [pg $cell^{-1}$ d^{-1}]	4.05 ±0.21	3.76 ±0.50	3.47 ±0.34	2.35 ±0.36
	BSi [μg $cell^{-1}$ d^{-1}]	29.09 ±0.61	23.32 ±1.61	20.69 ±2.13	16.55 ±0.47
Ratios	C : N (pg:pg)	5.29 ±0.80	6.50 ±0.56	5.44 ±0.10	5.47 ±0.04
	C : Chl *a* (pg:pg)	61.67 ±4.70	68.51 ±5.01	60.44 ±5.72	67.87 ±6.56
Primary production	NPP [mol C (mol Chl $a)^{-1}$ d^{-1}]	1407 ±124	1676 ±243	1158 ±1.19	914 ±142
Electrons transport	ETR_{24h} [mol e^{-1} (mol Chl $a)^{-1}$ d^{-1}]	3852 ±195	3468 ±332	3949 ±395	4383 ±433
Energy conversion	$\Phi_{e,C}$ [mol e^- (mol C)$^{-1}$]	2.74 ±0.38	2.07 ±0.50	3.41 ±0.78	4.81 ±1.22

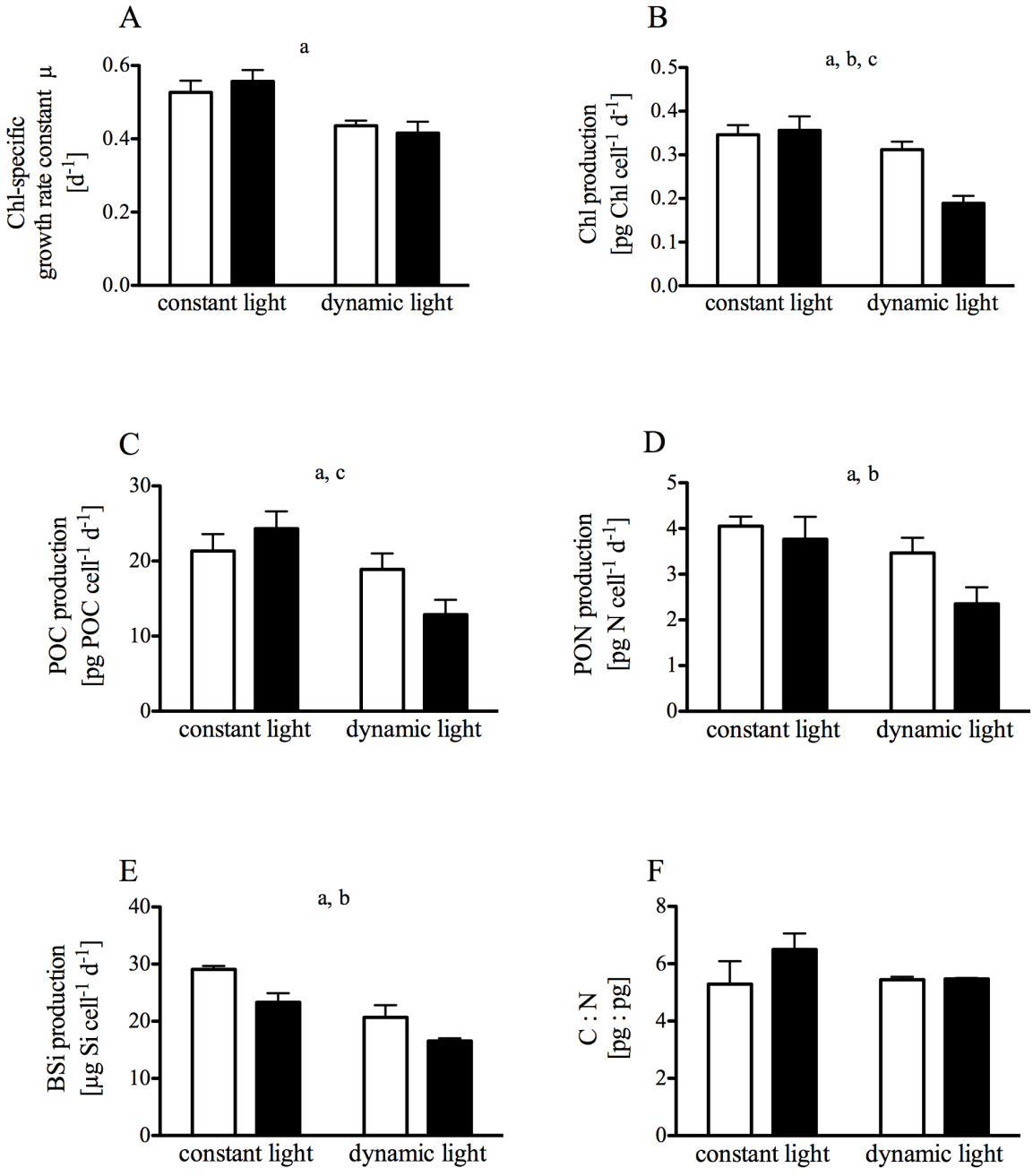

Figure 5.2: - Chl *a*-specific rowth rates (A), production rates of Chl *a* (B), POC (C), PON (D) and BSi (E) as well as cellular C:N ratios (F) of *C. debilis* at pCO_2 levels of 390 μatm (open bars) and 1000 μatm (filled bars) under constant and dynamic light regimes (n=3; mean $\pm$1 s.d.). Letters indicate significant ($p<0.05$) differences between light treatments (a), pCO_2 treatments (b) and significant interactions between light and pCO_2 treatments (c).

F=6; p=0.047). Both factors also had an interactive effect on production rates (ANOVA,F=21; p=0.002), which led to a significant decrease in Chl *a* production under dynamic light and increasing pCO_2 (post-hoc, p<0.001). The ratio of Chl *a* : C (Table 5.3) was not significantly affected by any treatment.

Cellular quota of particulate organic carbon (POC; Table 5.3) under constant light did not differ between ambient and high pCO_2, whereas they significantly decreased with increasing pCO_2 under dynamic light (post-hoc test, p=0.010; significant ANOVA interaction between pCO_2 and light, F=9; p=0.018). Overall, POC production (Table 5.3, Figure 5.2C) under constant light was not significantly affected by pCO_2 or light. Under dynamic light conditions, however, POC production significantly decreased with increasing pCO_2 (post-hoc, p=0.009), resulting in a significant interaction term between pCO_2 and light conditions (ANOVA, F=9; p=0.018).

Cellular quota of particulate organic nitrogen (PON; Table 5.3) were significantly reduced under high compared to ambient pCO_2 (ANOVA, F=14; p=0.006), irrespective of the light conditions applied. Also the production of PON (Table 5.3, Figure 5.2 D) decreased significantly with decreasing pCO_2 (ANOVA, F=11; p=0.01). PON production was significantly higher under constant compared to dynamic light (ANOVA, F=23; p=0.001). Under constant light, C : N ratios significantly increased with increasing pCO_2 (Table 5.3, Figure 5.2 F; post-hoc, p=0.017). Under dynamic light, no such response was observed. Significant differences in C : N ratios between the light treatments were observed under high pCO_2 only (post-hoc, p=0.033).

Cultures exhibited a highly significant decline in the cellular quota of biogenic silica (BSi; Table 5.3) with increasing pCO_2 (ANOVA, F=38; p<0.001), irrespective of the applied light treatment. The decline in BSi quota under dynamic light was smaller than under constant light, but also significant (ANOVA, F=9; p=0.020). We also observed a highly significant decrease in BSi production (Table 5.3, Figure 5.2 E) with increasing pCO_2 (ANOVA, F= 38; p<0.001). Furthermore, BSi production was significantly lower under dynamic compared to constant light (ANOVA, F=90; p<0.001).

5.4.3 Chl *a*-specific net primary production

Chl *a*-specific net primary production (NPP; Table 5.3, Figure 5.3) under constant light increased slightly, yet insignificantly, with increasing pCO_2. Under dynamic light, NPP was lower than under constant light (ANOVA, F=27; p<0.001). Under these conditions, NPP was furthermore significantly decreased with increasing pCO_2 (post-hoc, p<0.001), resulting in a significant interaction between pCO_2 and light conditions (ANOVA, F=7; p=0.034).

5.4.4 Chl *a* fluorescence-based photophysiology

The dark-acclimated quantum yield efficiency of PSII (F_v/F_m; Table 5.4) was similar in all treatments with values of 0.53 ±0.01. The effective quantum yield efficiency under the average daily irradiance (90 μmol photons m^{-1} s^{-1} ;$F_q'/F_m'_{90}$; Table 5.4) measured after 4h of darkness was significantly higher in the dynamic compared to constant light treatments (ANOVA, F=165; p<0.001), irrespectively of the pCO_2 applied. No relationship between the dark-acclimated functional absorption cross-section of PSII (σ_{PSII} ; Table 5.4) or the functional absorption cross-section of PSII acclimated to the average light intensity ($\sigma_{PSII}'_{90}$; Table 5.4) and the applied treatments was observed. The dark-adapted connectivity between PSII reaction centres (ρ; Table 5.4), however, was significantly lower under constant compared to dynamic light (ANOVA, F=50; p<0.001) as well as significantly larger under ambient compared to high pCO_2 (ANOVA, F=6; p=0.036). The connectivity under average daily irradiances (ρ'_{90}; Table 5.4) was significantly higher under dynamic compared to constant light (ANOVA, F=88; p<0.001), but not affected by pCO_2. The dark-acclimated re-oxidation time after saturation of PSII (τ; Table 5.4) as well as the re-oxidation time under average daily irradiance (τ'_{90}) was not affected by pCO_2 or light treatments. Neither non-photochemical quenching (NPQ) at 490 μmol photons m^{-1} s^{-1} (Table 5.4) nor at 650 μmol photons m^{-1} s^{-1} (data not shown) was affected by the applied treatments.

Also the fitted parameters of nighttime FRRf-based PI curves were only slightly influenced by the experimental treatments. The maximal electron transport rates through PSII (ETR_{max}; Table 5.4) did not differ between treatments. In addition, also the maximum PSII light-use efficiency (α; Table 5.4) was similar under all applied conditions. The PSII light-saturation point (I_K; Table 5.4), however, was significantly higher under dynamic compared to constant light (ANOVA, F=37; p<0.001), while pCO_2 levels had no effect.

Cumulative electron transport rates over 24h (ETR_{24h}; Table 5.3) of the treatments were not significantly different. The electron requirement for carbon fixation ($\Phi_{e,C}$; Table 5.3), however, was significantly higher under dynamic compared to constant light (Figure 3; ANOVA, F=117; p<0.001). While $\Phi_{e,C}$ decreased with increasing pCO_2 under constant light (post-hoc, p=0.023), the opposite trend was observed under dynamic light (post-hoc, p=0.002). This led to a highly significant interaction term between light treatments and pCO_2 levels (ANOVA, F=28; p<0.001).

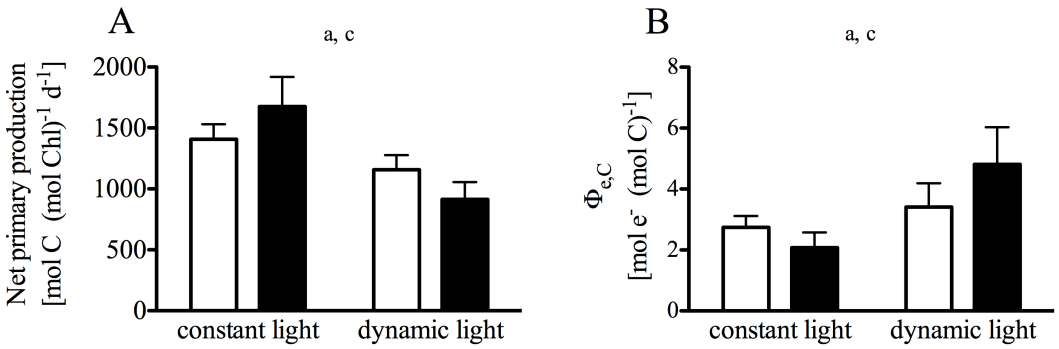

Figure 5.3: - Chl *a*-specific net primary production (NPP [μmol C (μmol Chl *a*)$^{-1}$ d^{-1}]; A) and electron requirement for carbon fixation ($\Phi_{e,C}$ [mol e$^-$ (mol C)$^{-1}$]; B) at pCO$_2$ levels of 390 μatm (open bars) and 1000 μatm (filled bars) under constant and dynamic light regimes (n=3; mean $\pm$1 s.d.).Letters indicate significant ($p<0.05$) differences between light treatments (a), pCO$_2$ treatments (b) and significant interactions between light and pCO$_2$ treatments (c).

Table 5.4: FRR-flourometrical PSII photochemistry measurements - Quantum yield, functional absorption cross-section [$Å^2$ quantum^{-1}], connectivity, re-oxidation time of the plastoquinone pool [μs] and NPQ at 490 μmol photons m^{-2} s^{-1} after dark and integrated in-situ light acclimation (90 μmol photons m^{-2} s^{-1}), light-saturated, maximal absolute electron transfer rates through PSII (ETR$_{max}$ [mol e$^-$ [mol Chl$a$]$^{-1}$ s^{-1}]), light saturation index (I$_K$ [μmol photons m^{-2} s^{-1}]) and the maximum light-use efficiency (initial slope α [mol e$^-$ m^2 (mol Chl$a$)$^{-1}$ (mol photons)$^{-1}$]) at night (4h after the onset of darkness) under two pCO_2 levels at constant and dynamic light regimes (n=3; mean ±1 s.d.).

Parameter		**Constant light**		**Dynamic light**	
		390 μatm CO$_2$	**1000 μatm CO$_2$**	**390 μatm CO$_2$**	**1000 μatm CO$_2$**
Quantum yield	F$_v$/F$_m$	0.52 ±0.01	0.53 ±0.01	0.54 ±0.01	0.54 ±0.01
	F$_q$'/F$_m$'$_{90}$	0.37 ±0.01	0.37 ±0.01	0.45 ±0.01	0.44 ±0.01
Functional absorption cross-section	σ_{PSII}	4.36 ±0.20	4.19 ±0.14	4.34 ±0.10	4.41 ±0.17
	σ_{PSII}'$_{90}$	4.01 ±0.19	4.06 ±0.07	4.08 ±0.11	4.21 ±0.15
Connectivity	ρ	0.42 ±0.02	0.40 ±0.01	0.46 ±0.01	0.45 ±0.01
	ρ'$_{90}$	0.15 ±0.02	0.15 ±0.02	0.29 ±0.02	0.30 ±0.01
Reoxidation time	τ	581 ±14	601 ±15	582 ±16	581 ±23
	τ'$_{90}$	6oo ±15	598 ±21	594 ±18	581 ±21
Non-photochemical quenching	NPQ$_{90}$	1.18 ±0.31	1.09 ±0.10	0.86 ±0.27	0.78 ±0.15
Maximum electron transport rates	ETR$_{max}$	0.21 ±0.03	0.21 ±0.02	0.20 ±0.02	0.23 ±0.01
PSII light saturation index	I$_K$	139 ±10	128 ±10	177 ±16	170 ±9
PSII light use efficiency	α	0.0010 ±0.0001	0.0011 ±0.0002	0.0012 ±0.0003	0.0014 ±0.0001

5.5 Discussion

5.5.1 Dynamic light exerts high metabolic costs

Prevailing strong winds lead to deeply mixed surface layers and highly dynamic light regimes in the SO (Nelson & Smith 1991). Phytoplankton species occurring in this environment can therefore be expected to cope well with dynamic light conditions. In fact, cellular POC and PON quotas as well as C : Chl *a* at 390 atm μatm pCO_2 did not differ between the light treatments in *C. debilis* (Table 5.3). The maintenance of cellular stoichiometry under dynamic light was achieved at the expense of growth and biomass build-up (Table 5.3, Figures 5.2 and 5.3). A decline in growth rates under dynamic light is an overarching pattern observed in several studies (Van de Poll et al. 2007, Mills et al. 2010, Boelen et al. 2011, Shatwell et al. 2012). Cells grown under dynamic light furthermore had a higher light-saturation point (I_K; Table 5.4). Such changes in I_K are normally associated with an increase in irradiance levels (Behrenfeld et al. 2004), but also seem to be an acclimation response to dynamic light regimes. Even though the resulting daily integrated ETR_{24h} were not affected by the different light regimes (Table 5.3), NPP (Figure 5.3) and biomass build-up (Figure 5.2) under dynamic light were significantly lowered. This implies that under dynamic light, the overall energy conversion efficiency from photochemistry to biomass production was substantially reduced (Wagner et al. 2006, Ihnken et al. 2011, Su et al. 2012, Jin et al. 2013).

In fact, the electron requirement of carbon fixation ($\Phi_{e,C}$; Figure 5.3) was significantly higher under these conditions, hinting towards an increase in other electron consuming processes such as photorespiration or alternative electron cycling (Prásil et al. 1996, Badger et al. 2000, Waring et al. 2010, Thamatrakoln et al. 2013). While theoretically, $\Phi_{e,C}$ should be 4-6 mol e^- (mol C)$^{-1}$ (Genty et al. 1989, Suggett et al. 2009), the estimates for $\Phi_{e,C}$ in this study range between roughly 2 and 5 mol e^- (mol C)$^{-1}$ (Table 5.3). Values between 1.2 and 54.3 mol e^- (mol C)$^{-1}$ have been previously observed in field studies and laboratory experiments (Suggett et al. 2009, Lawrenz et al. 2013). $\Phi_{e,C}$ <4 mol e^- (mol C)$^{-1}$ have been attributed to systematic errors in the ETR calculations (Lawrenz et al. 2013). In addition, differences in temporal scales between measures (e.g. Kromkamp & Forster 2003), short-term light acclimation as well as normalization procedures may lead to a systematic underestimation of ETRs. Irrespectively, the observed trend indicates comparably low energy transfer efficiency under dynamic light, which may explain the observed decrease in growth and NPP compared to constant light.

Diatom cells growing under dynamic light need to adjust their photosynthetic apparatus to achieve a balance between photoprotection at high light and effective light-harvesting at low light. In line with other studies on dynamic light (van de Poll et al. 2007,

Kropuenske et al. 2009, Alderkamp et al. 2012, Su et al. 2012), we did not observe an increase in NPQ capacity (Table 5.4). Successful photoprotection may be achieved via other processes such as increased connectivity ρ (Table 5.4; Trimborn et al. 2014) or the induction of alternative electron pathways (e.g. Mehler reaction, electron flow around PSII or PSI) that can supplement the xanthophyll cycle in diatoms (Prásil et al. 1996, Asada et al. 1999, Waring et al. 2010). These could have contributed to the observed increase in $\Phi_{e,C}$ (Figure 5.3) under dynamic compared to constant light.

In addition, an insensitivity of electron transport towards high-light stress does not mean that no photodamage of reaction centres occurs. In fact, an uncoupling of between PSII inactivation and the rate of electron flow has been described as a common mechanism for phytoplankton occurring under natural light regimes (Behrenfeld et al. 1998). The uncoupling can be explained by the presence of 'excess PSII capacity', i.e. more reaction centres than actually needed, allowing for high photochemical efficiencies even if light-dependent photoinactivation of PSII increases (Behrenfeld et al. 1998). This overproduction and subsequent repair of PSII, including the susceptible D1 subunit and associated proteins, imposes high metabolic costs for the phytoplankton cell (Raven 2011). Whether or not the costs, being associated with the high-light phases of the dynamic light treatment, get compensated for by the subsequent period of low light depends on the rates of both, the changes in light intensity and D1 repair (Behrenfeld et al. 1998, Marshall et al. 2000). In the here tested scenarios, we did not observe the manifestation of photoinhibition (Figure SI5.1). Therefore, we postulate that a large fraction of the decline in energy conversion efficiency from photochemistry to biomass production under dynamic light ($\Phi_{e,C}$; Figure 5.3, Table 5.3) results from increased metabolic costs of elevated D1 turnover at high light in combination with the consequences of light limitation in the low light phases.

5.5.2 Ocean Acidification increases energy use efficiency under constant light

CO_2 has been shown to differentially affect SO diatoms on the species level (Boelen et al. 2011, Hoogstraten et al. 2012a, Hoogstraten et al. 2012b, Trimborn et al. 2013, Trimborn et al. 2014) as well as in natural communities (Tortell et al. 2008, Feng et al. 2010, Hoppe et al. 2013). The Antarctic diatom *C. debilis* was shown to exhibit increased energy use efficiencies (i.e. higher growth rates, but lower O_2 evolution) as well as decreased dark respiration under high pCO_2 and constant light (Trimborn et al. 2013, Trimborn et al. 2014). In the present study, C : N ratios were higher under OA and constant light, while growth rates and primary production (NPP) of *C. debilis* were only slightly stimulated under these conditions (Table 5.3, Figures 5.2 and 5.3). Similarly, two other species of *Chaetoceros* showed little or no

growth response to OA, but results seemed to also depend on the applied light levels (Boelen et al. 2011, Ihnken et al. 2011). In CO_2 manipulation experiments with SO phytoplankton communities, *Chaetoceros* was found to benefit from elevated pCO_2 as this genus dominated the applied OA treatments (Tortell et al. 2008, Feng et al. 2010). Such responses have often been attributed to the mode of CCMs, which can differ in the ability to reach rate-saturation and to respond to environmental changes as well as in the associated costs of these processes. In the case of diatoms, CCMs have been shown to be very effective avoiding carbon limitation, but also to be regulated as a function of external CO_2 concentration (e.g. Raven & Johnston 1991, Trimborn et al. 2009, Hopkinson et al. 2011). Elevated pCO_2 is thought to lead to a down-regulating of CCM activity, thereby reducing the overall costs of carbon acquisition (Burkhardt et al. 2001, Rost et al. 2003, Hopkinson et al. 2011). Even though Trimborn et al. (2013) observed a rather constitutively expressed CCM for *C. debilis*, it can be speculated that higher gross CO_2 uptake under elevated pCO_2 may have caused the observed stimulation in growth. In conclusion, the often documented beneficial OA effects at constant light may, to a large degree, be explained by overall lowered costs of the CCM.

Through the regulation of CCMs and RubisCO concentrations also photoacclimation can be influenced by CO_2 concentrations, as it changes the amount of electrons being used during carbon fixation (Tortell et al. 2000, Reinfelder 2011). Trimborn et al. (2014) showed strong effects of short-term exposure to low pCO_2 levels on various photophysiological parameters in *C. debilis*. In the current study, most photophysiological parameters such as NPQ_{490} or σ_{PSII} did not change. The connectivity between reaction centres ρ, however, decreased with increasing pCO_2 under constant light (Table 5.4), maybe indicating a decreased need for photoprotection. With respect to the balance between light and dark reaction of photosynthesis, however, we observed a significant decrease in $\Phi_{e,C}$ (Figure 5.3) with increasing pCO_2 under constant light. This implies that the Calvin cycle acts as a better energy sink under elevated pCO_2, as has been proposed by Trimborn et al. (2014). A significant decrease in $\Phi_{e,C}$ also means that the electron use efficiency increased, which could explain the beneficial effects of OA (Figures 5.2 and 5.3).

5.5.3 Dynamic light reverses the responses to Ocean Acidification

In line with previous findings on *Chaetoceros* (Boelen et al. 2011, Ihnken et al. 2011), we observed slight, yet insignificant enhancement in growth, POC production and NPP with increasing pCO_2 (Figures 5.2 and 5.3). In other studies, growth or NPP of *Chaetoceros* were strongly stimulated under elevated pCO_2 and constant light conditions (Tortell et al. 2008, Feng et al. 2010, Trimborn et al. 2013, Hoppe et al. 2013). When comparing these trends with the OA responses from the dynamic light treatments, a completely

different picture emerges: POC production and NPP decrease under OA by about 30 and 50%, respectively. The putatively beneficial effects of elevated pCO_2 seem not only to be dampened but even reversed under dynamic light as cells significantly slow down biomass production. Surprisingly, no such strong differences between light treatments were evident in the photophysiology under OA. For example, there was no sign of photoinhibition after short-term exposure to irradiances up to 650 μmol photons m^{-2} s^{-1} in any of the treatments (Figure SI5.1). At higher irradiances, however, rETRs in *C. debilis* were found to decrease (Trimborn et al. 2014). The photophysiological results therefore suggest that the excess capacity of photosynthesis (Behrenfeld et al. 1998) was sufficient to prevent chronic photoinhibition under the applied assay irradiances (Figure SI5.1). As these photophysiological results do not explain the decline in POC production and NPP observed under OA and dynamic light (Figure 5.2 and 5.3), the underlying reason may be associated with an imbalance between light and dark reactions of photosynthesis.

There is increasing evidence that diatoms are more susceptible to D1 inactivation and photoinhibition under OA compared to ambient pCO_2 levels (Wu et al. 2010, Gao et al. 2012a, McCarthy et al. 2012). Li & Campbell (2013) observed that under OA, *Thalassiosira pseudonana* has enhanced growth rates under low, but not high light, a finding that is in line with studies on cyanobacteria and coccolithophores (Kranz et al. 2010, Rokitta & Rost 2012). As photosynthesis progressively shifts from light towards carbon limitation under increasing irradiance, also the CCM activity needs to be increased under these conditions (Beardall 1991, Rost et al. 2006). The CCM, however, is typically down-regulated under OA (Burkhardt et al. 2001, Rost et al. 2003), which could restrict the capacity to rapidly sink more electrons in the Calvin cycle or to drain excess energy by HCO_3^- cycling under short-term high-light stress (Tchernov et al. 1997, Rost et al. 2006). This could cause a lower capability to cope with high light and may increase photoinactivation of PSII under OA (Beardall & Giordano 2002, Ihnken et al. 2011, Gao et al. 2012b), shifting the susceptibility towards photoinhibition to lower irradiances. The proposed mechanism implies that under dynamic light, cells exposed to higher pCO_2 levels experience high-light stress for longer time periods compared to cells grown under ambient pCO_2. Under constant light, no photoacclimation to high-light phases would be needed, so that the OA-induced surplus of energy could be directly used to build more biomass (Figure 5.2 and 5.3; Tortell et al. 2008, Trimborn et al. 2013). Under dynamic light, however, this extra energy may lead to higher metabolic costs for photoacclimation and D1 repair during high-light phases, which apparently cannot be compensated by lowered operational costs of CCMs, all together explaining the observed increase in $\Phi_{e,C}$ and decline in NPP (Figure 5.3).

Under the here applied conditions, *C. debilis* seems to be able to circumvent measurable photoinhibition, even though we speculate that this comes at a high cost, especially under OA combined with dynamic light. Under higher pCO_2 levels as well as higher average or more dynamic irradiances, however, OA may induce measurable damage to the photosynthetic apparatus in addition to presumably high metabolic costs incurring from D1 turnover and photosystems repair (Raven 2011, Li & Campbell 2013). Therefore, also the modulation of OA responses may vary depending on the light regime applied. Particularly, response pattern may also be modulated by depth-dependent changes in the spectral composition of light (Falkowski & LaRoche 1991), which were not investigated in the present study. In view of the generally high plasticity of photoacclimation in diatoms (Wagner et al. 2006, Lavaud et al. 2007), the here described interactive effects may be even more pronounced in other phytoplankton taxa. In any case, our data has demonstrated that a combination of OA and dynamic light may pose significantly more stress onto phytoplankton than previously thought.

5.5.4 Implications for ecology and biogeochemistry

Our results have important implications for the current understanding of OA effects on marine phytoplankton. Even though knowledge from studies obtained under constant light can be used to explain the responses under dynamic light, the strong modulation of OA responses is surprising and highlights the need to investigate both physiological (e.g. photophysiology) and integrated (e.g. growth rates) responses in multifactorial experimental approaches (Boyd & Hutchins 2012). As has been shown for several environmental variables such as temperature (Fu et al. 2007, Tatters et al. 2013) or nutrient concentrations (Fu et al. 2010, Lefebvre et al. 2012, Hoppe et al. 2013), interactive effects need to be considered when predicting future productivity and ecosystem functioning. As major characteristic of oceanic environments, dynamic light is an especially important aspect (Mitchell et al. 1991, MacIntyre 2000), which has been neglected in most OA studies so far. If our results are representative, the proposed CO_2 fertilisation may be dampened or even reversed in many natural environments. In this context, it is important to consider that anthropogenic CO_2 emissions do not only lead to OA, but also to a warming of the surface ocean (Sarmiento et al. 2004). A concomitant shoaling of the upper mixed layer would change the integrated intensity and variability of the light regimes phytoplankton cells encounter (Rost et al. 2008, Steinacher et al. 2010). The genus of *Chaetoceros* has been considered a potential winner of OA (Tortell et al. 2008, Trimborn et al. 2013). In view of the present study, however, potential winners would be species that benefit from easier carbon acquisition and are able to cope with potentially higher light stress under OA. This does not seem to be the case for *C. debilis*.

Regarding the SO, especially interactions between light and iron stress need to be considered (Boyd 2002, de Baar et al. 2005, Alderkamp et al. 2012). It is likely that synergistic effects of iron limitation and dynamic light, both dominant features of this region, jointly lower the potential benefits of OA. Even though difficult to obtain, more results on the interaction of these three drivers are desirable. Under iron-enriched conditions, as in the present study, diatom taxa such as *Chaetoceros* and *Fragilariopsis* have been shown to dominate OA treatments under constant light, suggesting higher potential for export production (Tortell et al. 2008, Hoppe et al. 2013). The lowered NPP under OA and dynamic light, however, questions the reliability of such predictions. Also the aspect of ballasting has to be considered, as siliceous frustules make diatoms efficient vectors for carbon (Sartou et al. 2005). In line with Milligan et al. (2004), we observed a decline in both cellular BSi quotas and production rates with increasing pCO_2 (Table 5.3, Figure 5.2), which further argue against a stimulation of the biological carbon pump. Up to now, the effects of dynamic light on OA-responses observed in this study were unknown. This knowledge will change our perception of phytoplankton under climate change.

Acknowledgements

We would like to thank D. Campbell, N. Schuback as well as two anonymous reviewers for very helpful comments on an earlier version of this manuscript. We also would like to thank T. Brenneis, J. Hölscher, U. Richter, N. Schuback and S. Beszteri for laboratory assistance. C.J.M.H. and B.R. were funded by the European Research Council (ERC) under the European Communitys Seventh Framework Programme (FP7 2007-2013), ERC grant agreement no. 205150. L.-M.H. was funded by the German Federal Ministry of Education and Research, project ZeBiCa^2 (31P7279). S.T. was funded by the Helmholtz Impulse Fond (HGF Young Investigator Group EcoTrace).

5.6 References

Alderkamp, A.-C., Kulk, G., Buma, A.G.J., Visser, R.J.W., Van Dijken, G.L., Mills, M.M. & Arrigo, K.R. (2012) The effect of iron limitation on the photophysiology of *Phaeocystis antarctica* (Prymnesiophyceae) and *Fragilariopsis cylindrus* (Bacillariophyceae) under dynamic iradiance. Journal of Phycology 48, 45-59

Asada, K. (1999) The waterwater cycle in chloroplasts: scavenging of active oxygens and dissipation of excess photons. Annual Review of Plant Physiology and Plant Molecular Biology, 50, 601639

Arrigo, K. R., Mills, M. M., Kropuenske, L. R., van Dijken, G. L., Alderkamp, A.-C. & Robinson, D. H. (2010) Photophysiology in two major Southern Ocean phytoplankton taxa: Photosynthesis and growth of *Phaeocystis antarctica* and *Fragilariopsis cylindrus* under different irradiance levels. Integrative and Comparative Biology, 50, 950-966

Badger, M.R., Andrews, T.J., Whitney, S.M., Ludwig, M., Yellowlees, D.C., Leggat, W. & Price, G.D. (1998) The diversity and coevolution of Rubisco, plastids, pyrenoids, and chloroplast-based CO_2-concentrating mechanisms in algae. Canadian Journal of Botany-Revue Canadienne De Botanique, 76(6), 1052-1071

Badger, M.R., von Caemmerer, S., Ruuska, S. & Nakano, H. (2000) Electron flow to oxygen in higher plants and algae: rates and control of direct photoreduction (Mehler reaction) and rubisco oxygenase. Philosophical Transactions of the Royal Society of London, 355, 1433-1446

Beardall, J. (1991) Effects of photon flux density on the 'CO_2-concentrating mechanism' of the cyanobacterium *Anabaena variabilis*. Journal of Plankton Research, 13, 133-141

Beardall, J. & Giordano, M. (2002) Ecological implications of microalgal and cyanobacterial CO_2 concentrating mechanisms, and their regulation. Functional Plant Biology, 29(3), 335-347

Behrenfeld, M., Prásil, O., Kolber, Z., Babin, M. & Falkowski, P. (1998) Compensatory changes in Photosystem II electron turnover rates protect photosynthesis from photoinhibition. Photosynthesis Research, 58(3), 259-268

Behrenfeld, M.J., Prásil, O., Babin, M. & Bruyant, F. (2004) In search of a physiological basis for covariations in light-limited and light-saturated photosynthesis. Journal of Phycology, 40(1), 4-25

Behrenfeld, M.J., Halsey, K.H. & Milligan, A.J. (2008) Evolved physiological responses of phytoplankton to their integrated growth environment. Philosophical Transactions of the Royal Society, 363, 2687-2703

Boelen, P., van de Poll, W.H., van der Strate, H.J., Neven, I.A., Beardall, J. & Buma, A.G.J. (2011) Neither elevated nor reduced CO_2 affects the photophysiological performance of the

marine Antarctic diatom *Chaetoceros brevis*. Journal of Experimental Marine Biology and Ecology, 406(1-2), 38-45

Boyd, P.W. (2002) Environmental factors controlling phytoplankton processes in the Southern Ocean. Journal of Phycology 38, 844-861

Brewer, P.G., Bradshaw, A.L. & Williams, R.T. (1986) Measurement of total carbon dioxide and alkalinity in the North Atlantic ocean in 1981, in: Trabalka, J.R., Reichle, D.E. (Eds.), The Changing Carbon Cycle −A Global Analysis Springer Verlag, Heidelberg Berlin, pp. 358381

Brzezinski, M.A., Villareal, T.A. & Lipschultz, F. (1998) Silica production and the contribution of diatoms to new and primary production in the central North Pacific. Marine Ecology Progress Series, 167, 89-104

Burkhardt, S., Amoroso, G., Riebesell, U. & Sültemeyer, D. (2001) CO_2 and HCO_3^- uptake in marine diatoms acclimated to different CO_2 concentrations. Limnology and Oceanography, 46, 1378-1391

de Baar et al. (2005) Synthesis of iron fertilization experiments: From the Iron Age in the Age of Enlightenment. Journal of Geophysical Research, 110(C9), C09S16

Denman, K.L. & Gargett, A.E. (1983) Time and space scales of vertical mixing and advection of phytoplankton in the upper ocean. Limnology and Oceanography, 28(5), 801-815

Dickson, A.G. (1990) Standard potential of the reaction: AgCl(s) + 1/2 H_2(g) = Ag(s) + HCl(aq), and the standard acidity constant of the ion HSO_4- in synthetic seawater from 273.15 to 318.15 K. Journal of Chemical Thermodynamics, 22, 113-127

Dickson, A.G. & Millero, F.J. (1987) A comparison of the equilibrium constants for the dissociation of carbonic acid in seawater media. Deep-Sea Research, 34, 1733 1743

Dickson, A.G., Sabine, C.L. & Christian, J.R. (2007) Guide to best practices for ocean CO_2 measurements. PICES Special Publication 3, pp. 191

Falkowski, P.G. & LaRoche, J. (1991) Acclimation to spectral irradiance in algae. Journal of Phycology, 27, 8-14

Falkowski, P.G. & Raven, J.A. (1997) Aquatic photosynthesis, Blackwell Publishers

Feng, Y., Warner, M.E., Zhang, Y., Sun, J., Fu, F.-X., Rose, J.M. & Hutchins, D.A. (2008) Interactive effects of increased pCO_2, temperature and irradiance on the marine coccolithophore *Emiliania huxleyi* (Prymnesiophyceae). European Journal of Phycology, 43(1), 87 - 98

Feng et al. (2010) Interactive effects of iron, irradiance and CO_2 on Ross Sea phytoplankton. Deep Sea Research Part I: Oceanographic Research Papers, 57(3), 368-383

Fu, F.X., Warner, M.E., Zhang, Y., Feng, Y., & Hutchins, D.A. (2007) Effects of increased temperature and CO_2 on photosynthesis, growth, and elemental ratios in marine *Synechococcus* and *Prochlorococcus* (Cyanobacteria). Journal of Phycology, 43(3), 485-496

Fu, F.X., Place, A.R., Garcia, N.S. & Hutchins, D.A. (2010) CO_2 and phosphate availability control the toxicity of the harmful bloom dinoflagellate *Karlodinium veneficum*. Aquatic Microbial Ecology, 59(1), 55-65

Gao, K. et al. (2012a) Rising CO_2 and increased light exposure synergistically reduce marine primary productivity. Nature Climate Change, 2(7), 519-523

Gao, K., Helbling, E.W., Häder, D.-P. & Hutchins, D.A. (2012b) Responses of marine primary producers to interactions between ocean acidification, solar radiation, and warming. Marine Ecology Progress Series, 470, 167-189

Genty, B., Briantais, J.-M. & Baker, N.R. (1989) The relationship between the quantum yield of photosynthetic electron transport and quenching of chlorophyll fluorescence. Biochimica et Biophysica Acta, 990, 87-92

Guillard, R.R.L. & Ryther, J.H. (1962) Studies of marine planktonic diatoms. I. *Cyclothella nana* Hustedt and *Detonula confervacea* Cleve Canadian Journal of Microbiology, 8, 229-239

Gurney et al. (2004) Transcom 3 inversion intercomparison: Model mean results for the estimation of seasonal carbon sources and sinks. Global Biogeochemical Cycles, 18(1), GB1010

Hoogstraten, A., Timmermans, K.R. & de Baar, H.J.W. (2012a) Morphological and physiological effects in *Proboscia alata* (Bacillariophyceae) grown under different light and CO_2 concentrations of the modern Southern Ocean. Journal of Phycology, 48(3), 559-568

Hoogstraten, A., Peters, M., Timmermans, K. R. & de Baar, H. J. W. (2012b) Combined effects of inorganic carbon and light on *Phaeocystis globosa* Scherffel (Prymnesiophyceae). Biogeosciences, 9, 1885-1896

Hoppe, C.J.M., Langer, G., Rokitta, S.D., Wolf-Gladrow, D.A. & Rost, B. (2012) Implications of observed inconsistencies in carbonate chemistry measurements for ocean acidification studies. Biogeosciences 9, 24012405

Hoppe, C.J.M., Hassler, C.S., Payne, C.D., Tortell, P.D., Rost, B. & Trimborn, S. (2013) Iron limitation modulates ocean acidification effects on Southern Ocean phytoplankton communities. PLoSONE, 8(11): e79890

Hopkinson, B.M., Dupont, C.L., Allen, A.E. & Morel, F.M.M. (2011) Efficiency of the CO_2-concentrating mechanism of diatoms. Proceedings of the National Academy of Sciences 108, 3830-3837

Ihnken, S., Eggert, A. & Beardall, J. (2010) Exposure times in rapid light curves affect photosynthetic parameters in algae. Aquatic Botany, 93(3), 185-194

Ihnken, S., Roberts, S. & Beardall, J. (2011) Differential responses of growth and photosynthesis in the marine diatom *Chaetoceros muelleri* to CO_2 and light availability. Phycologia, 50(2), 182-193

Jin, P., Gao, K., Villafañe, V.E., Campbell, D.A. & Helbling, E.W. (2013) Ocean Acidification alters the photosynthetic responses of a coccolithophorid to fluctuating ultraviolet and visible radiation. Plant Physiology, 162(4), 2084-2094

Kaffes, A., Thoms, S. Trimborn, S. Rost, B., Langer, G. Richter, K.-U. Khler, A. Norici, A. & Giordano, M. (2010) Carbon and nitrogen fluxes in the marine coccolithophore *Emiliania huxleyi* grown under different nitrate concentrations. Journal of Experimental Marine Biology and Ecology, 393, 1-8

Khatiwala, S., Primeau, F. & Hall, T. (2009) Reconstruction of the history of anthropogenic CO_2 concentrations in the ocean. Nature, 462(7271), 346-349

Knap, A., Michaels, A., Close, A., H., D. & Dickson, A.e. (1996) Protocols for the Joint Global Ocean Flux Study (JGOFS) Core Measurements. In JGOFS Report Nr. 19, UNESCO, pp. 170

Kolber, Z.S., Prásil, O. & Falkowski, P.G. (1998) Measurements of variable chlorophyll fluorescence using fast repetition rate techniques. I. Defining methodology and experimental protocols. Biochem. Biophys. Acta, 1367, 88-106

Koroleff, F. (1983) Determination of silicon. In Methods of Seawater Analysis, K. Grasshoff, M. E., K. Kremling (ed.), Verlag Chemie, Weinheim pp. 174183

Kramer, D.M., Cruz, J.A. & Kanazawa, A. (2003) Balancing the central roles of the thylakoid proton gradient. Trends in plant science, 8(1), 27-32

Kranz, S.A., Levitan, O., Richter, K.-U., Pril, O., Berman-Frank, I. & Rost, B. (2010) Combined Effects of CO_2 and Light on the N_2-Fixing Cyanobacterium *Trichodesmium* IMS101: Physiological Responses. Plant Physiology, 154(1), 334-345

Kromkamp, J.C. & Forster, R.M. (2003) The use of variable fluorescence measurements in aquatic ecosystems: differences between multiple and single turnover measuring protocols and suggested terminology. European Journal of Phycology, 38, 103-112

Kropuenske, L.R., Mills, M.M., van Dijken, G.L., Bailey, S., Robinson, D.H., Welschmeyer, N.A. & Arrigo, K.R. (2009) Photophysiology in two major Southern Ocean phytoplankton taxa: Photoprotection in *Phaeocystis antarctica* and *Fragilariopsis cylindrus*. Limnology and Oceanography, 54(4), 1176-1196

Langer, G., Nehrke, G., Probert, I., Ly, J. & Ziveri, P. (2009) Strain-specific responses of *Emiliania huxleyi* to changing seawater carbonate chemistry. Biogeosciences, 6, 2637-2646

Lavaud, J., Strzepek, R. F. & Kroth, P. G. (2007) Photoprotection capacities differ among plankton diatoms: Possible consequence on their spatial distribution related to fluctuations in the underwater light climate. Limnology and Oceanography, 52, 1188-1194

Lawrenz, E., Silsbe, G., Capuzzo, E., Ylöstalo, P., Forster, R.M., Simis, S.G.H., Pril, O., Kromkamp, J.C., Hickman, A.E., Moore, C.M., Forget, M.-H., Geider, R.J. & Suggett, D.J.

(2013) Predicting the Electron Requirement for Carbon Fixation in Seas and Oceans. PLoS ONE, 8, e58137

Lefebvre, S.C., Benner, I., Stillman, J.H., Parker, A.E., Drake, M.K., Rossignol, P.E., Okimura, K.M., Komada, T. & Carpenter, E.J. (2012) Nitrogen source and pCO_2 synergistically affect carbon allocation, growth and morphology of the coccolithophore *Emiliania huxleyi*: potential implications of ocean acidification for the carbon cycle. Global Change Biology, 18(2), 493-503

Li, G. & Campbell, D.A. (2013) Rising CO_2 interacts with growth light and growth rate to alter photosystem II photoinactivation of the coastal diatom *Thalassiosira pseudonana*. PLoS ONE, 8(1), e55562

MacIntyre, H.L., Kana, T.M. & Geider, R.J. (2000) The effect of water motion on short-term rates of photosynthesis by marine phytoplankton. Trends in Plant Science, 5(1), 12-17

Marinov, I., Gnanadesikan, A., Toggweiler, J.R. & Sarmiento, J.L. (2006) The Southern Ocean biogeochemical divide. Nature, 441(7096), 964-967

Marshall, H.L., Geider, R.J. & Flynn, K.J. (2000) A Mechanistic Model of Photoinhibition. New Phytologist, 145(2), 347-359

Martin, J.H. (1990) Glacial-interglacial CO_2 change: The Iron Hypothesis. Paleoceanography, 5(1), 1-13

McCarthy, A., Rogers, S.P., Duffy, S.J. & Campbell, D.A. (2012) Elevated carbon dioxide differentially alters the photophysiology of *Thalassiosira pseudonana* (Bacillariophyceae) and *Emiliania huxleyi* (Haptophyta). Journal of Phycology, 48(3), 635-646

McKew, B.A., Davey, P., Finch, S.J., Hopkins, J., Lefebvre, S.C., Metodiev, M.V., Oxborough, K., Raines, C.A., Lawson, T. & Geider, R.J. (2013) The trade-off between the light-harvesting and photoprotective functions of fucoxanthin-chlorophyll proteins dominates light acclimation in *Emiliania huxleyi* (clone CCMP 1516). New Phytologist, 200, 74-85.

Mehrbach, C., Culberson, C.H., Hawley, J.E. & Pytkowicz, R.M. (1973) Measurement of the apparent dissociation constants of carbonic acid in seawater at atmospheric pressure. Limnology and Oceanography, 18, 897907

Milligan, A.J., Varela, D.E., Brzezinski, M.A. & Morel, F.M.M. (2004) Dynamics of Silicon Metabolism and Silicon Isotopic Discrimination in a Marine Diatom as a Function of pCO_2. Limnology and Oceanography, 49(2), 322-329

Mills, M. M., Kropuenske, L. R., van Dijken, G. L., Alderkamp, A.-C., Berg, G. M., Robinson, D. H., Welschmeyer, N. A. & Arrigo, K. R. (2010) Photophysiology in two Southern Ocean phytoplankton taxa: Photosynthesis of *Phaeocystis antarctica* (Prymnesiophyceae) and *Fragilariopsis cylindrus* (Bacillariopyceae) under simulated mixed-layer irradiance. Journal of Phycology, 46, 1114-1127

Mitchell, B.G., Brody, E.A., Holm-Hansen, O., McClain, C. & Bishop, J. (1991) Light limitation of phytoplankton biomass and macronutrient utilization in the Southern Ocean. Limnology and Oceanography, 36(8), 1662-1677

Moore, J.K., Abbott, M.R., Richman, J.G. & Nelson, D.M. (2000) The southern ocean at the Last Glacial Maximum: A strong sink for atmospheric carbon dioxide. Global Biogeochemical Cycles, 14(1), 455-475

Nelson, D.M. & Smith, W.O.J. (1991) Sverdrup revisited: Critical depths, maximum chlorophyll levels, and the control of Southern Ocean productivity by the irradiance-mixing regime. Limnology and Oceanography, 36, 1650-1661

Nelson, D.M., Treguer, P., Brzezinski, M.A., Leynaert, A. & Queguiner, B. (1995) Production and dissolution of biogenic silica in the ocean - revised global estimates, comparison with regional data and relationship to biogenic sedimentation. Global Biogeochemical Cycles, 9(3), 359-372

Oxborough, K. (2012) FastPro8 GUI and FRRf3 systems documentation. Chelsea Technologies Group Ltd

Oxborough, K., Moore, C.M., Suggett, D.J., Lawson, T., Chan, H.G. & Geider, R.J. (2012) Direct estimation of functional PSII reaction center concentration and PSII electron flux on a volume basis: a new approach to the analysis of Fast Repetition Rate fluorometry (FRRf) data. Limnology and Oceanography Methods, 10, 142-154

Pierrot, D.E., Lewis, E. & Wallace, D.W.R. (2006) MS Exel Program Developed for CO_2 System Calculations, (ORNL/CDIAC-105a). Carbon Dioxide Information Analysis Centre, O. R. N. L. ed. US Department of Energy

Prásil, O., Kolber, Z., Berry, J. & Falkowski, P. (1996) Cyclic electron flow around Photosystem II in vivo. Photosynthesis Research, 48(3), 395-410

Raven, J.A. (2011) The cost of photoinhibition. Physiologia Plantarum, 142(1), 87-104

Raven, J.A. & Johnston, A.M. (1991) Mechanisms of inorganic-carbon acquisition in marine phytoplankton and their implications for the use of other resources. Limnology and Oceanography, 36(8), 1701-1714

Reinfelder, J.R. (2011) Carbon Concentrating Mechanisms in Eukaryotic Marine Phytoplankton. Annual Review of Marine Science, 3(1), 291-315

Riebesell, U., Wolf-Gladrow, D.A. & Smetacek, V. (1993) Carbon dioxide limitation of marine phytoplankton growth rates. Nature, 361(6409), 249-251

Rokitta, S.D. & Rost, B. (2012) Effects of CO_2 and their modulation by light in the life-cycle stages of the coccolithophore *Emiliania huxleyi*. Limnology and Oceanography, 57(2), 607-618

Rost, B., Riebesell, U., Burkhardt, S. & Sültemeyer, D. (2003) Carbon acquisition of bloom-forming marine phytoplankton. Limnology and Oceanography, 48, 55 - 67

Rost, B., Riebesell, U., & Sültemeyer, D. (2006) Carbon acquisition of marine phytoplankton: Effect of photoperiod length. Limnology and Oceanography 51(1), 12-20

Rost, B., Zondervan, I. & Wolf-Gladrow, D. (2008) Sensitivity of phytoplankton to future changes in ocean carbonate chemistry: current knowledge, contradictions and research directions. Marine Ecology Progress Series, 373, 227-237

Sakshaug, E., Slagstad, D. & Holm-Hansen, O. (1991) Factors controlling the development of phytoplankton blooms in the Antarctic Ocean a mathematical model. Marine Chemistry 35, 259-271

Sarmiento, J.L., Slater, R., Barber, R., Bopp, L., Doney, S.C., Hirst, A.C., Kleypas, J., Matear, R., Mikolajewicz, U., Monfray, P., Soldatov, V., Spall, S.A. & Stouffer, R. (2004) Response of ocean ecosystems to climate warming. Global Biogeochemical Cycles, 18(3), GB3003

Sarthou, G., Timmermans, K.R., Blain, S. & Trguer, P. (2005) Growth physiology and fate of diatoms in the ocean: a review. Journal of Sea Research, 53(12), 25-42

Shatwell, T., Nicklisch, A. & Khler, J. (2012) Temperature and photoperiod effects on phytoplankton growing under simulated mixed layer light fluctuations. Limnology and Oceanography, 57(2), 541-553

Sigman, D.M., Hain, M.P. & Haug, G.H. (2010) The polar ocean and glacial cycles in atmospheric CO_2 concentration. Nature, 466(7302), 47-55

Silsbe, G.M. & Kromkamp, J.C. (2012) Modeling the irradiance dependency of the quantum efficiency of photosynthesis. Limnology and Oceanography Methods, 10, 645-652

Smith Jr, W. O., Tozzi, S. , Long, M. C., Sedwick, P. N., Peloquin, J. A., Dunbar, R. B., Hutchins, D. A., Kolber, Z. & DiTullio, G. R. (2013) Spatial and temporal variations in variable fluoresence in the Ross Sea (Antarctica): Oceanographic correlates and bloom dynamics. Deep Sea Research Part I: Oceanographic Research Papers, 79, 141-155

Steinacher, M., Joos, F., Frlicher, T. L., Bopp, L., Cadule, P., Cocco, V., Doney, S. C., Gehlen, M., Lindsay, K., Moore, J. K., Schneider, B. & Segschneider, J. (2010) Projected 21st century decrease in marine productivity: a multi-model analysis. Biogeosciences, 7, 979-1005

Stoll, M.H.C., Bakker, K., Nobbe, G.H. & Haese, R.R. (2001) Continous-flow analysis of dissolved inorganic carbon content in seawater. Analytical Chemistry, 73(17), 4111-4116

Su, W., Jakob, T. & Wilhelm, C. (2012) The impact of nonphotochemical quenching of fluorescence on the photon ballance in diatoms under dynamic light conditions. Journal of Phycology, 48(2), 336-346

Suggett, D.J., MacIntyre, H.L., Kana, T.M. & Geider, R.J. (2009) Comparing electron transport with gas exchange: parameterising exchange rates between alternative photosynthetic currencies for eukaryotic phytoplankton. Aquatic Microbial Ecology, 56, 147-162

Sugie, K. & Yoshimura, T. (2013) Effects of pCO_2 and iron on the elemental composition and cell geometry of the marine diatom *Pseudo-nitzschia pseudodelicatissima* (Bacillariophyceae). Journal of Phycology, 49(3), 475488

Takahashi et al. (2002) Global sea-air CO_2 flux based on climatological surface ocean pCO_2, and seasonal biological and temperature effects. Deep Sea Research Part II: Topical Studies in Oceanography, 49, 1601-1622

Takahashi et al. (2009) Climatological mean and decadal change in surface ocean pCO_2, and net sea-air CO_2 flux over the global oceans. Deep Sea Research Part II: Topical Studies in Oceanography, 56(810), 554-577

Tatters, A.O., Roleda, M.Y., Schnetzer, A., Fu, F., Hurd, C.L., Boyd, P.W., Caron, D.A., Lie, A.A.Y., Hoffmann, L.J. & Hutchins, D.A. (2013) Short- and long-term conditioning of a temperate marine diatom community to acidification and warming. Philosophical Transactions of the Royal Society B: Biological Sciences, 368(1627)

Taylor, A.R., Chrachri, A., Wheeler, G., Goddard, H. & Brownlee, C. (2011) A voltage-gated H^+ channel underlying pH homeostasis in calcifying coccolithophores. PLoS Biol, 9(6), e1001085

Tchernov, D., Hassidim, M., Luz, B., Sukenik, A., Reinhold, L. & Kaplan, A. (1997) Sustained net CO_2 evolution during photosynthesis by marine microorganism. Current Biology 7, 723-728

Thamatrakoln, K., Bailleul, B., Brown, C.M., Gorbunov, M.Y., Kustka, A.B., Frada, M., Joliot, P.A., Falkowski, P.G. & Bidle, K.D. (2013) Death-specific protein in a marine diatom regulates photosynthetic responses to iron and light availability. Proceedings of the National Academy of Sciences, 110, 20123-20128

Tortell, P.D. (2000) Evolutionary and ecological perspectives on carbon acquisition in phytoplankton. Limnology and Oceanography, 45(3), 744-750

Tortell, P.D., Payne, C.D., Li, Y., Trimborn, S., Rost, B., Smith, W.O., Riesselman, C., Dunbar, R.B., Sedwick, P. & DiTullio, G.R. (2008) CO_2 sensitivity of Southern Ocean phytoplankton. Geophysical Research Letters, 35(4), L04605

Trimborn, S., Lundholm, N., Thoms, S., Richter, K.-U., Krock, B., Hansen, P.J. & Rost, B. (2008) Inorganic carbon acquisition in potentially toxic and non-toxic diatoms: the effect of pH-induced changes in seawater carbonate chemistry. Physiologia Plantarum, 133(1), 92-105

Trimborn, S., Brenneis, T., Sweet, E. & Rost, B. (2013) Sensitivity of Antarctic phytoplankton species to ocean acidification: Growth carbon aquisition, and species interaction. Limnology and Oceanography, 58, 997-1007

Trimborn, S., Thoms, S., Petrou, K., Kranz, S. A. & Rost, B. (2014) Photophysiological responses of Southern Ocean phytoplankton to changes in CO_2 concentrations: Short-term versus acclimation effects. Journal of Experimental Marine Biology and Ecology, 451: 44-45

van de Poll, W.H., Visser, R.J.W. & Buma, A.G.J. (2007) Acclimation to a dynamic irradiance regime changes excessive irradiance sensitivity of *Emiliania huxleyi* and *Thalassiosira weissflogii*. Limnology and Oceanography, 52(4), 1430-1438

van Leeuwe, M.A., van Sikkelerus, B., Gieskes, W.W.C. & Stefels, J. (2005) Taxon-specific differences in photoacclimation to fluctuating irradiance in an Antarctic diatom and a green flagellate. Marine Ecology-Progress Series, 288, 9-19

Volk, T. & Hoffert, M. I. (1985) Ocean carbon pumps: analysis of relative strengths and efficiencies in ocean-driven atmospheric CO_2 changes. In The carbon cycle and atmospheric CO_2: natural variation archean to present, eds. Sunquist, E. T. & Broecker, W. p. 99 - 110. Washington, D.C: American Geophysical Union, Geophysical Monographs

Wagner, H., Jakob, T. & Wilhelm, C. (2006) Balancing the energy flow from captured light to biomass under fluctuating light conditions. New Phytologist, 169(1), 95-108

Waring, J., Klenell, M., Bechtold, U., Underwood, G.J.C. & Baker, N.R. (2010) Light-induced responses of oxygen photoreduction, reactive oxygen species production and scavenging in two diatom species. Journal of Phycology, 46, 1206-1217.

Wilson, K.E., Ivanov, A.G., Quist, G., Grodzinski, B., Sarhan, F. & Huner, N.P.A. (2006) Energy balance, organellar redox status, and acclimation to environmental stress. Canadian Journal of Botany, 84, 1355-1370.

Wu, Y., Gao, K. & Riebesell, U. (2010) CO_2-induced seawater acidification affects physiological performance of the marine diatom *Phaeodactylum tricornutum*. Biogeosciences, 7(9), 2915 - 2923

Supporting Information:

Table 5.5: Cellular quotas and ratios statistics - Results from two-way ANOVAs for all measured acclimation parameters. The significance level was set to p values <0.05.

Source of variation	μ		**C:N**		**Chl *a*: POC**	
	F	**p**	**F**	**p**	**F**	**p**
light	50.9	<0.001	2.4	0.160	0.2	0.797
pCO_2	0.1	0.757	4.8	0.06	2.4	0.158
light × pCO_2	2.3	0.164	4.4	0.071	0.1	0.993

Source of variation	**Chl *a* cell^{-1}**		**POC cell^{-1}**		**PON cell^{-1}**		**BSi cell^{-1}**	
	F	**p**	**F**	**p**	**F**	**p**	**F**	**p**
light	5.5	0.047	3.7	0.093	1.0	0.358	8.5	0.020
pCO_2	27.6	<0.001	3.1	0.116	13.7	0.006	38.1	<0.001
light × pCO_2	21.0	0.002	8.9	0.018	2.4	0.158	2.8	0.136

Source of variation	**Chl *a* cell^{-1} day^{-1}**		**POC cell^{-1} day^{-1}**		**PON cell^{-1} day^{-1}**		**BSi cell^{-1} day^{-1}**	
	F	**p**	**F**	**p**	**F**	**p**	**F**	**p**
light	56.2	<0.001	30.9	<0.001	22.6	0.001	89.7	<0.001
pCO_2	18.0	0.003	1.5	0.261	11.1	0.010	38.3	<0.001
light × pCO_2	24.8	0.001	12.9	0.007	3.8	0.086	1.0	0.339

Table 5.6: Chl *a*-fluorescence based parameters - Results from two-way ANOVAs for measured Chl *a*- fluorescence-based parameters, net primary production and the electron requirement for carbon fixation. The significance level was set to p values <0.05.

Source of variation	**F_v/F_m**		**σ_{PSII}**		**ρ**		**τ**	
	F	**p**	**F**	**p**	**F**	**p**	**F**	**p**
light	4.2	0.064	1.9	0.199	49.9	<0.001	1.4	0.257
pCO_2	0.0	1	0.5	0.5	5.5	0.036	1.2	0.288
light × pCO_2	0.5	0.510	1.9	0.190	0.2	0.702	1.5	0.243

Source of variation	**F_q'/F_m'**		**σ_{PSII}'**		**ρ'**		**τ'**	
	F	**p**	**F**	**p**	**F**	**p**	**F**	**p**
light	165	<0.001	2.9	0.112	87.6	<0.001	1.5	0.239
pCO_2	0.1	0.819	1.6	0.226	0.1	0.938	0.7	0.432
light × pCO_2	0.1	0.819	0.3	0.594	0.2	0.969	0.4	0.555

Source of variation	**ETR_{max}**		**I_K**		**α**		**NPQ_{490}**	
	F	**p**	**F**	**p**	**F**	**p**	**F**	**p**
light	0.3	0.622	4.6	0.065	37.1	<0.001	0.2	0.694
pCO_2	1.1	0.336	2.3	0.166	2.1	0.182	4.9	0.058
light × pCO_2	1.1	0.336	0.4	0.559	0.1	0.808	0.1	0.821

Source of variation	**ETR_{24h}**		**NPP**		**$\Phi_{e,C}$**	
	F	**p**	**F**	**p**	**F**	**p**
light	5.3	0.050	26.6	<0.001	117.1	<0.001
pCO_2	0.1	0.912	0.1	0.905	1.8	0.222
light × pCO_2	3.5	0.100	6.9	0.028	28.0	<0.001

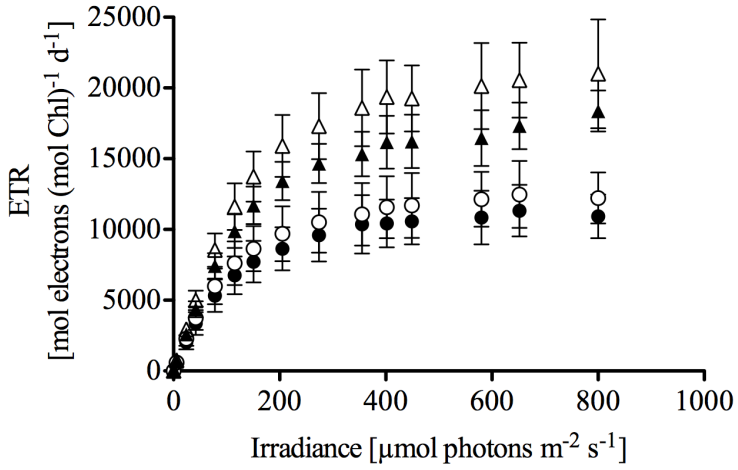

Figure 5.4: - Night time development of Chl *a*-specific ETR with increasing irradiance from constant (filled circles) and dynamic light treatments (filled triangles) at 390 μatm pCO_2 as well as from constant (open circles) and dynamic light treatments (open triangles) at 1000 μatm pCO_2 (n=3).

Chapter 6

Publication IV

Controls of primary production in two phytoplankton blooms in the Antarctic Circumpolar Current

Controls of primary production in two phytoplankton blooms in the Antarctic Circumpolar Current

Hoppe, C.J.M.[1]*, Ossebaar, S.[3], Soppa, M. A.[1], Cheah, W.[1], Klaas, C.[1], Rost, B.[1], Wolf-Gladrow, D.[1], Hoppema, M.[1], Bracher, A.[1,2], Strass, V.[1], de Baar, H.J.W.[3], and Trimborn, S.[1]

[1]Alfred Wegener Institute - Helmholtz Centre for Polar and Marine Research, 27570 Bremerhaven, Germany

[2]Institute of Environmental Physics, University Bremen, 28359 Bremen, Germany

[3]NIOZ - Royal Netherlands Institute for Sea Research, 't Horntje (Texel), The Netherlands

*** Corresponding author (Clara.Hoppe@awi.de)**

To be submitted to Deep-Sea Research II

6.1 Abstract

The Antarctic Circumpolar Current has a high potential for primary production and carbon sequestration through the biological pump. Development of phytoplankton blooms in this area is controlled by a complex interaction of light, iron and silica limitation as well as a strong impact of grazing. In the current study, two large-scale blooms were characterised with respect to standing stocks, primary production and nutrient budgets. While net primary productivity was similar in both blooms, chlorophyll *a*-specific photosynthesis was more efficient in the bloom closer to the island of South Georgia (39°W, 50°S) compared to the bloom further east (12°W, 51°S). Nutrient deficit ratios indicated a higher dependence on regenerated nutrients at 12°W compared to 39°W, leading to a lower potential of the biological pump. Differences between the two blooms could be explained by their distance to the shelf and concomitant differences in iron availability.

Keywords: Biological pump; nutrient deficits; Southern Ocean; primary productivity

6.2 Introduction

The phytoplankton populations of the world's oceans account for about half of the global primary production, providing the basis of marine food webs and exerting a major control on biogeochemical cycles and global climate (Field et al. 1998, Falkowski et al. 1998). The concentrations of nutrients such as nitrate, phosphate and silicic acid do not only define an upper limit of phytoplankton productivity, but also determine the potential of the biologically-mediated export of organic material to the deep ocean, the so-called biological pump (Volk and Hoffert 1985, Longhurst and Harrison 1989). Its strength generally depends on the degree to which these nutrients are consumed and recycled in the surface ocean as well as the ratio of carbon relative to these nutrients in the organic matter sinking to depth (Sigman and Hain 2012). According to the concept of Dugdale and Goering (1967), on larger spatial and temporal scales, only an increase in new production (i.e. production based on the uptake of inorganic nutrients being newly brought into the euphotic zone) can lead to both, larger standing stocks of higher trophic levels and an increase in the strength of the biological carbon pump (Jenkins and Goldman 1985, Falkowski et al. 1998). Primary production based on recycled nutrients (e.g. the use of regenerated nitrogen sources such as ammonia) is thought to have no net effect on the biological carbon pump (Dugdale and Goering 1967), even though a decoupling between carbon and nitrogen in sinking matter can change this picture on shorter temporal scales (Coale et al. 4004, Smetacek et al. 2012).

One area with a great potential for an increase in both new and total production is the region of the Antarctic Circumpolar Current (ACC). As concentrations of nitrate and phosphate are high, primary production is limited by other controlling factors (Priddle et al. 1992, Moore et al. 2000a). More specifically, productivity in the ACC region is considered to be controlled by complex interactions between light (Mitchell and Holm-Hansen 1991, Nelson and Smith 1991), iron (Martin 1990, de Baar et al. 1995) as well as silica limitation (Brzezinski et al. 2003), and the effect of grazing (Dubischar and Bathmann 1997, Atkinson et al. 2001). Changes in these factors are thought to alter productivity and carbon sequestration, thereby influencing atmospheric CO_2 concentrations on geological timescales (Moore et al. 2000b, Sigman et al. 2010). On the one hand, light-limitation due to deep mixed layers as well as low availability of iron and other trace metals restrain phytoplankton biomass build-up in the open ocean areas of the ACC for most part of the year (de Baar et al. 1995, Bathmann et al. 1997). On the other hand, large phytoplankton blooms do occur and account for a significant proportion of the global primary production and substantial export of organic matter to depth (Schlitzer 2002). Phytoplankton blooms in open ocean areas of the ACC tend to occur downstream of land masses and have been associated with fronts, islands and bathymetric

features, which increase the input of iron and other trace metals into the surface waters and also positively affect water column stability (Moore et al. 1999, Blain et al. 2001, Strass et al. 2002, Borrione and Schlitzer 2013). In the Atlantic sector of the Southern Ocean, high phytoplankton standings stocks and production rates have been observed in the Antarctic Polar Frontal zone (APF; Read et al. 1995; Bathmann et al. 1997; Bracher et al. 1999, Moore and Abbott 2000, Tremblay et al. 2002). It has been proposed that, in the APF, an alleviation of light-limitation in spring leads to the development of phytoplankton blooms after deep-mixing in winter. The termination of blooms is often caused by a combination of grazing pressure as well as iron and silica limitation (Abbott et al. 2000, Tremblay et al. 2002).

The effects of these controlling factors are not only difficult to disentangle, they also interact with each other (e.g. iron limitation decreases photoadaptive capabilities, thereby affecting light limitation; Sunda and Huntsman 1997). The aim of the present study was therefore to characterise two different large-scale phytoplankton blooms in the APF region with respect to biomass, primary production and nutrient usage in order to understand how different environmental factors influence ACC phytoplankton blooms and their potential for carbon sequestration.

6.3 Material and methods

6.3.1 Cruise track and sampling locations

Sampling was conducted in the framework of the 'Eddy-Pump' project during the ANT-XXVIII/3 expedition on-board *RV Polarstern*. Between January and March 2011, the cruise covered 121 stations, which were distributed on a transect along 10°E between 44°S and 53°S as well as in two survey areas, one located around 12°W, 51°S and the other around 38°W, 50°S. In addition to physical properties, nutrient and chlorophyll a (Chl *a*) concentrations, primary production was determined at 10 stations in a bloom area at 50 - 52°S and 13.5 - 11.5°W (hereafter 12°W bloom) and 9 stations in a bloom area at 48 - 52°S and 37 - 39°W (hereafter 39°W bloom; Figure 6.1). All water samples were obtained from Niskin bottles attached to the Conductivity Temperature Depth (CTD) rosette at different depth (10, 20, 40, 60, 80 and 100 m).

6.3.2 Nutrient measurements and nutrient deficiency calculations

Macronutrients were measured colorimetrically using a ship-board Technicon TRAACS 800 auto-analyzer (Seal Analytics). Ortho-phosphate ($PO_4{}^{3-}$) was measured at 880 nm after the formation of molybdophosphate-complexes (Murphy and Riley 1962). Ortho-silicate ($Si(OH)_4$) was measured at 820 nm after formation of silica-molybdenum complexes with oxalic acid being added to prevent the formation of phosphate-molybdenum (Strickland and Parsons 1968). After nitrate reduction through a copperized cadmium coil, nitrate plus nitrite ($NO_3{}^- + NO_2{}^-$) was measured at 550 nm after complexation with sulphanylamide and naphtylethylene-diamine (Grasshoff et al. 1983). Complex formation without the reduction step was used to determine nitrite concentrations. Nitrate is calculated by subtracting the nitrite value from the 'NO_3+NO_2' value (Grasshoff et al. 1983).

Prior to analysis, all samples and standards were brought to 22°C in about 2h; concentrations were recorded in μmol L^{-1} at this temperature. Calibration standards were diluted from stock solutions of the different nutrients in 0.2 μm filtered low nutrient seawater. During every run, a daily freshly diluted mixed nutrient standard, containing silicate, phosphate and nitrate, the so-called 'NIOZ nutrient cocktail', was measured in triplicate. Every 2 weeks, a sterilized 'Reference Material Nutrient Sample' (JRMNS, Kanso Technos, Japan) containing known concentrations of silicate, phosphate, nitrate and nitrite in Pacific Ocean water was analyzed in triplicate. The cocktail and the JRMNS were both used to monitor the performance of the analyzer. Finally, the NIOZ nutrient cocktail was used to adjust all data by means of a correction factor. The average standard deviation of

the NIOZ nutrient cocktail measurements were 0.02 μmol L^{-1} for phosphate, 0.59 μmol L^{-1} for silicate and 0.13 μmol L^{-1} for nitrate (n=113).

Surface nutrient concentrations were calculated as the average of the measured values for 10-60 m sampling depth, accounting for differences in sampling frequency with increasing depth. Nutrient deficits for each station were calculated as the differences between the nutrient concentration in remnant Antarctic Winter Water (AWW) in the layer below the seasonal pycnocline and the average concentrations above (Jennings et al. 1984, Rubin et al. 1998, Hoppema et al. 2000). The latter were calculated from nutrient measurements integrating 10-120 m depths. It should be noted that nutrient deficits are suitable estimates for annual net community production only if vertical and lateral mixing in both the temperature minimum and the surface layer are small (Jennings et al. 1984, Hoppema et al. 2000, Hoppema et al. 2007). The AWW layer, which is characterised by a well-defined potential temperature minimum visible in CTD profiles, was situated at 150 ±20 m water depth during the present cruise. Deficit ratios presented in the paper are calculated by averaging the quotients of the nutrient deficits at each station.

6.3.3 Irradiance estimates

Solar irradiance was measured using a RAMSES hyperspectral radiometer (TriOS GmbH) placed at the monkey deck of the ship to avoid shading. The sensor measured downwelling incident sunlight from 350 nm to 950 nm with a spectral resolution of about 3.3 nm. Plane photosynthetically active radiation (PAR) was calculated as the integral of irradiances at 400 nm to 700 nm. Prior to the summation, the measurements at each wavelength were converted from energy content per time [W m^{-2} s^{-1}] to photon content per time [μmol photons m^{-2} s^{-1}] using the Planck's equation. The integrated PAR [μmol photons m^{-2} d^{-1}] to which samples in the on-deck incubator were exposed, was calculated based on the incubation time of each sample.

6.3.4 Chlorophyll *a*

Chl *a* concentrations were determined by two methods: Fluorometry (Chl a_{FLUO}) and high performance liquid chromatography (HPLC; Chl a_{HPLC}). Except for stations PS79/160 and PS79/175, where Chl a_{FLUO} data is used, Chl a_{HPLC} data are used for Chl *a* estimates. The two Chl *a* data sets of this cruise produced similar results, showing a significant correlation with hardly any differences (r^2=0.98, p<0.01, n=104, Chl a_{HPLC} = 0.978* Chl a_{FLUO} - 0.0584).

For the Chl a_{FLUO} determination, samples were filtered onto 25 mm diameter GF/F filters (Whatman) at a vacuum of <100 mmHg. Filters were immediately transferred into

centrifuge tubes containing 10 mL of 90% acetone and 1 cm^3 of glass beads. The tubes were sealed and stored at -20°C for at least 30 min and up to 24 h. Chl *a* was extracted by placing the centrifuge tubes in a grinder for 3 min followed by centrifugation at 0°C. The supernatant was poured into quartz tubes and the Chl *a* content was quantified in a 10-AU fluorometer (Turner). Calibration of the fluorometer was carried out at the beginning and at the end of the cruise, diverging by 2%. Chl *a* content was calculated using the equation given in Knap et al. (1996) and the average parameter values from the two calibrations.

For the Chl a_{HPLC} determination, water samples were shock-frozen in liquid nitrogen and stored at -80°C until analysis in the home laboratory following the method described by Hoffmann et al. (2006) adjusted as detailed by Taylor et al. (2011). For calculating Chl a_{HPLC} the sum of concentrations of monovinyl- and divinyl chlorophyll *a* and chlorophyllide a (divinyl chlorophyll *a* was not detected in our samples) was taken.

6.3.5 Particulate organic carbon and nitrogen

Samples for particulate organic carbon (POC) and nitrogen (PON) were filtered onto pre-combusted (15h, 500°C) glass fibre filters (GF/F 0.6 μm nominal pore size; Whatman). Filters were stored at -20°C and processed according to Lorrain et al. (2003). Analysis was performed using a CHNS-O elemental analyser (Euro EA 3000, HEKAtech).

6.3.6 Primary Production

Net primary production (NPP) rates were determined in duplicate by the incubation of 20 mL seawater sample spiked with 20 μCi $NaH^{14}CO_3$ (53.1 mCi $mmol^{-1}$; Perkin Elmer) in a 20 mL glass scintillation vial for 24h in a seawater cooled on-deck incubator. Seawater samples were incubated at different irradiances for 24h on-deck. Irradiance levels were achieved with neutral density filters decreasing incoming PAR to 25, 12.5, 6.3, 3.1, 1.6 and 0.8%.

After the addition of the $NaH^{14}CO_3$ spike, 0.1 ml aliquots were immediately removed and mixed with 10 mL of scintillation cocktail (Ultima Gold AB, PerkinElmer). After 2h, these samples were counted with a liquid scintillation counter (Tri-Carb 2900TR, PerkinElmer) to determine the total amount of added $NaH^{14}CO_3$ (100%). For blank determination, one additional replicate per sample was immediately acidified with 0.5 ml 6N HCl. After the outdoor incubation of the samples over 24h, ^{14}C incorporation was stopped by adding 0.5 ml 6N HCl to each vial. The vials were then left to degas overnight, thereafter 15 ml of scintillation cocktail (Ultima Gold AB) were added and samples were measured after 2h with the same liquid scintillation counter. NPP rates [mg C m^{-3} d^{-1}] at each sample depth were calculated as follows:

$$\text{NPP [mg C m}^{-3}\text{ d}^{-1}] = ([\text{DIC}] \times (\text{DPM}_{\text{sample}} - \text{DPM}_{\text{blank}}) \times 1.05)/(\text{DPM}_{100\%} \times \text{t}) \quad (6.1)$$

where DIC is the concentration of dissolved inorganic carbon [μmol kg^{-1}], t is the incubation time [days], DPM$_{blank}$, DPM$_{sample}$ and DPM$_{100\%}$ are the disintegration per minute measured by the scintillation counter for the blank, the sample and the determination of the total amount of added NaH^{14}CO$_3$, respectively. Chl *a*-specific carbon fixation (P^b [mg C [mg Chl *a*]$^{-1}$ d^{-1}]) was calculated by dividing the depth-specific NPP value by the depth-specific Chl *a* concentrations. Column-integrated NPP and P^b were derived by integrating values for 100 m depth.

^{14}C-based photosynthesis-irradiance (PI) curves were conducted with samples from 20 and 60 m water depth. Samples were prepared and measured as those for the 24h incorporation experiments. The PI samples were placed for 1 h in a temperature controlled (3 $\pm$0.5°C) photosynthetron equipped with warm-white light-emitting diodes (LEDs; Avago Technologies) providing light intensities of 15, 30, 50, 80, 200, and 500 μmol photons m^{-2} s^{-1}. Light intensities were measured using a LI-1400 data logger (Li-Cor) equipped with a 4π-sensor (Walz). Irradiance-dependent behaviour of Chl *a*-specific carbon fixation was described by fitting the data to the following equation (Kaffes et al. 2010):

$$\text{P}^{\text{b}} = \text{P}^{\text{b}}_{\text{max}} * (1 - \text{e}^{-(\alpha/\text{P}^{\text{b}}_{\text{max}})*(\text{I}-\text{I}_{\text{K}})}) \quad (6.2)$$

where Pb is the Chl *a*-specific rate of carbon fixation [mg C [mg Chl *a*]$^{-1}$ d^{-1}] at a given light, P$^b_{max}$ is the light-saturated, maximal Chl *a*-specific carbon fixation [mg C (mg Chl *a*)$^{-1}$ d^{-1}], α is light-use efficiency [(mg Chl *a*)$^{-1}$ m^2 s^{-1} μmol photons^{-1}], I is the irradiance [μmol photons m^{-2} s^{-1}] and I$_K$ is the light saturation index [μmol photons m^{-2} s^{-1}].

6.3.7 Satellite chlorophyll *a* maps

Weekly satellite maps of Chl *a* were used to study the development of the blooms. The comparison of satellite derived Chl *a* concentrations with the in-situ values measured at the two bloom locations was based on daily maps. The Chl *a* maps were derived using the POLYMER level-3 product of the Medium Resolution Imaging Spectrometer (MERIS) data at 0.02° spatial resolution (Steinmetz et. al. 2011). POLYMER is an improved atmospheric correction algorithm for pixels contaminated by sun glint, thin clouds or heavy aerosol plumes and therefore is providing better spatial coverage than using operational Chl *a* data product from MERIS, SeaWiFS, MODIS and the merged GlobColour Chl *a* data product of these

three satellite sensors. The Chl *a* concentrations are retrieved using the standard OC4Me algorithm (Morel et al. 2007).

6.4 Results

6.4.1 Temporal and spatial development of the blooms

During late austral summer 2011/12, two large-scale phytoplankton blooms were observed in the APF zone (Figure 6.1 A). The in-situ Chl *a* concentrations were plotted on top of the satellite Chl *a*, averaged for the time when the in-situ samples were taken. The Chl *a* data from both data sets are in very good agreement, showing a nearly perfect match for the 12°W bloom. A reasonable agreement was observed for the 39°W bloom north of South Georgia, where the satellite data underestimated especially the high Chl *a* values in that area.

In case of the 12°W bloom (Figure 6.1 C), satellite Chl *a* maps indicated that the bloom developed in mid December 2011 and peaked in the first two weeks of January 2012 with Chl *a* concentrations of around 3 mg m^{-3}. Our in-situ sampling took place between January 26th and February 15th, in the declining phase of the bloom. Within these three weeks, a

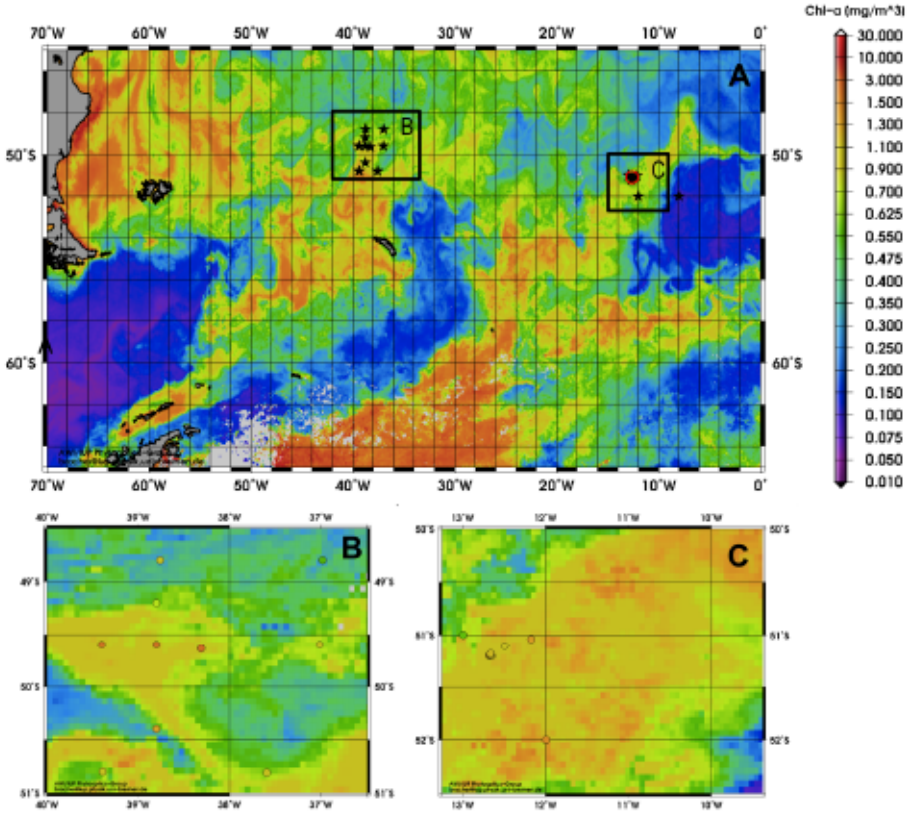

Figure 6.1: - Mean Chl a concentrations (mg m^{-3}) during February 2012 derived from satellite MERIS Polymer product. Stars indicate sampling locations during the ANT-XXVIII/3 cruise. Detailed view on the 39°W bloom north of South Georgia (B) and the 12°W bloom (C); red circle indicates time-series station.

central station in the initial centre (at 12°6'W, 51°2'S) of the 12°W bloom was re-visited six times to investigate the temporal development of the bloom. The satellite data indicated Chl *a* concentration were <1 mg Chl *a* m^{-3} everywhere in the area within 5 days after the last sampling day. The second phytoplankton bloom (Figure 6.1 A, B) was located in the Georgia Basin, north of the island of SG at 48 - 52°S and 41 - 3°W. Satellite Chl *a* maps indicated that the 39°W bloom developed already in mid October and peaked in mid December with surface Chl *a* concentrations reaching values higher than 3 mg Chl *a* m^{-3}. Sampling took place between February 16th and March 3rd, in the declining phase of the bloom. Satellite data indicates that Chl *a* concentrations above 0.5 mg Chl *a* m^{-3} persisted at least until mid March. The investigations of this bloom were focussed on the spatial rather than the temporal variability, with stations being located within a larger grid of oceanographic stations.

6.4.2 Phytoplankton standing stocks and primary production

While the Chl *a* standing stocks, i.e. 100 m-depth integrated Chl *a* concentrations (Table 6.1), were as low as 9 mg m^{-2} outside the 12°W bloom area, the concentrations in the bloom ranged from 52 to 118 mg Chl *a* m^{-2} and were on average 120 ±41 mg Chl *a* m^{-2}. NPP (Table 6.1) in this bloom was on average 1751 ±747 mg C m^{-2} d^{-1} and ranged from 796 to 2816 mg C m^{-2} d^{-1}, all being much higher than those measured outside the bloom area (161 mg C m^{-2} d^{-1}). Chl *a*-specific carbon fixation P^b (Table 6.1), a measure of photosynthetic efficiency, varied between 10.1 and 17.3 mg C [mg Chl *a*]$^{-1}$ d^{-1} (on average 14.4 ±2.6 mg C [mg Chl *a*]$^{-1}$ d^{-1}) in the 12°W bloom. The average 100 m integrated POC:PON ratios (Table 6.2) in this area were 4.6 ±0.4 mol POC (mol PON)$^{-1}$. Average daily PAR during primary production measurements in the 12°W bloom was 12.3 ±5.1 mol photons m^{-2} d^{-1}.

In the 39°W bloom north of SG, Chl *a* standing stocks (Table 6.1) ranged from 25 to 129 mg Chl *a* m^{-2}, with an average of 63 ±29 mg Chl *a* m^{-2}. NPP (Table 6.1) in this region varied between 573 and 3023 mg C m^{-2} d^{-1} (on average 1365 ±832 mg C m^{-2} d^{-1}). With measured values between 14.4 and 30.3 mg C [mg Chl *a*]$^{-1}$ d^{-1} and an average of 19.4 ±5.5 mg C [mg Chl *a*]$^{-1}$ d^{-1}, P^b in the 39°W bloom area was significantly higher compared to the 12°W bloom (Table 6.1, t-test, T= 2.447, p=0.027). In the 39°W bloom, 100m integrated POC:PON ratios (Table 6.2) in this area were on average 4.3 ±0.3 mol POC (mol PON)$^{-1}$. Average daily PAR during primary production measurements in this bloom was 15.7 ±6.1 mol photons m^{-2} d^{-1}.

Exemplary Chl *a*-specific PI curves with samples from 20 m and 60 m depth of both blooms revealed a high level of variability between stations within one bloom area (Figure 6.2). In addition, $P^b{}_{max}$ measured the 12°W bloom area was higher in the surface samples compared to the deep samples, while the opposite trend was observed in the 39°W bloom.

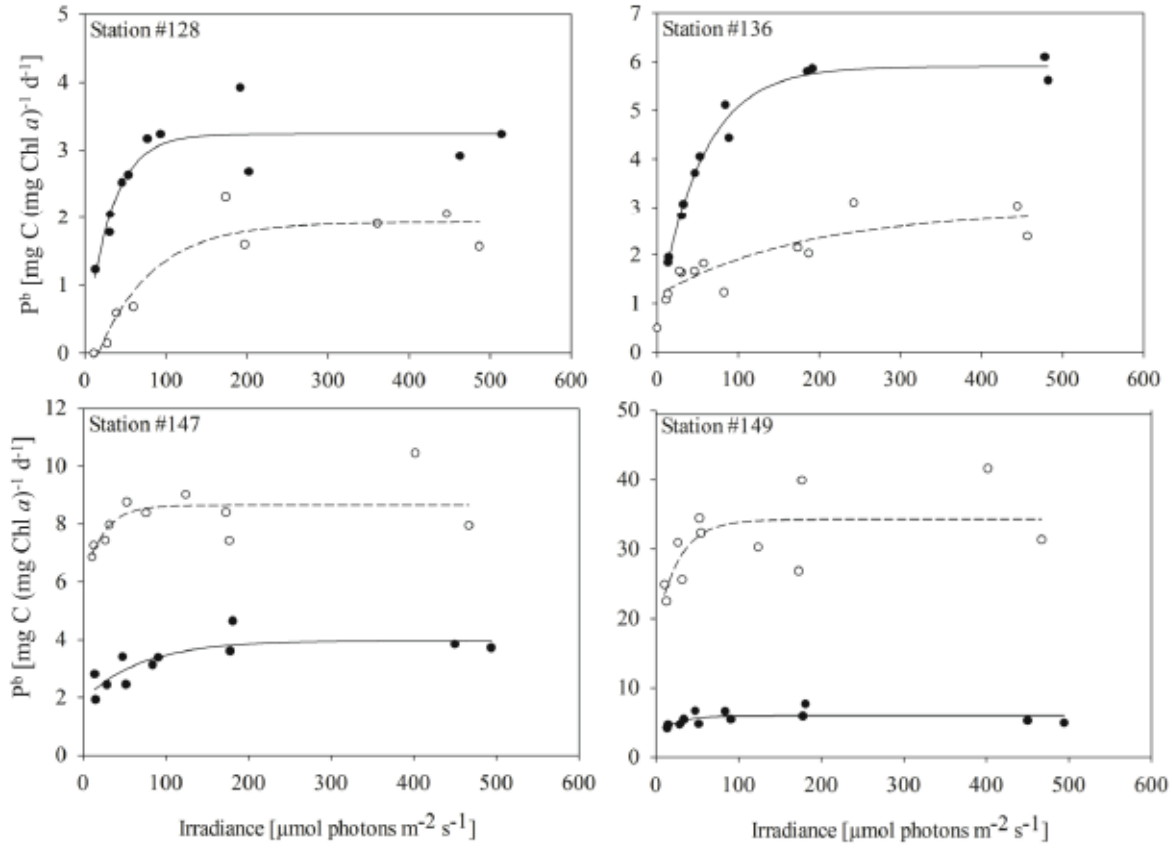

Figure 6.2: - Exemplary Chl *a*-specific photosynthesis-irradiance curves with curve fits for samples from 20 m (closed symbols; solid fit curve) and 60 m depth (open symbols; dashed fit curve) from the 12°W bloom (A, B) and the 39°W bloom (C, D).

Table 6.1: 100m depth-integrated Chl *a* standing stocks [mg Chl *a* m^{-2}], primary production [mg C m^{-2} d^{-1}], photosynthetic efficiency Pb [mg C (mg Chl *a*)$^{-1}$ d^{-1}], total PAR during on-deck incubations [μmol photons m^{-2} d^{-1}]. n.d. denotes missing data, $\star$ denote central station in 12°W bloom.

Area	Station	Date	Long °W	Lat °S	Chl *a*	NPP	P^b	PAR
Outstation	PS79/085-3	26.01.12	8.00	52.00	9	161	17.6	14.45
12°W bloom	PS79/086-2	29.01.12	11.99	52.00	180	2587	14.4	11.27
12°W bloom	PS79/091-5$\star$	03.02.12	12.67	51.21	166	2816	17.0	16.40
12°W bloom	PS79/114-1$\star$	08.02.12	12.67	51.20	143	2447	17.1	18.75
12°W bloom	PS79/128-10$\star$	12.02.12	12.65	51.21	117	1669	14.2	13.80
12°W bloom	PS79/136-8$\star$	14.02.12	12.66	51.20	85	1050	12.3	17.03
12°W bloom	PS79/137-7	15.02.12	12.17	51.04	136	1380	10.1	8.68
12°W bloom	PS79/138-2	15.02.12	12.49	51.11	88	1020	11.5	5.65
12°W bloom	PS79/139-3	15.02.12	12.99	51.00	52	796	15.4	6.01
12°W bloom	PS79/140-12$\star$	17.02.12	12.66	51.19	115	1998	17.3	19.31
39°W bloom	PS79/147-1	25.02.12	37.01	49.60	54	n.d.	n.d.	15.58
39°W bloom	PS79/149-1	25.02.12	36.98	48.80	25	573	22.7	13.17
39°W bloom	PS79/155-1	26.02.12	37.59	50.81	60	769	12.8	5.28
39°W bloom	PS79/160-1	27.02.12	38.80	50.40	n.d.	640	n.d.	5.27
39°W bloom	PS79/165-5	28.02.12	39.40	49.60	89	1644	18.4	17.29
39°W bloom	PS79/168-1	29.02.12	38.76	48.80	73	1052	14.4	20.29
39°W bloom	PS79/169-1	29.02.12	38.80	49.20	39	786	20.3	19.06
39°W bloom	PS79/170-1	29.02.12	38.80	49.60	129	2220	16.1	19.61
39°W bloom	PS79/174-9	01.03.12	38.31	49.64	100	3023	30.3	17.76
39°W bloom	PS79/175-1	03.03.12	39.39	50.80	79	1575	20.0	19.49

6.4.3 Nutrient concentrations and deficits

In the area of the 12°W bloom, average surface nutrient concentrations (10 m depth, Figure 6.3) were 19.7 ±0.3 mmol NO_3 m^{-3}, 1.3 ±0.1 mmol PO_4 m^{-3}, and 4.1 ±3.1 mmol $Si(OH)_4$ m^{-3}. The average nutrient concentrations of the euphotic zone (10-60 m, Table 6.2) were 20.56 ±0.47 mmol NO_3 m^{-3}, 1.42 ±0.05 mmol PO_4 m^{-3}, and 6.63 ±2.68 mmol $Si(OH)_4$ m^{-3}. Average integrated nutrient deficits (Table 6.2) in this area were 1087 ±108 mmol NO_3 m^{-2}, 75 ±7 mmol PO_4 m^{-2}, and 2712 ±303 mmol $Si(OH)_4$ m^{-2}. Calculated $Si(OH)_4$:NO_3 deficit ratios were 2.5 ±0.3 and NO_3:PO_4 deficit ratios were 14 ±1(Table 6.2; Figure 6.4).

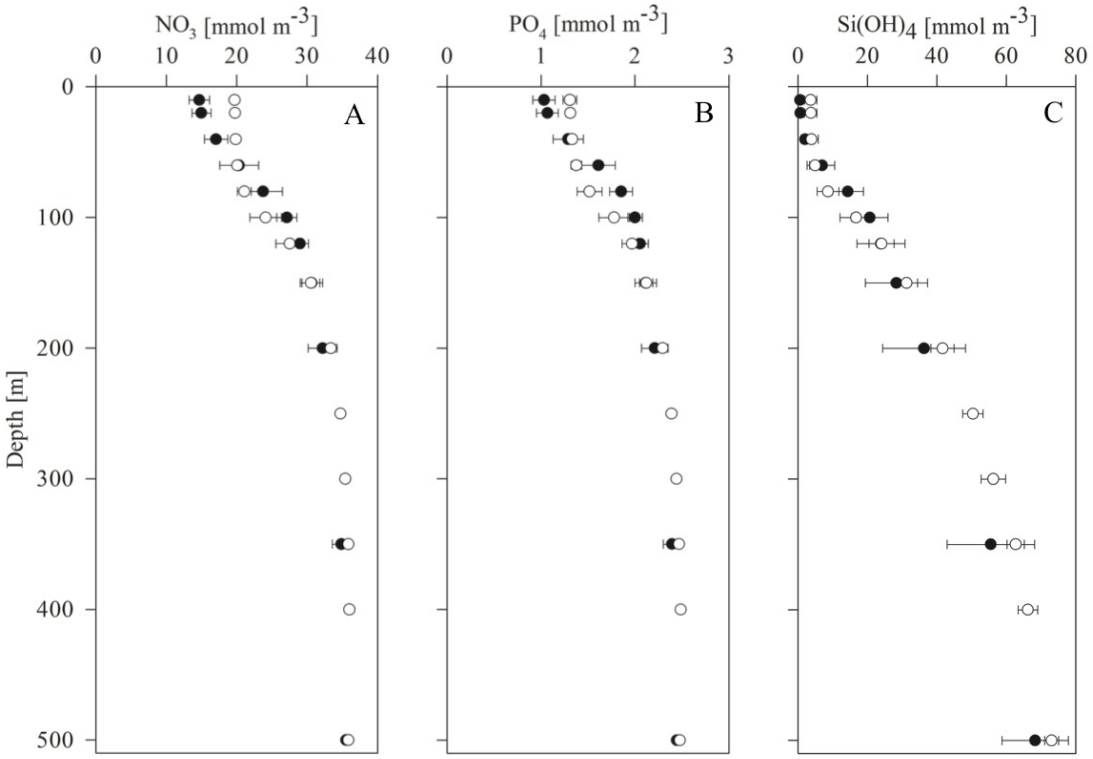

Figure 6.3: - Average profiles of nitrate (A), phosphate (B) and silicate (C) in the top 500 m from the 12°W bloom (open symbols) and the 39°W bloom north of South Georgia (filled symbols).

Table 6.2: Comparison of average (± 1 s.d.) estimates as phytoplankton biomass, productivity and POC:PON ratios as well as average 10-60 m nutrient concentrations and deficit ratios for the two bloom areas investigated.Values denote average (± 1 s.d.)

Parameter	**12°W bloom area**		**39°W bloom**	
Chl *a* [mg Chl *a* m^{-2}]	120 ±41	(n=9)	63 ±29	(n=8)
Primary production [mg C m^{-2} d^{-1}]	1751 ±747	(n=9)	1365 ±832	(n=9)
P^b [mg C (mg Chl *a*)$^{-1}$ d^{-1}]	14 ±3	(n=9)	19 ±5	(n=8)
POC:PON [μg:μg]	4.6 ±0.4	(n=23)	4.3 ±0.3	(n=28)
Total PAR [μmol photons m^{-2} d^{-1}]	12.2 ±5.1	(n=9)	15.7 ±6.1	(n=9)
NO_3 [mmol m^{-3}]	19.9 ±0.5	(n=33)	16.3 ±1.8	(n=28)
PO_4 [mmol m^{-3}]	1.3 ±0.1	(n=33)	1.2 ±0.1	(n=28)
$SiOH_4$ [mmol m^{-3}]	4.5 ±3.1	(n=33)	2.2 ±1.3	(n=28)
NO_3 deficit [mmol m^{-2}]	1087 ±108	(n=33)	1219 ±307	(n=28)
PO_4 deficit [mmol m^{-2}]	75 ±7	(n=33)	67 ±18	(n=28)
$SiOH_4$ deficit [mmol m^{-2}]	2712 ±303	(n=33)	2359 ±631	(n=28)
NO_3:PO_4 deficit	14.4 ±2.5	(n=33)	18.1 ±1.6	(n=28)
$SiOH_4$:NO_3 deficit	2.5 ±0.3	(n=33)	1.9 ±0.4	(n=28)

In the 39°W bloom area, average surface (10 m) nutrient concentrations (Figure 6.3) were 14.9 ±1.8 mmol NO_3 m^{-3}, 1.0 ±0.1 mmol PO_4 m^{-3}, and 0.6 ±0.5 mmol $Si(OH)_4$ m^{-3}. Average nutrient concentrations of the euphotic zone (10-60 m, Table 6.2) were 16.3 ±1.8 mmol NO_3 m^{-3}, 1.2 ±0.1 mmol PO_4 m^{-3} and 2.2 ±1.3 mmol $Si(OH)_4$ m^{-3}. Resulting average integrated surface nutrient deficits (Table 6.2) in the 39°W bloom area were 1219 ±307 mmol NO_3 m^{-2}, 68 ±18 mmol PO_4 m^{-2} and 2359 ±631 mmol $Si(OH)_4$ m^{-2}, resulting in $Si(OH)_4$:NO_3 deficit ratios of 1.9 ±0.4 and NO_3:PO_4 deficit ratios of 17 ±1 in this region (Table 6.2; Figure 6.4). Due to the high variability, no significant differences in nutrient concentrations or deficits were observed (Table 6.2). The ratios of $Si(OH)_4$:NO_3 deficits (Table 6.2; Figure 6.4), however, were significantly higher in the 39°W area compared to the 12°W bloom (t-test, $p<0.001$), while the ratios of NO_3:PO_4 deficits were significantly lower at 39°W (t-test, $p<0.001$).

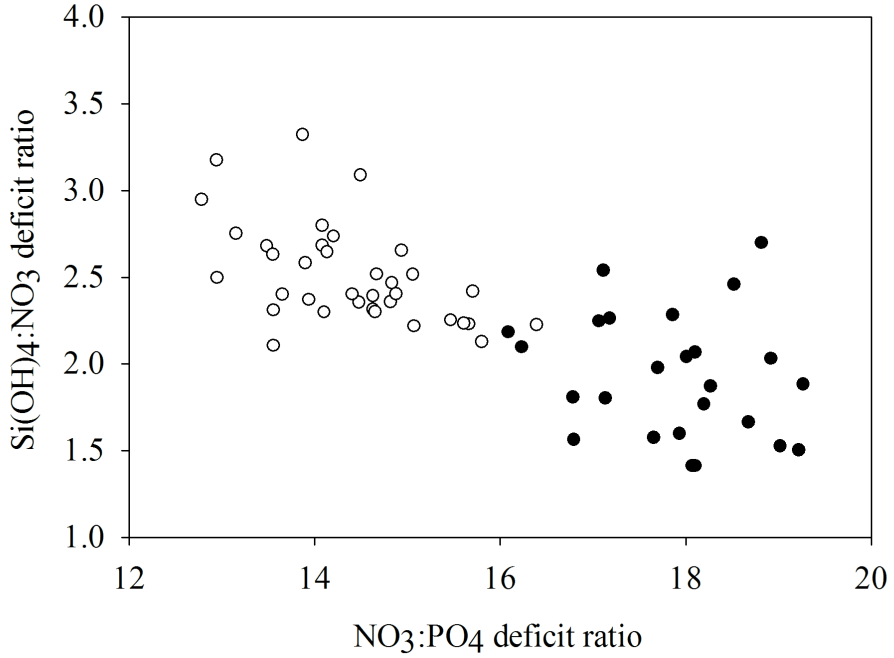

Figure 6.4: - Deficiency ratios for $Si(OH)_4$:NO_3 versus NO_3:PO_4 for all stations in the 12°W bloom (open symbols) and the 39°W bloom (filled symbols).

6.5 Discussion

6.5.1 High variability of primary production in the APF region

During the presented cruise, two large-scale phytoplankton blooms in the Atlantic sector of the ACC were observed (Figure 6.1). Both blooms were located between 50°S and 52°S in the APF region. In fact, phytoplankton blooms regularly develop in this region during spring and summer (e.g. Laubscher et al. 1993, Bathmann et al. 1997, Tremblay et al. 2002). The occurrence of blooms in SO frontal zones has been associated with their oceanographic features such as meanders, mesoscale eddies and west-east zonal flow, which can both lead to increased iron and silicate availability and high vertical stability of the water column (de Jong et al. 1998, Bracher et al. 1999, Strass et al. 2002, Tremblay et al. 2002), thereby alleviating nutrient and light limitation for phytoplankton growth.

Being a highly productive area within the otherwise high-nutrient low-chlorophyll (HNLC) region, the APF has been the destination of many research cruises and gained considerable attention over the past decades. Estimates of primary production vary between 100 and 6000 mg C m^{-2} d^{-1} (El-Sayed et al. 1983, Mitchell and Holm-Hansen 1991, Bracher et al. 1999, Moore and Abbott 2000, Strass et al. 2002, Tremblay et al. 2002, Hiscock et al. 2003, Vaillancourt et al. 2003, Korb and Whitehouse 2004, Park et al. 2010). The data observed in the present study (about 160 - 3020 mg C m^{-2} d^{-1}; Table 6.1) are highly variable, but fall well within this range. Generally, Antarctic phytoplankton productivity in this region has been reported to exhibit strong spatial (Veth et al. 1992, Arrigo et al. 1998), seasonal (Smith et al. 2000, Hiscock et al. 2003) and inter-annual variations (Clarke and Leakey 1996, Park et al. 2010). Sporadic and patchy sampling during research cruises therefore makes it difficult to measure the specific productivity. These sampling opportunities are nonetheless useful to investigate the variability of productivity in the region.

During sampling in the 12°W bloom, one station in the initial centre of the bloom was investigated over a 2 weeks period (Figure 6.1, Table 6.1). Estimates of primary production at this central sampling station varied between 1050 and 2816 mg C m^{-2} d^{-1} (Table 6.1). The observed temporal variability, which was lower than the spatial variability in the 12°W region (796 - 2816 mg C m^{-2} d^{-1}), probably reflects a combination of the changes in light availability due to cloud cover as well as the movement of water masses. The development of the phytoplankton bloom was also an important factor, as a primary production decreased over time indicating bloom erosion (Table 6.1). During the investigations of the 39°W bloom, special emphasis was put on the spatial variability of productivity (Figure 6.1, Table 6.1). In this bloom, primary production varied stronger compared to the first area (573 - 3023 mg C m^{-2} d^{-1}; Table 6.1), which next to temporal aspects could be explained by the higher

spatial coverage. Nonetheless, even at three consecutive stations sampled on the same day (PS79/168-70) and within half a degree distance to each other, primary production varied between 786 and 2220 mg C m^{-2} d^{-1} (Table 6.1), demonstrating significant small-scale variability in the 39°W bloom area.

The high degree of variability, both spatial and temporal, emphasises once more the difficulties in estimating the productivity in this highly dynamic region (Abbott et al. 2000). Even though satellite Chl *a* estimates have drawbacks compared to in-situ measurements (Schlitzer 2002, Korb and Whitehouse 2004, Whitehouse et al. 2008), they provide higher spatial and temporal coverage of phytoplankton biomass at mesoscale resolution. The satellite Chl *a* from the MERIS Polymer-Chl-product used in this study has been validated globally and regionally within the current ESA Climate Change Initiative for Ocean colour and was chosen as the best algorithm for MERIS data processing (Brewin et al. in press, Müller et al. in revision). A comparison of surface Chl *a* concentrations (<10m) derived by HPLC measurements with MERIS Polymer Chl *a* from the same day and within the respective satellite pixel revealed a reasonable correlation coefficient ($r^2 = 0.67$), low bias (0.17 mg m^{-3}) and percent error (33%) between the two data sets. Therefore, the quality of the satellite Chl *a* data is sufficient to allow for reconstructing the temporal and spatial development of the two phytoplankton blooms at the surface.

As satellite Chl *a* data only cover the oceans surface layer (i.e. the first optical depth), primary production estimates can only be derived using a model that incorporate satellite-based estimates of Chl *a*, sea surface temperature and PAR (e.g. Antoine and Morel 1996). Shipboard data are therefore needed to verify satellite-derived products and to give information on the layers lower than the first optical depth. Regarding ^{14}C-based estimates, they tend to overestimate primary production due to the exclusion of loss terms (e.g. sinking, grazing) and biases in applied irradiance (e.g. Gall et al. 2001). Nonetheless, they can be used to investigate the underlying mechanisms for the patterns observed in satellite-derived maps.

6.5.2 Similarities and differences between the two blooms

In the following, the two blooms are compared based on their general characteristics rather than investigating differences between single stations because their relationship to the environmental conditions have to be considered on a wider scale.

In terms of depth-integrated primary production, the two blooms were quite similar (Table 6.1). In the depth-integrated photosynthetic efficiencies derived from Chl *a*-specific carbon fixation (P^b), however, higher values were found in the 39°W bloom area (Table 6.1). In the 12°W bloom, lower P^b-values indicate that the phytoplankton is less efficient

in photosynthesis (Behrenfeld et al. 2008), having a lower capacity of acclimating to its environment (Korb and Whitehouse 2004). This hypothesis is supported by patterns in the Chl *a*-specific photosynthesis vs. irradiance (P^bI) behaviour of the different phytoplankton assemblages (Figure 6.5). While the 12°W bloom exhibits a typical PI dependent saturation curve, no such pattern was observed in the 39°W bloom samples. Photosynthesis of the deep samples from the 12°W bloom might have been light-limited, whereas the samples from the same depth (i.e. similar light intensity) in the 39°W bloom were able to adapt to low light levels by increasing their photosynthetic efficiency. Classical PI curves (Figure 6.2) with surface and deep samples (20 and 60 m depth) revealed that in the 12°W bloom the Pb at a given irradiance as well as $P^b{}_{max}$ were higher for the surface compared to the deep sample, yet the opposite was true for the 39°W bloom area. This is further evidence that while depth-acclimated phytoplankton was able to increase light-harvesting in the 39°W area, this was not the case in the 12°W bloom. The absence of photoinhibition in PI curves furthermore indicates that the increased light-harvesting efficiencies of the depth-acclimated samples from the 39°W bloom must have been accompanied by sufficient photoprotective capacities (Figure 6.2). Hence, despite similar net primary production in both areas (Table 6.2), there are apparent differences in the photosynthetic efficiencies (Figures 6.2 and 6.5), which most likely are caused by differences in the physico-chemical environment as discussed in the following.

6.5.3 Nutrient deficits indicate differences in iron availability

In both blooms, $Si(OH)_4$ concentrations in the surface were low and were likely affecting diatom growth (Figure 6.3; Nelson et al. 2001). As the two blooms, however, did not differ regarding integrated and surface $Si(OH)_4$ concentrations, silicate limitation is probably affecting NPP in both blooms but not causing the differences between them.

In the winter, nutrients in surface waters are replenished by deep mixing. During the growing season, phytoplankton take up and export these nutrient to a certain degree, which is expressed as the nutrient deficits (Le Corre and Minas 1983, Jennings et al. 1984; Table 6.2). These proxies for net community production as well as their ratios differed between bloom areas (Figure 6.4). While the ratios of $Si(OH)_4$:NO_3 deficits were significantly higher in the 12°W compared to the 39°W bloom area, the opposite trend was observed with respect to the NO_3:PO_4 deficit ratios. These results indicate differences in the nutrient assimilation capacities of the two phytoplankton assemblages, which could be explained by different levels of iron availability in the two regions. More specifically, iron limitation was probably more pronounced in the 12°W than in the 39°W bloom down-stream of SG. As iron is needed by phytoplankton for the assimilation of nitrate, and to a lesser degree of phosphate, its absence

leads to lower uptake capacities (de Baar et al. 1997, Hutchins and Bruland 1998). Drifter buoy trajectories indicate that water masses at the 39°W sampling locations originate from the SG shelf (Meredith et al. 2003), most likely transporting iron and other trace metals to the sampling site (Korb and Whitehouse 2004, Nielsdóttir et al. 2012, Borrione and Schlitzer 2013). The 12°W bloom, however, was much more distant from any shelf region and trace metal input is thus strongly restricted.

Iron measurements during the cruise, however, do not indicate clear differences in dissolved (0.1-0.2 nM), leachable and particulate iron (0.2-0.8 nM) concentrations between the two areas (L. Laglera, unpubl. results). Since only two stations have been sampled in the 39°W bloom, this comparison is of limited value. Given the development and intensity of the blooms, as inferred from satellite data, iron concentrations must have been much higher at the onset of blooms, yet they were already depleted by phytoplankton activity and particle scavenging at the time of sampling (Boyd and Ellwood 2010). As iron-limitation generally leads to lower photosynthetic capacities, differences in the 'iron history' of the two blooms could also explain the patterns in P^b (Greene et al. 1991; Figure 6.2, Figure 6.5). More intense iron limitation hampers photoacclimating (Figure 6.5 A, B), while slightly higher iron availability may allow phytoplankton to optimise photosynthesis according to their integrated light environment (Figure 6.5 C, D).

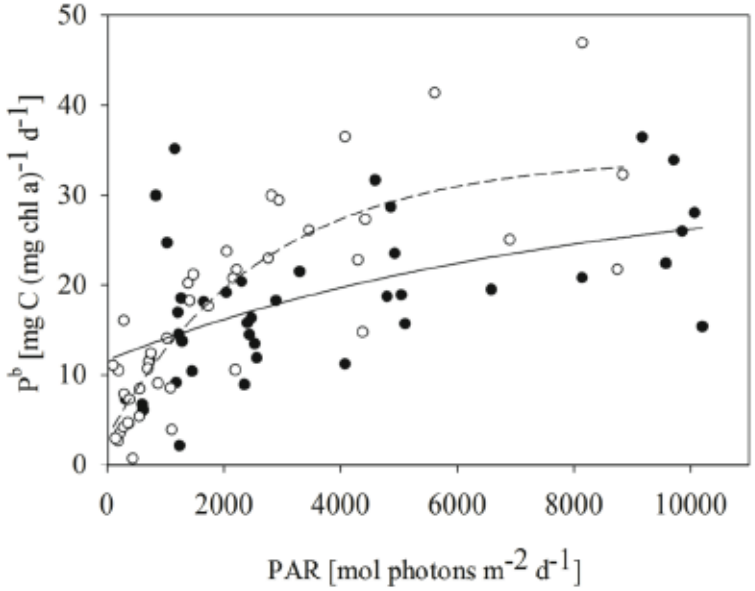

Figure 6.5: - Chl *a*-specific photosynthesis vs. irradiance (P^bI) relationship of 24h on-deck incubations from stations in the 12°W bloom (open symbols) and the 39°W bloom (closed symbols). PI curve fits were applied to both datasets individually (dashed and solid line for 12°W and 39°W blooms, respectively).

6.5.4 Different fractions of new and regenerated production

Nutrient deficits are not only used as indicators for iron limitation, but also as an estimation of season-integrated net community production, which can be used as a proxy for new production (Jennings et al. 1984, Hoppema et al. 2000, Whitehouse et al. 2012). Production rates calculated from nutrient deficits, however, can potentially be biased by altered nutrient concentrations due to vertical mixing, alternative nutrient sources (e.g. ammonium), remineralisation in surface waters, as well as changes in stoichiometry of organic matter (Jennings et al. 1984, Hoppema et al. 2007, Whitehouse et al. 2012). In the case of the present dataset, the comparison of estimates based on ^{14}C-uptake and nutrient deficits can give further insight into the proportions of new and regenerated production (Whitehouse et al. 2012).

In agreement with Laubscher et al. (1993), stronger nutrient depletion in the APF co-occurred with higher photosynthetic efficiencies (Table 6.2). The estimates of primary production (Table 6.1) and POC:PON ratios (Table 6.2) were in a similar range for both blooms, but nutrient deficits indicate lower nitrate usage in the 12°W bloom (Figure 6.4). Phytoplankton growth must have therefore been supported by other nitrogen sources in the latter area. In fact, phytoplankton are known to counteract the nitrogen deficiency arising from the decreased NO_3^- uptake capacities under iron-limitation by using a larger proportion of regenerated nitrogen sources such as ammonia (Brzezinski et al. 2003). This implies that in the 12°W bloom more active recycling of nutrients took place, which decreases the proportion of primary productivity being exported by the biological pump (Dugdale and Goering 1967, Epply and Petterson 1979). Shipboard carbonate chemistry measurements during the cruise revealed higher deficits in dissolved inorganic carbon (DIC) and a stronger CO_2 uptake from the atmosphere in the 39°W bloom area compared to the 12°W bloom (Jones et al. in prep.), supporting the hypothesis raised above. In conclusion, even if net primary production was similar in the two blooms, the potential for carbon sequestration was probably larger in the 39°W bloom compared to the 12°W bloom.

6.5.5 From bottom-up towards top-down control

All available data from our study suggest that the phytoplankton in the 39°W bloom area are able to acclimate more efficiently to their light environment and therefore have higher photosynthetic efficiencies (Table 6.2). It is therefore surprising that standing stocks and net primary production are not higher compared to the less efficient 12°W bloom. Our estimates of primary production, however, are prone to underestimate loss terms such as grazing (Gall et al. 2001). We therefore speculate that during the time of sampling, top-down control

was more strongly developed in the 39°W bloom north of SG compared to the 12°W bloom area. In fact, average zooplankton biomass in the SG area has been found to be larger than anywhere else in the SO (Atkinson et al. 2001).

Zooplankton samples (net catches and stable isotope analysis) from the presented cruise furthermore showed that, despite high spatial variability, the zooplankton community near at 39°W was further developed compared to the 12°W bloom area, where the proportion of small organisms and early developmental stages was higher (E. Pakomov and B. Hunt, unpubl. data). Also sediment trap data support this hypothesis, as during the sampling period the organic matter export fluxes and E_z-ratios (exported organic matter : NPP ratio; Buesseler and Boyd 2009) were indicating higher grazing activity in the 39°W bloom compared to the 12°W bloom area (M. Iversen, unpub. results). As the control of phytoplankton dynamics can shift from bottom-up to top-down within a few weeks (Abbott et al. 2000), a slightly earlier bloom development at 39°W could have been enough to lead to this result. Diatom-dominated blooms, as observed in this study (C. Klaas, unpubl. results; also indicated by silicate depletion in the surface waters, Figure 6.3), are mainly grazed by larger zooplankton. One can therefore assume that the usual time lag between bloom and grazer development (Smetacek et al. 1978) was still having an effect on the 12°W bloom, while grazers already imposed a strong control on the 39°W bloom. Satellite Chl *a* maps of the two bloom areas in fact show that the 39°W bloom developed around 8 weeks earlier than the 12°W bloom.

6.5.6 Conclusions and biogeochemical implications

In agreement with the general opinion (e.g. Priddle et al. 1992, Abbott et al. 2000, Boyd 2002), the results of this study suggest that a combination of different factors strongly affect primary production in phytoplankton blooms in the SO. While iron availability seems to be a master variable (i.e. also influencing the effects of other nutrients and light) controlling the build-up of a bloom, top-down processes are more important determining the phytoplankton standing stock at the late bloom stage, i.e. when sampling took place. Based on our data, one can conclude that ^{14}C-based estimates of primary production alone are insufficient for the assessment of ecological and biogeochemical effects of phytoplankton blooms in the ACC. These effects may depend on the intensity of iron limitation, determining how strongly production has to be fuelled by recycled rather than 'new' nutrients and thereby setting upper limits for the strength of the biological pump. It should also be kept in mind that the other 'main controlling factor' light is thought to be especially important for bloom development early in the season (Bracher et al. 1999, Smith et al. 2000, Abbott et al. 2001, Landry et al. 2002), a time which is not covered by the present cruise dataset.

Priddle et al. (1992) concluded that due to the complex matrix of and interactions between processes, it is "virtually impossible" to translate primary production into carbon export. Even though there is without doubt a lack of knowledge, more and more light has been shed onto these interactions. In the present study, we were able to link differences in measured primary production and photosynthetic efficiencies with observations on nutrient deficits. Furthermore, it was possible to disentangle some of the underlying mechanisms when considering the time scales of the individual measurements. Most likely, the observed patterns can be explained by differences in iron availability and grazing pressure. This work helps to better understand the development of blooms in the ACC and their implications for the biological pump under different environmental settings.

Acknowledgements

We would like to thank all scientists as well as the captain, officers and crew of RS Polarstern for their work and support during the ANT-XXVIII/3 cruise. Especially, we would like to thank M. Iversen, E. Jones and L. Laglera for helpful discussions on the present dataset. E. Jones provided DIC measurements. We thank S. Wiegmann for help with the HPLC analysis and F. Steinmetz (HYGEOS) for supplying Polymer-MERIS CHL data and ESA for MERIS level-1 satellite data. Furthermore, we would like to thank F. Altvater, D. Kottmeier, R. Kottmeier, T. Rueger, V. Schourup-Kristensen for their help during the cruise as well as A. Terbrüggen, K.-U. Richter and U. Richter for help with the cruise preparations. C.J.M.H. and B.R. were funded by the European Research Council (ERC) under the European Communitys Seventh Framework Programme (FP7 2007-2013), ERC grant agreement no. 205150. S.T. was funded by the German Science Foundation (DFG), project TR 899/2. Funding to M.S. was supplied by CAPES, Brazil, and to A.B. by the Helmholtz Innovation Fund Phytooptics. M.H. and H.J.W.d.B were supported through EU FP7 project CARBOCHANGE which received funding from the European Communitys Seventh Framework Programme under grant agreement no. 264879. This work was furthermore supported by the Deutsche Forschungsgemeinschaft (DFG) in the framework of the priority programme "Antarctic Research with comparative investigations in Arctic ice areas" by a grant HO 4680/1.

6.6 References

Abbott, M.R., Richman, J.G., Letelier, R. M., Bartlett, J. S. (2000) The spring bloom in the Antarctic polar frontal zone as observed from a mesoscale array of bio-optical sensors. Deep Sea Research Part II: Topical Studies in Oceanography 47:3285-3314

Abbott, M. R., Richman, J. G., Nahorniak, J. S., Barksdale, B. S. (2001) Meanders in the Antarctic polar frontal zone and their impact on phytoplankton. Deep Sea Research Part II: Topical Studies in Oceanography 48:3891-3912

Antoine, D., Morel, A. (1996). Oceanic primary production: I. Adaptation of a spectral light-photosynthesis model in view of application to satellite chlorophyll observations, Global Biogeochemical Cycles 10:43-55

Arrigo, K. R., Worthen, D., Schnell, A., Lizotte, M. P. (1998) Primary production in Southern Ocean waters. Journal of Geophysical Research: Oceans 103:15587-15600

Atkinson, A., Whitehouse, M. J., Priddle, J., Cripps, G. C., Ward, P., Brandon, M. A. (2001) South Georgia, Antarctica: A productive, cold water, pelagic ecosystem. Marine Ecology Progress Series 216:279-308

Bathmann, U. V., Scharek, R., Klaas, C., Dubischar, C. D., Smetacek, V. (1997) Spring development of phytoplankton biomass and composition in major water masses of the Atlantic sector of the Southern Ocean. Deep Sea Research Part II: Topical Studies in Oceanography 44:51-67

Behrenfeld, M. J., Halsey, K. H., Milligan, A. J. (2008) Evolved physiological responses of phytoplankton to their integrated growth environment. Philosophical Transactions of the Royal Society B: Biological Sciences 363:2687-2703

Blain, S., et al. (2001) A biogeochemical study of the island mass effect in the context of the iron hypothesis: Kerguelen islands, Southern Ocean. Deep Sea Research Part I: Oceanographic Research Papers 48:163-187

Borrione, I., Schlitzer, R. (2013) Distribution and recurrence of phytoplankton blooms around South Georgia, Southern Ocean. Biogeosciences 10:217-231

Boyd, P. W. (2002) Environmental factors controlling phytoplankton processes in the Southern Ocean. Journal of Phycology 38:844-861

Boyd, P. W., Ellwood, M. J. (2010) The biogeochemical cycle of iron in the ocean. Nature Geoscience 3:675-682

Bracher, A. U., Kroon, B. M. A., Lucas, M. I. (1999) Primary production, physiological state and composition of phytoplankton in the Atlantic sector of the Southern Ocean. Marine Ecology Progress Series 190: 1-16

Brewin. R, et al. (in press) The Ocean Colour Climate Change Initiative: III. A round-robin comparison on bio-ioptical algorithms. Remote Sensing of Environment

Brzezinski, M. A., Dickson, M.-L., Nelson, D. M., Sambrotto, R. (2003) Ratios of Si, C and C uptake by microplankton in the Southern Ocean. Deep Sea Research Part II: Topical Studies in Oceanography 50:619-633

Buesseler, K. O., Boyd, P. W. (2009) Shedding light on processes that control particle export and flux attenuation in the twilight zone of the open ocean. Limnology and Oceanography 54: 1210-1232

Clarke, A., Leakey, R. J. (1996) The seasonal cycle of phytoplankton, macronutrients, and the microbial community in a nearshore antarctic marine ecosystem. Limnology and Oceanography 41:1281-1294

Coale, K. H., et al. (2004) Southern Ocean Iron Enrichment Experiment: Carbon Cycling in High- and Low-Si Waters. Science 304:408-414

de Baar, H. J. W., de Jong, J. T. M., Bakker, D. C. E., Loscher, B. M., Veth, C., Bathmann, U., Smetacek, V. (1995) Importance of iron for plankton blooms and carbon dioxide drawdown in the Southern Ocean. Nature 373:412-415

de Baar, H. J. W., Van Leeuwe, M. A., Scharek, R., Goeyens, L., Bakker, K. M. J., Fritsche, P. (1997) Nutrient anomalies in *Fragilariopsis kerguelensis* blooms, iron deficiency and the nitrate/phosphate ratio (A. C. Redfield) of the Antarctic Ocean. Deep Sea Research Part II: Topical Studies in Oceanography 44:229-260

de Jong, J. T. M., den Das, J., Bathmann, U., Stoll, M. H. C., Kattner, G., Nolting, R. F., de Baar, H. J. W. (1998) Dissolved iron at subnanomolar levels in the Southern Ocean as determined by ship-board analysis. Analytica Chimica Acta 377:113-124

Dubischar, C. D., Bathmann, U. V. (1997) Grazing impact of copepods and salps on phytoplankton in the Atlantic sector of the Southern Ocean. Deep Sea Research Part II: Topical Studies in Oceanography 44:415-433.

Dugdale, R. C., Goering, J. J. (1967) Uptake of new and regenerated forms of nitrogen in primary productivity. Limnology and Oceanography 12:196206

El-Sayed, S. Z., Biggs, D. C., Holm-Hansen, O. (1983) Phytoplankton standing crop, primary productivity, and near-surface nitrogenous nutrient fields in the Ross Sea, Antarctica. Deep Sea Research Part A Oceanographic Research Papers 30:871-886

Eppley, R. W., Peterson, B. J. (1979) Particulate organic matter flux and planktonic new production in the deep ocean. Nature 282: 677-680

Falkowski, P. G., Barber, R. T., Smetacek, V. (1998) Biogeochemical controls and feedbacks on ocean primary production. Science 281:200-206

Field, C. B., Behrenfeld, M. J., Randerson, J. T., Falkowski, P. (1998) Primary production of the biosphere: Integrating terrestrial and oceanic components. Science 281:237-240

Gall, M. P., Strzepek, R., Maldonado, M., Boyd, P. W. (2001) Phytoplankton processes. Part 2: Rates of primary production and factors controlling algal growth during the southern ocean iron release experiment (soiree). Deep Sea Research Part II: Topical Studies in Oceanography 48:2571-2590

Grasshoff, K., Kremling, K., Ehrhardt, M. (1999) Methods of Seawater Analysis, Weinheim, Wiley-VCH

Greene, R. M., Geider, R. J., Falkowski, P. G. (1991) Effect of iron limitation on photosynthesis in a marine diatom. Limnology and Oceanography 36:1772-1782

Hiscock, M. R., et al. (2003) Primary productivity and its regulation in the pacific sector of the southern ocean. Deep-Sea Research II 50:533-558

Hoffmann, L. J., Peeken, I., Lochte, K., Assmy, P., Veldhuis, M. (2006) Different reactions of Southern Ocean phytoplankton size classes to iron fertilization, Limnology and Oceanography 51: 1217-1229

Hoppema, M., Goeyens, L., Fahrbach, E. (2000) Intense nutrient removal in the remote area off Larsen Ice Shelf (Weddell Sea). Polar Biology 23:85-94

Hoppema, M., Middag, R., de Baar, H. J. W., Fahrbach, E., van Weerlee, E. M., Thomas, H. (2007) Whole season net community production in the Weddell Sea. Polar Biology 31:101-111

Hutchins, D., Bruland, K. (1998) Iron-limited diatom growth and Si:N uptake ratios in a coastal upwelling regime. Nature 393:561

Jenkins, W. J., Goldman, J. C. (1985) Seasonal oxygen cycling and primary production in the Sargasso Sea. Journal of Marine Research 43:465-491

Jennings, J. C., Gordon, L. I., Nelson, D. M. (1984) Nutrient depletion indicates high primary productivity in the Weddell Sea. Nature 309:51-54

Jones, E., Hoppema, M., et al. (in prep): Mesoscale features are hotspots of carbon uptake in the Antarctic Circumpolar Current

Kaffes, A., Thoms, S., Trimborn, S., Rost, B., Langer, G., Richter, K.-U., Köhler, A., Norici, A., Giordano, M. (2010) Carbon and nitrogen fluxes in the marine coccolithophore *Emiliania huxleyi* grown under different nitrate concentrations. Journal of Experimental Marine Biology and Ecology 393:1-8

Knap, A., Michaels, A., Close, H. D., Dickson, A. (1996) Protocols for the joint global ocean flux study (JGOFS) core measurements, UNESCO

Korb, R. E., Whitehouse, M. (2004) Contrasting primary production regimes around South Georgia, Southern Ocean: Large blooms versus high nutrient, low chlorophyll waters. Deep Sea Research Part I: Oceanographic Research Papers 51:721-738

Landry, M. R., Selph, K. E., Brown, S. L., Abbott, M. R. et al. (2002) Seasonal dynamics of phytoplankton in the Antarctic polar front region at 170°W. Deep Sea Research Part II: Topical Studies in Oceanography 49:1843-1865

Le Corre, P., Minas, H. J. (1983) Distributions et évolution des éléments nutritifs dans le secteur indien de l'Océan Antarctique en fin de période estivale. Oceanologica Acta 6:365-381

Laubscher, R. K., Perissinotto, R., McQuaid, C. D. (1993) Phytoplankton production and biomass at frontal zones in the Atlantic sector of the Southern Ocean. Polar Biol 13:471-481

Longhurst, A., Glen, R., Harrison, W. (1989) The biological pump: Profiles of plankton production and consumption in the upper ocean. Progress In Oceanography 22:47-123

Lorrain, A., Savoye, N., Chauvaud, L., Paulet, Y.-M., Naulet, N. (2003) Decarbonation and preservation method for the analysis of organic C and N contents and stable isotope ratios of low-carbonated suspended particulate material. Analytica Chimica Acta 491:125-133

Martin, J. H. (1990) Glacial-interglacial CO_2 change: The iron hypothesis. Paleoceanography 5:1-13

Meredith, M. P., et al. (2003) An anticyclonic circulation above the northwest Georgia Rise, Southern Ocean. Geophysical Research Letters 30:2061

Mitchell, B. G., Holm-Hansen, O. (1991) Observations and modeling of the Antarctic phytoplankton crop in relation to mixing depth. deep Sea Research 38:981-1007

Müller, D, et al. (in revision) The Ocean Colour Climate Change Initiative: I. An Assessment of Atmospheric Correction Processors based on in-situ measurements. Remote Sensing of Environment

Moore, J. K., Abbott, M. R. (2000a) Phytoplankton chlorophyll distributions and primary production in the Southern Ocean. Journal of Geophysical Research: Oceans 105:28709-28722

Moore, J. K., Abbott, M. R., Richman, J. G., Nelson, D. M. (2000b) The Southern Ocean at the last glacial maximum: A strong sink for atmospheric carbon dioxide. Global Biogeochem Cycles 14:455-475

Moore, J. K., et al. (1999) SeaWiFs satellite ocean color data from the Southern Ocean. Geophysical Research Letters 26:1465-1468

Morel, A., Huot, Y., Gentili, B., Werdell, P. J., Hooker, S. B., Franz, B. A. (2007) Examining the consistency of products derived from various ocean color sensors in open ocean waters in the perspective of a multi-sensor approach. Remote Sensing of Environment 111: 69-88

Murphy, J., Riley, J. P. (1962) A modified single solution method for the determination of phosphate in natural waters. Analytica Chimica Acta 27:31-36

Nelson, D. M., Brzezinski, M. A., Sigmon, D. E., Franck, V. M. (2001) A seasonal progression of Si limitation in the pacific sector of the Southern Ocean. Deep Sea Research Part II: Topical Studies in Oceanography 48:3973-3995

Nelson, D. M., Smith, W. O. J. (1991) Sverdrup revisited: Critical depths, maximum chlorophyll levels, and the control of Southern Ocean productivity by the irradiance-mixing regime. Limnology and Oceanography 36: 1650-1661

Nielsdóttir, M. C., Bibby, T. S., Moore, C. M., Hinz, D. J., Sanders, R., Whitehouse, M., Korb, R., Achterberg, E. P. (2012) Seasonal and spatial dynamics of iron availability in the Scotia Sea. Marine Chemistry 130:62-72

Park, J., Oh, I.-S., Kim, H.-C., Yoo, S. (2010) Variability of SeaWiFs Chlorophyll-a in the southwest Atlantic sector of the Southern Ocean: Strong topographic effects and weak seasonality. Deep Sea Research Part I: Oceanographic Research Papers 57:604-620

Priddle, J., Smetacek, V., Bathmann, U., Stromberg, J.-O., Croxall, J. P. (1992) Antarctic marine primary production, biogeochemical carbon cycles and climatic change. Philosophical Transactions of the Royal Society of London Series B: Biological Sciences 338:289-297

Read, J. F., Pollard, R. T., Morrison, A.I., Symon, C. (1995) On the southerly extent of the Antarctic Circumpolar Current in the southeast Pacific. Deep Sea Research Part II: Topical Studies in Oceanography 42:933-954

Rubin, S. I., Takahashi, T., Chipman, D. W., Goddard, J. G. (1998) Primary productivity and nutrient utilization ratios in the Pacific sector of the Southern Ocean based on seasonal changes in seawater chemistry. Deep Sea Research Part I: Oceanographic Research Papers 45:1211-1234

Schlitzer, R. (2002) Carbon export fluxes in the Southern Ocean: results from inverse modeling and comparison with satellite based estimates. Deep-Sea Research II 49:1623-1644

Sigman, D. M., Hain, M. P. (2012) The biological productivity of the ocean: Section 3. Nature Education Knowledge 3:19

Sigman, D. M., Hain, M. P., Haug, G. H. (2010) The polar ocean and glacial cycles in atmospheric CO_2 concentration. Nature 466:47-55

Smetacek, V., Bröckel, K., Zeitzschel, B., Zenk, W. (1978) Sedimentation of particulate matter during a phytoplankton spring bloom in relation to the hydrographical regime. Mar Biol 47:211-226

Smetacek, V., et al. (2012) Deep carbon export from a Southern Ocean iron-fertilized diatom bloom. Nature 487:313-319

Smith Jr, W. O., Marra, J., Hiscock, M. R., Barber, R. T. (2000) The seasonal cycle of phytoplankton biomass and primary productivity in the Ross Sea, Antarctica. Deep Sea Research Part II: Topical Studies in Oceanography 47:3119-3140

Steinmetz, F., Deschamps, P. Y., Ramon, D. (2011) Atmospheric correction in presence of sun glint: application to MERIS. Optics express 19: 9783-9800

Strass, V. H., Naveira Garabato, A. C., Pollard, R. T., Fischer H. I., Hense, I., Allen, J. T., Read, J. F., Leach, H., Smetacek, V. (2002) Mesoscale frontal dynamics: Shaping the environment of primary production in the Antarctic Circumpolar Current. Deep Sea Research Part II: Topical Studies in Oceanography 49:3735-3769

Strickland, J. D. H, Parsons, T. R. (1968) A pracitcal handbook of seawater analysis, Bulletin. No 167. Fisheries Research Board of Canada

Sunda, W. G., Huntsman, S. A. (1997) Interrelated influence of iron, light and cell size on marine phytoplankton growth. Nature 390:389-392

Taylor, B. B., Torrecilla, E., Bernhardt, A., Taylor, M. H., Peeken, I., Röttgers, R., Piera, J., Bracher, A. (2011) Bio-optical provinces in the eastern Atlantic Ocean. Biogeosciences 8: 3609-3629

Tremblay, J. E., Lucas, M. I., Kattner, G., Pollard, R., Bathmann, U., Strass, V., Bracher, A. (2002) Significance of the Polar Frontal Zone for large-sized diatoms and new production during summer in the Atlantic Sector of the Southern Ocean. Deep-Sea Research II 49 18: 3793-3811

Vaillancourt, R. D., Marra, J., Barber, R. T., Smith Jr, W. O. (2003) Primary productivity and in situ quantum yields in the Ross Sea and pacific sector of the Antarctic Circumpolar Current. Deep Sea Research Part II: Topical Studies in Oceanography 50:559-578

Veth, C., Lancelot, C., Ober, S. (1992) On processes determining the vertical stability of surface waters in the marginal ice zone of the north-western Weddell Sea and their relationship with phytoplankton bloom development. Polar Biol 12:237-243

Volk, T., Hoffert, M. I. (1985) Ocean carbon pumps: analysis of relative strengths and efficiencies in ocean-driven atmospheric CO_2 changes. In The carbon cycle and atmospheric CO_2: natural variation archean to present, eds. Sunquist ET, Broecker WS, 99 - 110. Washington, D.C, American Geophysical Union, Geophysical Monographs

Whitehouse, M. J., Atkinson, A., Korb, R. E., Venables, H. J., Pond, D. W., Gordon, M. (2012) Substantial primary production in the land-remote region of the central and northern Scotia Sea. Deep Sea Research Part II: Topical Studies in Oceanography 5960:47-56

Whitehouse, M. J., Korb, R. E., Atkinson, A., Thorpe, S. E., Gordon, M. (2008) Formation, transport and decay of an intense phytoplankton bloom within the high-nutrient low-chlorophyll belt of the Southern Ocean. Journal of Marine Systems 70:150-167

Chapter 7

Synthesis

7.1 Main findings of this thesis

The aim of this thesis was to understand the modulation of OA effects on SO phytoplankton. Until recently, the interactions of pCO_2 with other environmental factors were largely unknown. In the past 3 years, a lot more knowledge was gained (see Boyd & Hutchins 2012, Gao et al. 2012b for reviews). For the SO, however, such information is still scarce. The publications presented in this thesis represent some of the first attempts to understand OA effects in the framework of multiple stressors in the SO.

In order to meaningfully interpret and extrapolate response patterns observed in OA experiments, we first need to strictly constrain the carbonate chemistry organisms are exposed to. *Publication I* describes uncertainties associated with inconsistencies between different input parameters and associated calculations of the carbonate system. The observed discrepancies between pCO_2 values calculated from different measured parameter pairs (TA & DIC, TA & pH, and DIC & pH) were as high as 30%. These discrepancies hamper the comparability and quantitative validity of past and future OA studies. Until the reasons are found and abolished, it is suggested to agree on one set of parameters (i.e. TA & pH) to increase comparability between different studies. The implications arising from this will be discussed in chapter 7.2.

Applying the knowledge gained in the first study, the responses of SO phytoplankton to OA were investigated. In *Publication II*, the modulation of OA effects by iron availability was investigated. For a natural phytoplankton community from the SO, iron limitation was shown to drastically alter the responses to OA. After iron enrichment, primary production increased with increasing pCO_2 levels, whereas OA had no influence on carbon fixation under iron limitation. The changes in primary production under iron-enriched conditions were accompanied by a pronounced taxonomic shift from weakly to heavily silicified diatoms, while under iron-depleted conditions, no such functional shift was observed. This suggests that under increased iron availability, OA could potentially lead to a stimulation of primary as well as export production. For large parts of the SO, however, iron limitation could restrict the possible 'CO_2 fertilization' effect.

In addition to the modulation by iron, also the effects of different light regimes on OA responses were investigated. In *Publication III*, dynamic light was found to strongly alter the effects of OA on an Antarctic strain of the diatom *Chaetoceros debilis*. High pCO_2 had no effect on primary production under constant but a strong negative effect under dynamic light. Photophysiological results indicate increased susceptibility to high-light stress under OA, even though efficient electron transport was sustained in all treatments. The observed patterns can be explained by increased metabolic costs for photosystem turnover. In view

of the highly dynamic light fields experienced by phytoplankton in the oceans, these results stress that understanding and predicting the effects on OA is only possible, if experiments also include dynamic changes in other environmental conditions such as light. The potential consequences arising from synergistic or antagonistic interactions between light, iron and OA will be discussed in chapter 7.3.

To understand how different environmental conditions control SO phytoplankton blooms and their potential for carbon sequestration, also knowledge from more complex and realistic systems is needed. To investigate this, the abiotic controls of two large-scale phytoplankton blooms from the ACC were compared in *Publication IV*. The results indicated that blooms were controlled by interactions between iron and light limitation as well as grazing. Furthermore, it highlighted the need to study processes such as productivity on different spatial and temporal scales, e.g. because measurements of net primary production based on 24h incubations do not allow for the estimation of primary and export production over the whole season. The aspect of different scales relevant for phytoplankton productivity will be discussed in 7.4.

Building on the findings presented in these four publications, the results of this thesis will be exploited to make overall predictions for the SO (chapter 7.5). Lastly, some important perspectives for future research will be highlighted (chapter 7.6).

7.2 How our methods determine our results

It goes without saying that the design of an experiment will influence its outcome. In the fast growing OA research community, however, this fact was not recognized for a long time. The responses of phytoplankton to OA were thought to be straightforward in the 'early days', but more and more contradictory results were published over time (Gattuso & Hansson 2011). The complexity of carbonate chemistry and the various options for its manipulation was held responsible for deviating results from different studies (e.g. Riebesell et al. 2000 versus Iglesias-Rodrigues 2008). To overcome these problems, 'best practise guides' for experimental setup and carbonate chemistry measurements have been published (Dickson et al. 2007, Riebesell et al. 2010). While different methods of carbonate chemistry manipulation have proven not to alter the response patterns of organisms to OA (Hoppe et al. 2011, *Appendix*), inter- and intraspecific variability were identified as important reasons for the differences in OA responses (Langer et al. 2006, Langer et al. 2009, Trimborn et al. 2009, Hoppe et al. 2011, Trimborn et al. 2013).

Different experimental setups and ways to measure physiological parameters are another key to explain apparent divergent patterns of OA responses. For example, *Publication*

I demonstrated that responses of organisms to a certain pCO_2 scenario could be severely over- or underestimated depending on the choice of carbonate chemistry parameters used for pCO_2 calculations. The inconsistencies and consequently also the potential misinterpretations are most pronounced at high pCO_2 levels. This adds more uncertainty to pCO_2 estimations under conditions where carbonate chemistry gets progressively unstable due to the lower buffering capacity under OA (Egleston et al. 2010) and for which reference materials do not exist (*Publication I*). As most experimental studies compare an ambient CO_2 level with one derived from future CO_2 emission scenarios (e.g. 750 or 1000 ppm), predicted trends are often based on two treatments only. If we assume a bell-shaped response curve of overall fitness to OA (as has been proposed for coccolithophores; Ridgwell et al. 2009, Bach et al. 2011), the described inconsistencies in calculated pCO_2 values can lead to very different conclusions on organism responses to OA (Figure 7.1). Depending on the pair of input parameters used and the type of response pattern observed, predicted trends could even reverse. The described phenomenon can be especially problematic if studies aim to identify 'tipping points', which are requested by policy makers. Furthermore, also the experimental validation of paleooceanographic proxies may be flawed. As described in *Publication I* , the

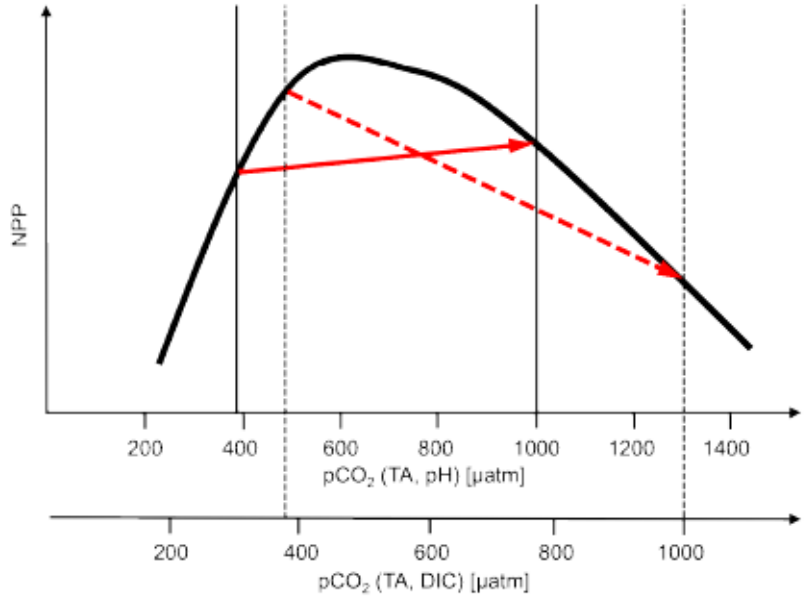

Figure 7.1: - Simplified illustration phytoplankton responses to increased pCO_2 levels as described for coccolithophores (e.g. Langer et al. 2009, Bach et al. 2011). Taking the observed inconsistency in carbonate chemistry calculation can reverse trends in parameters like net primary production (NPP) when comparing ambient and future pCO_2 scenarios (380 and 1000 μatm, respectively). Calculations yielded different pCO_2 levels based on TA and pH (lower x-axis) and TA and DIC (upper x-axis), leading either increasing (solid arrow) or decreasing trends (dashed arrow), respectively.

inconsistencies can furthermore unravel some of the apparent differential responses described in the literature (cf. Langer et al. 2009, Hoppe et al. 2011).

But also the parameters that are not considered in an experimental matrix and therefore are kept constant (i.e. light, temperature, nutrients) can greatly affect the experiment's outcome. For example, light levels were shown to modulate OA response patterns in various phytoplankton taxa (Kranz et al. 2010, Rokitta & Rost 2012, Li & Campbell 2013). Going one step beyond this, *Publication II* and *III* demonstrate how a shift from standard experimental conditions (i.e. replete nutrients and constant light) to more realistic scenarios for the SO (i.e. iron limitation in *Publication II* and dynamic light in *Publication III*) can even reverse the effects of OA. In addition to light and iron availability, also changes in macronutrients or temperatures have been shown to significantly affect organism responses to OA by complex interactions (e.g. Hutchins et al. 2007, Feng et al. 2009, Lefebvre et al. 2012, Tatters et al. 2013). Furthermore, differences in timing and duration of measurements (e.g. at different phases of the cell cycle; Halsey et al. 2011), acclimation and adaptation times (Lohbeck et al. 2012, Collins et al. 2013) and the parameters investigated (e.g. photosynthesis estimated from electrons, O_2 evolution, carbon uptake, biomass build-up; Behrenfeld et al. 2008, Suggett et al. 2009, *Publication III*) will pick up 'snapshots' of response patterns on different scales. Investigations that are limited in scale or experimental approach can therefore lead to biased predictions on OA effects.

Predictions of the effects of climate change are only possible, if the effects of OA are investigated in a framework of important co-varying conditions in the environment of interest. A better knowledge of environmental key drivers, independent of the CO_2 problem, moreover helps to narrow down research questions and experimental matrixes for OA research. For example, various field datasets (e.g. *Publication IV*) as well as largescale fertilisation experiments (e.g. Smetacek et al. 2012) have shown that the availability of iron, light and silicate are exerting major controls on SO primary production. It can therefore be deduced, that the changes in their availabilities have the potential to strongly modulate OA responses of SO phytoplankton while the interactions with nitrate or phosphate limitation are probably not that important, as these nutrients are rarely limiting in the SO.

7.3 The whole is greater (or smaller) than the sum of its parts

As outlined above, organisms will always experience a wide range of changing environmental drivers and stressors (e.g. nutrients, light, temperature). Similarly, phytoplankton cells always have to balance various physiological processes (e.g. light and dark reactions of

photosynthesis, synthesis of proteins and storage compounds) that compete for energy and/or substrates, which themselves show different dependencies towards environmental conditions. Therefore, it is not sufficient to investigate the effects of different environmental conditions in isolation and add them up theoretically. Substantial efforts have been made to understand how multiple drivers interactively affect organisms (Folt et al. 1999, Saito et al. 2008, Boyd & Hutchins 2012). Combined effects can be additive, i.e. equal to the sum of the effects of individual drivers. In most cases, however, the combined effects are multiplicative, i.e. either greater (synergistic) or smaller than (antagonistic) their sum (Folt et al. 1999).

The main aim of this thesis was to understand how OA responses of SO phytoplankton will be modulated by the key controlling factors iron and light. The antagonistic effects between OA and iron-limitation observed in *Publication II* (Figure 7.2 A) can be explained by two mechanisms: As iron is needed for central physiological processes in phytoplankton cells (photosynthesis, nitrate assimilation; Geider & La Roche 1994, Behrenfeld & Milligan 2013), its shortage will limit their ability to benefit from facilitated carbon acquisition. More surprisingly, the bioavailability of iron decreases with increasing pCO_2 and declining seawater pH (Shi et al. 2010, Sugie et al. 2013, *Publication II*). This shows that iron limitation and OA also interact in a purely chemical way, which in turn leads to more severe iron limitation of phytoplankton under high pCO_2 levels (Figure 7.2 A).

Also, differences in irradiance significantly alter the responses of phytoplankton to OA (e.g. Kranz et al. 2010, Gao et al. 2012b, *Publication III*), as irradiances directly alter the level of energization of phototrophic cells. Under constant light, the manifestation of OA responses is different between treatments with subsaturating, saturating and supersaturating irradiances, because light harvest needs to be balanced by carbon acquisition and metabolism (Behrenfeld et al. 2004). Under light-limitation, phytoplankton cells will benefit most from

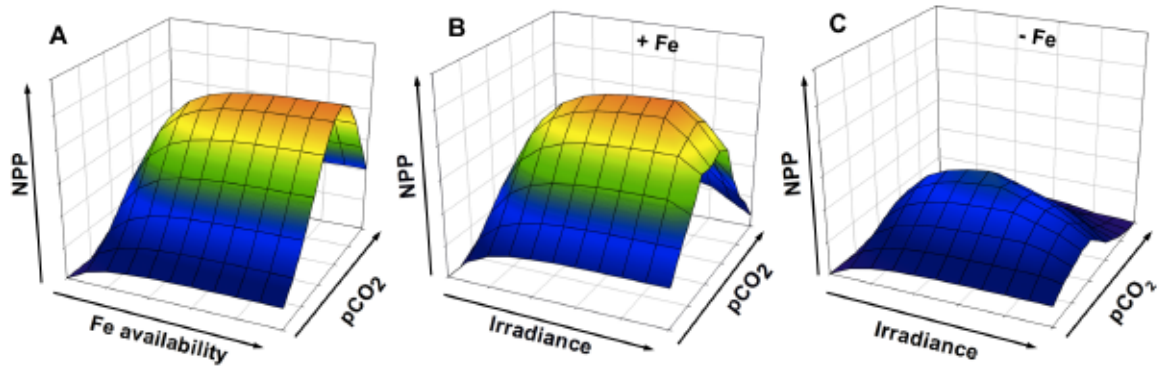

Figure 7.2: - Conceptual illustrations of interactive effects on net primary production (NPP) of SO phytoplankton. Observed effects of iron availability (A) and light (B) as well as proposed combined effects of both parameters on OA responses (C).

OA and the thus decreased costs for carbon acquisition (Kranz et al. 2010, Kranz et al. 2011, Rokitta & Rost 2012), and the often observed increased susceptibility towards photoinhibition under OA (Wu et al. 2010, McCarthy et al. 2012, Li & Campbell 2013) does not manifest under the low light levels applied. Under supersaturating light, however, the CO_2-dependent down-regulation of CCM activities decreases the cells options to sink excess energy in the dark reactions of the Calvin cycle, thereby leading to an over-reduction of the photosynthetic apparatus and thus photoinhibition (Tchernov et al. 1997, Rost et al. 2006). Interactions with the applied light levels can explain at least some of the contradicting results published on phytoplankton under OA. For example, the growth rates of the diatom *Thalassiosira pseudonana* have been described to be positively, negatively and not at all affected by increased pCO_2 levels of 750-1000 μatm (Sobrino et al. 2008, Gao et al. 2012b, McCarthy et al. 2012, Li & Campbell 2013). While positive OA associated trends in growth rates were observed at roughly 30-200 μmol photons m^{-2} s^{-1}, no net effect was observed between about 200-400 μmol photons m^{-2} s^{-1}. Decreasing growth rates under increasing pCO_2 levels were found at high irradiances of 1000 μmol photons mm^{-2} s^{-1}, only. In conclusion, the effects of irradiances on OA-responses could, similarly to the growth response to pCO_2 itself (Ridgwell et al. 2009, Bach et al. 2011), be described by an optimum curve.

All these experiments applied homogenous, non-fluctuation light. In the water columns of the oceans, however, phytoplankton experience highly dynamic light fields. Regarding the associated physiology, different acclimation strategies have been observed: While some studies suggested that phytoplankton cells acclimate to average light intensities (van Leeuwe et al. 2005), others implied that acclimation responds to the highest irradiances of a certain light regime (van de Poll et al. 2007). In *Publication III*, OA effects were altered under dynamic light compared to constant light, demonstrating the antagonistic effects pCO_2 and light regime (Figure 7.2 B), a response similar to the observed interaction between pCO_2 and iron limitation.

Interactions between two environmental factors (i.e. pCO_2 levels with either iron availability or light dynamics; Figure 2 A & B) were investigated in *Publications II* and *III*. In the natural SO environment, however, phytoplankton will experience iron and light stress simultaneously. While it is difficult to control three parameters (pCO_2, light and iron) simultaneously, all possible combinations of two of these were successfully investigated (e.g. Timmermans et al. 2001, van Oijen et al. 2004, Alderkamp et al. 2012, *Publication II* and *Publication III*). Apparently, iron limitation and dynamic light exhibit synergistic effects: As iron limitation leads to inefficient energy transfer in the photosynthetic apparatus and hampers chlorophyll synthesis, it strongly amplifies the negative effects of light limitation (Folt et al. 1999, Saito et al. 2008). At the same time, iron limitation intensifies the effects

of high-light stress in marine phytoplankton, as disrupted electron transfer chains are more prone to photodamage compared to iron replete situations (Greene et al. 2001). Also the effects of dynamic light under iron limitation have been studied in previous experiments (Alderkamp et al. 2012) as well as field studies (e.g. Boyd et al. 2001, Alderkamp et al. 2010, Petrou et al. 2011, *Publication IV*). Alderkamp et al. (2012) showed that in iron-limited cells of *Fragilariopsis cylindrus*, energy conversion efficiency from photochemistry to biomass production were drastically reduced under dynamic compared to constant light. Furthermore, a higher fraction of reduced (i.e. closed) PSII reaction centres suggested a higher susceptibility towards photodamage under these conditions. As both, iron limitation and dynamic light synergistically decrease the energy transfer efficiency and biomass build-up, even larger antagonistic effects under OA can be expected in the field (cf. Moore et al. 2007, Figure 7.2 C). In conclusion, iron limitation and dynamic light jointly decrease the probability of 'CO_2 fertilisation', which has been observed in conventional OA experiments (e.g. Riebesell et al. 1993, Hutchins et al. 2007, Tortell et al. 2008a).

If experiments aim to predict changes in primary and export production in offshore SO waters, they need to consider limiting iron concentrations and dynamic light fields. It must furthermore be noted that complex interactions with other drivers also exist. For example, the thickness of diatom frustules is known to increase under iron limitation (Hutchins & Bruland 1998, Takeda 1998, Marchetti & Harrison 2007). Similar responses have been described for elevated pCO_2 levels (Milligan et al. 2004, *Publication III*). Therefore, interactive effects between silicate, iron limitation and OA may change the potential for BSi production. Changes therein would, due to the ballasting effect of biogenic silica, have strong implications on the strength of the biological pump and its potential for carbon sequestration (Nelson et al. 1995). Implications arising from responses to multiple stressors on the biogeochemistry of the SO will be discussed in chapter 7.5.

7.4 A question of scale

The ultimate goal of research on OA effects is the up-scaling of findings to predict future changes in productivity and biogeochemical cycles. This requires an understanding of the relationship between different spatial and temporal scales as well as knowledge on the validity of measurements to cover respective scales (Figure 7.3). In *Publication II* and *III*, measurements of electron transport rates (ETR) through PSII reaction centres are presented, which occur on very small spatial (approx. 10^{-10} m) and temporal scales (approx. 10^{-12} days; Figure 7.3). These measurements are compared with estimates of net primary production, a parameter that integrates cellular processes on time scales of days and spatial

scales of cells (approx 10^{-6} m). By comparing these measures, assumptions for processes on the intermediate scales can be made. For example, lowered energy transfer efficiencies, which are indicated by divergent trends of ETR and net primary production, can be explained by various processes down-stream of PSII such as cyclic electron transport, alternative electron sinks or increased mitochondrial respiration (Behrenfeld et al. 2008).

Publication IV also compared productivity estimates on different scales. Net primary production, on the one hand, is assessed in small incubation bottles covering 24 hours and specifically measures the incorporation rates of carbon into phytoplankton biomass. An estimation from nutrient deficit calculations, on the other hand, integrate several weeks or months of changing temperatures, irradiances and nutrient concentrations and depend on the succession of different phytoplankton taxa and their grazers as well as processes such as upwelling, sinking and remineralization (Whitehouse et al. 2012). It is therefore not surprising that the two approaches yield completely different results. Being put into the right context, i.e. the right scale, both can jointly help to infer information about intermediate processes (*Publication IV*). With increasing temporal and spatial coverage, also the complexity of observations increases and nonlinearity of dynamics can occur. As a consequence, the uncertainty of long-term predictions increases (Benincá et al. 2002). Large-scale incubation experiments such as mesocosms (e.g. Riebesell et al. 2008) and field observations (e.g. Pollard et al. 2009) can help to unravel general or overarching patterns,

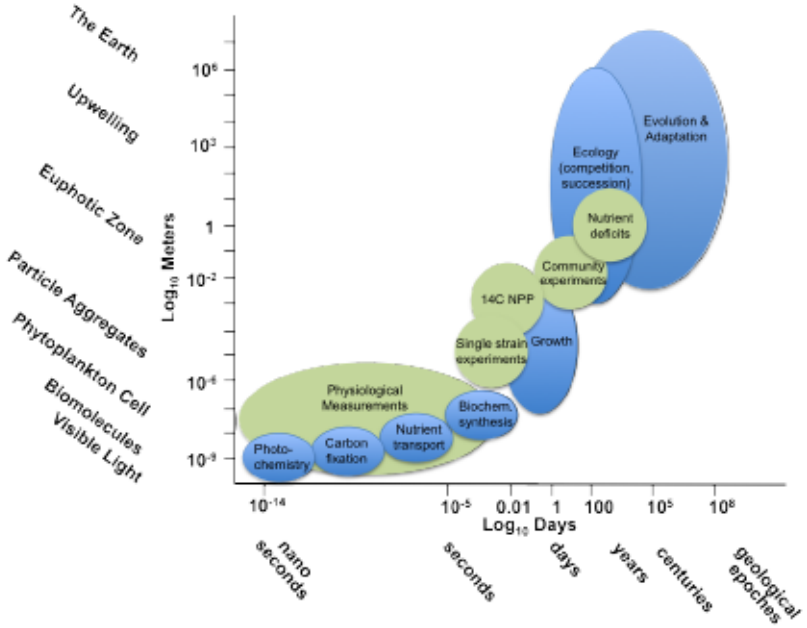

Figure 7.3: - Illustration of the different temporal and spatial scales of relevant process for phytoplankton physiology, ecology and evolution. Modified after Moore et al. (2013).

while detailed small-scale investigations on physiological processes (e.g. Rokitta et al. 2012) are needed to gain an understanding of the underlying mechanisms.

In this thesis, a large range of temporal and spatial levels was covered. It comprises many different pieces of a larger puzzle and although not all aspects are covered (e.g. effects on higher trophic levels, phytoplankton adaptation), a glimpse on 'the big picture' can be caught. In fact, the results and hypotheses from the different studies and measurements fit well together, indicating that the most important environmental drivers and ecophysiological mechanisms were covered by the different approaches. It therefore seems justified to speculate about likely consequences of OA on SO phytoplankton in a more general sense.

7.5 The Southern Ocean in a high CO_2 world

Especially regarding new research questions, the confidence in scientific concepts and results can vary over time (Kuhn 1969). The impacts of OA on phytoplankton productivity and biogeochemical cycling are far more variable and complex than expected about two decades ago. In the past years, however, also many explanations and underlying mechanisms for the differential response patters have been identified. In the context of this thesis, the most important reason is the modulation of OA effects by other environmental parameters. In agreement with the general opinion, *Publication IV* identified interactions between iron and light as the most important bottom-up controls on productivity and ecophysiology of SO phytoplankton (e.g. Boyd 2002, de Baar et al. 2005, Strzepek et al. 2012). It is therefore reasonable to assume that, besides top-down controls like grazing, iron and light are the prime suspects to modify the effects of OA in the SO. And even though *Publication II* and *III* are not covering the whole range of spatio-temporal variability and complexity, their results are in agreement with the current understanding of multiple drivers in the context of climate change and SO phytoplankton ecophysiology. For example, isolated strains as well as natural diatom-dominated phytoplankton communities have been shown to possess highly efficient and/or regulated CCMs (Tortell et al. 2008b, Neven et al. 2011, Trimborn et al. 2013). Therefore, the interactions between OA, CCM regulation and high-light stress proposed for *Chaetoceros debilis* (*Publication III*) may be extrapolated to other species. Furthermore, the interactions between seawater pH and iron bioavailability have been confirmed in single species incubations (Sugie & Yoshimura 2013) as well as phytoplankton communities from the Bering Sea (Sugie et al. 2013).

In general, SO regimes can be divided into 'coastal' (i.e. land- and or shelf-influenced) and 'oceanic' (i.e. land-remote) areas. As these regimes are characterised by strong differences in iron availability, they must be considered separately. Coastal SO phytoplankton

communities are known to form blooms that provide the basis for large stocks of higher trophic levels (Atkinson et al. 2001) and facilitate significant drawdown of atmospheric CO_2 (Arrigo et al. 1999). Coastal habitats are characterised by relatively high and constant iron availability to phytoplankton due to various input modes (e.g. dissolution from the shelf, dust deposition; Boyd & Ellwood 2010). With respect to light dynamics, shallower MLD cause higher integrated light intensities (Cisewski et al. 2005), even though higher turbidity, due to melt water input, can lead to steep light gradients (MacIntyre 2000, Dierssen et al. 2002). Under current conditions, ample iron supply in coastal regions allows phytoplankton to adapt efficiently to dynamic light (Sunda & Huntsman 1997, Strzepek & Harrison 2004), yielding high biomass on a regular basis (Wefer & Fischer 1991, Arrigo et al. 2008, Figure 7.4 A). The oceanic HNLC regions of the SO are defined by low average phytoplankton concentrations (e.g. de Baar et al. 1994). This is thought to be caused by particularly low iron supply from the distant continents and shelf seas (Martin 1990, Duce et al. 1991) in combination with light limitation and/or stress resulting from deep MLDs (van Oijen et al. 2004, Alderkamp et al. 2010). Nonetheless, also oceanic phytoplankton blooms with substantial drawdown of carbon occur. These are usually associated with increased average light intensities due to stronger surface stratification in late spring or early summer combined with increased iron availabilities originating from previous events of deep-water upwelling (Moore et al. 1999, Abbott et al. 2000, Blain et al. 2001, *Publication IV*; Figure 7.4 A).

Future projections on SO productivity and the strength of the biological pump critically depend on the expected changes in iron input and light environments. Unfortunately, no consensus on these questions exists and model predictions often lack agreement (Boyd & Ellwood 2010, Breitbart et al. 2010). Especially with respect to the future iron availability, several different input sources and their characteristics need to be considered. For example, atmospheric iron deposition depends on continental aridity, sea level as well as wind and

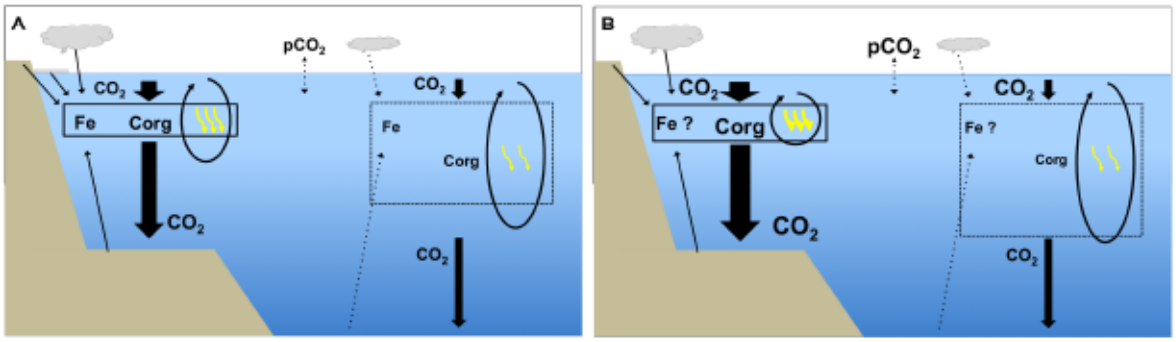

Figure 7.4: - Simplified illustration of the current (A) and potential future (B) development of production and export of organic matter (C_{org}) production via the biological carbon pump depending on mixing regimes and iron input for the coastal and oceanic regions of the SO.

ocean current patterns and strengths (Breitbart et al. 2010). The bioavailability of the newly supplied iron will change with ligand and siderophore (and thus microbial) composition as well as seawater pH (Shi et al. 2010, Hassler et al. 2012). Furthermore, the availability of iron to phytoplankton in the euphotic zone depends on the depth and temporal development of the surface mixed layer (Boyd & Ellwood 2010). As the effects of climate change on iron input mechanisms into the SO remain unknown (Boyd & Ellwood 2010), only changes in MLD und upwelling are considered in the following.

For most parts of the world's oceans, increased sea surface temperatures are proposed to also intensify surface stratification and thus decrease MLD (Steinacher et al. 2010). At least in the oceanic regions of the SO, future MLD dynamics are probably more governed by wind patterns than by thermal stratification (Lovenduski & Gruber 2005). On-going changes in the leading mode of climate variability in the Southern Hemisphere troposphere, known as the Southern Annular Mode (SAM), lead to stronger westerly winds south of 45°S (Thompson & Solomon 2002, Marshall 2003). Thus, MLDs are thought to decline along the Antarctic continent but increase in offshore waters (Lovenduski & Gruber 2005, Hauck et al. 2013). One could therefore hypothesise that in coastal waters, stratification increases and phytoplankton experience less dynamic and higher integrated irradiances. In view of the generally high iron availabilities in coastal waters, changes in stratification probably will not lead to pronounced iron limitation in these areas. For the oceanic areas, most studies focussed on the effects of stronger winds on upwelling and subsequent out-gassing of CO_2 from the SO (Le Quéré et al. 2007, Zickfeld et al. 2008, Le Quéré et al. 2008). Accounting for effects on primary production and subsequent carbon sequestration via the biological pump, modelling results suggest that an increase in MLD in the oceanic waters of the SO will lead to increased primary and export production due to increased iron supply from deeper waters (Hauck et al. 2013). According to the latter study, the benefits of increased iron availabilities are expected to cancel out the negative effects of lower integrated and more dynamic irradiances.

Taking into account the interactive effects of OA, iron and light regimes, this thesis yields different predictions for the SO, which furthermore depend on the region considered. The results from *Publication III* question whether a slight alleviation of iron limitation by higher upwelling of nutrients in the oceanic areas will be able to compensate for the increased metabolic costs of dynamic light and the lowered energy availability due to deeper mixing (Strzepek et al. 2012, *Publication III*). Moreover, decreasing iron bioavailabilities with decreasing pH could even intensify iron limitation in the future (Shi et al. 2010, *Publication II*). Higher susceptibility towards photoinhibition under OA could furthermore intensify the high-light stress experienced in the high-light peaks at the sea surface (McCarthy et al. 2012, *Publication III*). Iron-limited phytoplankton communities therefore unlikely benefit from the

lowered metabolic costs for carbon acquisition (*Publication II*), causing primary production to be unaltered by OA. Also, there are no indications for functional shifts towards more silicified diatoms that may enhance the export efficiency (*Publication II*).

For the coastal areas of the SO, however, a completely different picture emerges. Under the relatively high iron concentrations, phytoplankton cells should be able to acclimate to their light environment and therefore benefit from a shoaling of the MLD (Strzepek et al. 2012, *Publication II*). The correspondingly lower variability in irradiance could furthermore decrease the costs for photoacclimation (Arrigo et al 2010, *Publication III*). These changes in capacity and cost of photoacclimation may compensate for the likely higher susceptibility towards photoinhibition under OA (McCarthy et al. 2012, *Publication III*). Under these conditions, phytoplankton may even benefit from lowered metabolic costs for carbon acquisition, causing primary production to increase under OA (Tortell et al. 2008a, *Publication II*). Under iron-replete conditions, as they occur in coastal areas, OA induced taxonomic shift towards strongly silicified diatom species, which are more efficient vectors for carbon export (*Publication II*, Figure 7.4 B). Alderkamp et al. (2012) suggested that the relative contribution of diatoms to the total phytoplankton biomass may increase with a future shoaling of the MLD, representing another positive feedback on export production. In conclusion, while there may be substantial potential for the proposed 'CO_2 fertilisation' of primary and export production in land-influenced coastal waters, this is unlikely for the most parts of the land-remote regions of the SO (Figure 7.4 B).

7.6 Perspectives for future research

As this thesis investigated several aspects and levels of OA effects on SO phytoplankton, also the emerging gaps in knowledge and further research directions are plentiful. On the level of scientific attainment, the implications of unknown or high uncertainties of predictions have been discussed above. For experiments, all different levels of uncertainties should be investigated in order to assign an overall (un)certainty of scientific findings (e.g. as done in the IPCC reports). For example, to better estimate the uncertainties in carbonate chemistry calculations described in *Publication I*, an inter-laboratory comparison of TA, DIC and pH measurements of ambient and high pCO_2 samples has been initiated in cooperation with Prof. Andrew Dickson and his co-workers from Scripps Institution (USA).

With respect to the modulation of OA effects by key environmental variables (*Publication II* and *III*), further research is necessary to predict SO phytoplankton responses with higher confidence. Most importantly, the interactive effects of OA, iron limitation and dynamic light should be investigated further (cf. Feng et al. 2010). To date, scientific insights

into these interactions are often hindered by the need for highly sophisticated experimental setup, which is the reason why data is scarce. In addition, the impact of different iron sources and their bioavailabilities under decreasing seawater pH should be investigated. A successful projection of future SO phytoplankton responses will also depend on our abilities to estimate and predict changes in the different iron input modi (Boyd & Ellwood 2010).

The effects of different frequencies and amplitudes of dynamic light field should also have a high research priority. If OA responses are put into the context of photosystem repair, D1 protein turnover and associated metabolic costs, a process-based understanding of the interactions between OA and dynamic light can be gained. There is more and more evidence that increasing pCO_2 levels lead to changes in the balance between light and dark reactions of photosynthesis (Kranz et al. 2010, Rokitta & Rost 2012, *Publication III*) as well as carbon and energy fluxes in phytoplankton cells (Rokitta et al. 2012, Beszteri et al. in prep). To understand these interactions, thorough investigations of small-scale processes such as the up- or down-regulation of metabolic pathways via gene expression studies (i.e. transcriptomics) and subsequent metabolite composition (i.e. metabolomics) are needed (Fiehn 2002). For example, the composition and turnover of photosystems as well as storage compounds (e.g. fatty acid composition) could be particularly helpful for understanding the fluxes of energy and carbon under multiple stressors.

An increased understanding of OA effects on different levels of complexity is required for the mathematical modelling of cells, ecosystem dynamics and global elemental fluxes (Follows et al. 2007). Even though this thesis investigated the combined effects of pCO_2, iron and light dynamics on various temporal and spatial scales, some levels are obviously missing (e.g. intraspecific plasticity, potential for adaptation, interactions with higher trophic levels). In order to better relate the responses from different temporal and spatial scales to each other, field observations should be linked to perturbation experiments with natural communities as well as in-depth physiological approaches of single species in a systematic way. In this context, it could be useful to investigate development of a phytoplankton bloom in-situ in concert with bottle incubations to disentangle the effects of different drivers (e.g. iron, light) as well as their modulation by OA. In subsequent laboratory studies on isolated strains from the different manipulations, intra- and interspecific variability as well as their physiological plasticity could be investigated. In such an experimental framework, the specific traits of an organism leading to competitive advantages could be identified (Litchman & Klausmeier 2008). This may allow for an understanding of the relative importance of key traits (e.g. efficiency of iron or carbon acquisition) and the trade-offs between them. Such a holistic approach could help to understand the current and future relationships between ecosystem

structure (e.g. species composition and diversity) and functioning (e.g. primary and export production).

7.7 Conclusions

In this thesis, the general importance as well as the underlying mechanisms of interactions between increasing pCO_2, light and iron availability have been identified, with the conclusion that there is no such thing as 'the OA effect'. Even when specifying the organism or region of interest, the manifestation of OA effects strongly depends on the abiotic environmental settings, influencing energization or resource availability, as well as biotic interactions with competitors and grazers. These interdependencies may help to explain the often seemingly contradicting results from an increasing volume of scientific literature that is concerned with OA. With increasing understanding of the effects of multiple drivers on marine ecophysiology and biogeochemistry, predictions can be developed with higher confidence.

Chapter 8

References

Abbott, M. R., Richman, J. G. R., Letelier, M., Bartlett, J. S. (2000) The spring bloom in the Antarctic Polar Frontal Zone as observed from a mesoscale array of bio-optical sensors. Deep Sea Research Part II: Topical Studies in Oceanography, 47, 3285-3314

Abelmann, A., Gersonde, R., Cortese, G., Kuhn, G., Smetacek, V. (2006) Extensive phytoplankton blooms in the Atlantic sector of the glacial Southern Ocean. Paleoceanography, 21, PA1013

Alderkamp, A.-C., de Baar, H. J. W., Visser, R. J. W., Arrigo, K. R. (2010) Can photoinhibition control phytoplankton abundance in deeply mixed water columns of the Southern Ocean? Limnology and Oceanography, 55, 12481264

Alderkamp, A.-C., Kulk, G., Buma, A. G. J., Visser, R. J. W., Van Dijken, G. L., Mills, M. M., Arrigo, K. R. (2012) The effect of iron limitation on the photophysiology of *Phaeocystis antarctica* (Prymnesiophyceae) and *Fragilariopsis cylindrus* (Bacillariophyceae) under dynamic iradiance. Journal of Phycology, 48, 45-59

Arrigo, K. R., Worthen, D., Schnell, A., Lizotte, M. P. (1998) Primary production in Southern Ocean waters. Journal of Geophysical Research: Oceans, 103, 15587-15600

Arrigo, K. R., Robinson, D. H., Worthen, D. L., Dunbar, R. B., DiTullio, G. R., VanWoert, M., Lizotte, M. P. (1999) Phytoplankton Community Structure and the Drawdown of Nutrients and CO_2 in the Southern Ocean. Science, 283, 365-367

Arrigo, K. R., van Dijken, G., M. Long, M. (2008) Coastal Southern Ocean: A strong anthropogenic CO_2 sink. Geophysical Research Letters, 35, L21602

Asada, K. (1999) The waterwater cycle in chloroplasts: scavenging of active oxygens and dissipation of excess photons. Annual Review of Plant Physiology and Plant Molecular Biology, 50, 601639

Atkinson, A., Whitehouse, M. J., Priddle, J., Cripps, G. C., Ward, P., Brandon, M. A. (2001) South Georgia, Antarctica: a productive, cold water, pelagic ecosystem. Marine Ecology Progress Series, 216, 279-308

Bach, L. T., Riebesell, U., Schulz, K. G. (2011) Distinguishing between the effects of ocean acidification and ocean carbonation in the coccolithophore *Emiliania huxleyi*. Limnology and Oceanography, 56, 2040-2050

Badger, M. R., Andrews, T. J., Whitney, S. M., Ludwig, M., Yellowlees, D. C., Leggat, W., Price,G. D. (1998) The diversity and coevolution of Rubisco, plastids, pyrenoids, and chloroplast-based CO_2-concentrating mechanisms in algae. Canadian Journal of Botany-Revue Canadienne De Botanique, 76, 1052-1071

Banse, K. (1996) Low seasonality of low concentrations of surface chlorophyll in the Subantarctic water ring: underwater irradiance, iron, or grazing? Progress In Oceanography, 37, 241-291

Bareille, G., Labracherie, M., Labeyrie, L., Pichon, J.-J., Turon, J.-L. (1991) Biogenic silica accumulation rate during the Holocene in the southeastern Indian Ocean. Marine Chemistry, 35, 537-551

Bathmann, U. V., Scharek, R., Klaas, C., Dubischar, C. D., Smetacek, V. (1997) Spring development of phytoplankton biomass and composition in major water masses of the Atlantic sector of the Southern Ocean. Deep Sea Research Part II: Topical Studies in Oceanography, 44, 51-67

Beardall, J., Giordano, M. (2002) Ecological implications of microalgal and cyanobacterial CO_2 concentrating mechanisms, and their regulation. Functional Plant Biology, 29, 335-347

Behrenfeld, M. J., Milligan, A. J. (2013) Photophysiological Expressions of Iron Stress in Phytoplankton. Annual Review of Marine Science, 5, 2687-2703

Behrenfeld, M. J., Halsey, K. H., Milligan, A. J. (2008) Evolved physiological responses of phytoplankton to their integrated growth environment. Philosophical Transactions of the Royal Society B: Biological Sciences, 363, 2687-2703

Behrenfeld, M. J., Prásil, O., Babin, M., Bruyant, F. (2004) In search of a physiological basis for covariations in light-limited and light-saturated photosynthesis. Journal of Phycology, 40, 4-25

Bekker, A., Holland, H. D., Wang, P. L., Rumble, D., Stein, H. J., Hannah, J. L., Coetzee, L. L., Beukes, N. J. (2004) Dating the rise of atmospheric oxygen. Nature, 427, 117-120

Benincá, E., Huisman, J., Heerkloss, R., Johnk, K. D., Branco, P., Van Nes, E. H., Scheffer, M., Ellner, S. P. (2008) Chaos in a long-term experiment with a plankton community. Nature, 451, 822-825

Beszteri, S., Hoppe, C., Bachmann, J., Frickenhaus, S., Trimborn, S., Rost, B.: Interactive effects of CO_2 and dynamic light on the transcriptome of *Chaetoceros debilis*. In preparation

Bindoff, N. L., Willebrand, J., Artale, V., Cazenave, A., Gregory, J. M., Gulev, S., Hanawa, K., Le Quéré, C., Levitus, S., Nojiri, Y., Shum, C. K., Talley, L. D., Unnikrishnan, A. S., Josey, S. A., Tamisiea, M., Tsimplis, M., Woodworth, P. (2007) Observations: oceanic climate change and sea level. In Climate change 2007: the physical science basis. Contribution of Working Group I. , ed. S. Q. Solomon, D.; Manning, M.; Chen, Z.; Marquis, M.; Averyt, K.B.; Tignor, M.; Miller, H.L., 385-428. Cambridge: Cambridge University Press

Blain, S., Tréguer, P., Belviso, S., Bucciarelli, E., Denis, M., Desabre, S., Fiala, M., Martin Jézéquel, V., Le Févre, J., Mayzaud, P., Marty, J.-C., Razouls, S. (2001) A biogeochemical study of the island mass effect in the context of the iron hypothesis: Kerguelen Islands, Southern Ocean. Deep Sea Research Part I: Oceanographic Research Papers, 48, 163-187

Böning, C. W., Dispert, A., Visbeck, M., Rintoul, S. R., Schwarzkopf, F. U. (2008) The response of the Antarctic Circumpolar Current to recent climate change. Nature Geoscience, 1, 864-869

Boyd, P. W. (2002) Environmental factors controlling phytoplankton processes in the Southern Ocean. Journal of Phycology, 38, 844-861

Boyd, P. W., Hutchins, D. A. (2012) Understanding the responses of ocean biota to a complex matrix of cumulative anthropogenic change. Marine Ecology Progress Series, 470, 125-135

Boyd, P. W., Ellwood,M. J. (2010) The biogeochemical cycle of iron in the ocean. Nature Geoscience, 3, 675-682

Boyd, P. W., Crossley, A. C., DiTullio, G. R., Griffiths, F. B., Hutchins, D. A., Queguiner, B., Sedwick, P. N. Trull, T. W. (2001) Control of phytoplankton growth by iron supply and irradiance in the subantarctic Southern Ocean: Experimental results from the SAZ Project. Journal of Geophysical Research: Oceans, 106, 31573-31583

Boyd, P. W., Watson, A. J., Law, C. S., Abraham, E. R., Trull, T., Murdoch, R., Bakker, D. C. E., Bowie, A. R., Buesseler, K. O., Chang, H., Charette, M., Croot, P., Downing, K., Frew, R., Gall, M., Hadfield, M., Hall, J., Harvey, M., Jameson, G., LaRoche, J., Liddicoat, M., Ling, R., Maldonado, M. T., McKay, R. M., Nodder, S., Pickmere, S., Pridmore, R., Rintoul, S., Safi, K., Sutton, P., Strzepek, R., Tanneberger, K., Turner, S., Waite, A., Zeldis, J. (2000) A mesoscale phytoplankton bloom in the polar Southern Ocean stimulated by iron fertilization. Nature, 407, 695-702

Boyd, P. W., Strzepek, R., Fu, F., Hutchins, D. A., Tait, A. (2010) Environmental control of open-ocean phytoplankton groups: Now and in the future. Journal Limnology and Oceanography, 55, 1353-1376

Boye, M., van den Berg, C. M. G., de Jong, J. T. M., Leach, H., Croot, P., de Baar, H. J. W. (2001) Organic complexation of iron in the Southern Ocean. Deep Sea Research Part I: Oceanographic Research Papers, 48, 1477-1497

Boye, M., Nishioka, J., Croot, P., Laan, P., Timmermans, K. R., Strass, V. H., Takeda, S., de Baar, H. J. W. (2010) Significant portion of dissolved organic Fe complexes in fact is Fe colloids. Marine Chemistry, 122, 20-27

Breitbarth, E., Achterberg, E. P., Ardelan, M. V., Baker, A. R., Bucciarelli, E., Chever, F., Croot, P. L., Duggen, S., Gledhill, M., Hassellev, M., Hassler, C., Hoffmann, L. J., Hunter, K. A., Hutchins, D. A., Ingri, J., Jickells, T., Lohan, M. C., Nielsdottir, M. C., Sarthou, G., Schoemann, V., Trapp, J. M., Turner, D. R., Ye, Y. (2010) Iron biogeochemistry across marine systems - progress from the past decade. Biogeosciences, 7,1075-1097

Broecker, W. S., Clark, E. (2002) A major dissolution event at the close of MIS 5e in the western equatorial Atlantic. Geochemistry, Geophysics, Geosystems, 3, 1-5

Broecker, W. S., Peng, T.-H. (1992) Interhemispheric transport of carbon dioxide by ocean circulation. Nature, 356, 587-589

Brzezinski, M. A., Dickson, M.-L., Nelson, D. M., Sambrotto, R. (2003) Ratios of Si, C and N uptake by microplankton in the Southern Ocean. Deep Sea Research Part II: Topical Studies in Oceanography, 50, 619-633

Buesseler, K. O. (1998) The decoupling of production and particulate export in the surface ocean. Global Biogeochemical Cycles, 12, 297-310

Burkhardt, S., Zondervan, I., Riebesell, U. (1999) Effect of CO_2 concentration on C: N: P ratio in marine phytoplankton: A species comparison. Limnology and Oceanography, 44, 683-690

Caldeira, K., Wickett, M. E. (2003) Oceanography: Anthropogenic carbon and ocean pH. Nature, 425

Canadell, J. G., Le Quéré, C., Raupach, M. R., Field, C. B., Buitenhuis, E. T., Ciais, P., Conway, T. J., Gillett, N. P., Houghton, R. A., Marland, G. (2007) Contributions to accelerating atmospheric CO_2 growth from economic activity, carbon intensity, and efficiency of natural sinks. Proceedings of the National Academy of Sciences of the United States of America, 104, 18866-18870

Cassar, N., Laws, E. A., Bidigare, R. R., Popp, B. N. (2004) Bicarbonate uptake by Southern Ocean phytoplankton. Global Biogeochemical Cycles, 18, GB2003

Cisewski, B., Strass, V. H., Prandke, H. (2005) Upper-ocean vertical mixing in the Antarctic Polar Front Zone. Deep Sea Research Part II: Topical Studies in Oceanography, 52, 1087-1108

Collins, S., Rost, B., Rynearson, T. A. (2013) Evolutionary potential of marine phytoplankton under ocean acidification. Evolutionary Applications, in press

Cooper, L. (1937) Some conditions governing the solubility of iron. Proceedings of the Royal Society of London. Series B, Biological Sciences, 124, 299-307

de Baar, H. J. W. (1994) von Liebig's law of the minimum and plankton ecology (1899-1991). Progress In Oceanography, 33, 347-386

de Baar, H. J. W., Boyd, P. W., Coale, K. H., Landry, M. R., Tsuda, A., Assmy, P., Bakker, D. C. E., Bozec, Y., Barber, R. T., Brzezinski, M. A., Buesseler, K. O., Boyé, M., Croot, P. L., Gervais, F., Gorbunov, M. Y., Harrison, P. J., Hiscock, W. T., Laan, P., Lancelot, C., Law, C. S., Levasseur, M., Marchetti, A., Millero, F. J., Nishioka, J., Nojiri, Y., van Oijen, T., Riebesell, U., Rijkenberg, M. J. A., Saito, H., Takeda, S., Timmermans, K. R., Veldhuis, M. J. W., Waite, A. M., Wong, C.-S. (2005) Synthesis of iron fertilization experiments: From the Iron Age in the Age of Enlightenment. Journal of Geophysical Research, 110, C09S16

De La Rocha, C. L., Passow, U. (2007) Factors influencing the sinking of POC and the efficiency of the biological carbon pump. Deep Sea Research Part II: Topical Studies in Oceanography, 54, 639-658

Denman, K., Gargett, A. (1983) Time and space scales of vertical mixing and advection of phytoplankton in the upper ocean. Oceanography, 28

Dickson, A. G. (1981) An exact definition od total alkalinity and a procedure for the alkalinity and total inorganic carbon from titration data. Deep-Sea Research 28, 609 - 623

Dickson, A. G., Sabine, C. L., Christian, J. R. (2007) Guide to best practices for ocean CO_2 measurements. 191. PICES Special Publication 3

Dierssen, H. M., Smith, R. C., Vernet, M. (2002) Glacial meltwater dynamics in coastal waters west of the Antarctic peninsula. Proceedings of the National Academy of Sciences, 99, 1790-1795

Dong, S., Sprintall, J., Gille, S. T., Talley, L. (2008) Southern Ocean mixed-layer depth from Argo float profiles. Journal of Geophysical Research: Oceans, 113, C06013

Dubischar, C. D., Bathmann, U. V. (1997) Grazing impact of copepods and salps on phytoplankton in the Atlantic sector of the Southern Ocean. Deep Sea Research Part II: Topical Studies in Oceanography, 44, 415-433

Duce, R., Liss, P., Merrill, J., Atlas, E., BuatMenard, P., Hicks, B., Miller, J., Prospero, J., Arimoto, R., Church, T. (1991) The atmospheric input of trace species to the world ocean. Global Biogeochemical Cycles, 5, 193-259

Dugdale, R. C., Goering, J. J. (1967) Uptake of new and regenerated forms of nitrogen in primary productivity. Limnology and Oceanography, 12, 196206

Egleston, E. S., Sabine, C. L., Morel, F. M. M. (2010) Revelle revisited: Buffer factors that quantify the response of ocean chemistry to changes in DIC and alkalinity. Global Biogeochemical Cycles, 24, GB1002

Eppley, R. W., Peterson, B. J. (1979) Particulate organic matter flux and planktonic new production in the deep ocean. Nature, 282, 677-680

Fabry, V. J., McClintock, J. B., Mathis, J. T., Grebmeier, J. M. (2009) Ocean Acidification at High Latitudes: The Bellweather. Oceanography, 22, 161-171

Falkowski, P. G., Raven, J. A. (1997) Aquatic photosynthesis. Blackwell Publishers

Falkowski, P. G., Katz, M. E., Knoll, A. H., Quigg, A., Raven, J. A., Schofield, O., Taylor, F. J. R. (2004) The Evolution of Modern Eukaryotic Phytoplankton. Science, 305, 354-360

Falkowski, P. G., Barber, R. T., Smetacek, V. (1998) Biogeochemical Controls and Feedbacks on Ocean Primary Production. Science, 281, 200-206

Feely, R. A., Doney, S. C., Cooley, S. R. (2009) Ocean Acidification: Present Conditions and Future Changes in a High-CO_2 World. Oceanography, 22, 3647

Feng, Y., Warner, M. E., Zhang, Y., Sun, J., Fu, F.-X., Rose, J. M., Hutchins, D. A. (2008) Interactive effects of increased pCO_2, temperature and irradiance on the marine

coccolithophore *Emiliania huxleyi* (Prymnesiophyceae). European Journal of Phycology, 43, 87-98

Feng, Y., Hare, C., K. Leblanc, J. Rose, Y. Zhang, G. DiTullio, P. Lee, S. Wilhelm, J. Rowe, J. Sun, N. Nemcek, C. Gueguen, U. Passow, I. Benner, C. Brown & D. Hutchins (2009) Effects of increased pCO_2 and temperature on the North Atlantic spring bloom. I. The phytoplankton community and biogeochemical response. Marine Ecology Progress Series, 388, 13-25

Feng, Y., Hare, C. E., Rose, J. M., Handy, S. M., DiTullio, G. R., Lee, P. A., Smith Jr, W. O., Peloquin, J., Tozzi, S., Sun, J., Zhang, Y., Dunbar, R. B., Long, M. C., Sohst, B., Lohan, M., Hutchins, D. A. (2010) Interactive effects of iron, irradiance and CO_2 on Ross Sea phytoplankton. Deep Sea Research Part I: Oceanographic Research Papers, 57, 368-383

Fiehn, O. (2002) Metabolomics - the link between genotypes and phenotypes. Plant Molecular Biology, 48, 155-171

Field, C. B., Behrenfeld, M. J., Randerson, J. T., Falkowski, P. (1998) Primary Production of the Biosphere: Integrating Terrestrial and Oceanic Components. Science, 281, 237-240

Follows, M. J., Dutkiewicz, S., Grant, S., Chisholm, S. W. (2007) Emergent Biogeography of Microbial Communities in a Model Ocean. Science, 315, 1843-1846

Folt, C., Chen, C., Moore, M., Burnaford, J. (1999) Synergism and antagonism among multiple stressors. Limnology and Oceanography, 44, 864-877

Galbraith, E. D., Gnanadesikan, A., Dunne, J. P., Hiscock, M. R. (2010) Regional impacts of iron-light colimitation in a global biogeochemical model. Biogeosciences, 7, 1043-1064

Gao, K., Xu, J., Gao, G., Li, Y., Hutchins, D. A., Huang, B., Wang, L., Zheng, Y., Jin, P., Cai, X., Hader, D.-P., Li, W., Xu, K., Liu, N., Riebesell, U. (2012a) Rising CO_2 and increased light exposure synergistically reduce marine primary productivity. Nature Climate Change, 2, 519-523

Gao, K., Helbling, E. W., Häder, D.-P., Hutchins, D. A. (2012b) Responses of marine primary producers to interactions between ocean acidification, solar radiation, and warming. Marine Ecology Progress Series, 470, 167-189

Gattuso, J.-P., Hansson, L. (2011) Ocean acidification: background and history. In Ocean acidification, eds. J.-P. Gattuso & L. Hansson, 1-20. Oxford: Oxford University Press

Geider, R., LaRoche, J. (1994) The role of iron in phytoplankton photosynthesis, and the potential for iron-limitation of primary productivity in the sea. Photosynthesis Research, 39, 275-301

Goeyens, L., Tréguer, P., Baumann, M. E. M., Baeyens, W., Dehairs, F. (1995) The leading role of ammonium in the nitrogen uptake regime of Southern Ocean marginal ice zones. Journal of Marine Systems, 6, 345-361

Gran, H. H. (1931) On the conditions for the production of plankton in the sea. Rapports et Proces verbaux des Rgunions, Conseil International pour le exploration de la Met, 75, 37-46

Greene, R. M., Geider, R. J., Falkowski, P. G. (1991) Effect of Iron Limitation on Photosynthesis in a Marine Diatom. Limnology and Oceanography, 36, 1772-1782

Gruber, N., Gloor, M., Mikaloff Fletcher, S. E., Doney, S. C., Dutkiewicz, S., Follows, M. J., Gerber, M., Jacobson, A. R., Joos, F., Lindsay, K., Menemenlis, D., Mouchet, A., Müller, S. A., Sarmiento, J. L., Takahashi, T. (2009) Oceanic sources, sinks, and transport of atmospheric CO_2. Global Biogeochemical Cycles, 23, GB1005

Halsey, K. H., Milligan, A. J., Behrenfeld, M. J. (2011) Linking time-dependent carbon-fixation efficiencies in *Dunaliella tertiolecta* (Chlorophyceae) to underlying metabolic pathways. Journal of Phycology, 47, 66-76

Wedepohl, K. H. (1995) The composition of the continental crust. Geochimica et Cosmochimica Acta, 59, 1217-1232

Hare, C. E., DiTullio, G. R., Riseman, S. F., Crossley, A. C., Popels, L. C., Sedwick, P. N., Hutchins, D. A. (2007) Effects of changing continuous iron input rates on a Southern Ocean algal assemblage. Deep Sea Research Part I: Oceanographic Research Papers, 54, 732-746

Hart, T. J. (1934) On the phytoplankton of the Southwest Atlantic and the Bellingshausen Sea 1929-1931. Discovery Reports, 8, 1-268

Hassler , C. S., Schoemann, V., Boye, M., Tagliabue, A., Rozmarynowycz, M., McKay, R. M. L. (2012) Iron Bioavailability in the Southern Ocean. In Oceanography and Marine Biology: An Annual Review, eds. R. N. Gibson, R. J. A. Atkinson, J. D. M. Gordon, Hughes, R. N., 164. London: CRC Press

Hassler, C. S., Schoemann, V., Nichols, C. M., Butler, E. C. V., Boyd, P. W. (2011) Saccharides enhance iron bioavailability to Southern Ocean phytoplankton. Proceedings of the National Academy of Sciences, 108, 1076-1081

Hauck, J., Völker, C., Wang, T., Hoppema, M., Losch, M., Wolf-Gladrow, D. A. (2013) Seasonally different carbon flux changes in the Southern Ocean in response to the Southern Annular Mode. Global Biogeochemical Cycles, 2013GB004600

Heinze, C., Maier-Reimer, E., Winn, K. (1991) Glacial pCO_2 Reduction by the World Ocean: Experiments With the Hamburg Carbon Cycle Model. Paleoceanography, 6, 395-430

Hoegh-Guldberg, O., Bruno, J. F. (2010) The Impact of Climate Change on the Worlds Marine Ecosystems. Science, 328, 1523-1528

Holland, H. D. (1984) The chemical evolution of the atmosphere and oceans. Princeton: Princeton University Press

Hoppe, C. J. M., Langer, G., Rost, B. (2011) *Emiliania huxleyi* shows identical responses to elevated pCO_2 in TA and DIC manipulations. Journal of Experimental Marine Biology and Ecology, 406, 54-62

Hutchins, D. A., Bruland, K. W. (1998) Iron-limited diatom growth and Si:N uptake ratios in a coastal upwelling regime. Nature, 393, 561-564

Hutchins, D., Fu, F.-X., Zhang, Y., Warner, M., Feng, Y., Portune, K., Bernhardt, P., Mulholland, M. (2007) CO_2 control of *Trichodesmium* N_2 fixation, photosynthesis, growth rates, and elemental ratios: Implications for past, present, and future ocean biogeochemistry. Limnol. Oceanogr., 52, 1293

Iglesias-Rodriguez, D. M., Halloran, P., Rickaby, R., Hall, I., Colmenero-Hidalgo, E. (2008) Phytoplankton calcification in a high-CO_2 world. Science, 320, 336

IPCC Core Writing Team Pachauri, R. K. R., A. (eds.) (2007) Climate Change 2007: Synthesis Report. Contribution of Working Groups I, II and III to the Fourth Assessment Report of the Intergovernmental Panel on Climate Change. Geneva, Switzerland

Johnson, K. S., Gordon, R. M., Coale, K. H. (1997) What controls dissolved iron concentrations in the world ocean? Marine Chemistry, 57, 137-161

Kasting, J. F., Toon, O. B., Pollack, J. B. (1988) How climate evolved on the terrestrial planets. Scientific American, 258, 90-97

Katz, M., Finkel, Z., Grzebyk, D., Knoll, A., Falkowski, P. (2005) Evolutionary trajectories and biogeochemical impacts of marine eukaryotic phytoplankton. Annual Review of Ecological Systems, 35, 523

Keeling, C. D. (1973) Industrial production of carbon dioxide from fossil fuels and limestone. Tellus A, 25

Khatiwala, S., Primeau, F., Hall, T. (2009) Reconstruction of the history of anthropogenic CO_2 concentrations in the ocean. Nature, 462, 346-349

Kranz, S. A., Sültemeyer, D., Richter, K.-U., Rost, B. (2009) Carbon acquisition in Trichodesmium: the effect of pCO_2 and diurnal changes. Limnology and Oceanography, 54, 548-559

Kranz, S. A., Levitan, O., Richter, K.-U., Prásil, O., Berman-Frank, I., Rost, B. (2010) Combined Effects of CO_2 and Light on the N_2-Fixing Cyanobacterium *Trichodesmium* IMS101: Physiological Responses. Plant Physiology, 154, 334-345

Kranz, S., Eichner, M., Rost, B. (2011) Interactions between CCM and N_2 fixation in *Trichodesmium*. Photosynthesis Research, 109, 73-84

Kuhn, T. S. (1970) The structure of scientific revolutions, 2nd. Chicago: University of Chicago Press

Landry, M. R., Selph, K. E., Brown, S. L., Abbott, M. R., Measures, C. I., Vink, S., Allen, C. B., Calbet, A., Christensen, S., Nolla, H. (2002) Seasonal dynamics of phytoplankton in the Antarctic Polar Front region at 170°W. Deep Sea Research Part II: Topical Studies in Oceanography, 49, 1843-1865

Langer, G., Nehrke, G., Probert, I., Ly, J., Ziveri, P. (2009) Strain-specific responses of *Emiliania huxleyi* to changing seawater carbonate chemistry. Biogeosciences, 6, 2637-2646

Langer, G., Geisen, M., Baumann, K.-H., Kläs, J., Riebesell, U., Thoms, S., Young, J. R. (2006) Species-specific responses of calcifying algae to changing seawater carbonate chemistry. Geochemistry Geophysics Geosystems, 7

Lavaud, J. (2007) Fast regulation of photosynthesis in diatoms: mechanisms, evolution and ecophysiology. Functional Plant Science and Biotechnology, 1, 267-287

Le Quéré, C., Rödenbeck, C., Buitenhuis, E. T., Conway, T. J., Langenfelds, R., Gomez, A., Labuschagne, C., Ramonet, M., Nakazawa, T., Metzl, N., Gillett, N., Heimann, M. (2007) Saturation of the Southern Ocean CO_2 Sink Due to Recent Climate Change. Science, 316, 1735-1738

Le Quéré, C., Rödenbeck, C., Buitenhuis, E. T., Conway, T. J., Langenfelds, R., Gomez, A., Labuschagne, C., Ramonet, M., Nakazawa, T., Metzl, N., Gillett, N., Heimann, M. (2008) Response to Comments on "Saturation of the Southern Ocean CO_2 Sink Due to Recent Climate Change". Science, 319, 570

Lefebvre, S. C., Benner, I., Stillman, J. H., Parker, A. E., Drake, M. K., Rossignol, P. E., Okimura, K. M., Komada, T., Carpenter, E. J. (2012) Nitrogen source and pCO_2 synergistically affect carbon allocation, growth and morphology of the coccolithophore *Emiliania huxleyi*: potential implications of ocean acidification for the carbon cycle. Global Change Biology, 18, 493-503

Levitan, O., Rosenberg, G., Setlik, I., Setlikova, E., Grigel, J., Klepetar, J., Prasil, O., Berman-Frank, I. (2007) Elevated CO_2 enhances nitrogen fixation and growth in the marine cyanobacterium *Trichodesmium*. Global Change Biology, 13, 531-538

Levitus, S., Antonov, J., Boyer, T. (2005) Warming of the world ocean, 1955-2003. Geophysical Research Letters, 32, L02604.

Li, G., Campbell, D. A. (2013) Rising CO_2 Interacts with Growth Light and Growth Rate to Alter Photosystem II Photoinactivation of the Coastal Diatom *Thalassiosira pseudonana*. PLoS ONE, 8, e55562

Lindeman, R. L. (1942) The Trophic-Dynamic Aspect of Ecology. Ecology, 23, 399-417

Litchman, E., Klausmeier, C. A., Schofield, O. M., Falkowski, P. G. (2008) The role of functional traits and trade-offs in structuring phytoplankton communities: scaling from cellular to ecosystem level. Ecology Letters, 10, 1170-1181

Lohbeck, K. T., Riebesell, U., Reusch, T. B. H. (2012) Adaptive evolution of a key phytoplankton species to ocean acidification. Nature Geosciences, 346-351

Longhurst, A. R., Harrison, W. G (1989) The biological pump: Profiles of plankton production and consumption in the upper ocean. Progress In Oceanography, 22, 47-123

Lovenduski, N. S., Gruber, N. (2005) Impact of the Southern Annular Mode on Southern Ocean circulation and biology. Geophysical Research Letters, 32, L11603

Lüthi, D., Le Floch, M., Bereiter, B., Blunier, T., Barnola, J.-M., Siegenthaler, U., Raynaud, D., Jouzel, J., Fischer, H., Kawamura, K., Stocker, T. F. (2008) High-resolution carbon dioxide concentration record 650,000-800,000 years before present. Nature, 453, 379-382

Macdonald, A. M., Wunsch, C. (1996) An estimate of global ocean circulation and heat fluxes. Nature, 382, 436-439

MacIntyre, H. L., Kana, T. M., Geider, R. J. (2000) The effect of water motion on short-term rates of photosynthesis by marine phytoplankton. Trends in Plant Science, 5, 12-17

Marchetti, A., Harrison, P. J. (2007) Coupled changes in the cell morphology and elemental (C, N, and Si) composition of the pennate diatom *Pseudo-nitzschia* due to iron deficiency. Limnology and Oceanography, 52, 2270-2284

Marshall, G. J. (2003) Trends in the Southern Annular Mode from Observations and Reanalyses. Journal of Climate, 16, 4134-4143

Marshall, J., Speer, K. (2012) Closure of the meridional overturning circulation through Southern Ocean upwelling. Nature Geoscience, 5, 171-180

Martin, J. H. (1990) Glacial-interglacial CO_2 change: The Iron Hypothesis. Paleoceanography, 5, 1-13

Martin, J., Fitzwater, S., Gordon, R. (1990) Iron Deficiency Limits Phytoplankton Growth in Antarctic Waters. Global Biogeochemical Cycles, 4, 5-12

McCarthy, A., Rogers, S. P., Duffy, S. J., Campbell, D. A. (2012) Elevated carbon dioxide differentially alters the photophysiology of *Thalassiosira pseudonana* (Bacillariophyceae) and *Emiliania huxleyi* (Haptophyta). Journal of Phycology, 48, 635-646

McKay, R. M. L., Geider, R. J., LaRoche, J. (1997) Physiological and Biochemical Response of the Photosynthetic Apparatus of Two Marine Diatoms to Fe Stress. Plant Physiology, 114, 615-622

Millenium Ecosystem Assesment Board (2005) Ecosystems and Human Well-being: Synthesis. In Island Press, ed. P. Reid. Washington, DC

Milligan, A. J., Varela, D. E., Brzezinski, M. A., Morel, F. M. M. (2004) Dynamics of Silicon Metabolism and Silicon Isotopic Discrimination in a Marine Diatom as a Function of pCO_2. Limnology and Oceanography, 49, 322-329

Mitchell, B. G., Brody, E. A., Holm-Hansen, O., McClain, C., Bishop, J. (1991) Light limitation of phytoplankton biomass and macronutrient utilization in the Southern Ocean. Limnology and Oceanography, 36, 1662-1677

Mitchell, J. F. B. (1989) The "Greenhouse" effect and climate change. Reviews of Geophysics, 27, 115-139

Moore, C. M., Mills, M. M., Arrigo, K. R., Berman-Frank, I., Bopp, L., Boyd, P. W., Galbraith, E. D., Geider, R. J., Guieu, C., Jaccard, S. L., Jickells, T. D., La Roche, J., Lenton, T. M., Mahowald, N. M., Maranon, E., Marinov, I., Moore, J. K., Nakatsuka, T., Oschlies, A., Saito, M. A., Thingstad, T. F., Tsuda, A., Ulloa, O. (2013) Processes and patterns of oceanic nutrient limitation. Nature Geosciences, 6, 1123-1129

Moore, C. M., Seeyave, S., Hickman, A. E., Allen, J. T., Lucas, M. I., Planquette, H., Pollard, R. T., Poulton, A. J. (2007) Ironlight interactions during the CROZet natural iron bloom and EXport experiment (CROZEX) I: Phytoplankton growth and photophysiology. Deep Sea Research Part II: Topical Studies in Oceanography, 54, 2045-2065

Moore, J. K., Abbott, M. R., Richman, J. G., Smith, W. O., Cowles, T. J., Coale, K. H., Gardner, W. D., Barber, R. T. (1999) SeaWiFS satellite ocean color data from the Southern Ocean. Geophysical Research Letters, 26, 1465-1468

Nelson, D. M., Brzezinski, M. A., Sigmon, D. E., Franck, V. M. (2001) A seasonal progression of Si limitation in the Pacific sector of the Southern Ocean. Deep Sea Research Part II: Topical Studies in Oceanography, 48, 3973-3995

Nelson, D. M., Smith Jr, W. O., Muench, R. D., Gordon, L. I., Sullivan, C. W., Husby, D. M. (1989) Particulate matter and nutrient distributions in the ice-edge zone of the Weddell Sea: relationship to hydrography during late summer. Deep Sea Research Part A. Oceanographic Research Papers, 36, 191-209

Nelson, D., Tréguer, P., Brzezinski, M. A., Leynaert, A., Quéguiner, B. (1995) Production and dissolution of biogenic silica in the ocean: Revised global estimates, comparison with regional data and relationship to biogenic sedimentation. Global Biogeochemical Cycles, 9, 359

Neven, I. A., Stefels, J., van Heuven, S. M. A. C., de Baar, H. J. W., Elzenga, J. T. M. (2011) High plasticity in inorganic carbon uptake by Southern Ocean phytoplankton in response to ambient CO_2. Deep Sea Research Part II: Topical Studies in Oceanography, 58, 2636-2646

Niyogi, K. K. (1999) Photoprotection revisited: Genetic and Molecular Approaches. Annual Review of Plant Physiology and Plant Molecular Biology, 50, 333-359

Orr, J., Fabry, V., Aumont, O., Bopp, L., Doney, S. (2005) Anthropogenic ocean acidification over the twenty-first century and its impact on calcifying organisms. Nature, 437, 681

Park, J., Oh, I.-S., Kim, H.-C., Yoo, S. (2010) Variability of SeaWiFs chlorophyll-a in the southwest Atlantic sector of the Southern Ocean: Strong topographic effects and weak seasonality. Deep Sea Research Part I: Oceanographic Research Papers, 57, 604-620

Peterson, C. H., Lubchenco, J. (1997) Marine ecosystem services. In Nature's services: societal dependence on natural ecosystems, ed. G. C. Daily. Washington, DC: Island Press

Petit, J. R., Jouzel, J., Raynaud, D., Barkov, N. I., Barnola, J.-M., Basile, I., Bender, M., Chappellaz, J., Davis, M., Delaygue, G., Delmotte, M., Kotlyakov, V. M., Legrand, M., Lipenkov, V. Y., Lorius, C., Pepin, L., Ritz, C., Salzman, E., Stievenard, M. (1999) Climate and atmopsheric history of the past 420,000 years from the Vostok ice core, Antarctica. Nature, 399, 429-436

Petrou, K., Hassler, C. S., Doblin, M. A., Shelly, K., Schoemann, V. r., van den Enden, R., Wright, S., Ralph, P. J. (2011) Iron-limitation and high light stress on phytoplankton populations from the Australian Sub-Antarctic Zone (SAZ). Deep Sea Research Part II: Topical Studies in Oceanography, 58, 2200-2211

Pollard, R. T., I. Salter, R. J. Sanders, M. I. Lucas, C. M. Moore, R. A. Mills, P. J. Statham, J. T. Allen, A. R. Baker, D. C. E. Bakker, M. A. Charette, S. Fielding, G. R. Fones, M. French, A. E. Hickman, R. J. Holland, J. A. Hughes, T. D. Jickells, R. S. Lampitt, P. J. Morris, F. H. Nedelec, M. Nielsdottir, H. Planquette, E. E. Popova, A. J. Poulton, J. F. Read, S. Seeyave, T. Smith, M. Stinchcombe, S. Taylor, S. Thomalla, H. J. Venables, R. Williamson & M. V. Zubkov (2009) Southern Ocean deep-water carbon export enhanced by natural iron fertilization. Nature, 457, 577-580

Prásil, O., Kolber, Z., Berry, J., Falkowski, P. (1996) Cyclic electron flow around Photosystem II in vivo. Photosynthesis Research, 48, 395-410

Priddle, J., Smetacek, V., Bathmann, U., Stromberg, J.-O., Croxall, J. P. (1992) Antarctic Marine Primary Production, Biogeochemical Carbon Cycles and Climatic Change [and Discussion]. Philosophical Transactions of the Royal Society of London. Series B: Biological Sciences, 338, 289-297

Raupach, M. R., Marland, G., Ciais, P., Le Quéré, C., Canadell, J. G., Klepper, G., Field, C. B. (2007) Global and regional drivers of accelerating CO_2 emissions. Proceedings of the National Academy of Sciences USA, 104, 10288-10293

Raven, J., Evans, M. W., Korb, R. (1999) The role of trace metals in photosynthetic electron transport in O_2-evolving organisms. Photosynthesis Research, 60, 111-150

Raven, P. H., Evert, R. F., Eichhorn, S. E. (2005) Biology of Plants. New York: W. H. Freeman

Raven, J. A., Cockell, C. S., De La Rocha, C. L. (2008) The evolution of inorganic carbon concentrating mechanisms in photosynthesis. Philosophical Transactions of the Royal Society B: Biological Sciences, 363, 2641-2650

Reinfelder, J. R. (2011) Carbon Concentrating Mechanisms in Eukaryotic Marine Phytoplankton. Annual Review of Marine Science, 3, 291-31

Ridgwell, A., Schmidt, D. N., Turley, C., Brownlee, C., Maldonaldo, M. T., Tortell, P. D., Young, J. R. (2009) From laboratory manipulations to earth system models. Biogeosciences, 6, 2611-2623

Riebesell, U., Wolf-Gladrow, D. A., Smetacek, V. (1993) Carbon dioxide limitation of marine phytoplankton growth rates. Nature, 361, 249-251

Riebesell, U., Zondervan, I., Rost, B., Tortell, P. D., Zeebe, R. E., Morel, F. M. M. (2000) Reduced calcification of marine phytoplankton in response to increased atmospheric CO_2. Nature, 407, 364-367

Riebesell, U., Bellerby, R., Grossart, H.-P., Thingstad, F. (2008) Mesocosm CO_2 perturbation studies: from organism to community level. Biogeosciences, 5, 1157-1164

Riebesell, U., Fabry, V. J.,Hansson, L., Gattuso, J.-P. (2010) Guide to best practices for ocean acidification research and data reporting

Rintoul, S. R., Sokolov, S. (2001) Baroclinic transport variability of the Antarctic Circumpolar Current south of Australia (WOCE repeat section SR3). Journal of Geophysical Research: Oceans, 106, 2815-2832

Rintoul, S. R. (2009) The Southern Ocean in the Earth System. In Science Diplomacy Antarctica, Science, and the Governance of International Spaces, eds. P. A. Berkman, M. A. Lang, D. W. H. Walton & O. R. Young. Washington D.D.: Smithsonian Institution Scholarly Press

Rokitta, S. D., Rost B. (2012) Effects of CO_2 and their modulation by light in the life-cycle stages of the coccolithophore *Emiliania huxleyi*. Limnology and Oceanography, 57, 607-618

Rokitta, S. D., John, U., Rost, B. (2012) Ocean Acidification Affects Redox-Balance and Ion-Homeostasis in the Life-Cycle Stages of *Emiliania huxleyi*. PLoS ONE, 7

Rost, B., Riebesell, U. (2004) Coccolithophores and the biological pump: responses to environmental changes. In Coccolithophores: from molecular processes to global impact, eds. H. R. Thierstein & J. R. Young, 99-125. Berlin, Springer

Rost, B., Zondervan, I., Wolf-Gladrow, D. (2008) Sensitivity of phytoplankton to future changes in ocean carbonate chemistry: Current knowledge, contradictions and research needs. Theme Section 'Effects on ocean acidification on marine ecosytems'. Marine Ecology Progress Series 373, 227-237

Rost, B., Zondervan, I., Riebesell, U. (2002) Light-dependent carbon isotope fractionation in the coccolithophorid *Emiliania huxleyi*. Limnology and Oceanography, 47, 120-128

Rost, B., Riebesell, U., Sültemeyer, D. (2006) Carbon acquisition of marine phytoplankton: Effect of photoperiod length. Limnology and Oceanography, 51, 12-20

Rost, B., Riebesell, U., Burkhardt, S., Sültemeyer, D. (2003) Carbon acquisition of bloom-forming marine phytoplankton. Limnology and Oceanography, 48, 55 - 67

Rowley, R. J., Kostelnick, J. C., Braaten, D., Li, X., Meisel, J. (2007) Risk of rising sea level to population and land area. Eos, Transactions American Geophysical Union, 88, 105-107

Sabine, C. L., Feely, R. A., Gruber, N., Key, R. M., Lee, K., Bullister, J. L., Wanninkhof, R., Wong, C. S., Wallace, D. W. R., Tilbrook, B., Millero, F. J., Peng, T.-H., Kozyr, A., Ono, T., Rios, A. F. (2004) The Oceanic Sink for Anthropogenic CO_2. Science, 305, 367-371

Sachs, O., Sauter, E. J., Schlüter, M., Rutgers van der Loeff, M. M., Jerosch, K., Holby, O. (2009) Benthic organic carbon flux and oxygen penetration reflect different plankton provinces in the Southern Ocean. Deep Sea Research Part I: Oceanographic Research Papers, 56, 1319-1335

Saito, M. A., Goepfert, T. J., Ritt, J. T. (2008) Some thoughts on the concept of colimitation: Three definitions and the importance of bioavailability. Limnology and Oceanography, 53, 276

Sakshaug, E., Slagstad, D. (1991) Light and productivity of phytoplankton in polar marine ecosystems: a physiological view. Polar Research, 10, 69-86

Sarmiento, J., Bender, M. (1994) Carbon biogeochemistry and climate change. Photosynthesis Research, 39, 209-234

Sarthou, G., Timmermans, K. R., Blain, S., Tréguer, P. (2005) Growth physiology and fate of diatoms in the ocean: a review. Journal of Sea Research, 53, 25-42

Schlitzer, R. (2002) Carbon export fluxes in the Southern Ocean: results from inverse modeling and comparison with satellite-based estimates. Deep Sea Research Part II: Topical Studies in Oceanography, 49, 1623-1644

Schmitz, W. J. (1996) On the world ocean circulation. Volume II, the Pacific and Indian Oceans/a global update. Woods Hole Oceanographic Institution

Schorr, D. K. (2004) Healthy fisheries, sustainable trade: crafting new rules on fishing subsidies in the World Trade Organization. WWF

Sciandra, A., Harlay, J., Lefevre, D., Lemee, R., Rimmelin, P., Denis, M., Gattuso, J. P. (2003) Response of coccolithophorid *Emiliania huxleyi* to elevated partial pressure of CO_2 under nitrogen limitation. Marine Ecology-Progress Series, 261, 111-122

Shi, D., Xu, Y., Hopkinson, B. M., Morel, F. M. M. (2010) Effect of Ocean Acidification on Iron Availability to Marine Phytoplankton. Science, 327, 676-679

Sigman, D. M., Hain, M. P., Haug, G. H. (2010) The polar ocean and glacial cycles in atmospheric CO_2 concentration. Nature, 466, 47-55

Sims, P., Mann, D., Medlin, L. (2006) Evolution of the diatoms: Insights from fossil, biological and molecular data. Phycologia, 45, 361

Smetacek, V. (1999) Diatoms and the Ocean Carbon Cycle. Protist, 150, 25-32

Smetacek, V., Klaas, C., Strass, V. H., Assmy, P., Montresor, M., Cisewski, B., Savoye, N., Webb, A., d/'Ovidio, F., Arrieta, J. M., Bathmann, U., Bellerby, R., Berg, G. M., Croot, P., Gonzalez, S., Henjes, J., Herndl, G. J., Hoffmann, L. J., Leach, H., Losch, M., Mills, M. M., Neill, C., Peeken, I., Röttgers, R., Sachs, O., Sauter, E., Schmidt, M. M., Schwarz, J., Terbrüggen, A., Wolf-Gladrow, D. (2012) Deep carbon export from a Southern Ocean iron-fertilized diatom bloom. Nature, 487, 313-319

Sobrino, C., Ward, M. L., Neale, P. J. (2008) Acclimation to elevated carbon dioxide and ultraviolet radiation in the diatom *Thalassiosira pseudonana*: Effects on growth, photosynthesis, and spectral sensitivity of photoinhibition. Limnology and Oceanography, 53, 494-505

Sorhannus, U. (2007) A nuclear-encoded small-subunit ribosomal RNA timescale for diatom evolution. Marine Micropaleontology, 65, 1-12

Steinacher, M., Joos, F., Frölicher, T. L., Bopp, L., Cadule, P., Cocco, V., Doney, S. C., Gehlen, M., Lindsay, K., Moore, J. K., Schneider B., Segschneider, J. (2010) Projected 21st century decrease in marine productivity: a multi-model analysis. Biogeosciences, 7, 979-1005

Strzepek, R. F., Harrison, P. J. (2004) Photosynthetic architecture differs in coastal and oceanic diatoms. Nature, 431, 689-692

Strzepek, R. F., Hunter, K. A., Frew, R. D., Harrison, P. J., Boyd, P. W. (2012) Iron-light interactions differ in Southern Ocean phytoplankton. Limnology and Oceanography, 57, 1182-1200

Suggett, D. J., MacIntyre, H. L., Kana, T. M., Geider, R. J. (2009) Comparing electron transport with gas exchange: parameterising exchange rates between alternative photosynthetic currencies for eukaryotic phytoplankton. Aquatic Microbial Ecology, 56, 147-162

Sugie, K., Yoshimura, T. (2013) Effects of pCO_2 and iron on the elemental composition and cell geometry of the marine diatom *Pseudo-nitzschia pseudodelicatissima* (Bacillariophyceae). Journal of Phycology, 49, 475488

Sugie, K., Endo, H., Suzuki, K., Nishioka, J., Kiyosawa, H., Yoshimura, T. (2013) Synergistic effects of pCO_2 and iron availability on nutrient consumption ratio of the Bering Sea phytoplankton community. Biogeosciences, 10, 6309-6321

Sunda, W. G., Huntsman, S. A. (1997) Interrelated influence of iron, light and cell size on marine phytoplankton growth. Nature, 390, 389-392

Sundquist, E. T. (1985) Geological Perspectives on Carbon Dioxide and the Carbon Cycle. In The Carbon Cycle and Atmospheric CO_2: Natural Variations Archean to Present, 55-59. American Geophysical Union

Takahashi, T., Sutherland, S. C., Sweeney, C., Poisson, A., Metzl, N., Tilbrook, B., Bates, N., Wanninkhof, R., Feely, R. A., Sabine, C., Olafsson, J., Nojiri, Y. (2002) Global sea-air CO_2

flux based on climatological surface ocean pCO_2, and seasonal biological and temperature effects. Deep Sea Research Part II: Topical Studies in Oceanography, 49, 1601-1622

Takeda, S. (1998) Influence of iron availability on nutrient consumption ratio of diatoms in oceanic waters. Nature, 393, 774-777

Tatters, A. O., Roleda, M. Y., Schnetzer, A., Fu, F., Hurd, C. L., Boyd, P. W., Caron, D. A., Lie, A. A. Y., Hoffmann, L. J., Hutchins, D. A. (2013) Short- and long-term conditioning of a temperate marine diatom community to acidification and warming. Philosophical Transactions of the Royal Society B: Biological Sciences, 368

Tchernov, D., Hassidim, M., Luz, B., Sukenik, A., Reinhold, L., Kaplan, A. (1997) Sustained net CO_2 evolution during photosynthesis by marine microorganism. Current Biology, 7, 723-728

Thompson, D. W. J., Solomon, S., Kushner, P. J., England, M. H., Grise, K. M., Karoly, D. J. (2011) Signatures of the Antarctic ozone hole in Southern Hemisphere surface climate change. Nature Geoscience, 4, 741-749

Timmermans, K. R., Davey, M. S., van der Wagt, B., Snoek, J., Geider, R. J., Veldhuis, M. J. W., Gerringa, L. J. A., de Baar, H. J. W. (2001) Co-limitation by iron and light of *Chaetoceros brevis*, *C. dichaeta* and *C. calcitrans* (Bacillariophyceae). Marine Ecology Progress Series, 217, 287-297

Toggweiler, J. R., Key, R. M. (2003) Ocean circulation/thermohaline circulation. In Encyclopedia of Atmospheric Sciences, 15491555. San Diego: Academic Press

Tortell, P. D. (2000) Evolutionary and ecological perspectives on carbon acquisition in phytoplankton. Limnology and Oceanography, 45, 744-750

Tortell, P. D., Payne, C. D., Li, Y., Trimborn, S., Rost, B., Smith, W. O., Riesselman, C., Dunbar, R. B., Sedwick, P., DiTullio, G. R. (2008a) CO_2 sensitivity of Southern Ocean phytoplankton. Geophysical Research Letters, 35, L04605

Tortell, P. D., Payne, C., Gueguen, C., Strzepek, R. F., Boyd, P. W., Rost, B. (2008b) Inorganic carbon uptake by Southern Ocean phytoplankton. Limnology and Oceanography, 53, 1266-1278

Tortell, P. D., DiTullio, G. R., Sigman, D. M., Morel, F. M. M. (2002) CO_2 effects on taxonomic composition and nutrient utilization in an Equatorial Pacific phytoplankton assemblage. Marine Ecology-Progress Series, 236, 37-43

Tréguer, P., Nelson, D. M., Van Bennekom, A. J., DeMaster, D. J., Leynaert, A., Quéguiner, B. (1995) The Silica Balance in the World Ocean: A Reestimate. Science, 268, 375-379

Trimborn, S., Wolf-Gladrow, D., Richter, K.-U., Rost, B. (2009) The effect of pCO_2 on carbon acquisition and intracellular assimilation in four marine diatoms. Journal of Experimental Marine Biology and Ecology, 376, 26-36

Trimborn, S., Brenneis, T., Sweet E., Rost, B. (2013) Sensitivity of Antarctic phytoplankton species to ocean acidification: Growth carbon aquisition, and species interaction. Limnology and Oceanography, 58, 997-1007

van de Poll, W. H., Visser, R. J. W., Buma, A. G. J. (2007) Acclimation to a dynamic irradiance regime changes excessive irradiance sensitivity of *Emiliania huxleyi* and *Thalassiosira weissflogii*. Limnology and Oceanography, 52, 1430-1438

van Leeuwe, M. A., van Sikkelerus, B., Gieskes, W. W. C., Stefels, J. (2005) Taxon-specific differences in photoacclimation to fluctuating irradiance in an Antarctic diatom and a green flagellate. Marine Ecology-Progress Series, 288, 9-19

van Oijen, T., van Leeuwe, M. A., Granum, E., Weissing, F. J., Bellerby, R. G. J., Gieskes, W. W. C., de Baar, H. J. W. (2004) Light rather than iron controls photosynthate production and allocation in Southern Ocean phytoplankton populations during austral autumn. Journal of Plankton Research, 26, 885-900

Volk, T., Hoffert, M. I. (1985) Ocean Carbon Pumps: Analysis of Relative Strengths and Efficiencies in Ocean-Driven Atmospheric CO_2 Changes. In The Carbon Cycle and Atmospheric CO_2: Natural Variations Archean to Present, 99-110. American Geophysical Union

Wagner, H., Jakob, T., Wilhelm, C. (2006) Balancing the energy flow from captured light to biomass under fluctuating light conditions. New Phytologist, 169, 95-108

Wefer, G., Fischer, G. (1991) Annual primary production and export flux in the Southern Ocean from sediment trap data. Marine Chemistry, 35, 597-613

Whitehouse, M. J., Atkinson, A., Korb, R. E., Venables, H. J., Pond, D. W., Gordon, M. (2012) Substantial primary production in the land-remote region of the central and northern Scotia Sea. Deep Sea Research Part II: Topical Studies in Oceanography, 5960, 47-56

Wilson, K. E., Ivanov, A. G., Quist, G., Grodzinski, B., Sarhan, F., Huner, N. P. A. (2006) Energy balance, organellar redox status, and acclimation to environmental stress. Canadian Journal of Botany, 84, 1355-1370

Wolf-Gladrow, D. A., Zeebe, R. E., Klaas, C., Körtzinger, A., Dickson, A. G. (2007) Total alkalinity: The explicit conservative expression and its application to biogeochemical processes. Marine Chemistry, 106, 287-300

Wolf-Gladrow, D. A., Riebesell, U., Burkhardt, S., Bijma, J. (1999) Direct effects of CO_2 concentration on growth and isotopic composition of marine plankton. Tellus B, 51, 461-476

Wu, Y., Gao, K., Riebesell, U. (2010) CO_2-induced seawater acidification affects physiological performance of the marine diatom *Phaeodactylum tricornutum*. Biogeosciences, 7, 2915-2923

Ye, Y., Völker, C., Wolf-Gladrow, D. A. (2009) A model of Fe speciation and biogeochemistry at the Tropical Eastern North Atlantic Time-Series Observatory site. Biogeosciences, 6, 2041-2061

Zeebe, R. E., Wolf-Gladrow,D. A. (2001) CO_2 in Seawater: Equilibrium, Kinetics, Isotopes. Amsterdam: Elsevier Science

Zickfeld, K., Eby, M., Weaver, A. J. (2008) Carbon-cycle feedbacks of changes in the Atlantic meridional overturning circulation under future atmospheric CO_2. Global Biogeochemical Cycles, 22, GB3024

9

Appendix

Emiliania huxleyi shows identical responses to elevated pCO_2 in TA and DIC manipulations

Journal of Experimental Marine Biology and Ecology 406 (2011) 54–62

Contents lists available at ScienceDirect

Journal of Experimental Marine Biology and Ecology

journal homepage: www.elsevier.com/locate/jembe

Emiliania huxleyi shows identical responses to elevated pCO_2 in TA and DIC manipulations

C.J.M. Hoppe *, G. Langer, B. Rost

Alfred Wegener Institute for Polar and Marine Research, Am Handelshafen 12, 27570 Bremerhaven, Germany

ARTICLE INFO

Article history:
Received 28 February 2011
Received in revised form 6 June 2011
Accepted 8 June 2011
Available online 2 July 2011

Keywords:
Calcification
CO_2 manipulation
Coccolithophores
Ocean acidification
Photosynthesis

ABSTRACT

With respect to their sensitivity to ocean acidification, calcifiers such as the coccolithophore *Emiliania huxleyi* have received special attention, as the process of calcification seems to be particularly sensitive to changes in the marine carbonate system. For *E. huxleyi*, apparently conflicting results regarding its sensitivity to ocean acidification have been published (Iglesias-Rodriguez et al., 2008a; Riebesell et al., 2000). As possible causes for discrepancies, intra-specific variability and different effects of CO_2 manipulation methods, i.e. the manipulation of total alkalinity (TA) or total dissolved inorganic carbon (DIC), have been discussed. While Langer et al. (2009) demonstrate a high degree of intra-specific variability between strains of *E. huxleyi*, the question whether different CO_2 manipulation methods influence the cellular responses has not been resolved yet. In this study, closed TA as well as open and closed DIC manipulation methods were compared with respect to *E. huxleyi's* CO_2-dependence in growth rate, POC- and PIC-production. The differences in the carbonate chemistry between TA and DIC manipulations were shown not to cause any differences in response patterns, while the latter differed between open and closed DIC manipulation. The two strains investigated showed different sensitivities to acidification of seawater, RCC1256 being more negatively affected in growth rates and PIC production than NZEH.

1. Introduction

Since the industrial revolution, anthropogenic activities such as the burning of fossil fuels or changes in land use have increased atmospheric pCO_2 values from about 280 μatm to 385 μatm (Lüthi et al., 2008; Tans, 2009). About one third of the emitted CO_2 has already been taken up by the oceans, leading to increased DIC concentrations in surface waters (Wolf-Gladrow et al., 1999). The subsequent changes in speciation, such as increased CO_2 concentrations [CO_2] and decreased CO_3^{2-} concentrations [CO_3^{2-}], lead to decreasing oceanic pH values (Broecker et al., 1971). This process, commonly referred to as ocean acidification, has diverse effects on marine organisms, communities and ecosystems (e.g. Bijma et al., 1999; Kleypas et al., 1999; Raven et al., 2005; Tortell et al., 2002).

There have been several studies investigating ocean acidification effects on phytoplankton on the single species and community level (for review see Fabry et al., 2008; Rost et al., 2008). CO_2 perturbation experiments are the prime tools to mimic future CO_2 scenarios and to study organism responses. These experiments can be conducted by i) equilibrating with air of a certain pCO_2, ii) the addition of $NaHCO_3$, Na_2CO_3, or iii) the addition of a strong acid or base (Riebesell et al., 2010). In any of these perturbations, the seawater carbonate system will react by increasing or decreasing the relative proportions of the carbonate species or the DIC concentration according to its new equilibrium state. The most common perturbation methods, leading to very similar speciation with regard to pH, [CO_2], [CO_3^{2-}] and Ω_{Ca} (calcite saturation state), are the manipulation of dissolved inorganic carbon (DIC) by aeration with a certain pCO_2 (while keeping total alkalinity (TA) constant) and manipulation of the TA by the addition of HCl or NaOH (while DIC stays constant). DIC manipulations reflect current changes in the marine carbonate chemistry. Even though TA perturbations differ regarding the quantity manipulated, they mimic the carbonate speciation as occurring during ocean acidification quite closely (Schulz et al., 2009).

With regard to climate change and its effects on the world's oceans, calcifying organisms are of major importance. Coccolithophores are considered to account for a significant fraction of the pelagic biogenic carbonate precipitation (Baumann et al., 2004; Milliman, 1993) and are mainly responsible for creating and maintaining the oceans vertical gradient in total alkalinity (Wolf-Gladrow et al., 1999). This group of marine calcifying phytoplankton has received special attention within the framework of ocean acidification research as they were shown to exhibit distinct sensitivity to elevated pCO_2 values (Fabry et al., 2008; Rost et al., 2008). Riebesell et al. (2000) reported a reduction in calcification in the most prominent coccolithophore *Emiliania huxleyi* under future CO_2 scenarios. Since then, several studies have confirmed the sensitivity of this species to acidification (Delille et al., 2005; Feng

* Corresponding author. Tel.: +49 471 4831 1630; fax: +49 471 4831 1425.
E-mail address: Clara.Hoppe@awi.de (C.J.M. Hoppe).

0022-0981/$ – see front matter © 2011 Elsevier B.V. All rights reserved.
doi:10.1016/j.jembe.2011.06.008

9. Appendix

et al., 2008; Langer et al., 2009; Sciandra et al., 2003). These findings have recently been challenged by Iglesias-Rodriguez et al. (2008a), who observed enhanced calcification under elevated pCO_2 in *E. huxleyi*. The authors attributed these striking differences to the application of different manipulation methods. As the TA manipulation used in Riebesell et al. (2000) do not mimic future scenarios as closely as DIC manipulations, Iglesias-Rodriguez et al. (2008a, 2008b) claimed that their results represent more realistic responses of *E. huxleyi* to ocean acidification.

As two different strains were used in these studies (PLYB92/11 in Riebesell et al., 2000; NZEH in Iglesias-Rodriguez et al., 2008a), intra-specific variability between *E. huxleyi* strains may have also caused differences in the response patterns. Intra-specific variability has been shown to lead to different responses for four strains of *E. huxleyi* (Langer et al., 2009). The strains used in Langer et al. (2009), however, neither included the one used by Riebesell et al. (2000) nor the one used by Iglesias-Rodriguez et al. (2008a). Therefore, the findings by Langer et al. (2009) are suggestive but not unambiguous with regard to the discrepancy between Riebesell et al. (2000) and Iglesias-Rodriguez et al. (2008a). Shi et al. (2009) compared responses of one *E. huxleyi* strain (NZEH) in growth, POC and PIC quota and production from closed TA and open DIC manipulations. Even though the cells were responding differently in the two manipulations, it remains unclear whether this was due to differences in the carbonate chemistry or mechanical effects of gas bubbling, occurring in the open DIC manipulation only.

As the reasons for differences between Riebesell et al. (2000) and Iglesias-Rodriguez et al. (2008a) are still unresolved, the aim of this study was to compare the effects of different CO_2 manipulation methods. To this end, the responses of two strains of *E. huxleyi* to changing carbonate chemistry were investigated in three different manipulation approaches. First, ecophysiological responses to TA (as applied by Riebesell et al., 2000) and DIC manipulations (as applied by Iglesias-Rodriguez et al., 2000a) were compared. Additionally, to further investigate the differences between TA and open DIC manipulations as found by Shi et al. (2009), the effect of mechanical perturbation was examined by comparing closed pre-equilibrated with open continuously aerated DIC manipulated incubations.

2. Material and methods

2.1. Cultures and media preparation

Monoclonal cultures of two strains of the coccolithophore *E. huxleyi* (NZEH / PLY M219, isolated near New Zealand, supplied by the Plymouth Culture Collection, http://www.mba.ac.uk/culturecollection.php; RCC1256, isolated near Iceland, supplied by the Roscoff Culture Collection, http://www.sb-roscoff.fr/Phyto/RCC) were grown in 0.1 µm sterile-filtered North Sea seawater. The salinity was 32.38 (Guildline Autosal 8400B salinometer, Ontario, Canada).

The seawater was enriched with vitamins and trace metals according to f/2 media (Guillard and Ryther, 1962; except for iron which was added in a concentration of 1.94 µmol L^{-1} $FeCl_3$). Seawater was also enriched with nitrate (NO_3^-) and phosphate (HPO_4^{2-}) to yield concentrations of 100 and 6 µmol L^{-1}, respectively. Nutrient concentrations were measured colorimetrically using a continuous flow analyzer (Evolution III, Alliance Instruments, Salzburg, Austria).

Dilute-batch cultures were grown in 2 L borosilicate bottles at 15 ± 0.2 °C. Daylight lamps (Lumilux De Luxe T8, Osram, München, Germany) provided light intensities of 170 ± 15 µmol photons m^{-2} s^{-1} as measured with a Li-Cor datalogger (Li-Cor, Lincoln, USA) equipped with a 4π-sensor (Walz, Effeltrich, Germany). A light: dark cycle of 16:8 h was applied and all samples were taken between 6 and 10 hours after the beginning of the light phase.

In order to keep cultures in exponential growth phase and to prevent significant changes in carbonate chemistry as well as attrition of nutrients in the media, cultures were diluted regularly (cell densities never exceeded 72,000 cells mL $^{-1}$). Cultures were kept at experimental temperatures, light intensities and cell densities for at least two weeks, followed by another week being pre-acclimated to experimental pCO_2 levels (5–7 generations).

2.2. CO_2 perturbation experiments

Different CO_2 manipulation methods (closed TA, closed and open DIC manipulation) were applied to test ecophysiological responses to different CO_2 concentrations. In the alkalinity manipulations, carbonate chemistry was adjusted by addition of calculated amounts of HCl or NaOH (1 N Titrisol, Merck, Darmstadt, Germany) to seawater for which DIC concentrations were known. The manipulated media were stored in 2 L borosilicate bottles, which were sealed immediately with Teflon-lined screw caps without head space to avoid CO_2 exchange with the atmosphere.

DIC manipulations and incubations were conducted in 2 L borosilicate bottles equipped with glass frits for aeration. The media were sparged continuously with humidified, 0.2 µm-filtered air of different partial pressures of CO_2 (180, 380, 750 and 1000 µatm). Gas flow rates were 130 ± 10 mL min^{-1}. Gas mixtures were generated using a custom-made gas flow controller. CO_2-free air (<1 ppmv CO_2; Dominick Hunter, Willich, Germany) was mixed with pure CO_2 (Air Liquide Deutschland, Düsseldorf, Germany) by a mass flow controller based system (CGM 2000 MCZ Umwelttechnik, Bad Nauheim, Germany). The CO_2 concentration was regularly controlled with a non-dispersive infrared analyzer system (LI6252, LI-COR Biosciences, Bad Homburg, Germany) calibrated with CO_2-free air and purchased gas mixtures of 150 ± 10 and 1000 ± 20 ppmv CO_2 (Air Liquide Deutschland, Düsseldorf, Germany). Experiments were started after 48 h of aeration in order to ensure equilibration. Bottles of the closed DIC treatments were sealed without head space with Teflon-lined screw caps. A roller table was used to keep the cells in suspension. Bottles of the open DIC treatments (only applied to strain NZEH) were sparged continuously with the respective gases over the duration of the experiment. Sedimentation of cells was minimised by aeration and shaking of bottles twice a day.

2.3. Determination of carbonate chemistry

Samples for TA measurements were 0.6 µm-filtered and stored in 150 mL borosilicate bottles at 3 °C. TA was determined by duplicate potentiometric titrations (Brewer et al., 1986) using a TitroLine alpha plus autosampler (Schott Instruments, Mainz, Germany), and calculation from linear Gran plots (Gran, 1952). Certified Reference Materials (CRMs, Batch No. 54) supplied by A. Dickson (Scripps Institution of Oceanography, USA) were used to correct the measurements. The average reproducibility was ± 5 µmol kg^{-1} (n = 10).

DIC samples were filtered through 0.2 µm cellulose-acetate syringe-filters and stored head-space free in 5 mL gas-tight borosilicate bottles at 3 °C. DIC was measured colorimetrically in triplicates with a QuaAAtro autoanalyzer (Seal Analytical, Mequon, USA) with an average reproducibility of ± 5 µmol kg^{-1} (n = 20). CRMs (Batch No. 54) were used to correct the measurements. Shifts in DIC concentrations due to CO_2 exchange were prevented by opening the storage vials less than one minute prior to each measurement.

Seawater pH was determined potentiometrically on the NBS scale using a glass electrode/reference electrode cell (Schott Instruments, Mainz, Germany), which included a temperature sensor and was two-point calibrated with NBS buffers prior to every set of measurements. Average repeatability was found to be ± 0.02 pH units (n = 30).

Calculations of the carbonate system were based on measurements of DIC, pH, temperature, salinity und nutrient concentrations. They were performed with the programme CO_2sys (Pierrot et al., 2006). The dissociation constants of carbonic acid of Mehrbach et al.

(1973), refit by Dickson and Millero (1987) and the dissociation constants for H_2SO_4 of Dickson (1990) were used for calculations.

2.4. Ecophysiological responses

Cell densities were determined using a Coulter Multisizer III (Beckman-Coulter, Fullerton, USA). Growth rates (μ) were calculated as:

$$\mu = (\ln c_1 \quad \ln c_0)\,\Delta t^{\ 1} \tag{1}$$

where c_0 and c_1 are the initial and the final cell counts in cells mL^{-1}, respectively, and Δt is the time between both counts in days.

For analysis of total particulate carbon (TPC) and particulate organic carbon (POC), cells were filtered onto precombusted (15 h, 500 °C) glass fibre filters (GF/F 0.6 µm nominal pore size; Whatman, Maidstone, UK) within 7 to 9 h after onset of light phase. Filters were stored at −20 °C and dried for at least 12 h at 60 °C prior to sample preparation. Analysis was performed using an Automated Nitrogen Carbon Analyser mass spectrometer system (ANCA-SL 20–20, SerCon Ltd., Crewe, UK). Contents of TPC and POC were corrected for blank measurements and normalised to filtered volume and cell densities of culture media to yield cellular quotas. Particulate inorganic carbon contents (PIC) were calculated as the difference in carbon content between TPC and POC. The production of particulate organic carbon (P_{POC}) and the production of particulate inorganic carbon (P_{PIC}) were calculated as:

$$P_{POC} = \mu\left(\text{POC cell}^{-1}\right) \tag{2}$$

$$P_{PIC} = \mu\left(\text{PIC cell}^{-1}\right) \tag{3}$$

where the production rates are given in pg POC cell^{-1} d^{-1} and pg PIC cell^{-1} d^{-1}, respectively.

2.5. Statistics

Significant responses were determined by analysis of covariances of the trend in response variables over the pCO_2 range tested, which were based on univariate general linear models performed with SPSS 11 (IBM, Chicago, USA). The null hypothesis ('no difference in responses') was rejected if the respective p-value was <0.05.

3. Results

3.1. Carbonate chemistry

In the different manipulation methods, the final pCO_2 values ranged between 153 and 1283 µatm (Table 1). In the DIC manipulation (i.e. aeration of the media with air of a certain pCO_2), TA stayed quasi-constant at values of 2325 ± 27 µmol kg^{-1} while DIC varied between 1922 ± 17 µmol kg^{-1} at the lowest and 2184 ± 26 µmol kg^{-1} at the highest pCO_2 treatment. In the TA manipulation (i.e. addition of HCl or NaOH), DIC stayed quasi-constant at values of 2080 ± 21 µmol kg^{-1} while TA varied between 2541 ± 64 µmol kg^{-1} at the lowest and 2198 ± 41 µmol kg^{-1} at the highest pCO_2 treatment. Lowest calcite saturation state was 1.33. DIC and TA depletion by the cells over the course of the experiment were on average 3% and 4% for TA and DIC, respectively.

3.2. Ecophysiological responses to carbonate chemistry manipulations

Both *E. huxleyi* strains used in this study responded in growth rate and the production of POC and PIC to changes in pCO_2. The response patterns found did not differ noteworthy between TA and closed DIC manipulation (Table 2). Differences in response patterns were, however, observed between the two DIC manipulations (open vs. closed). In the following, responses in growth rates, PIC and POC quota and production are described for the two strains RCC1256 and NZEH.

The growth rates of strain RCC1256 showed virtually the same response to increasing pCO_2 in DIC and TA manipulations (Table 2, Fig. 1a). In both manipulations, growth rates stayed constant at about 1.2 d^{-1} up to a pCO_2 value of ~800 µatm and declined statistically significant (i.e. $p<0.05$) beyond 800 µatm to values of about 1.1 d^{-1} ($F=18.02$, $p<0.001$). With respect to POC quota and POC production, RCC1256 responded differently to closed DIC and TA manipulation ($F=11.27$, $p=0.004$ and $F=5.97$, $p=0.025$, respectively). With respect to increasing pCO_2 levels, POC quota (Table 2, Fig. 1c) did not change in the closed DIC treatment, while a statistically insignificant increase (~30%) was observed in the TA manipulations. While POC production (Table 2, Fig. 1d) did not change substantially in the TA manipulations, a slight yet statistically insignificant decrease (~10%) was observed in the closed DIC manipulations.

With regard to PIC quota and production, no differences were found between the two manipulation methods. PIC quota (Table 2, Fig. 1e) decreased significantly by about 30% over the pCO_2 range

Table 1
Measured and calculated carbonate chemistry parameters of the media at 15 °C at the end of all experiments ($n=3$). Following Hoppe et al. (2010), DIC and pH were used as input parameters for calculations. Numbers in bold characters denote the manipulated parameter.

Strain	Experiment	Measured			Calculated				
		TA [µmol kg^{-1}]	DIC [µmol kg^{-1}]	pH (NBS)	pCO_2 [µatm]	CO_2 [µmol kg^{-1}]	HCO_3^- [µmol kg^{-1}]	CO_3^{2-} [µmol kg^{-1}]	Ω_{Ca}
RCC1256	TA manipulation	2508 ± 82	2114 ± 10	8.32 ± 0.03	288 ± 20	11 ± 1	1882 ± 19	221 ± 11	5.38 ± 0.26
	closed	2299 ± 18	2097 ± 9	7.97 ± 0.05	672 ± 89	26 ± 3	1967 ± 17	104 ± 11	2.54 ± 0.27
		2173 ± 17	2063 ± 7	7.82 ± 0.01	946 ± 10	36 ± 0	1955 ± 6	73 ± 1	1.76 ± 0.03
		2160 ± 7	2082 ± 6	7.72 ± 0.01	1206 ± 30	46 ± 1	1978 ± 6	58 ± 2	1.42 ± 0.04
	DIC manipulation	2349 ± 7	**1940 ± 11**	8.44 ± 0.01	191 ± 3	7 ± 0	1670 ± 11	263 ± 3	6.38 ± 0.07
	closed	2344 ± 8	**2058 ± 5**	8.20 ± 0.02	379 ± 14	14 ± 1	1876 ± 2	167 ± 6	4.06 ± 0.14
		2316 ± 7	**2123 ± 7**	7.98 ± 0.01	656 ± 10	25 ± 0	1989 ± 7	108 ± 1	2.64 ± 0.03
		2342 ± 13	**2156 ± 8**	7.88 ± 0.01	846 ± 24	32 ± 1	2036 ± 8	88 ± 2	2.14 ± 0.05
NZEH	TA manipulation	2573 ± 19	2089 ± 6	8.40 ± 0.01	232 ± 3	9 ± 0	1823 ± 5	257 ± 3	6.26 ± 0.08
	closed	2366 ± 15	2070 ± 13	8.21 ± 0.03	369 ± 27	14 ± 1	1883 ± 20	173 ± 9	4.21 ± 0.21
		2257 ± 1	2046 ± 8	7.95 ± 0.03	680 ± 45	26 ± 2	1923 ± 4	98 ± 7	2.38 ± 0.16
		2236 ± 1	2081 ± 7	7.73 ± 0.06	1175 ± 157	45 ± 6	1976 ± 5	60 ± 9	1.47 ± 0.21
	DIC manipulation	2312 ± 17	**1912 ± 12**	8.14 ± 0.01	404 ± 7	15 ± 0	1759 ± 8	138 ± 4	3.34 ± 0.09
	closed	2276 ± 14	**2025 ± 30**	7.95 ± 0.02	673 ± 31	26 ± 1	1903 ± 30	97 ± 3	2.35 ± 0.07
		2295 ± 3	**2118 ± 2**	7.82 ± 0.03	957 ± 57	36 ± 2	2006 ± 4	76 ± 4	1.84 ± 0.10
		2311 ± 3	**2184 ± 21**	7.79 ± 0.01	1066 ± 28	40 ± 1	2071 ± 20	72 ± 2	1.76 ± 0.04
	DIC manipulation	2351 ± 8	**1913 ± 12**	8.51 ± 0.01	157 ± 3	6 ± 0	1610 ± 13	297 ± 3	7.23 ± 0.07
	open	2322 ± 7	**2051 ± 2**	8.24 ± 0.02	336 ± 18	13 ± 1	1854 ± 7	184 ± 8	4.47 ± 0.20
		2361 ± 3	**2211 ± 2**	7.86 ± 0.02	909 ± 45	35 ± 2	2090 ± 2	86 ± 4	2.10 ± 0.10

Table 2
Ecophysiological responses of *E. huxleyi* strains RCC1256 and NZEH to changing pCO_2 as found under TA, open DIC and closed DIC manipulations. a: significant ($p<0.05$) responses to pCO_2; b: significant ($p<0.05$) differences between TA and closed DIC manipulation; c: significant ($p<0.05$) differences between open and closed DIC manipulation.

Strain	Experiment	pCO_2	μ [d^{-1}]	POC [pg $cell^{-1}$]	P_{POC} [pg $cell^{-1} d^{-1}$]	PIC [pg $cell^{-1}$]	P_{PIC} [pg $cell^{-1} d^{-1}$]	PIC : POC
			a	*b*	*b*	*a*	*a*	*a, b*
RCC1256	TA manipulation	288	1.19 ± 0.03	10.35 ± 0.19	12.36 ± 0.22	10.19 ± 1.09	12.14 ± 0.85	0.98 ± 0.09
	closed	672	1.17 ± 0.03	12.39 ± 0.30	14.76 ± 0.18	8.86 ± 0.21	10.55 ± 0.38	0.72 ± 0.03
		946	1.10 ± 0.04	11.29 ± 0.71	12.42 ± 0.29	6.72 ± 0.00	7.19 ± 0.00	0.57 ± 0.00
		1206	1.06 ± 0.02	13.07 ± 0.93	13.82 ± 0.89	7.17 ± 0.42	7.59 ± 0.41	0.55 ± 0.06
			a	*b*	*b*	*a*	*a*	*a*
	DIC manipulation	191	1.17 ± 0.01	13.22 ± 1.10	15.41 ± 1.26	10.25 ± 0.30	11.95 ± 0.40	0.78 ± 0.08
	closed	379	1.17 ± 0.03	12.16 ± 0.18	14.27 ± 0.54	9.95 ± 0.60	11.68 ± 0.86	0.82 ± 0.05
		656	1.18 ± 0.04	11.93 ± 0.96	14.08 ± 1.22	8.48 ± 0.30	10.02 ± 0.64	0.71 ± 0.05
		846	1.10 ± 0.05	12.18 ± 0.97	13.46 ± 1.65	8.39 ± 0.99	9.28 ± 1.45	0.69 ± 0.03
				a		*a, b*	*a*	*a*
NZEH	TA manipulation	232	1.21 ± 0.07	9.90 ± 1.52	11.89 ± 1.19	10.97 ± 1.97	13.35 ± 3.16	1.15 ± 0.37
	closed	369	1.22 ± 0.04	10.35 ± 0.69	12.60 ± 1.18	10.78 ± 0.76	13.13 ± 1.30	1.04 ± 0.01
		680	1.22 ± 0.06	11.26 ± 0.88	13.67 ± 0.88	9.98 ± 0.77	12.11 ± 0.71	0.89 ± 0.01
		1175	1.18 ± 0.03	10.97 ± 0.41	12.93 ± 0.19	9.34 ± 0.68	10.99 ± 0.54	0.85 ± 0.03
			c	*a, c*	*a, c*	*a, b, c*	*a, c*	*a*
	DIC manipulation	404	1.22 ± 0.02	11.51 ± 0.29	14.03 ± 0.38	13.44 ± 2.88	14.42 ± 1.51	1.17 ± 0.28
	closed	673	1.25 ± 0.02	12.30 ± 0.20	15.33 ± 0.13	11.01 ± 0.93	13.74 ± 1.41	0.90 ± 0.09
		957	1.19 ± 0.04	12.22 ± 0.44	14.55 ± 0.80	10.71 ± 0.32	12.75 ± 0.74	0.88 ± 0.02
		1066	1.16 ± 0.06	13.35 ± 0.79	15.46 ± 1.66	10.28 ± 0.47	11.09 ± 0.96	0.77 ± 0.06
			c	*a, c*	*a, c*	*a, c*	*a, c*	*a*
	DIC manipulation	157	0.99 ± 0.12	8.57 ± 1.28	8.41 ± 0.87	8.92 ± 1.71	8.71 ± 0.83	1.04 ± 0.06
	open	336	1.08 ± 0.02	8.96 ± 0.46	9.68 ± 0.57	9.49 ± 0.51	10.25 ± 0.61	1.06 ± 0.10
		909	1.09 ± 0.04	9.73 ± 0.40	10.56 ± 0.48	7.37 ± 0.61	8.01 ± 0.79	0.76 ± 0.09

tested in both manipulation methods applied ($F=47.18$, $p<0.001$). Furthermore, PIC production (Table 2; Fig. 1f) decreased significantly in both manipulation methods by about 35–40% between 200 and 1200 μatm pCO_2 ($F=58.30$, $p<0.001$). The PIC:POC ratios (Table 2, Fig. 1b) decreased significantly with increasing pCO_2 by approximately 40% and 20% in TA and DIC manipulations, respectively ($F=43.21$, $p<0.001$). Absolute values and slopes differed significantly between the two kinds of manipulations ($F=11.17$, $p=0.004$).

The strain NZEH did not show any growth rate response to changes in pCO_2, neither in the TA manipulations nor in the closed DIC manipulations (Table 2, Fig. 2a). Average growth rate was 1.21 ± 0.03 d^{-1}. In the open DIC manipulations, however, growth rates were about 10–14% lower (leading to significant differences between the two DIC manipulations; $F=18.53$, $p<0.001$). In these manipulations, cells could not be held in suspension and sedimentation occurred below the gas frits. The POC quotas (Table 2, Fig. 2c) differed between the three manipulation methods (highest quota was found in the closed DIC manipulation and lowest in the open DIC manipulations, which significantly differed from the other treatments; $F=10.08$, $p=0.006$). The overall trend in all manipulations was a small, yet significant increase of about 10% in the range between 160 and 1200 μatm ($F=9.57$, $p=0.006$). POC production (Table 2, Fig. 2d) stayed more or less constant in TA manipulations, while in the closed DIC manipulations, POC production increased by about 10% below 600 μatm ($F=8.59$, $p=0.009$) and remained unaffected above this pCO_2 level. The pattern found in the open DIC manipulation significantly differed from those of the closed manipulations ($F=31.41$, $p<0.001$), with increased values of about 25% ($F=8.59$, $p=0.009$).

The PIC quotas (Table 2, Fig. 2e) differed between the manipulation methods ($F=6.09$, $p=0.023$), but showed the same significant trend of slightly decreasing values ($F=11.24$, $p=0.009$). PIC production (Table 2, Fig. 2f) decreased by about 30% with increasing pCO_2 ($F=9.63$, $p=0.007$) in both TA and closed DIC manipulations, while an optimum curve with maximum values at ~340 μatm was observed in the case of open DIC manipulations ($F=24.12$, $p<0.001$). The PIC:POC ratio (Table 2, Fig. 2b) was generally higher than that of RCC1256 and was found to decrease significantly from about 1.1 at low to 0.8 at high pCO_2 in all manipulation methods (15–20%; $F=14.04$, $p=0.001$).

4. Discussion

Differences in carbonate chemistry speciation between DIC and TA manipulation have been argued to be the reason for different ecophysiological responses of *E. huxleyi* to changing pCO_2 (Iglesias-Rodriguez et al., 2008a, 2008b). Other authors held differences in experimental protocols (Riebesell et al., 2008) or the intraspecific variability between *E. huxleyi* strains (Langer et al., 2009) responsible for these differences. Shi et al. (2009) found strain NZEH responding differently to TA manipulation and open DIC manipulation and argued that these differences are likely to be due to the mechanical effect of bubbling rather than to differences in carbon speciation.

4.1. Comparison of different manipulation methods

This study was able to show that the differences in the carbonate chemistry of the two manipulation methods (changing DIC with constant TA vs. changing TA with constant DIC) had no substantially different effect on the overall ecophysiology of two strains of *E. huxleyi* (Table 2, Figs. 1 and 2). Compared to the different responses between open and closed DIC manipulations, in which the carbonate chemistry did not differ, the differences between TA and DIC manipulation are negligible and probably due to variability in the organisms overall sensitivity.

The differences in the response patterns between open and closed DIC manipulations were probably caused by the mechanical effect of bubbling and/or the effect of sedimentation of cells in the open DIC manipulations. In the closed DIC manipulations cells were always kept in suspension by steady and gentle rotation of the culture flasks. In the open DIC manipulations, the aeration process established areas of low currents, where cells could sediment. In such cell congregations, changes in nutrient and light availability as well as carbonate chemistry may occur and influence the physiology of *E. huxleyi*. Differences in ecophysiological responses to increasing pCO_2 in this treatment could, however, also be caused by a sensitivity of *E. huxleyi* to stress imposed by bubbling (cf. Merchuk, 1991). The latter explanation was put forward by Shi et al. (2009), who reported reverse trends in POC and PIC production in TA and open DIC manipulations.

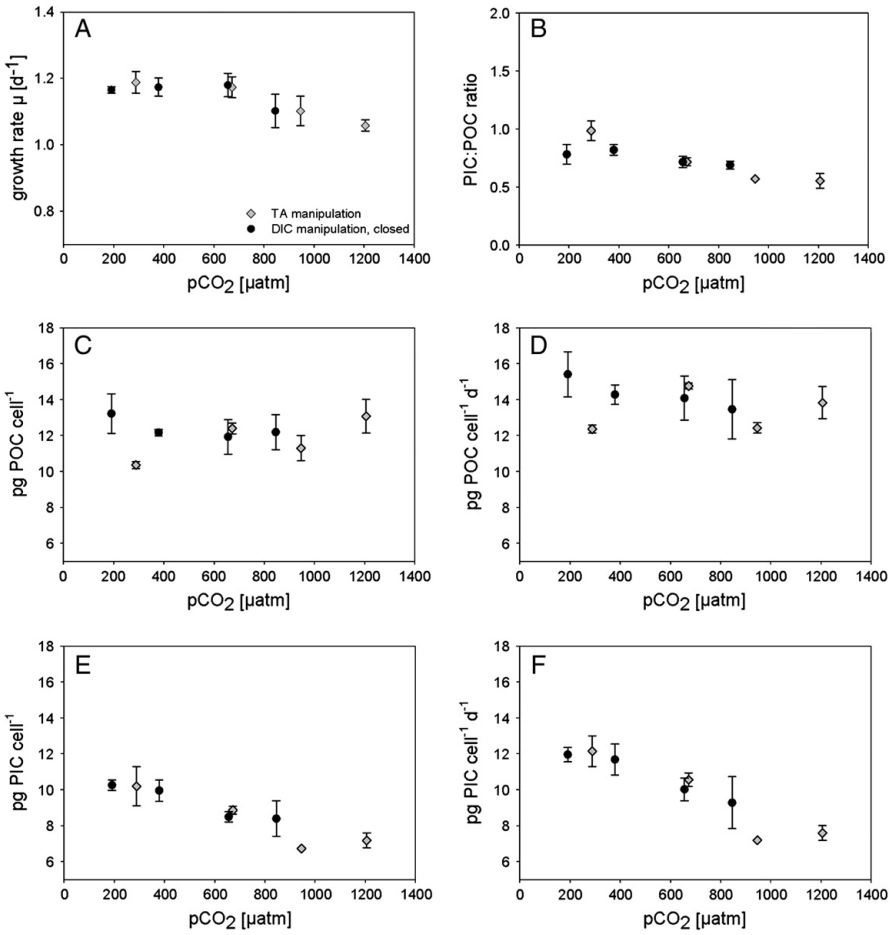

Fig. 1. Ecophysiological parameters of *E. huxleyi* strain RCC 1256 in response to changes in pCO_2 as observed in TA manipulation (grey symbols) and closed DIC manipulations (black symbols): A growth rates, B PIC:POC ratio, C POC quota, D POC production, E PIC quota, F PIC production.

The finding that differences in carbonate chemistry between DIC and TA manipulations do not cause changes in the ecophysiological response patterns is in agreement with other observations. Studies on coral recruitment and growth (Cohen and McCorkle, 2009; Schneider and Erez, 2006) obtained similar responses irrespective of the pCO_2 manipulation method applied. Our findings are in line with theoretical considerations raised by other authors (Hurd et al., 2009; Schulz et al., 2009), who argued that over the pCO_2 range tested, the physiological important components of the carbonate system ($[H^+]$, CO_3^{2-}, HCO_3^- as well as the calcite saturation state) do not differ significantly between the two manipulation methods.

4.2. Strain-specific responses of RCC1256 and NZEH

Strain-specific responses to increasing pCO_2 levels in *E. huxleyi* have been shown by Langer et al. (2009). In the following, the results for the two strains used in this study will be discussed with regard to the comparability to other findings on the same strains.

The sensitivity of strain RCC1256 to changes in carbonate chemistry seems to differ between studies. While Langer et al. (2009) found growth rates to decrease by 35% between 200 and 900 μatm, a decline of less than 10% was found in this study. It has to be noted, however, that the carbonate system in Langer et al. (2009) was calculated from TA and DIC, which can lead to an underestimation of pCO_2 (Hoppe et al., 2010). If the pCO_2 values are corrected for the discrepancies related to that combination of input parameters, as found for this particular set and quality of measurements, the same changes in growth rates, POC and PIC production spread over a wider pCO_2 range from 200 to 1200 μatm. Differences in growth rate responses of RCC1256 in the two studies now appear less pronounced. Both PIC quota and production significantly decreased with increasing pCO_2 in this study (Table 2; Fig. 1e; 1f), while in Langer et al. (2009) only production was found to decrease. In case of POC quota and production of RCC1256, no responses to changing pCO_2 levels were found in this study, while Langer et al. (2009) reported increasing POC quota and an optimum curve with a maximum at a (corrected) pCO_2 of about 800 μatm in case of production. The PIC:POC ratio declined with increasing pCO_2 in both studies. Whether the mentioned differences in responses between this study and Langer et al. (2009) are due to the fact that different light intensities and temperatures

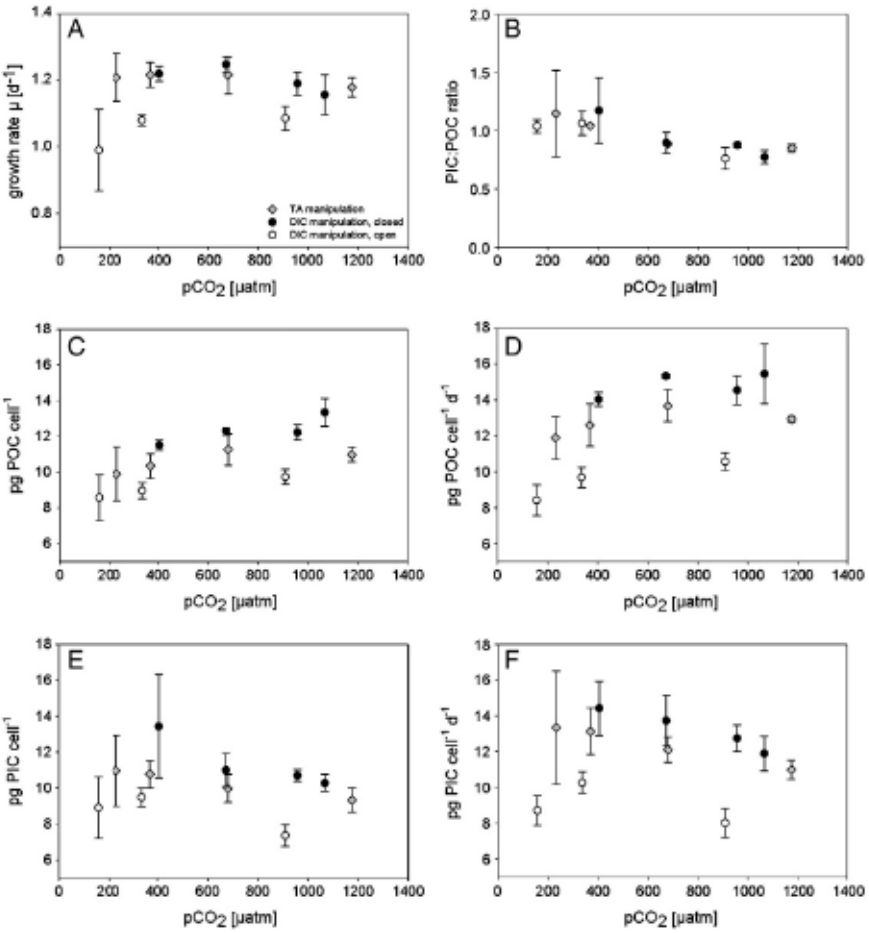

Fig. 2. Ecophysiological parameters of *E. huxleyi* strain NZEH in response to changes in pCO_2 as observed in TA manipulation (grey symbols), closed DIC manipulations (black symbols) and open DIC manipulations (white symbols): A growth rates, B PIC:POC ratio, C POC quota, D POC production, E PIC quota, F PIC production.

were used or simply reflect the natural variability in sensitivity of a single strain remains to be tested. Even if the latter is the case, major trends such as a decline or enhancement in physiological performance seem to be persistent in *E. huxleyi*.

The strain NZEH responded with slightly increased POC and slightly decreased PIC production under elevated pCO_2, while its growth rates remained constant over the pCO_2 range tested (Table 2, Fig. 2). These responses strikingly contradict the responses reported by Iglesias-Rodriguez et al. (2008a), who found the POC and PIC production of NZEH to increase by 150% and 80%, respectively, between pCO_2 values ranging from 280 to 750 μatm. This particular study, however, has been under debate because of shortcomings of its experimental protocol (Iglesias-Rodriguez et al., 2008b; Riebesell et al., 2008). As argued by Riebesell et al. (2008), the high cell densities of the pre-acclimations (up to 500.000 cells mL $^{-1}$) could have led to major changes in nutrient availability and carbonate chemistry. Furthermore, the actual experiments were run for 1 to 2 generations only. Even though physiological acclimation to changes in carbonate chemistry seems to be rather fast for this species (Barcelos e Ramos et al., 2009), a large proportion of the harvested biomass at the end of the experiment (25–50%) was probably produced prior to controlled experimental conditions and therefore cannot be interpreted as responses to the defined changes in pCO_2 levels. Further indications for the transfer of substantial biomass into the experiment from non-controlled pre-acclimations are the high numbers of detached coccoliths (Iglesias-Rodriguez et al., 2008a). Up to 80 detached coccoliths per cell, as observed in the high pCO_2 treatment (see their Table 1), are a strong indication for nutrient limitation having occurred. Another study on the same strain (Shi et al., 2009) also found PIC and POC production to increase with increasing pCO_2, even though to a lesser extent of about 36% and 69%, respectively. In Shi et al. (2009), cells were also not pre-acclimated, which could explain the agreement with Iglesias-Rodriguez et al. (2008a).

If these fundamental differences in the experimental approach were not the cause for the contradicting results, one would need to assume that the strains ecophysiological responses changed due to natural selection during long-term cultivation. Evolution in the lab was shown for bacterial cultures (Imhof and Schlotterer, 2001), a process that can be especially important when the number of transferred cells is low. Even though long-term cultivation of

phytoplankton strains is likely to put selection pressure on the population and to change its physiology compared to the ancestors in the field, it seems unlikely that similar cultivation conditions in culture collections lead to contrary ecophysiological responses as discussed above. The observation that absolute PIC and POC quotas and production vary between experiments, despite similar growth conditions, questions the reproducibility in terms of absolute values and numerically defined trends in ecophysiological studies. The general response patterns (i.e. decreasing growth rates at high pCO_2 values), however, seem to remain valid for a single strain and highlight the advantage of semi-quantitative or qualitative analysis when assessing the sensitivity of *E. huxleyi* (Fig. 3; cf. Fabry, 2008).

4.3. General response patterns of E. huxleyi

A noteworthy degree of intraspecific variability has been reported for *E. huxleyi* with regard to morphology, physiology and genetics (Iglesias-Rodríguez et al., 2006; Paasche, 2002; Young, 1994). Since Langer et al. (2009) published their study on the responses of four strains of *E. huxleyi* to changing carbonate chemistry, it is known that this also holds true for its responses to ocean acidification.

Over the last decade, several studies investigated responses to ocean acidification of eight different strains of *E. huxleyi* (Fig. 3). Most of the strains' growth rates were not influenced by increasing pCO_2. Furthermore, in those cases where changes have been observed (Iglesias-Rodriguez et al., 2008a; RCC1256 in: Langer et al., 2009; RCC1256 in this study), growth rates always declined. The latter is a strong hint that these cultures have been highly stressed, as *E. huxleyi* is usually capable to keep cell division rates constant over a wide range of conditions (Rost and Riebesell, 2004). More diverse responses have been found for the photosynthetic response in *E. huxleyi*. While in four experiments POC production (Feng et al., 2008; Langer et al., 2009; this study) did not change with increasing pCO_2, in four cases POC production increased (Iglesias-Rodriguez et al., 2008a; Riebesell et al., 2000; Shi et al., 2009; this study), a decrease was found in one study (Sciandra et al., 2003), and in two cases, strains showed optimum curves as response patterns (Langer et al., 2009). In summary, the CO_2-dependent changes in photosynthesis are highly variable and seem to differ between strains. With respect to PIC production, most of the studies found declining rates with increasing pCO_2, while in two studies a strain increased its PIC production rate (Iglesias-Rodriguez et al., 2008a; Shi et al., 2009) and one strain was found to be insensitive (Langer et al., 2009).

The comparison of morpho- (A, B and R; cf. Young et al., 2003) and ecotypes (oceanic vs. coastal strains) of all studies published so far does not reveal any group-specific patterns in the sensitivity to ocean acidification (Fig. 3; cf. Langer et al., 2009). With regard to the variable response patterns of different *E. huxleyi* clones (this study, Langer et al., 2009), it is at present merely possible to propose that this variability has a genetic basis, without defining its nature (Iglesias-Rodríguez et al., 2006; Langer et al., 2009). Taking all available data into account and considering some problems in the experimental setup of Iglesias-Rodriguez et al. (2008a) and Shi et al. (2009), the calcification process of *E. huxleyi* can be regarded as, although to a variable degree, sensitive to ocean acidification. It has to be kept in mind, however, that as long as the function and the ecological as well as evolutionary implications of coccolithophore calcification are unknown, the consequences of changes in calcification rates cannot be predicted with confidence. One fundamental question in this context is whether the process or the product of calcification is beneficial for the cell.

4.4. Implications for biogeochemical cycles

Similar trends were observed in several single-strain culture experiments, mesocosm experiments and field studies (e.g. Delille et al., 2005; Langer et al., 2009; Riebesell et al., 2000). Despite uncertainties in absolute quota and numerically defined trends obtained by these different ecophysiological studies, the same patterns of constant or increasing POC production and constant or declining PIC production were found in the majority of all studies mentioned. The predicted changes in coccolithophore carbon fixation and calcification have implications for future biogeochemical cycles, even though carbon fluxes also depend on other factors such as altered cellular elemental ratios and floristic shifts. Consequently, Earth system models critically depend on the input of ecophysiological responses of key functional groups such as marine calcifiers.

Based on the comparison of the data shown above, representative responses in form of absolute quota and trends with a certain slope appear oversimplified. Instead, uncertainties in the magnitude of

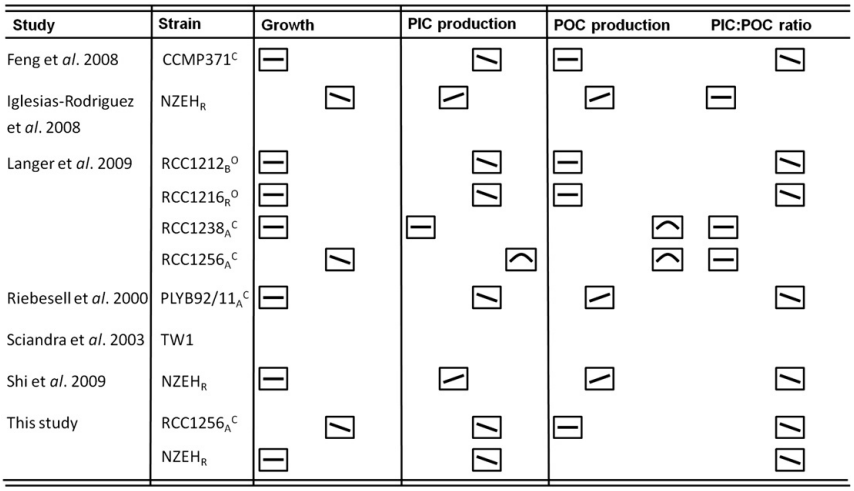

Fig. 3. Response patterns of *E. huxleyi* growth rates, POC production, PIC production and PIC:POC ratios as found in different studies. Subscript characters denote morphotype (A, B, R); superscript characters denote ecotype (C: coastal and O: oceanic). Modified after Fabry, 2008.

9. Appendix

calcification responses to ocean acidification remain and have to be accounted for in global carbon models. As the parameterisation of calcification in global carbon cycle models is based on the results of experiments (Ridgwell et al., 2009), also the model predictions on future impacts of anthropogenic CO_2 emissions depend on the reproducibility and transferability of laboratory studies. As modellers base their parameterizations on different ecophysiological studies (e.g. Gehlen et al., 2007; Hofmann and Schellnhuber, 2009), there is no agreement in the estimates for the amount of anthropogenic CO_2 taken up by the ocean due to the reduction in coccolithophore calcification. Applying a "Eppely curve" behaviour (Eppely, 1972) to the available data on biogenic calcification (cf. Fig. 3), Ridgwell et al. (2009) suggested a progressively decreasing net community calcification with increasing CO_2 to be used for the parameterisation of carbon cycle models. Further investigations of inter- and intraspecific response-variability as well as community and ecosystem responses to changing seawater carbonate chemistry will help understanding and predicting the future fate of calcifying phytoplankton.

5. Conclusions

Differences between TA and DIC manipulations do not cause differences in the ecophysiological responses of *E. huxleyi* to changing pCO_2 levels. Other differences in the experimental protocol (e.g. continuous bubbling *vs.* pre-bubbled), however, can lead to changes in growth rates and other ecophysiological parameters. Although strain-specific differences and overall trends were confirmed, the CO_2- sensitivity within single strains of *E. huxleyi* seems to vary over time. This favours the analysis of experimental data in a semi-quantitative way, defining trends rather than numerical relationships. After comparing the ecophysiological responses of all *E. huxleyi* strains described in the literature, this species can be regarded as moderately sensitive to ocean acidification.

Acknowledgements

This work was supported by the European Research Council under the European Community's Seventh Framework Programme (FP7/2007-20139)/ERC grant agreement No. 205140 and contributes to the "European Project on Ocean Acidification" (EPOCA) under the grant agreement No. 211284. G. Langer acknowledges financial support by BIOACID (Biological Impacts of Ocean Acidification; BMBF, FKZ 03F0608), and the European Community's Seventh Framework Programme under grant agreement 265103 (Project MedSeA). We thank Sebastian Rokitta, Karin Woudsma, Klaus-Uwe Richter und Ulrike Richter for laboratory assistance. **[SS]**

References

Barcelos e Ramos, J., Müller, M.N., Riebesell, U., 2009. Short-term response of the coccolithophore *Emiliania huxleyi* to abrupt changes in seawater carbon dioxide concentrations. Biogeosciences 7, 177–186.

Baumann, K.-H., Böckel, B., Frenz, M., 2004. Coccolith contribution to South Atlantic carbonate sedimentation. In: Thierstein, H.R., Young, J.R. (Eds.), Coccolithophores: from Molecular Processes to Global Impact. Springer, Berlin, pp. 367–402.

Bijma, J., Spero, H.J., Lea, D.W., 1999. Reassesing foraminiferal stable isotope geochemistry: impact of the oceanic carbonate system (experimental results). In: Fischer, G., Wefer, G. (Eds.), Use of Proxies in Paleoceanography: Examples from the South Atlantic. Springer, New York, pp. 489–521.

Brewer, P.G., Bradshaw, A.L., Williams, R.T., 1986. Measurement of total carbon dioxide and alkalinity in the North Atlantic Ocean in 1981. In: Trabalka, J.R., Reichle, D.E. (Eds.), The Changing Carbon Cycle — a Global Analysis. Springer Verlag, Heidelberg Berlin, pp. 358–381.

Broecker, W.S., Li, Y.H., Peng, T.H., 1971. Carbon dioxide — man's unseen artifact. In: Hood, D.W. (Ed.), Impingement of Man on the Ocean. Wiley-Interscience, New York, pp. 287–324.

Cohen, A.L., McCorkle, D.C., 2009. Morphological and conpositional changes in the skeletons of new coral recruits reared in acidified seawater: insights into the biomeneralization response to ocean acidification. Geochemistry Geophysics Geosystems 10.

Delille, B., Harlay, J., Zondervan, I., Jacquet, S., Chou, L., Wollast, R., Bellerby, R.G.J., Frankignoulle, M., Borges, A.V., Riebesell, U., Gattuso, J.P., 2005. Response of primary production and calcification to changes of pCO_2 during experimental blooms of the coccolithophorid *Emiliania huxleyi*. Global Biogeochemical Cycles 19 Gb2023.

Dickson, A.G., 1990. Standard potential of the reaction $AgCl(s) + ½\,H_2(g) = Ag(s) + HCl(aq)$, and the standard acidity constant of the ion HSO_4^- in synthetic seawater from 273.15 to 318.15 K. The Journal of Chemical Thermodynamics 22, 113–127.

Dickson, A.G., Millero, F.J., 1987. A comparison of the equilibrium constants for the dissociation of carbonic acid in seawater media. Deep-Sea Research 34, 1733–1743.

Eppely, R.W., 1972. Temperature and plankton growth in the sea. Fishery Bulletin 70, 1063–1085.

Fabry, V.J., 2008. Ocean science: marine calcifiers in a high-CO_2 ocean. Science 320, 1020–1022.

Fabry, V.J., Seibel, B.A., Feely, R.A., Orr, J.C., 2008. Impacts of ocean acidification on marine fauna and ecosystem processes. ICES Journal of Marine Science 65, 414–432.

Feng, Y., Warner, M.E., Zhang, Y., Sun, J., Fu, F.-X., Rose, J.M., Hutchins, D.A., 2008. Interactive effects of increased pCO_2, temperature and irradiance on the marine coccolithophore *Emiliania huxleyi* (Prymnesiophyceae). European Journal of Phycology 43, 87–98.

Gehlen, M., Gangsto, R., Schneider, B., Bopp, L., Aumont, O., Ethe, C., 2007. The fate of pelagic $CaCO_3$ production in a high CO_2 ocean: a model study. Biogeosciences 4, 505–519.

Gran, G., 1952. Determination of the equivalence point in potentiometric titrations of seawater with hydrochloric acid. Oceanologica Acta 5.

Guillard, R.R.L., Ryther, J.H., 1962. Studies of marine planktonic diatoms. I. Cyclothella nana Hustedt and Detonula confervacea Cleve Canadian Journal of Microbiology 8, 229–239.

Hofmann, M., Schellnhuber, H.-J., 2009. Oceanic acidification affects marine carbon pump and triggers extended marine oxygen holes. Proceedings of the National Academy of Sciences 106, 3017–3022.

Hoppe, C.J.M., Langer, G., Rokitta, S.D., Wolf-Gladrow, D., Rost, B., 2010. On CO_2 pertubation experiments: over-determination of carbonate chemistry reveals inconsistencies. Biogeosciences Discussion 7, 1707–1726.

Hurd, C.L., Hepburn, C.D., Currie, K.I., Raven, J.A., Hunter, K.A., 2009. Testing the effects of ocean acidification on algal metabolism: considerations for experimental designs. Journal of Phycology 45, 1236–1251.

Iglesias-Rodriguez, M.D., Buitenhuis, E.T., Raven, J.A., Schofield, O.M., Poulton, A.J., Gibbs, S., Halloran, P.R., Baar, H.J.W.d., 2008a. Phytoplankton calcification in a high-CO_2 world. Science 322, 336–340.

Iglesias-Rodriguez, M.D., Buitenhuis, E.T., Raven, J.A., Schofield, O.M., Poulton, A.J., Gibbs, S., Halloran, P.R., Baar, H.J.W.d., 2008b. Response to comment on "phytoplankton calcification in a high-CO_2 world". Science 322 1466c.

Iglesias-Rodríguez, M.D., Schofield, O.M., Batley, J., Medlin, L.K., Hayes, P.K., 2006. Intraspecific genetic diversity in the marine coccolithophore *Emiliania huxleyi* (Prymnesiophyceae): the use of microsatellite analysis in marine phytoplankton population studies. Journal of Phycology 42, 526–536.

Imhof, M., Schlotterer, C., 2001. Fitness effects of advantageous mutations in evolving *Escherichia coli* populations. Proceedings of the National Academy of Sciences of the United States of America 98, 1113–1117.

Kleypas, J.A., Buddemeier, R.W., Archer, D.E., Gattuso, J.-P., Langdon, C., Opdyke, B.N., 1999. Geochemical consequences of increased atmospheric carbon dioxide on coral reefs. Science 284, 118–120.

Langer, G., Nehrke, G., Probert, I., Ly, J., Ziveri, P., 2009. Strain-specific responses of *Emiliania hulxeyi* to changing seawater carbonate chemistry. Biogeosciences 6, 2637–2646.

Lüthi, D., Le Floch, M., Bereiter, B., Blunier, T., Barnola, J.-M., Siegenthaler, U., Raynaud, D., Jouzel, J., Fischer, H., Kawamura, K., Stocker, T.F., 2008. High-resolution carbon dioxide concentration record 650,000–800,000 years before present. Nature 453, 379–382.

Mehrbach, C., Culberson, C.H., Hawley, J.E., Pytkowicz, R.M., 1973. Measurement of the apparent dissociation constants of carbonic acid in seawater at atmospheric pressure. Limnology and Oceanography 18, 897–907.

Merchuk, J., 1991. Shear effects on suspended cells. in: Bioreactor Systems and Effects, Advances in Biochemical Engineering/Biotechnology. Springer, Berlin / Heidelberg 65–95.

Milliman, J.D., 1993. Production and accumulation od calcium-carbonate in the ocean — budget of a nonsteady state. Global Biogeochemical Cycles 7, 927–957.

Paasche, E., 2002. A review of the coccolithophorid *Emiliania huxleyi* (Prymnesiophyceae), with particular reference to growth, coccolith formation, and calcification-photosynthesis interactions. Phycologia 40, 503–529.

Pierrot, D.E., Lewis, E., Wallace, D.W.R., 2006. MS Exel Program Developed for CO_2 System Calculations, ORNL/CDIAC-105aCarbon Dioxide Information Analysis Centre. Oak Ridge National Laboratory, US Department of Energy.

Raven, J.A., Caldeira, K., Elderfield, H., Hoegh-Guldberg, O., Liss, P., Riebesell, U., Shepherd, J., Turley, C., Watson, A., 2005. Ocean Acidification Due to Increasing Atmospheric Carbon Dioxide. The Royal Society, Cardiff, UK.

Ridgwell, A., Schmidt, D.N., Turley, C., Brownlee, C., Maldonaldo, M.T., Tortell, P.D., Young, J.R., 2009. From laboratory manipulations to earth system models. Biogeosciences 6, 2611–2623.

Riebesell, U., Zondervan, I., Rost, B., Tortell, P.D., Zeebe, R.E., Morel, F.M.M., 2000. Reduced calcification of marine phytoplankton in response to increased atmospheric CO_2. Nature 407, 364–367.

Riebesell, U., Bellerby, R.G.J., Engel, A., Fabry, V.J., Hutchins, D.A., Reusch, T.B.H., Schulz, K.G., Morel, F.M.M., 2008. Comment on "phytoplankton calcification in a high CO_2-world". Science 322, 1466b.

9. Appendix

Riebesell, U., Fabry, V.J., Hansson, L., Gattuso, J.-P. (Eds.), 2010. Guide to best practices for ocean acidification research and data reporting. 260 p. Luxembourg: Publications Office of the European Union.

Rost, B., Riebesell, U., 2004. Coccolithophores and the biological pump: responses to environmental changes. In: Thierstein, H.R., Young, J.R. (Eds.), Coccolithophores: from Molecular Processes to Global Impact. Springer, Berlin, pp. 99–125.

Rost, B., Zondervan, I., Wolf-Gladrow, D., 2008. Sensitivity of phytoplankton to future changes in ocean carbonate chemistry: current knowledge, contradictions and research directions. Marine Ecology Progress Series 373, 227–237.

Schneider, K., Erez, J., 2006. The effect of carbonate chemistry on calcification and photosynthesis in the hermatypic coral *Acropora eurystoma*. Limnology and Oceanography 51, 1284–1293.

Schulz, K.G., Barcelos e Ramos, J., Zeebe, R.E., Riebesell, U., 2009. CO_2 perturbation experiments: similarities and differences between dissolved inorganic carbon and total alkalinity manipulations. Biogeoscience 6, 2145–2153.

Sciandra, A., Harlay, J., Lefevre, D., Lemee, R., Rimmelin, P., Denis, M., Gattuso, J.P., 2003. Response of coccolithophorid *Emiliania huxleyi* to elevated partial pressure of CO_2 under nitrogen limitation. Marine Ecology Progress Series 261, 111–122.

Shi, D., Xu, Y., Morel, F.M.M., 2009. Effects of the pH/pCO_2 control method on medium chemistry and phytoplankton growth. Biogeosciences 6, 1199–1207.

Tans, P., 2009. An accounting of the observed increase in oceanic and atmospheric CO_2 and an outlook for the future. Oceanography 22, 26–35.

Tortell, P.D., DiTullio, G.R., Sigman, D.M., Morel, F.M.M., 2002. CO_2 effects on taxonomic composition and nutrient utilization in an Equatorial Pacific phytoplankton assemblage. Marine Ecology Progress Series 236, 37–43.

Wolf-Gladrow, D.A., Riebesell, U., Burkhardt, S., Bijma, J., 1999. Direct effects of CO_2 concentration on growth and isotopic composition of marine plankton. Tellus B 51, 461–476.

Young, J.R., 1994. Function of coccoliths. In: Winter, A., Siesser, W.G. (Eds.), Coccolithophores. Cambridge University Press, Cambridge, pp. 63–82.

Young, J.R., Geisen, M., Cros, L., Kleijne, A., Probert, I., Ostergaard, J.B., 2003. A guide to extant coccolithophore taxonomy. Journal of Nannoplankton Research 111–132.

Declaration

Erklärung

Hiermit erkläre ich, dass ich die Doktorarbeit mit dem Titel:

Southern Ocean phytoplankton undermultiple stressors:
The modulation of Ocean Acidification effects by iron and light

selbstständig verfasst und geschrieben habe und ausser den angegebenen Quellen keine weiteren Hilfsmittel verwendet habe. Bei dieser Version handelt es sich um eine in Teilen überarbeitete, aber inhaltlich unveränderte Version der Doktorarbeit.

Ebenfalls erkläre ich hiermit, dass es sich bei den von mir abgegebenen Arbeiten um 3 identische Exemplare handelt.

Bremen, 19.12.2013

.....